SRR-CWDA-2011-00178
Revision 0

Saltstone Disposal Facility Stochastic Fate and Transport Model

January 2012

Prepared by: Savannah River Remediation LLC
Closure and Waste Disposal Authority
Aiken, SC 29808

Savannah River Remediation

Prepared for U.S. Department of Energy Under Contract No. DE-AC09-09SR22505

APPROVALS

Author:

1/10/2012

Barry Lester
Savannah River Remediation LLC
Closure & Waste Disposal Authority

Date

Technical Reviews:

1/10/2012

Steven Hommel
Navarro Research and Engineering, Inc.
Closure & Waste Disposal Authority

Date

1/10/2012

Richard Sheppard
Savannah River Remediation LLC
Closure & Waste Disposal Authority

Date

Approval:

1/10/2012

Kent Rosenberger
Savannah River Remediation LLC
Closure & Waste Disposal Authority

Date

TABLE OF CONTENTS

LIST OF FIGURES

LIST OF TABLES

ACRONYMS/ABBREVIATIONS

DOE	U.S. Department of Energy
FDC	Future Disposal Cell
GM	Geometric Mean
GSD	Geometric Standard Deviation
HDPE	High Density Polyethylene
HTF	H-Area Tank Farm
IHI	Inadvertent Human Intruder
LHS	Latin Hypercube Sampling
MCC	Moisture Characteristic Curve
MOP	Member of Public
NRC	U.S. Nuclear Regulatory Commission
PA	Performance Assessment
RAI	Request for Additional Information
SDF	Saltstone Disposal Facility
UA/SA	Uncertainty and Sensitivity Analyses

1.0 EXECUTIVE SUMMARY

This report documents the Saltstone Disposal Facility (SDF) Stochastic Fate and Transport Model (referred to herein as the SDF GoldSim model). The SDF GoldSim model is an object-oriented, probabilistic model designed to evaluate parameter sensitivity and the influence of parameter uncertainty on the potential for migration of radionuclides stored at the SDF to the accessible environment. For each realization of a Monte Carlo or Latin Hypercube Sampling (LHS) of data, the model is designed to calculate doses along a 100-meter boundary surrounding the disposal units at the SDF. The doses can be calculated from radionuclide concentrations generated by the model or calculated from concentrations generated by the SDF PORFLOW model. The deterministic advective-dispersive transport sub model that is repeatedly simulated in the analysis is an abstraction of the full 3-D SDF PORFLOW model that allows for a computationally efficient solution to the contaminant transport process, which is a necessity for multi-realization runs.

This report discusses the approach taken in the construction of the model including the use of the GoldSim software, the organization of the model, and the basic processes simulated. [GTG-2010c] This document also presents a compilation of the data used in the transport model and for the dose calculations.

The final section (Section 5.0) of this report documents the benchmark testing that was performed to show that the abstraction could be used as a surrogate for the full 3-D model. During the testing, results from the SDF PORFLOW model and the SDF GoldSim model were compared, showing that the abstraction can approximate the trends produced in the full 3-D model simulation results.

2.0 PURPOSE

The SDF GoldSim model is an object-oriented, probabilistic model designed to evaluate parameter sensitivity and the influence of parameter uncertainty on the potential for migration of radionuclides and non-radioactive contaminants in the SDF to the accessible environment. For the purpose of compliance, the accessible environment is defined by a 100-meter perimeter surrounding the Saltstone disposal units.

The SDF GoldSim model is comprised of two sub models; 1) the first is an abstraction of the SDF PORFLOW model, and 2) the second is a dose calculator. The abstraction is specifically designed to approximate the process of radionuclide transport from disposal units in a manner that would allow for uncertainty and sensitivity analyses to be performed in a time-efficient manner, while still allowing the influence of parameters on the transport processes to be examined. The model also includes a dose calculator, which can be used to evaluate dose at points of compliance based on the concentrations generated by the transport abstraction module or generated by the SDF PORFLOW model. This volume serves mainly as a documentation of Version 3.002 of the abstraction of the PORFLOW radionuclide transport model (as provided in the SDF GoldSim model file: SRS Saltstone v3.002.gsm, SRR-CWDA-2011-00189).

The two dose modules are documented in other sources, therefore discussion of the dose modules will be limited to directing the reader to those sources. This version (Version 3.002) of the SDF GoldSim model was constructed specifically for evaluating and comparing the Case A (Base Case) and Alternative Sensitivity Case K configurations of the SDF model. At a later date, a future version (tested and finalized for all cases) will be completed.

2.1 Advective-Dispersive Transport Model

The SDF GoldSim model solves the general equations for transport of dissolved radionuclides and non-radioactive species within the engineered barriers (the disposal units) and the natural barriers (the unsaturated zone and saturated zone). The SDF takes advantage of the GoldSim mixing cell-network elements and the 1-D analytical solution-based pipe elements to evaluate the advective-dispersive transport of contaminants through the engineered and natural barriers. The governing equation for 1-D advective-dispersive transport of a dissolved species in a unidirectional flow field can be written as follows:

$$\frac{\partial(\varphi RC)}{\partial t} = D\frac{\partial^2 C}{\partial l^2} - v\frac{\partial C}{\partial l} - \varphi R\lambda C + \sum_{i=1}^{Np}\varphi R\lambda_{pi}C_{pi} \qquad (2\text{-}1)$$

where:

C	=	solute concentration (m/L^3)
R	=	retardation coefficient
φ	=	effective porosity
t	=	time (T)
D	=	dispersion coefficient = $v\alpha + \varphi$ D_{eff} (L^2/T)
v	=	Darcy velocity (L/T)

α = dispersivity (L)

D_{eff} = effective diffusion coefficient (L^2/T)

λ = decay coefficient (T^{-1})

λ_{pi} = decay coefficient of the i^{th} parent (T^{-1})

Np = number of parent species

and:

l = transport pathway coordinate (L)

The transport module of the SDF GoldSim model simulates the transport of non-conservative species subject to sorption and either simple decay or ingrowth along decay chains. Other processes controlling the mass release from the disposal units include time-dependent physical and chemical degradation of grout and concrete zones, and for the future disposal cells (FDCs), the high-density polyethylene (HDPE) liners. The influence of mechanical dispersion (which is represented by the first term making up the dispersion coefficient) is not explicitly considered in the disposal unit structure, backfill, or unsaturated zone. In the saturated zone, dispersion is explicitly simulated. Matrix diffusion from the saltstone into the walls and from the walls to the backfill is also considered

2.2 Dose Calculator Model

In addition to calculating transport, the SDF GoldSim model also calculates receptor doses to the Member of Public (MOP) or to the Inadvertent Human Intruder (IHI), at points of compliance based on 1) the results from the transport abstraction module, 2) output from the SDF PORFLOW model or 3) estimated soil concentrations. The dose calculations are abstracted from conceptualizations of possible exposure pathways.

The possible exposure pathways for the SDF area are presented in the performance assessment (PA) for the SDF (SRR-CWDA-2009-00017), Tables 4.2-20 and 4.2-21. Note that there are two dose calculators found in the SDF Model (the original calculator described in the SDF PA and an updated calculator that is specifically used to evaluate Alternative Sensitivity Case K). Alternative Sensitivity Case K was developed in response to the SDF requests for additional information (RAIs) from the U.S. Nuclear Regulatory Commission (NRC) as described in the response to RAI PA-8. [SRR-CWDA-2011-00044] Differences between the two calculators are described in RAI responses B-2 and B-3. The approach taken in the original dose module is described in Sections 4.6 and 4.7 of the SDF PA. The approach used in Alternative Sensitivity Case K is an adaptation of the dose module used for the H-Tank Farm (HTF) SDF GoldSim model, which is documented in SRR-CWDA-2010-00093, Rev. 1, Sections 6, 7, and Appendix F. Modifications to this approach used in Alternative Sensitivity Case K are described in the response to RAI PA-8 found in SRR-CWDA-2011-00044.

Additionally, the intended use for the SDF GoldSim model is for GoldSim based dose calculations for the Base Case through E, with the exception of the dose due to the air and radon pathway, which is modeled using PORFLOW and documented in the SDF PA Section 4.5. PORFLOW based results are evaluated by a stand-alone GoldSim dose calculator as noted in Section 4.4.4.2.3 of the SDF PA. For Alternative Sensitivity Case K, both the GoldSim and

PORFLOW doses are evaluated within this model. The basic differences between the Base Case through E scenarios are presented in Table 2.2-1. The basic attributes of Alternative Sensitivity Case K are presented in Table 2.2-2.

Table 2.2-1: Saltstone Disposal Unit Configuration Summary

Case	Vault 1	Vault 4	FDCs
A	Base Case vault wall degraded, saltstone intact	Base Case vault wall degraded, saltstone intact	Base Case disposal unit wall intact, saltstone intact
B	N/A (no sheet drains)	Fast flow walls fast flow along walls from roof thru floor, vault wall degraded	Fast flow walls fast flow along walls from roof thru floor (including upper and lower mud mats)
C	Fast flow walls & crack fast flow along cracks from roof thru floor, vault wall degraded	Fast flow walls & crack fast flow along walls and cracks from roof thru floor vault wall degraded	Fast flow walls & columns fast flow along walls and columns from roof thru floor (including upper and lower mud mats)
D	N/A (no sheet drains)	Capillary break Base Case with capillary break at sheet drains	Capillary break Base Case with capillary break at sheet drains
E	Saltstone severely degraded vault wall degraded	Saltstone severely degraded vault wall degraded	Saltstone severely degraded disposal unit wall intact

[Table 4.4-4 from SRR-CWDA-2009-00017]

Table 2.2-2: Summary of Alternative Sensitivity Case K Attributes

Modeling Attributes	Change from Base Case (SRR-CWDA-2011-00044 response noted)	Impact on Base Case
Saltstone Physical Degradation	Complete degradation occurred within 10,000 years with degraded saltstone having a saturated hydraulic conductivity of 1.0E-06 cm/sec and an effective diffusion coefficient of 5.0E-06 cm^2/sec. Final degradation values are representative of soil properties (SP-1, SP-2, SP-7, and SP-17).	Increases the flow through the closure system and the release of contaminants
Moisture Characteristic Curves (MCCs)	MCCs were not used for cementitious material. Relative permeability and saturation were set equal to 1.0 for all suction levels for saltstone, clean cap, and disposal unit concrete (SP-3).	Increases the flow through the closure system and the release of contaminants
Saturated hydraulic conductivity for intact saltstone	Assumed to be 1.0E-08 cm/sec, largest value reported using simulants with a minimum of 90-day curing time and nominal curing temperature (SP-5).	Increases the flow through the closure system and the release of contaminants
Effective diffusivity of saltstone	For intact saltstone and clean cap, the initial value was unchanged from the Base Case but increased to 5.0E-06 cm^2/sec as the saltstone and clean cap degrade within 10,000 years (SP-6).	Increases the release of contaminants

Table 2.2-2: Summary of Alternative Sensitivity Case K Attributes (Continued)

Modeling Attributes	Change from Base Case (associated RAI)	Impact on Base Case
Pore volumes required to initiate E_h and pH transitions	E_h transition volume changed to 18 % of the Base Case value based on arbitrarily reducing by a factor of four, the reduction capacity of saltstone and applying a porosity correction. pH transition volume changed to 73 % of the Base Case value based on a porosity correction (SP-12).	Increases the release of the majority of contaminants
Technetium release via shrinking core model	Modified using a single porosity model that is based on the ISBN: 1-55899-189-1 approach; and using a semi-log fracture growth relationship with a final fracture spacing of 10 centimeters. Pertinent parameters (SP-13) are: • Constant diffusion coefficient of intact matrix of 1.0E-07 cm^2/sec • Reduction capacity of 0.206 meq e-/g (0.25 of Base Case value) • Dissolved oxygen concentration at fracture face is 1.06 meq e-/L	Increases surface area for oxygen diffusion and increases the oxidation of saltstone which accelerates the release of technetium from saltstone
Drainage layer performance	No Change (IEC-8) Time periods refined to capture significant changes to model parameters (C-22)	Increases flow into the closure system and contaminant release
Degradation of disposal unit concrete	Concrete fully degrades to representative soil properties with a saturated hydraulic conductivity of 1.0E-06 cm/sec and an effective diffusion coefficient of 5.0E-06 cm^2/sec • Initially for walls of Vaults 1 and 4 (VP-6) • Within 3,500 years for the roof of Vault 4 • Within 10,000 years for other disposal unit concrete (VP-2 and VP-3) • Non-degraded properties provided in SDF PA Table 4.2-16	Increases flow through the closure system without potentially diverting water away from saltstone caused by highly degraded walls in Vaults 1 and 4
Dose to the chronic intruder in vicinity of disposal units	Dose estimated based on water concentrations below Vault 4 and an FDC (II-2)	Increases potential dose to the intruder
Radionuclides analyzed	No change; all radionuclides identified in SDF PA Section 3.3.	No impact
Inventory	Vault 4 inventory reduced from the SDF PA Table 3.3-3 for Pu-238, Ra-226, Th-230, and U-234. FDC inventory reduced from the PA Table 3.3-5 for Ra-226 and Th-230 (IN-5).	Reduces the impact of radionuclides identified
Distribution Coefficient (K_d) values for saltstone, disposal unit concrete, and soil	Values updated based on latest issued reports (SP-10, SP-14, SP-15, FFT-2, and FFT-3)	Changes the impact of specific radionuclides
Dose methodology	Biotic transfer factors updated based on latest information (B-1) Inclusion of chicken and egg pathway (B-2) 25-year buildup of radionuclides in irrigated soil (B-3) Inclusion of leafy portion in plant transfer factor (B-4)	Changes the impact of specific radionuclides

[Table PA-8.1 from SRR-CWDA-2011-00044]

3.0 TRANSPORT MODEL TECHNICAL APPROACH

This section describes the approach taken in the development of the SDF GoldSim model. The first section describes the features of GoldSim used to develop the model. The second section presents the organization and makeup of the SDF GoldSim model.

3.1 GoldSim

The SDF GoldSim model was developed using GoldSim (Versions 10.11, SP3, 10.50 SP1 and 10.50 SP2), an object-oriented computer program designed to carry out dynamic, probabilistic simulations of external models (implemented as Dynamically Linked Libraries or DLLs) and/or self-contained models developed using GoldSim internal functions. [GTG-2010c] This software is qualified for use via acceptance testing as documented in *Software Acceptance Testing for GoldSim© Version 10.50 SP2*. [SRR-CWDA-2011-00166]

In addition to its use as a generalized stochastic analysis program, GoldSim contains contaminant and radionuclide transport modules that can be used to develop software for probabilistic simulations of the release of contaminants from engineered barriers, and the fate and transport of contaminants through natural barriers. GoldSim contaminant and radionuclide transport modules, approximate contaminant, or radionuclide transport processes analytically (or semi-analytically) using pipe elements (or networks of pipe elements) or numerically using networks of mixing cells (cell pathway elements). [GTG-2010]

Flow through the saltstone disposal units is a full 3-D process. For computational efficiency, the finite element SDF PORFLOW model takes advantage of the length of Vaults 1 and 4, perpendicular to the flow path, relative to the widths of the vaults in the flow direction, and approximates the 3-D system using 2-D slices through the vaults. In addition, the SDF PORFLOW model takes advantage of their mirror symmetry and simulates only half of the vault. Similarly, for the cylindrical FDCs the SDF PORFLOW model takes advantage of the radial symmetry and uses a quasi, 3-D radial approximation.

In the SDF GoldSim model, flow through the saltstone disposal units is approximated using a 2-D grid of mixing cells. The conceptual model simulated by PORFLOW is simplified in the SDF GoldSim model abstraction by assuming that the advective transport process is dominated by vertical flow. This assumption is consistent with the original SDF model as discussed in the PA. [SRS-CWDA-2009-00017] In areas of the saltstone disposal units where the horizontal component of flow is or becomes a controlling factor in the transport process, mass fluxes are apportioned between the cells below and cells in adjacent zones based upon changes in vertical volumetric fluxes.

The horizontal component of matrix diffusion, a major factor in the migration of radionuclides into the wall and to the backfill is explicitly modeled. The methodology for simulating of the horizontal component of matrix diffusion differs from the original semi-analytic solution approach has been replaced by discretizing the system of mixing cells horizontally and using diffusive links in the structure. This allows for a more rigorous handling of decay chains and time-dependent changes in parameters controlling the process of diffusion (K_ds and effective diffusion coefficients).

The disposal unit structure is divided into several groups of mixing cells, representing the saltstone, potential fast flow zones, sheet drains, walls, concrete floor, surrounding backfill, HDPE liners, and shotcrete for the FDCs. Note that certain design elements, such as the concrete roof and clean grout are not represented in the SDF GoldSim model but are represented in the SDF PORFLOW model. The floor beneath the disposal units is represented by a parallel set of 1-D mixing cell strings. Each string represents the floor beneath each of the zones making up the disposal unit. The unsaturated zone below the disposal units and surrounding backfill is also represented by a vertical 1-D string of mixing cells. The saturated zone immediately beneath the disposal unit is represented by a horizontal string of mixing cells. The saturated zone downgradient from the disposal unit is approximated using a pipe element.

3.1.1 GoldSim Cell Pathways

Cell pathway elements represent discrete, well-mixed environmental compartments or "mixing cells" that can be used to describe the environmental system being simulated. [GTG-2010c] A cell pathway element represents a specific volume of reference fluid (water for the SDF GoldSim model) and mass of solid(s). Within the cell, complete mixing takes place so there is no spatial differentiation of concentration within any phase. The dissolved species can migrate between cells, via advection or diffusion. The transport module of the SDF GoldSim model utilizes the GoldSim cell pathway elements to represent the transport pathways within the disposal-cell structure, the surrounding backfill, the unsaturated zone, and the saturated zone immediately beneath the disposal unit and just beyond the disposal unit. The concentrations just beyond the disposal units are used in the intruder dose calculations.

GoldSim cell-pathway elements are particularly amenable to simulating the transport processes within the disposal units because the SDF GoldSim model is designed to evaluate the fate and transport of radionuclide decay chains and can consider the influence of sorption on the radionuclide transport process. GoldSim allows for two types of mass links between cells, advective links, and diffusive links. The floor cells, unsaturated zone cells, and saturated zone cells are linked via advective links only. The disposal unit structure above the floor which is explicitly comprised of the saltstone, walls, backfill, fast zones (representing cracks and columns), sheet drains (Vault 4 and FDCs), shotcrete (FDCs), HDPE liners (FDCs), and surrounding backfill, utilizes vertical advective and horizontal diffusive links. The diffusive links are important because molecular diffusion controls the transport process into and through the walls and subsequently into the backfill. For computational efficiency, the horizontal advective links and vertical diffusive links are neglected. Note that the benchmarking exercise described in Section 5 indicates that the approximations used in the SDF GoldSim model can be used to approximate the results of the SDF PORFLOW model.

3.1.2 GoldSim Pipe Pathways

GoldSim pipe pathways are based on the Laplace transform approach to analytical solutions where an analytical solution is derived in the transformed then numerically inverted from the Laplace to the time domain. The pipe pathways provide analytical solutions for advective dominated transport problems, such as radionuclide transport in aquifer systems that can be approximated by a 1-D flow field. The solutions can simulate processes such as longitudinal

dispersion, retardation, decay, and ingrowth. The pipe pathways can also be used to simulate matrix diffusion, but this option is not used in the SDF Model.

The GoldSim SDF model uses pipe pathways to approximate the transport of radionuclides from under the disposal unit to the 100-meter boundary. The distance traveled is based on stream-trace measurements from disposal units to the boundary. The single-valued, Darcy velocity for each disposal unit is based on the time of travel for breakthrough curve peaks and associated aquifer porosity. The radionuclide concentrations at the end of the pipe pathway are used in the dose calculations.

3.1.3 GoldSim Sub Model Elements and Looping Structure

The transport module of the SDF GoldSim model takes advantage of the GoldSim Sub Model element to define the transport abstraction for the FDCs as a separate "inner model" (sub model) which is fed data from the main model. In addition, the FDC transport module utilizes GoldSim Looping Containers to allow the sub model to be run in do-loop mode for each of the 64 different FDCs. Vaults 1 and 4 are evaluated outside of this looping environment.

3.1.4 GoldSim Plume Function

The GoldSim transport module provides a built-in function that can be used to impose the influence of transverse (horizontal and vertical) dispersion on the results generated by the 1-D transport analysis. This function, called the plume function takes advantage of the fact that analytically the solution to 3-D advective-dispersive transport in a 1-D flow field can be defined as the product of solutions of point and/or integrated line sources in each of the three principal directions of a Cartesian coordinate system (see Figure 3.1-1).

Figure 3.1-1: GoldSim Plume Function Input

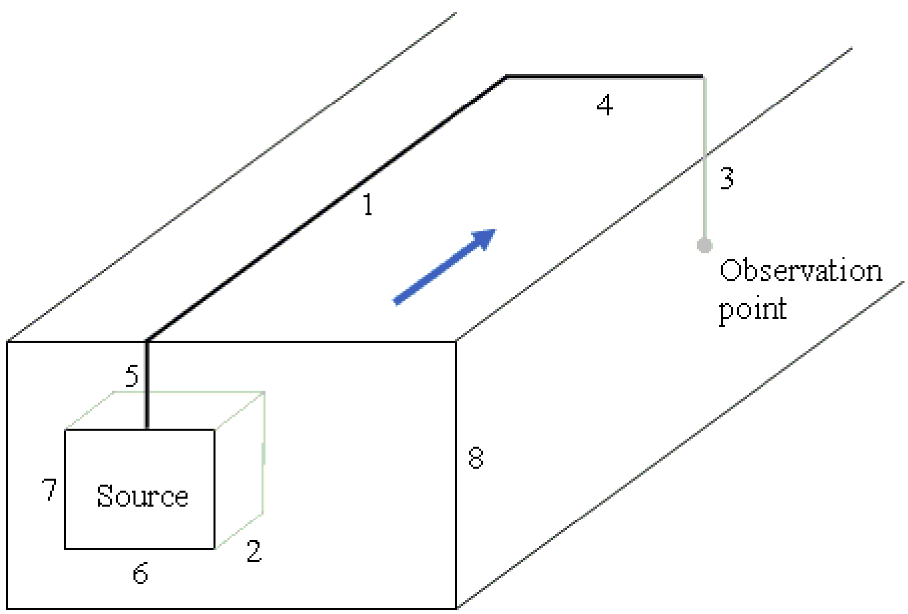

[GTG-2010]

By appropriate choice of point versus integrated line source solution for transport in each of the three principal directions, the product of the three solutions allows for the solution of advective-dispersive transport from a point, line, planar, or rectangular-prismatic source. The plume function is designed to use in conjunction with pipe elements, but can also be used with a set of cell pathway elements linked in series to represent a 1-D transport problem. The plume function, as designed, is evaluated independently from the solution for 1-D advective or advective-dispersive transport along a flow path. The plume function provides a dilution factor based on a specific transport length, a specific depth, and horizontal (transverse) distance or offset from the centerline (see Figure 3.1-1). The output from the plume function is a dilution factor, *DF*, which is the product of the analytic solutions for horizontal-transverse and vertical-transverse dispersion,

where:

$$DF = DF_{init} \times DF_T \times DF_V \tag{3.1-1}$$

and:

DF_{init} *is* the cross sectional area of the pipe (or of the cell pathway elements perpendicular to flow), DF_T is the component of the dilution factor based on the analytic solution for horizontal-transverse dispersion and DF_V is the component of the dilution factor based on the analytic solution for vertical-transverse dispersion.

The plume function returns a value designed to be used as a multiplier of concentrations (or fluxes) at the end of pipe pathway elements, to reflect the influence of transverse dispersion on the results. The plume function input parameters are as follows:

X_L*	=	length of the pipe or in a series of cells, the distance along the flow line to a line normal to the observation point [1]
A	=	cross-sectional area of pipe, or cells perpendicular to the flow line
L_S	=	length of the source parallel to the flow direction [2]
X_V	=	vertical position of the observation point [3]
X_T	=	transverse position of the observation point [4]
D_S	=	vertical depth to source top from top of aquifer or water table [5]
W_S	=	width of source transverse to flow direction [6]
b_S	=	source thickness [7]
b	=	aquifer thickness [8]
α_T	=	horizontal transverse dispersivity
α_V	=	vertical dispersivity

All of the plume function input parameters except the cross-sectional area (L^2) have dimensions of length (L) and where an input variable is depicted in Figure 3.1-1, the position of the variable in the input array is signified by brackets.

3.1.4.1 Analytical Solutions Used in the Plume Function

The plume function is used to expand the 1-D transport results along stream traces generated by PORFLOW into a 3-D approximation (plume), by taking into consideration the influence that spreading due to horizontal- and vertical-transverse dispersion would have on the 1-D stream-trace transport results. The plume function generates a more realistic value for concentrations at any wells crossed by a stream trace and allows for the influence of mass releases from disposal units to be considered at all observation wells whether or not they are crossed by specific stream traces.

3.1.4.1.1 Longitudinal Distance to the Observation Point

In a plume function analysis, GoldSim assumes that the longitudinal distance to the observation point (X_L), starts at the upgradient edge of the source. Prior to evaluation, the longitudinal distance to the observation point is adjusted to account for the change in longitudinal distance to the observation point from the beginning to end of the source. If the observation point is downgradient of the source, the longitudinal distance to the observation point (X_L) is adjusted as follows:

$$X_L^* = X_L - \frac{L_s}{2} \tag{3.1-2}$$

If the observation point is between the upgradient and downgradient edges of the source, the longitudinal distance to the observation point (X_L) is adjusted as follows:

$$X_L^* = \frac{X_L}{2} \tag{3.1-3}$$

This puts the upgradient edge of longitudinal distance to the observation point at the midpoint of the original longitudinal distance to the observation point. Note that an observation point upgradient of the source ($X_L \leq 0$) is not currently supported by GoldSim.

3.1.4.1.2 Horizontal Transverse Dispersion

There are two analytical solutions used in the plume function to describe the horizontal-transverse portion of the dilution factor. The first solution (Y_1) describes dispersive transport perpendicular to flow from a point source in an aquifer of infinite width is:

$$Y_1 = \frac{1}{\sqrt{4\pi\alpha_T X_L^*}}\left[\exp\left(\frac{-X_T^2}{4\alpha_T X_L^*}\right)\right] \tag{3.1-4}$$

The second solution (Y_2) describes dispersive transport perpendicular to flow from a line source in an aquifer of infinite width is:

$$Y_2 = \frac{1}{2W_s}\left[erf\left(\frac{X_T + \frac{W_s}{2}}{4\alpha_T X_L^*}\right) - erf\left(\frac{X_T - \frac{W_s}{2}}{4\alpha_T X_L^*}\right)\right] \tag{3.1-5}$$

The point source solution (Y_1) is invoked when the source width is very small relative to the distance from the center of the source to the position of the observation point, parallel to the flow direction X_L^*. The exact criteria used in the plume function, is as follows:

$$W_s < \frac{\sqrt{2\alpha_T X_L^*}}{100} \qquad (3.1\text{-}6)$$

where:

The value of 100 is "hard coded" into the function, and is based on the judgment of the developer. The line source solution (Y_2) is automatically invoked when the following criterion is met:

$$\frac{\sqrt{2\alpha_T X_L^*}}{100} < W_s < 1{,}000{,}000\sqrt{2\alpha_T X_L^*} \qquad (3.1\text{-}7)$$

If one of the criteria noted in Equations (3.1-6) and (3.1-7) is not met, the transverse dispersion is negligible, and the following criterion is used to determine whether the observation point falls within the plume or not:

$$\left| X_T \right| > \frac{W_s}{2} \qquad (3.1\text{-}8)$$

If the criterion stated in Equation (3.1-8) is met, the observation point is outside of the plume and the dilution factor DF_T is then set to zero. If not, DF_T is set equal to $1/W_s$.

3.1.4.1.3 Vertical Transverse Dispersion

There are two analytical solutions used in the plume function to describe the vertical-transverse portion of the dilution factor. Unlike the solutions for horizontal-transverse dispersion, the solutions for vertical-transverse dispersion take into consideration the finite depth of the aquifer. The influence of the top and bottom boundaries of the aquifer is accommodated using the method of images for both solutions, imposing zero-flux boundaries at the top and bottom of the aquifer. The method of images is based on superimposing equal strength sources on the opposite side of each boundary equidistant from the boundary. Since each image source will also need an image source across the boundary, it is not symmetrically opposed to an infinite series of images is produced. The first solution (Z_1) which describes dispersive transport perpendicular to flow from a point source in an aquifer of finite depth can be written as:

$$Z_1 = \frac{1}{\sqrt{4\pi\alpha_V X_L^*}} \sum_{n=-\infty}^{n=\infty} \left[\exp\left(\frac{-(2nb - X_V + D_s)^2}{4\alpha_V X_L^*} \right) + \exp\left(\frac{-(2nb - X_V - D_s)^2}{4\alpha_V X_L^*} \right) \right] \qquad (3.1\text{-}9)$$

The second solution (Z_2) describes vertical dispersive transport perpendicular to flow from a line source in an aquifer of finite depth is:

$$Z_2 = \frac{1}{2b_s} \sum_{n=-\infty}^{n=\infty} \left[erf\left(\frac{2nb + (X_V - D_s)}{4\alpha_V X_L^*} \right) - erf\left(\frac{2nb + (X_V - D_s - b_s)}{4\alpha_V X_L^*} \right) + erf\left(\frac{2nb - (X_V + D_s)}{4\alpha_V X_L^*} \right) - erf\left(\frac{2nb - (X_V + D_s + b_s)}{4\alpha_V X_L^*} \right) \right] \qquad (3.1\text{-}10)$$

Which solution is used or whether a simplified approximation can be made is automatically controlled by GoldSim according to the following set of criteria. In addition, the criteria are set so that Equations 3.1-9 and 3.1-10 can give a good approximation in nine terms or less.

If the aquifer thickness is small enough that the mass released from the source can be considered fully mixed with respect to depth at the distance along the flow path, where the observation point is located the dilution factor DF_V will be set to 1/b. The criterion for assuming that complete mixing takes place is:

$$b < \frac{\sqrt{2\alpha_V X_L^*}}{3} \tag{3.1-11}$$

If the aquifer is not thin enough for full mixing to occur, the suitability of using the method of images with nine images is examined. Image sources are invoked if the following criterion is met.

$$b < 1{,}000{,}000\sqrt{2\alpha_V X_L^*} \tag{3.1-12}$$

If the inequality is not met, than neither of the image sources solutions is used.

If an image source solution is used, the point source solution (Z_1) is chosen when the source thickness is very small relative to the distance from the center of the source to the position of the observation point, parallel to the flow direction X_L^*. Assuming that the complete mixing assumption is not used, the criteria used by the plume function, to invoke the point source solution is as follows:

$$\frac{\sqrt{2\alpha_V X_L^*}}{3} < b < \frac{\sqrt{2\alpha_V X_L^*}}{100} \tag{3.1-13}$$

where:

The value of 100 is "hard coded" into the function, and is based on the judgment of the developer. The line source solution (Z_2) is automatically invoked when the following criterion is met:

$$\frac{\sqrt{2\alpha_V X_L^*}}{100} < b < 1{,}000{,}000\sqrt{2\alpha_V X_L^*} \tag{3.1-14}$$

If the neither criteria noted in Equations (3.1-11) and (3.1-12) is met, the transverse dispersion is negligible, and the following criteria is used to determine whether the observation point falls within the plume or not:

$$|X_V| > \frac{b_s}{2} \tag{3.1-15}$$

If the criterion stated in Equation (3.1-15) is met, the observation point is outside of the plume, and the dilution factor, DF_V, is assigned a value of zero. If not, DF_V is assigned the value $1/b_s$.

3.1.4.1.4 Final Dilution Factor

The final dilution factor *DF* is then assembled from the dilution factor components described in Sections 3.1.4.1.1 through 3.1.4.1.3 as follows:

$$DF = DF_{init} \times DF_T \times DF_V \quad (3.1\text{-}16)$$

3.1.4.2 Application of the GoldSim Plume Function to the SDF GoldSim Model

The transport module of the SDF GoldSim model utilizes the matrix capability of the plume function by setting up two plume function elements, one for the northern disposal units and one for the southern disposal units, where all of the inputs are entered in matrix form. The matrix dimensions for the northern disposal units plume function are the number of disposal units in the northern zone (N_{dcn}=36) from which the radionuclides are released and the number of sectors ($N_{sectors}$= 6) where the stream traces cross the 100-meter boundary as shown in Figure 3.1-2. The matrix dimensions for the southern disposal units plume function are the number of disposal units (N_{dcs}=30) in the southern zone and the number of sectors ($N_{sectors}$= 6).

For each disposal unit, the observation well length (X_L) was evaluated by taking the distance along the stream trace from the disposal unit to the 100-meter boundary (Figures 3.1-3, 3.1-4, and 3.1-5). The stream traces from Vaults 1 and 4 are presented in Figures 3.1-3, 3.1-4 and the stream traces from the FDCs are presented in Figure 3.1-5. Note that, for clarity, stream traces presented in Figure 3.1-5 are plotted for only half of the disposal units. The distance between where a stream trace crosses the 100-meter boundary and the center point of each sector along the normal to the stream trace (X_T) is used as the observation point for determining the magnitude of the plume function.

Note that to reduce the memory storage, the concentrations are not rigorously solved at all points where the line normal to the observation well crosses the flow line. The concentrations are generated only at the point intersecting where the flow lines from the disposal units cross the 100-meter boundary. These concentrations are then used to generate the product of the 1-D analysis concentration and the plume function. The farther away an observation well is from the intersection point between the disposal unit stream-trace and the 100-meter boundary, the larger the concentration uncertainty. This approximation was considered to be acceptable because, in general, the magnitude of the component is smaller the farther away an observation well is from the stream trace intersection point.

Figure 3.1-2: SDF Modeling Showing Divisional Sectors

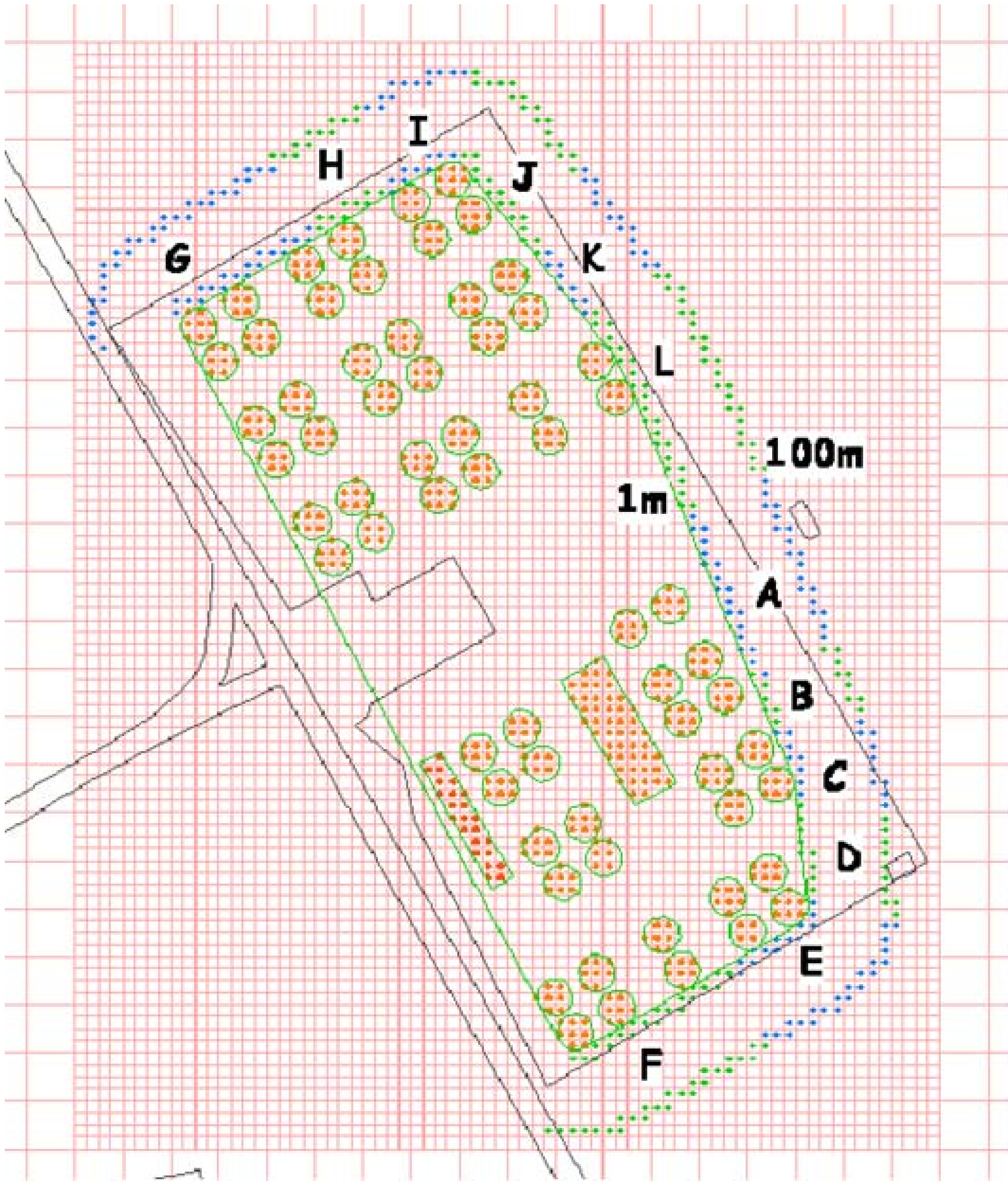

From Figure 4.4-16: SRS-CWDA-2009-00017, Rev. 0

Figure 3.1-3: SDF Vault 1 Modeling Showing Stream Tracers

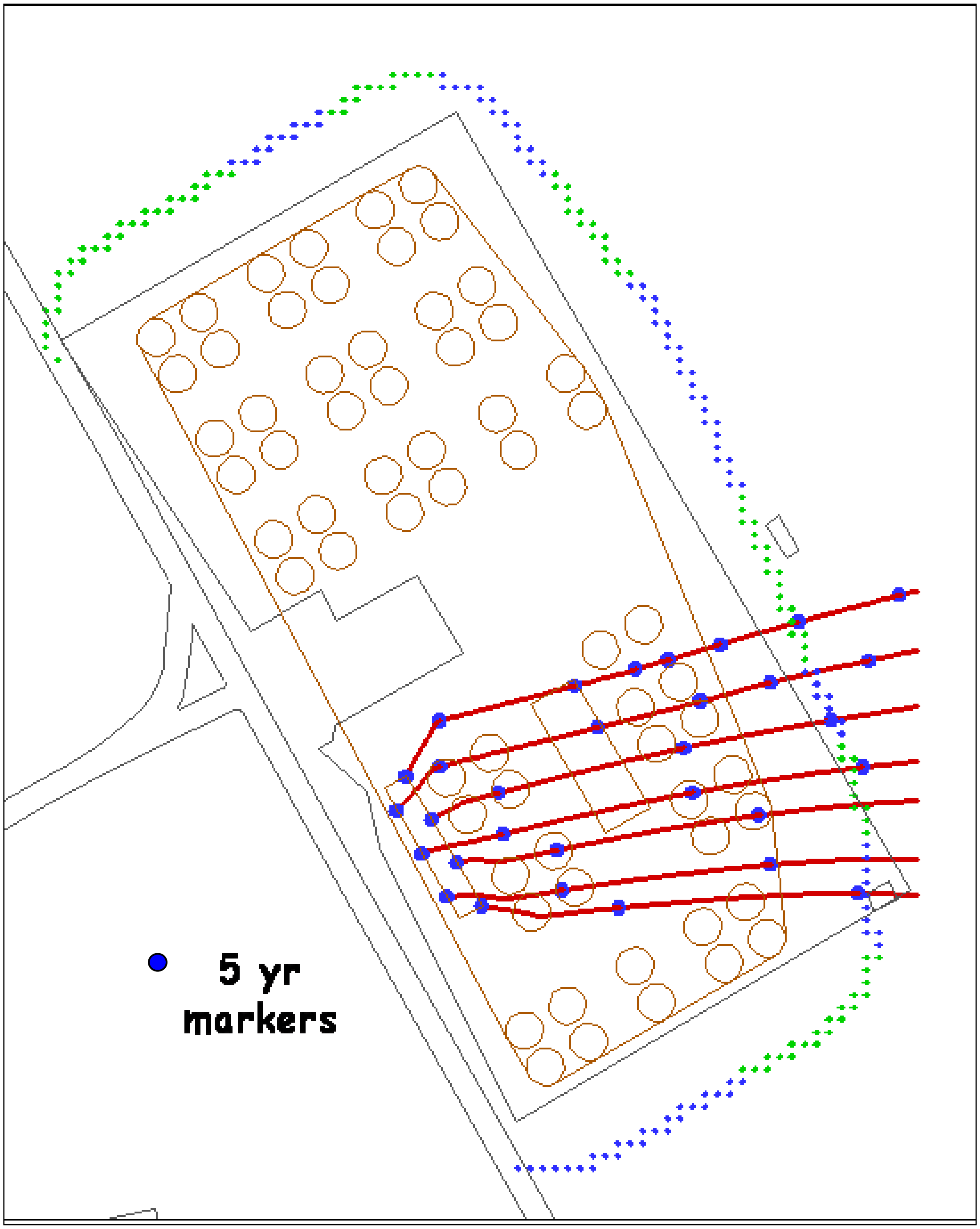

From Figure 4.4-17: SRS-CWDA-2009-00017, Rev. 0

Figure 3.1-4: SDF Vault 4 Modeling Showing Stream Tracers

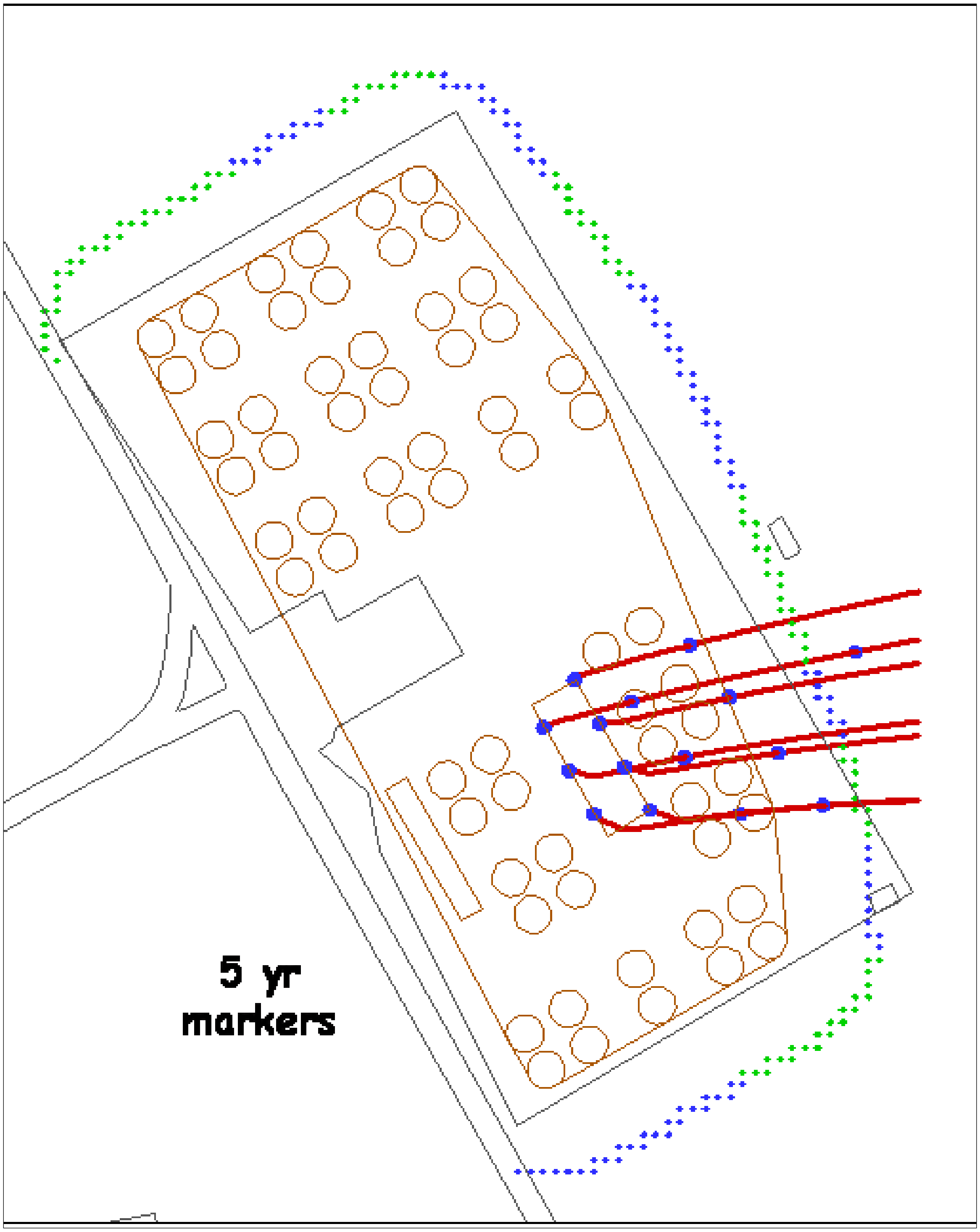

From Figure 4.4-18: SRS-CWDA-2009-00017, Rev. 0

Figure 3.1-5: SDF FDC Modeling Showing Stream Tracers

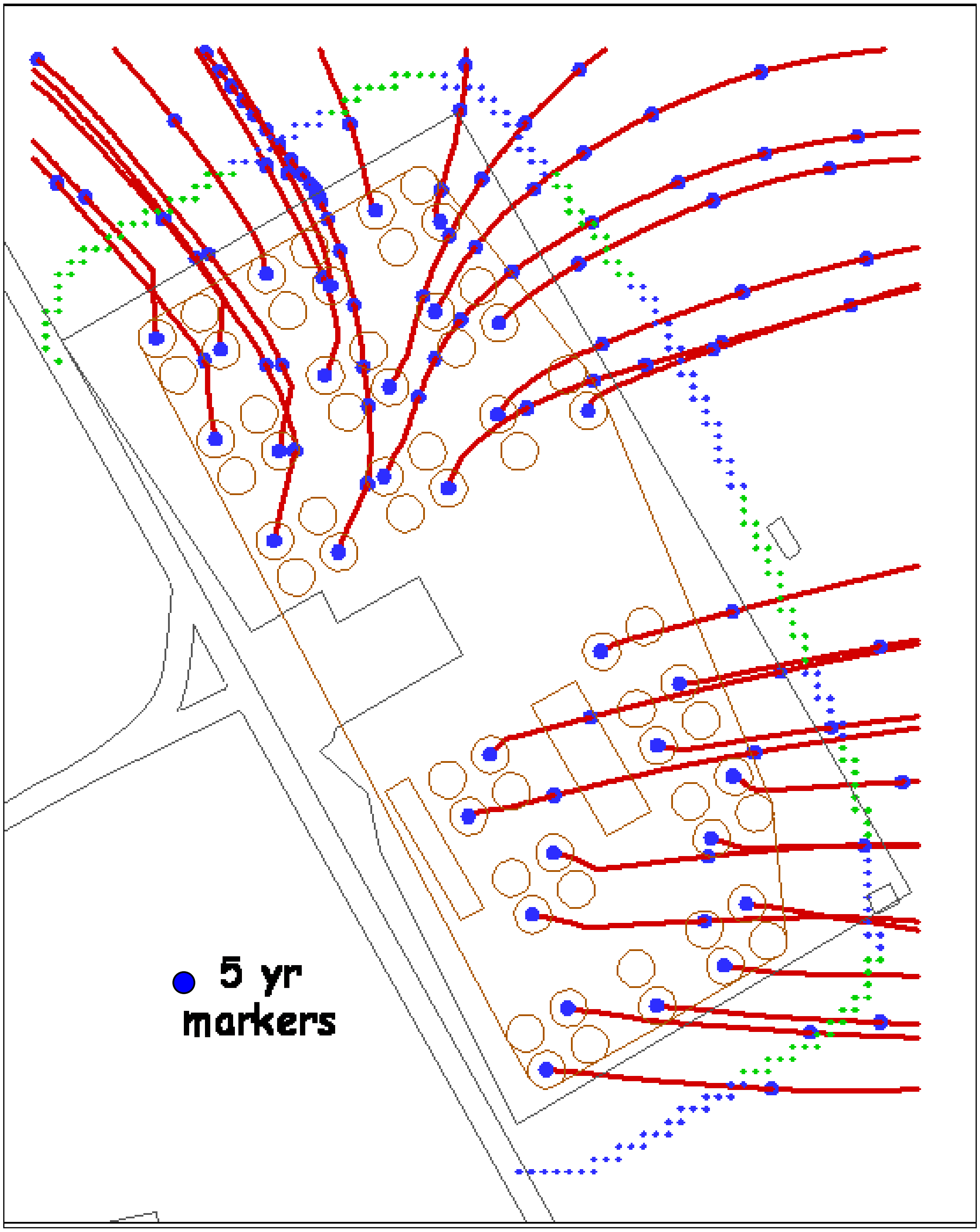

From Figure 4.4-19: SRS-CWDA-2009-00017, Rev. 0

3.1.5 Stochastic Elements

GoldSim stochastic elements are designed to represent explicitly the uncertainty in input parameters within a model. GoldSim uses the Monte Carlo method or an LHS method to carry out the probabilistic simulations. The traditional Monte-Carlo method randomly samples the data over the complete probabilistic range at each realization. The LHS approach divides each stochastic element's distribution P{0,1} into up to 10,000 strata of equal probability. The actual number used is the smaller of the number of realizations and 10,000 strata. The strata are then randomly "shuffled" into a new order and a random value is then picked from each stratum. The application of the LHS process ensures that a uniform spanning of sampling occurs. [GTG-2010c]

A typical GoldSim stochastic element used in the SDF GoldSim model is *Kd_Dist*, which is used to sample a K_d value, is depicted below in Figure 3.1-6, along with two expression elements used to define the geometric mean (GM) and geometric standard deviation (GSD) for all radionuclide species.

Figure 3.1-6: A Typical GoldSim Stochastic Element Used in the SDF GoldSim Model

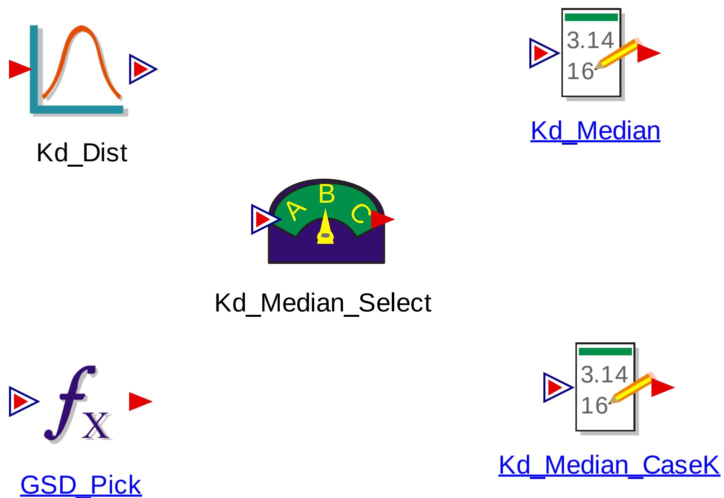

The sampling input is then added to the element as shown in Figure 3.1-7 below. Note that the stochastic element *Kd_Dist* is used to sample all species in the model and a pull-down menu can be used to look at species other than Ac-227. In addition, it can be seen that the probabilistic distribution used here is a log normal distribution with a GM of *Kd_Median_Select*, a GSD of *GSD_Pick*, a minimum of 0.25 x *GSD_Pick* and a maximum of 1.75 x *GSD_Pick*. The value *Kd_Median_Select* varies depending upon which configuration is chosen. Its value for the Base Case through E is *Kd_Median* and its value for Alternative Sensitivity Case K is *Kd_Median_CaseK*.

Figure 3.1-7: Sampling Input for a Typical GoldSim Stochastic Element Used in the SDF GoldSim Model

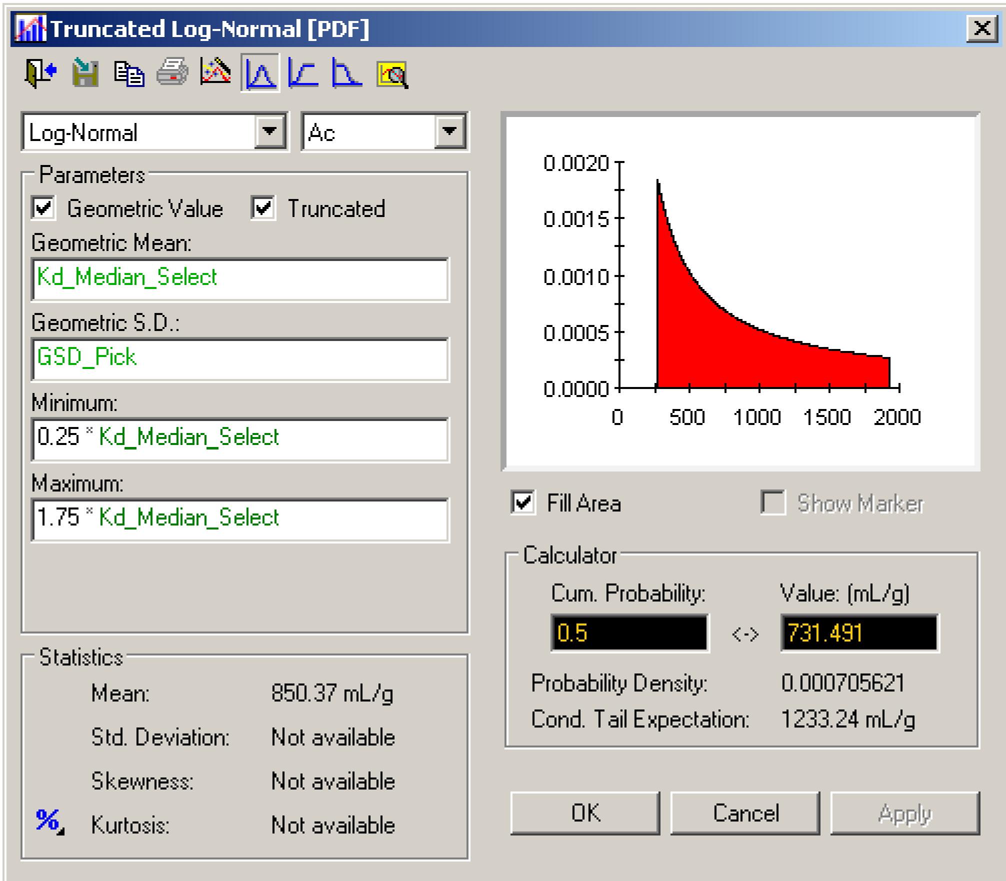

3.2 Model Organization

The SDF GoldSim model is partitioned into two main segments, 1) the Transport Module and 2) the Dose Calculation Modules. The Transport Module is comprised of an "outer model" in which are assembled all of the control elements and data input elements in addition to the elements used to define radionuclide transport in Vaults 1 and 4. The "inner model" (or sub model) is where all of the dynamic transport calculations for mass transport associated with FDC releases are made. As shown in Figure 3.2-1, the static portion of the Transport Module, in which all of the control elements and data input elements are assembled, is comprised of the following GoldSim containers:

- *Dashboards*
- *SimulationSettings*
- *UserInput*
- *Inventory*
- *Materials*
- *Transport*
- *Miscellaneous*

The first three containers (*Dashboards*, *SimulationSettings*, and *UserInput*) contain the control data for the model, and the other four containers (*Materials*, *Inventory*, *Transport,* and *Miscellaneous*) contain parameters describing the physical and chemical properties, flow system, and geometry of the system. The container, where all of the dynamic transport calculations for mass transport associated with disposal unit releases are made, is embedded in a series of containers, the uppermost being the *DisposalUnits* container (renamed from *TheVaults)*.

Figure 3.2-1: SDF GoldSim Model Organization

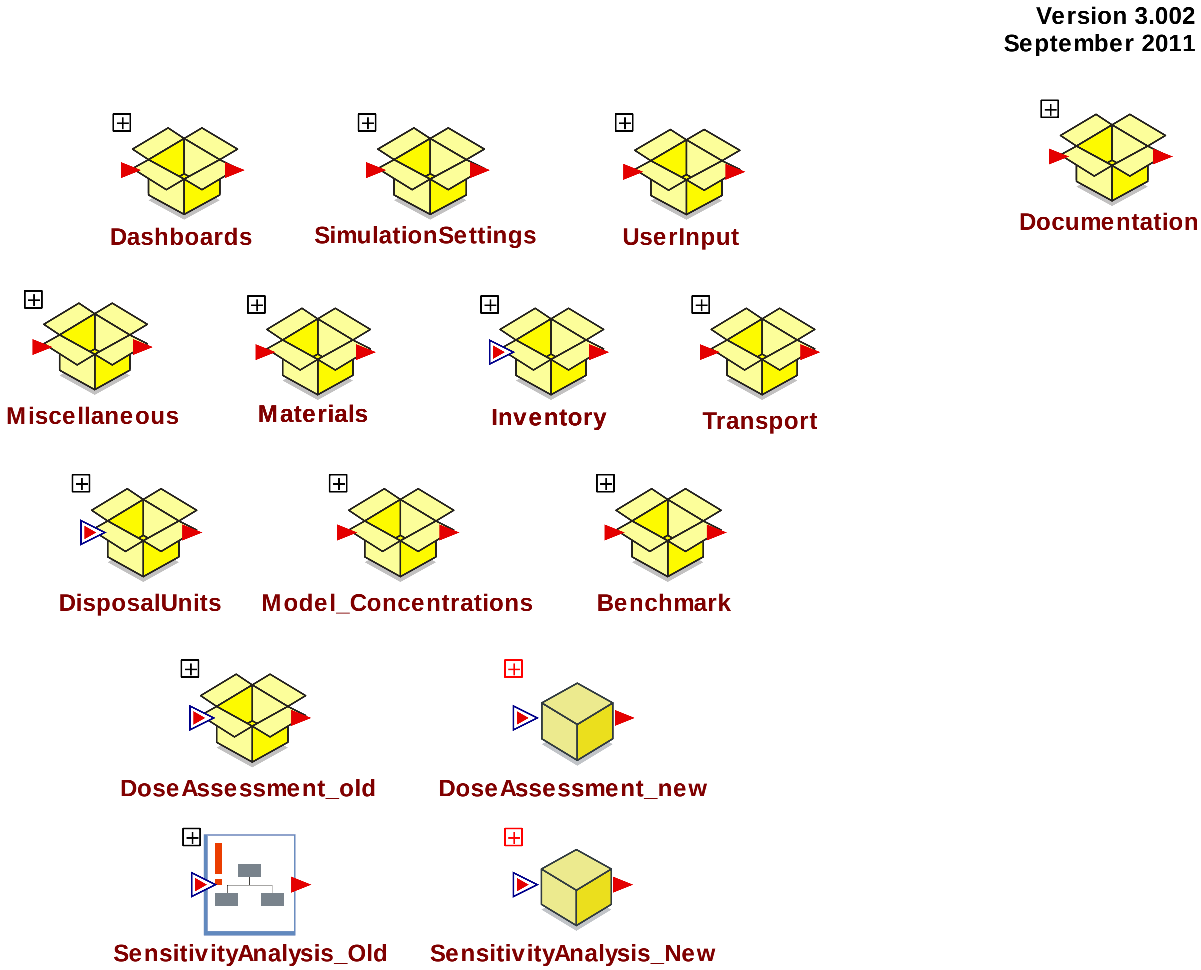

The *DisposalUnits* container is comprised of three containers (*Vault_1*, *Vault_4*, and *FDCs*). *Vault_1* and *Vault_4* contain the radionuclide transport logic for Vaults 1 and 4, respectively. The container *FDCs* contains the radionuclide logic for the 64 FDCs. Unlike Vaults 1 and 4, the FDCs are evaluated using a looping structure that repeatedly calls a radionuclide transport, sub model 64 times. The outermost of the nested containers in *FDCs* (Figure 3.2-2), contains the looping container *OuterLoop* (Figure 3.2-3), which loops through the 64 FDCs, calling the transport sub model 64 times. The two data elements in *FDCs* define the number of sources (*NFDC*) and a specified source area to run (*RunThisFDC*). If *RunThisFDC* is set to zero, the sub model will loop 64 times. If a specific source is defined (i.e., 1 for FDC V2A), only the requested source will be evaluated and results in the specified sub model can be saved.

Figure 3.2-2: Contents of Container *FDC_ TransportModel*

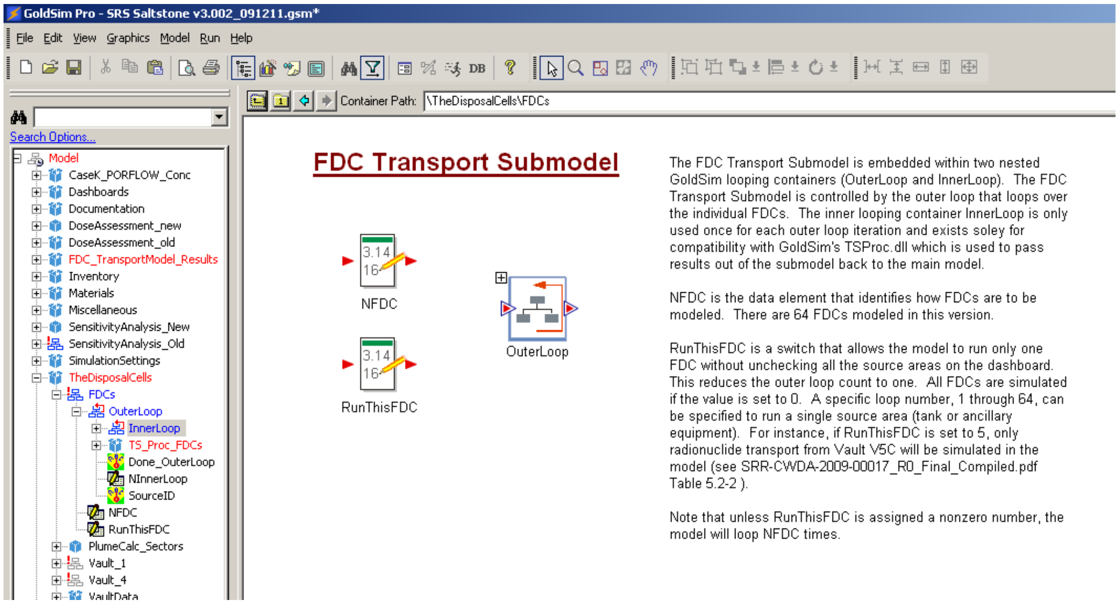

Figure 3.2-3: Contents of Container *HTFSourceLoop*

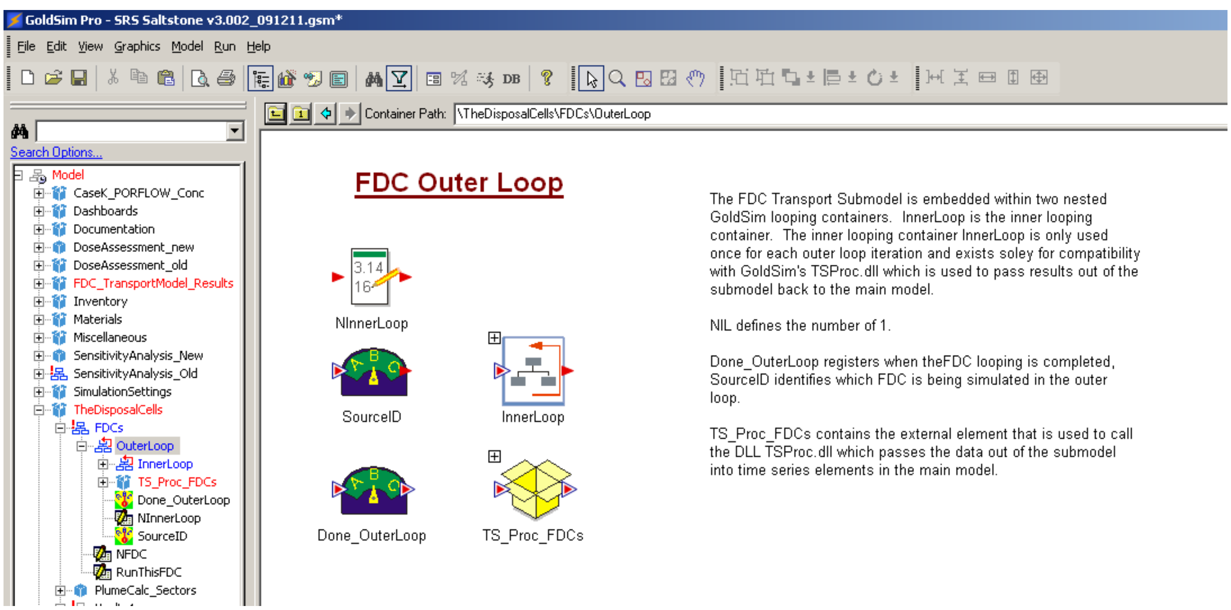

Figure 3.2-4: Contents of Container *InnerLoop*

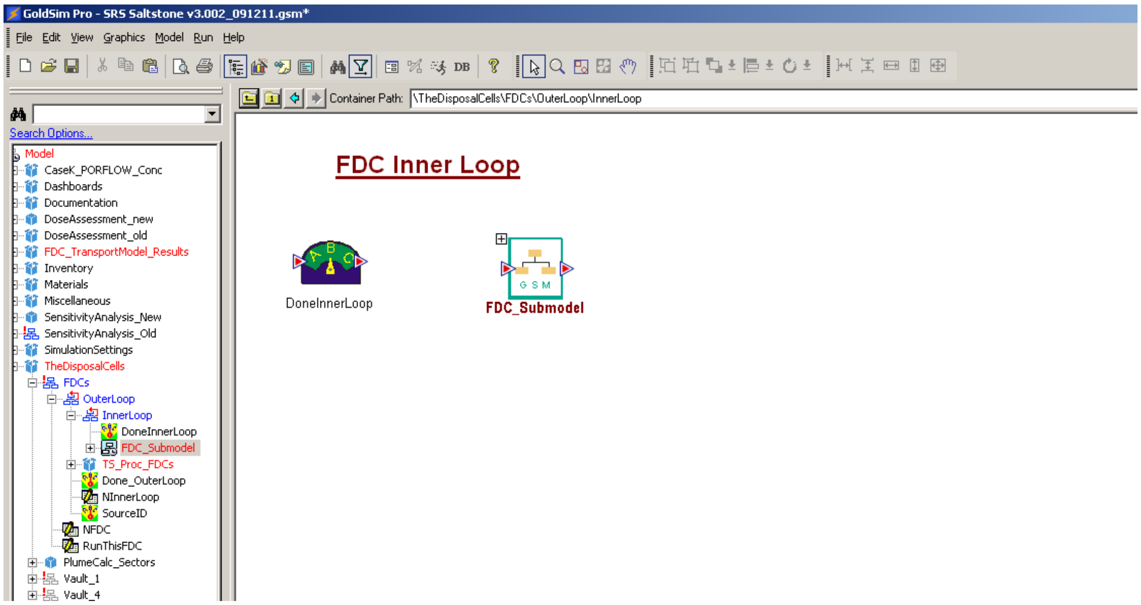

Nested inside the looping container *OuterLoop,* is an inner looping container, *InnerLoop* (Figure 3.2-4). The inner looping container is used only once for each outer loop iteration (as indicated by the data element *NIL)* and exists solely for compatibility with GoldSim C^{++} software *TSProc.dll* which is used to pass results out of the transport sub model back to the main model. *OuterLoop* also contains three selector elements, which are used to control the source being run, when the analysis is completed (Figure 3.2-3), and the container *TSProcFDCs* that contains the external element that controls the use of the *TSProc.dll* software.

The transport sub model *FDC_TransportSubmodel* is located within the innermost of the nested looping containers (Figure 3.2-4), and it is within this sub model that all the mass transport calculations, for FDCs, are performed. In addition to the transport sub model, *InnerLoop* contains a selector switch to indicate when the inner loop is finished.

TSProcFDCs contains an external element (Figure 3.2-5), that controls the use of *TSProc.dll,* which is used for copying time series associated with the disposal unit release analyses, from the sub model into the main model. For GoldSim Version 10.5, *TSProc.dll* is replaced by an updated version of *TSProc.dll for 32-bit* architectures and *TSProc_X64.dll* for 64-bit architectures. *TSProcFDCs* will require updating when the DLL name changes.

Figure 3.2-5: External Element Controlling *TSProc.dll orTSProc_x64.dll*

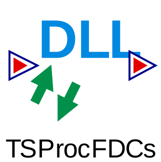

Several other upper-level containers are present in *FDC_TransportSubmodel* (Figure 3.2-6). Because *FDC* is a conditional container, time series elements (Figure 3.2-7) cannot be used

within these containers. Therefore, the time series elements used to transfer data from the sub model to the main model via *TSProc.dll* are assembled in the container *FDC_Transport_Results*.

Figure 3.2-6: Contents of *FDC_TransportSubmodel*

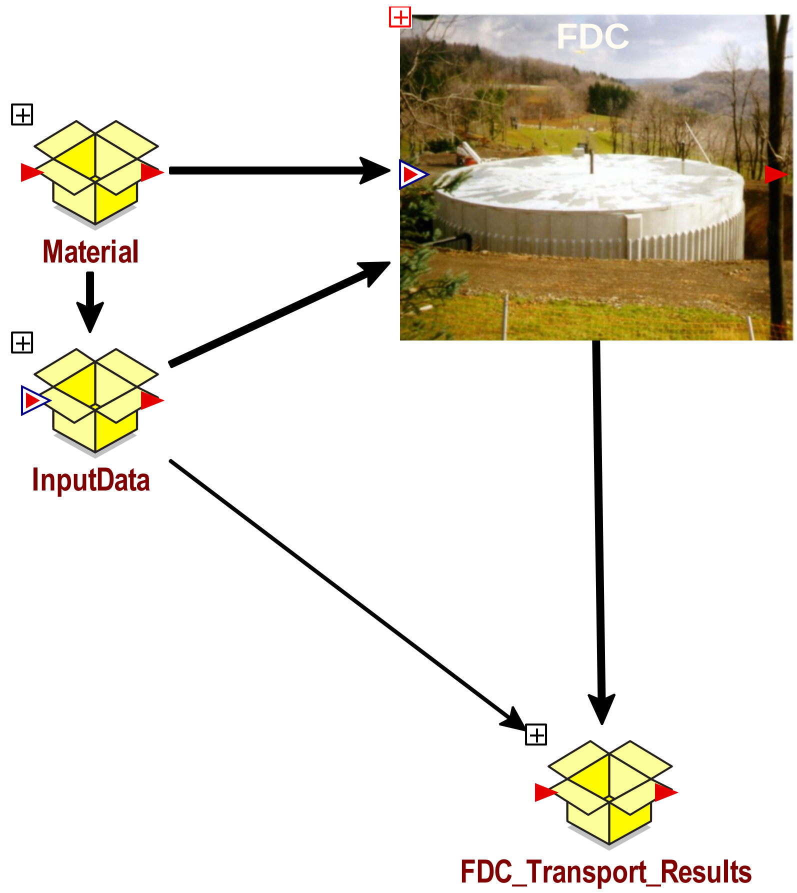

Figure 3.2-7: Typical GoldSim Time Series Element Used in *FDC_Transport_Results*

The species elements and reference fluid elements must also be separately defined in the main model and sub model. The species element and the base reference, fluid element for the sub model are located in the *Material* container (Figure 3.2-6).

The other upper-level container within *FDC_TransportSubmodel* is *InputData* (Figure 3.2-6), which serves as a transfer site for data passed from the main model to the sub model. The data from the main model to the sub model is passed directly though the sub model-interface in *FDC_TransportSubmodel* shown in Figure 3.2-8. Selector elements located in *InputData* serve an organizational purpose as they capture the data from the interface and reset the variable name to the name from the main model for consistency.

Figure 3.2-8: *SDF_TransportSubmodel* Sub Model Interface

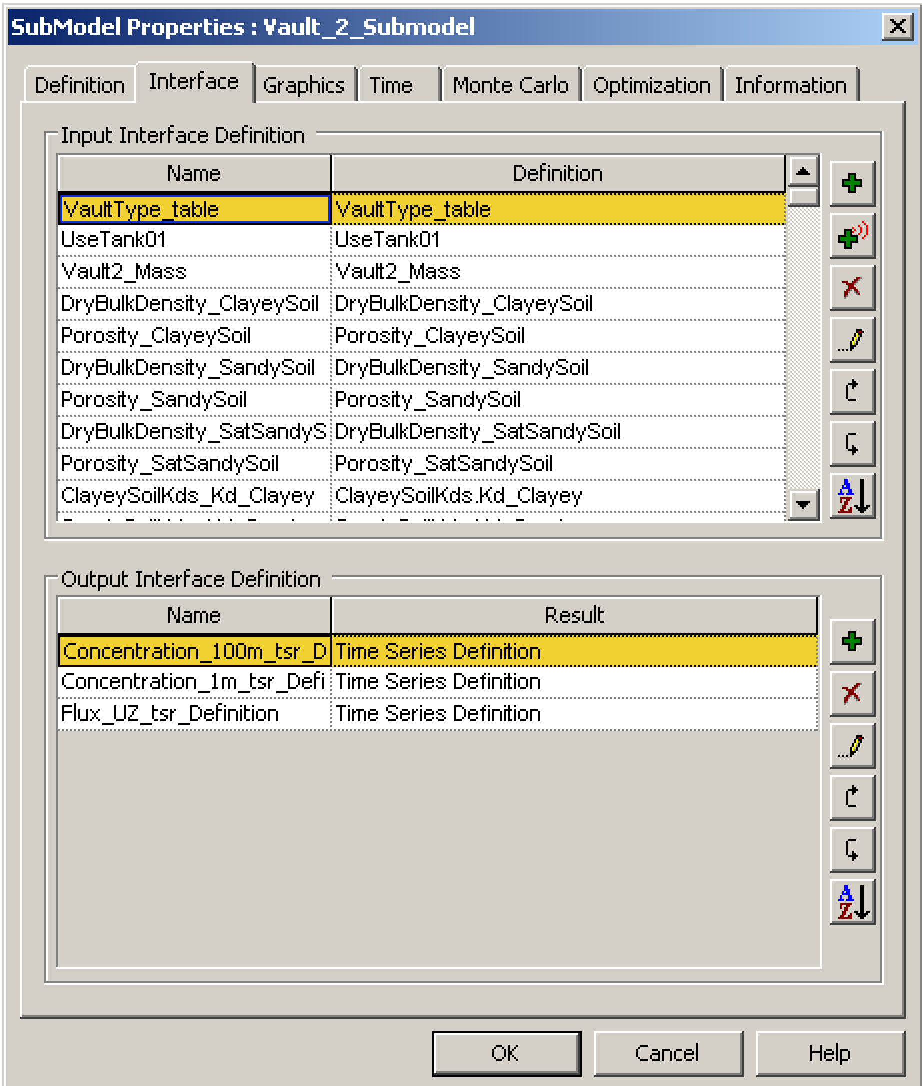

Also, note that data is output from the sub model through the interface. The output data is then returned to the main model using the software *TSProc.dll* or *TSProc_x64.dll* in conjunction with an external properties element.

Within the *FDC* container is located the cell networks that evaluate the transport of radionuclides and non-radioactive contaminants. Figure 3.2-9 depicts the organizational scheme within *FDC*.

Figure 3.2-9: Contents of the Container *FDC*

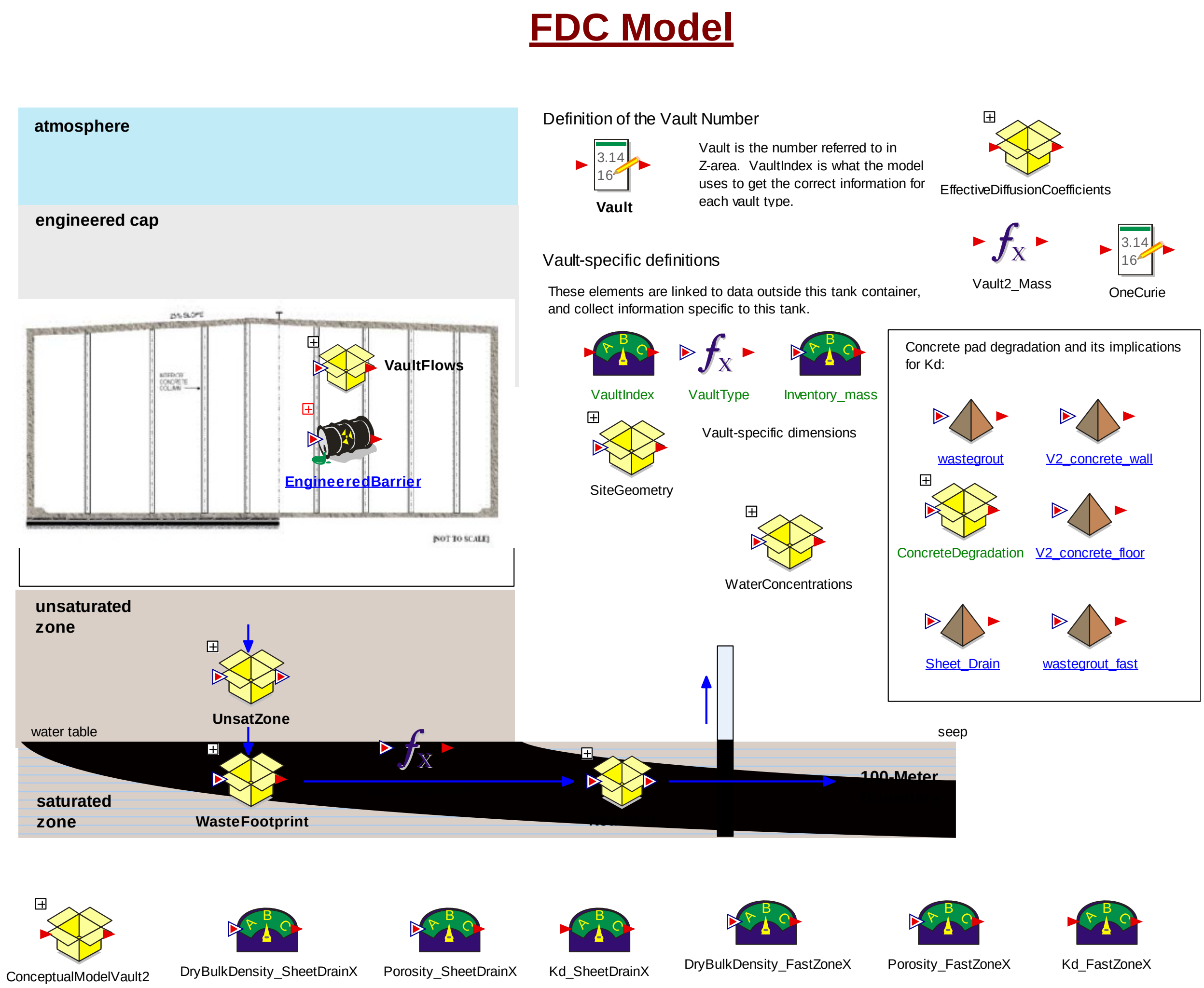

In the FDC model, the cell networks and pipe models are distributed within three upper level containers and a source element. The source element is a specialized type of container that is capable of performing functions associated with engineered barrier capabilities and based upon these functions can execute a controlled release into associated cells, which are defined by inserting them into the source element. [GTG-2010] In the FDC model, the source element contains the engineered barrier.

The upper-level containers in the FDC model (*FDCs)* that contain segments of the cell network are:

- *EngineeredBarrier*
- *UnsatZone*
- *WasteFootprint*
- *NearWell*

3.2.1 Engineered Barriers

The SDF has three types of disposal units, Vault 1, Vault 4, and the FDCs. In the SDF GoldSim model, the conceptual models of the three types of disposal units simulated using PORFLOW are simplified in the SDF GoldSim model abstraction by assuming that the advective transport process is dominated by vertical flow. This assumption is consistent with the SDF model discussed in the SDF PA. [SRR-CWDA-2009-00017]

In areas of the saltstone disposal units where the horizontal component of flow cannot be neglected in the transport process, mass fluxes are apportioned between the cells below and cells in adjacent zones based upon changes in vertical volumetric fluxes at the floor interface. The horizontal component of matrix diffusion, a major factor contributing to the migration of radionuclides into the wall and from the wall into the backfill is explicitly modeled.

In this version of the SDF GoldSim Model, the methodology used to simulate the horizontal component of matrix diffusion differs from the original semi-analytic solution approach used in the PA (see SRNL-STI-2009-00114). The original methodology has been replaced by assembling a 2-D mixing-cell network where diffusive mass flux links are used to connect cells horizontally and advective mass flux links are used to connect cells vertically. This numerical approach to simulating horizontal diffusion allows for a more rigorous handling of decay chains and time-dependent changes in parameters controlling the process of diffusion (K_ds and effective diffusion coefficients). In addition, this version of the SDF GoldSim uses the assigned inventories as initial conditions in the engineered barrier calculations, allowing for a more rigorous handling of the decay chains.

The conceptual model for Vault 1 is depicted in Figure 3.2-10. As with the SDF PORFLOW model, the SDF GoldSim model takes advantage of the symmetry of the structure and simulates radionuclide transport through only half of Vault 1. The SDF GoldSim model also disregards the direct influence of any transport processes above the saltstone. In the SDF GoldSim model, the simulated components of engineered barrier include the:

- saltstone
- fast flow zone
- wall
- surrounding backfill
- floor

Figure 3.2-10: Conceptual Model for SDF Vault 1

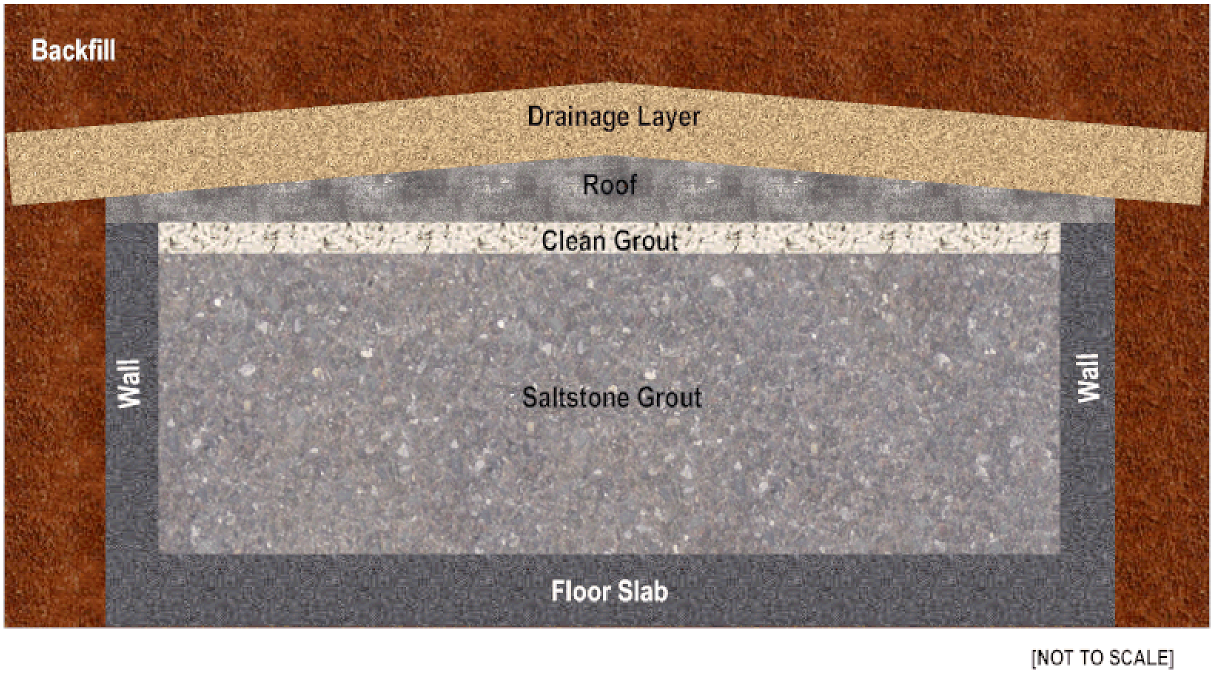

The Vault 1 structure is divided into several groups of mixing cells, representing the saltstone grout, potential fast flow zone, which is located between the saltstone cells, walls, concrete floor, and surrounding backfill. Note that the fast flow zone is a hypothetical fractured zone within the saltstone that acts as a pathway of low resistance to flow, enhancing the advective transport of the radionuclides through the saltstone and floor beneath.

The conceptual model for Vault 4 is depicted in Figure 3.2-11. As with the SDF GoldSim model for Vault 1, the SDF GoldSim model takes advantage of the symmetry of the structure and simulates radionuclide transport through only half of Vault 4. The SDF GoldSim model also disregards the direct influence of any transport processes above the saltstone. In the SDF GoldSim model, the simulated components of Vault 4 include the:

- saltstone
- fast flow zone (roof support column)
- sheet drains
- center wall
- outer wall
- floor
- backfill

The Vault 4 structure is divided into several groups of mixing cells, representing the saltstone, potential fast flow zone, which is located between two sets of saltstone cells, sheet drains, walls, the concrete floor, and surrounding backfill.

Figure 3.2-11: Conceptual Model for SDF Vault 4

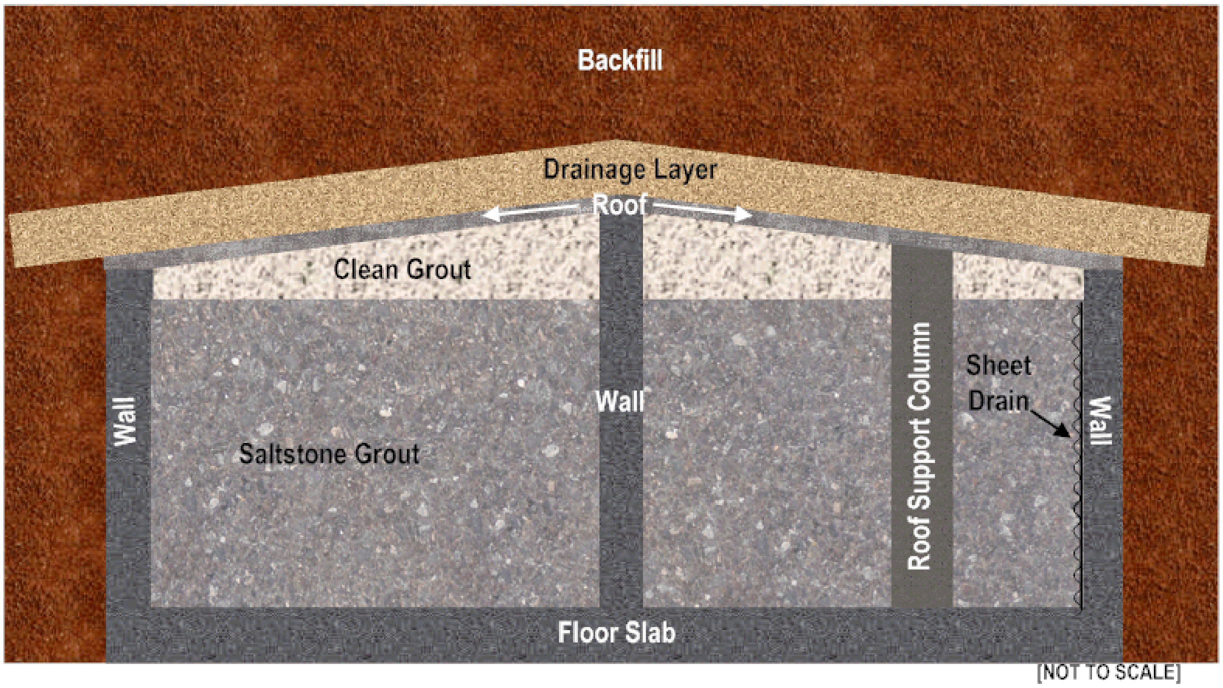

The conceptual model for a FDC is depicted in Figure 3.2-12. The SDF GoldSim takes advantage of the radial symmetry of the structure and simulates radionuclide transport, disposal unit center, outwards. The SDF GoldSim model also disregards the direct influence of any transport processes above the saltstone. In the SDF GoldSim model abstraction of the FDCs, the engineered barrier is comprised of the:

- saltstone
- fast flow zone
- sheet drain
- wall
- shotcrete
- vertical HDPE liner
- backfill
- floor

Figure 3.2-12: Conceptual Model for FDC (Typical)

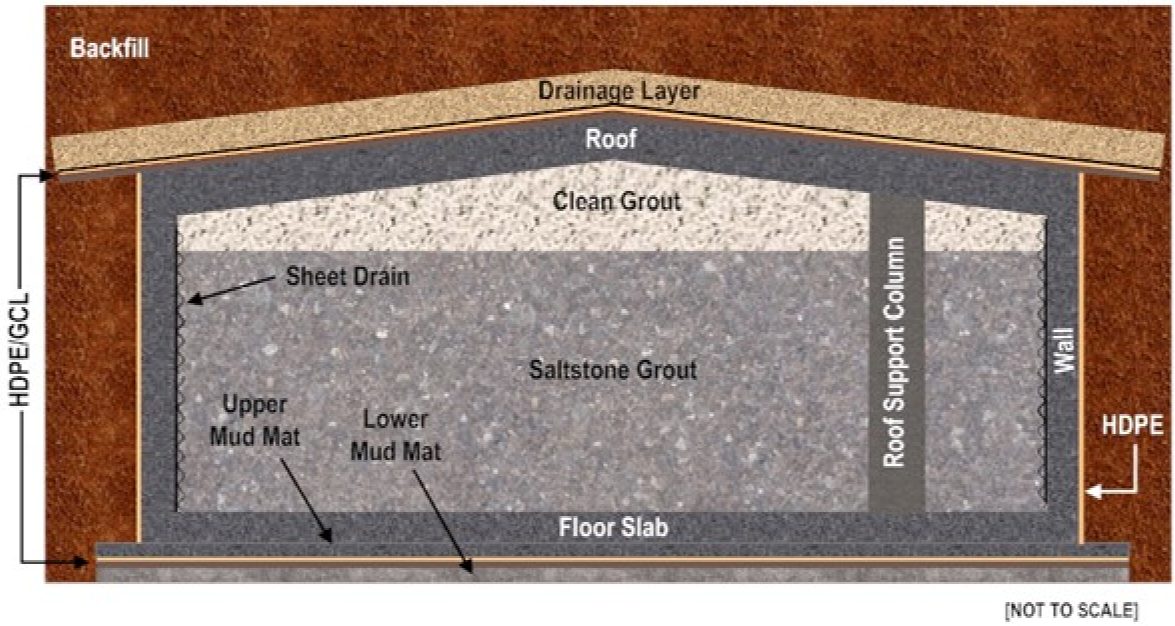

[SRR-CWDA-2009-00017 Figure 4.4-3]

Because the FDCs contain all of the possible zones in the model, the FDC structure will be used as an example of the how the cell networks are assembled.

The FDC structure is that of a mixing-cell network divided into several groups (or zones) of mixing cells, representing the saltstone, potential fast flow zones which are located between the saltstone cells, sheet drains, walls, shotcrete, the vertical HDPE liners, the concrete floor, and surrounding backfill. Note that certain design elements, such as the concrete roof and clean grout are not represented in the SDF GoldSim model but are represented in the SDF PORFLOW model. The influence of these design elements is implicitly considered in the flow fields, used in the SDF GoldSim model, which are abstracted from the SDF PORFLOW model. The floor beneath the disposal units is represented by a parallel set of 1-D mixing cell strings. Each string represents the floor beneath each of the zones making up the disposal unit.

Note that the SDF GoldSim model extends from the center of the FDC into the backfill, and the full model is simulated by determining the cell volumes based on cylindrical coordinates.

The engineered barrier is simulated using the source element, *EngineeredBarrier* (see Figure 3.2-9). Even though, source elements have special mass-release functionalities, these functionalities are presently not being used in the saltstone model therefore, the source element behaves as a standard container. Within the source element, *EngineeredBarrier*, a top-level container (*VaultCells*), houses the engineered barrier, mixing cell grid that is depicted in Figure 3.2-13, and represents the conceptual model depicted in Figure 3.2-12.

Figure 3.2-13: *EngineeredBarrier* Cell Structure

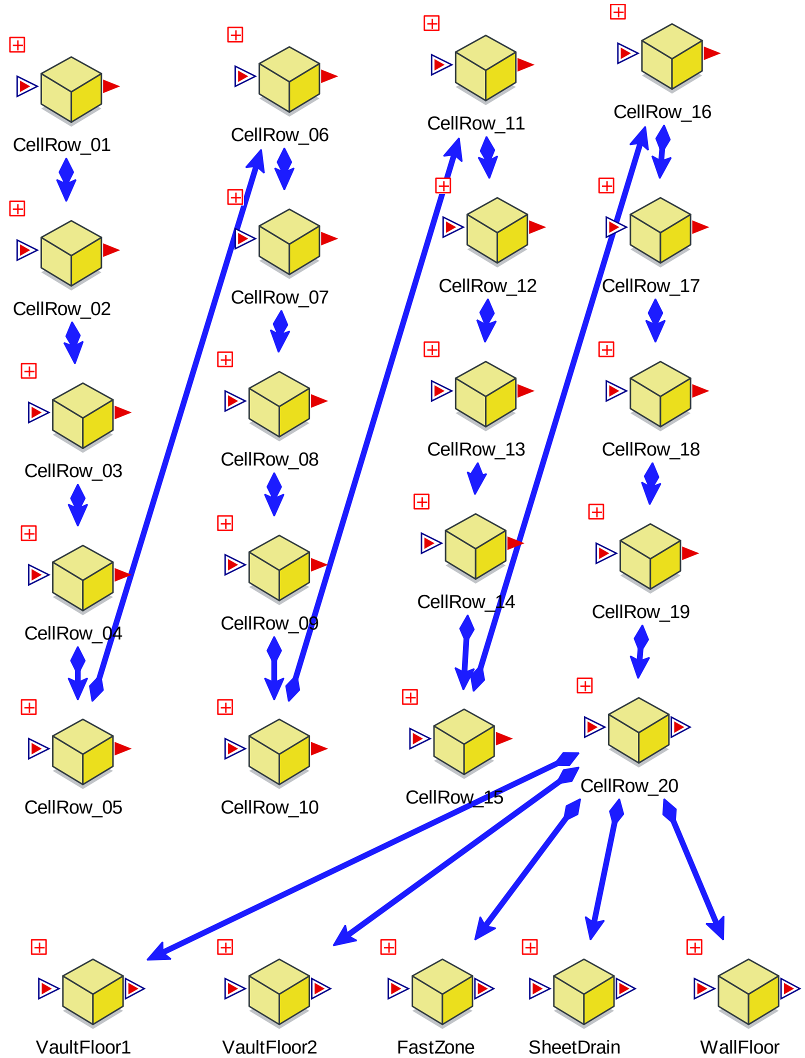

The containers *CellRow_01* to *CellRow_20* are each comprised of a horizontal string of mixing cells extending from the center of the disposal unit into the backfill. The top of the cells in container *CellRow_01* represents the contact between the clean and saltstone grout. The bottom of the cells in container *CellRow_20* represents the contact between the saltstone and the concrete floor. Note that the floor HDPE liner as well as the upper and lower mud mats are not explicitly simulated in this simplified model and are assumed as part of the floor. Their influence is implicitly reflected in the velocity fields.

Within each of the *CellRow* containers resides a set of containers containing the sets of cells defining specific zones as depicted in Figure 3.2-14.

Figure 3.2-14: Containers Making Up a Typical Row of Cells

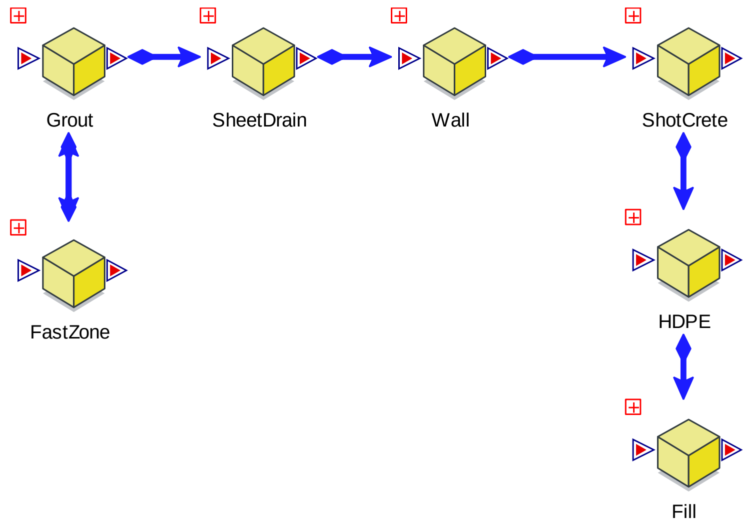

Note that the fast flow zone is located between two saltstone zones, but is kept in a separate container to allow for differences in diffusion coefficients (see Figures 3.2-14 and 3.2-15). A separate cloned water element is required in each of these containers to allow for the use of different diffusion coefficients in each of these zones. The container *Grout* includes two segments of the horizontal row of mixing cells connected by diffusive mass links, the first going from the center of the FDC to the fast flow zone (the roof support column) and the second going from the fast flow zone to the sheet drain (see Figures 3.2-14 and 3.2-16). The container *SheetDrain* includes the segment of the horizontal row of cells, between the saltstone and the wall (see Figures 3.2-14 and 3.2-17). *Wall* includes the segment of the horizontal row of cells, between the sheet drain and the shotcrete (see Figures 3.2-14 and 3.2-18). *Shotcrete* includes the segment of the horizontal row of cells, between the wall and the HDPE liner (see Figures 3.2-14 and 3.2-19). *HDPE* includes the segment of the horizontal row of cells, between the shotcrete and the backfill (see Figures 3.2-14 and 3.2-20). *Fill* includes the segment of the horizontal row of cells, representing the surrounding backfill (see Figures 3.2-14 and 3.2-21).

Figure 3.2-15: Contents of the *FastZone* Container

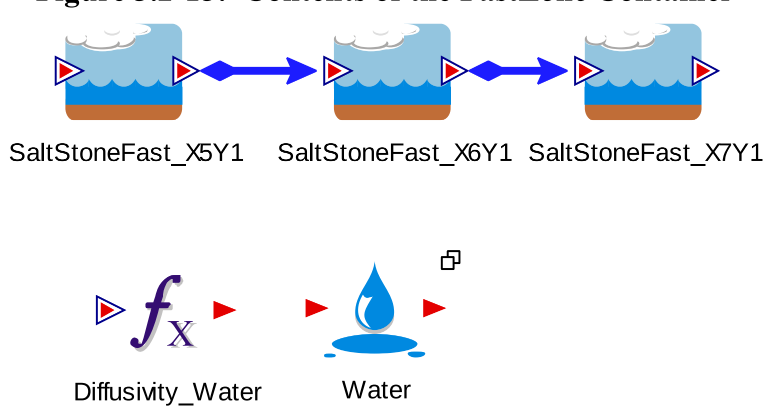

Figure 3.2-16: Contents of the *Grout* Container

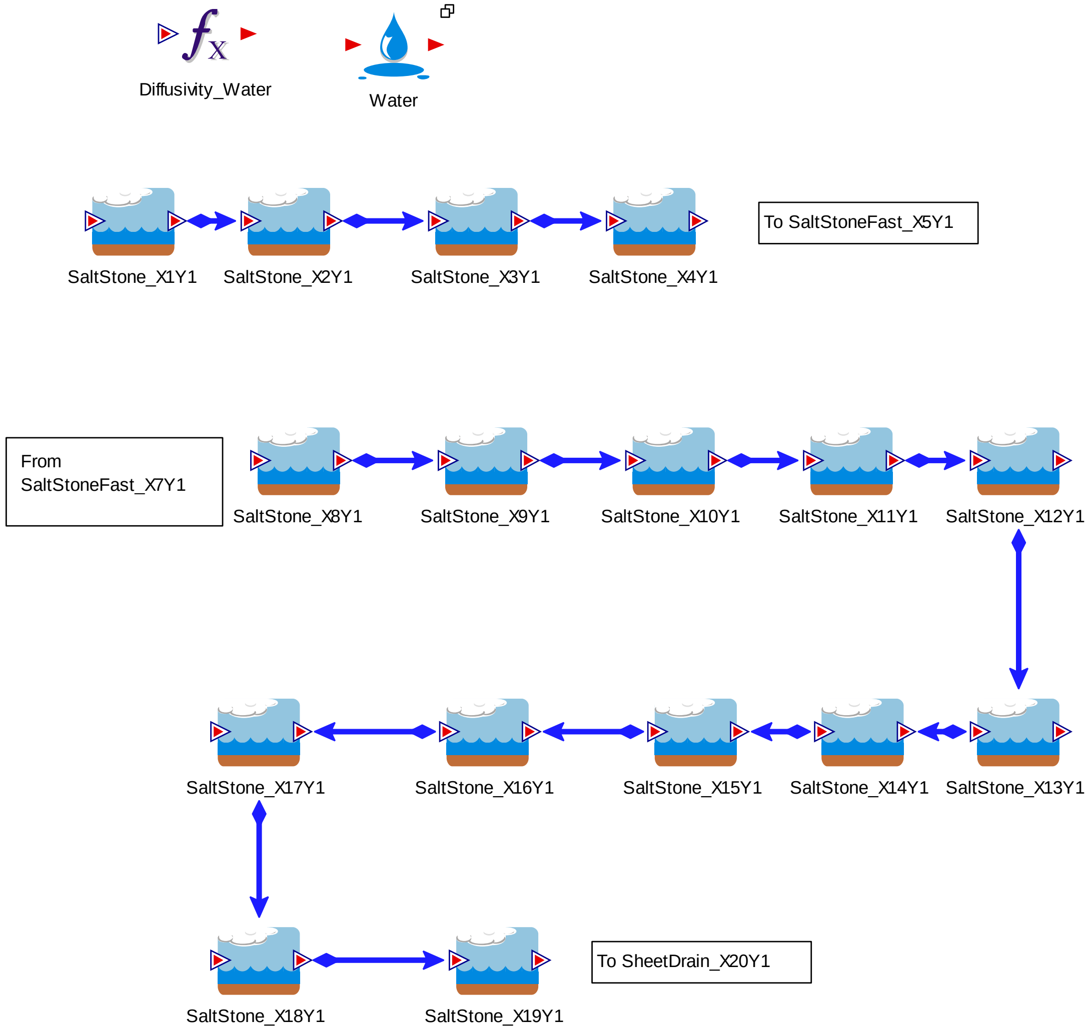

Figure 3.2-17: Contents of the *SheetDrain* Container

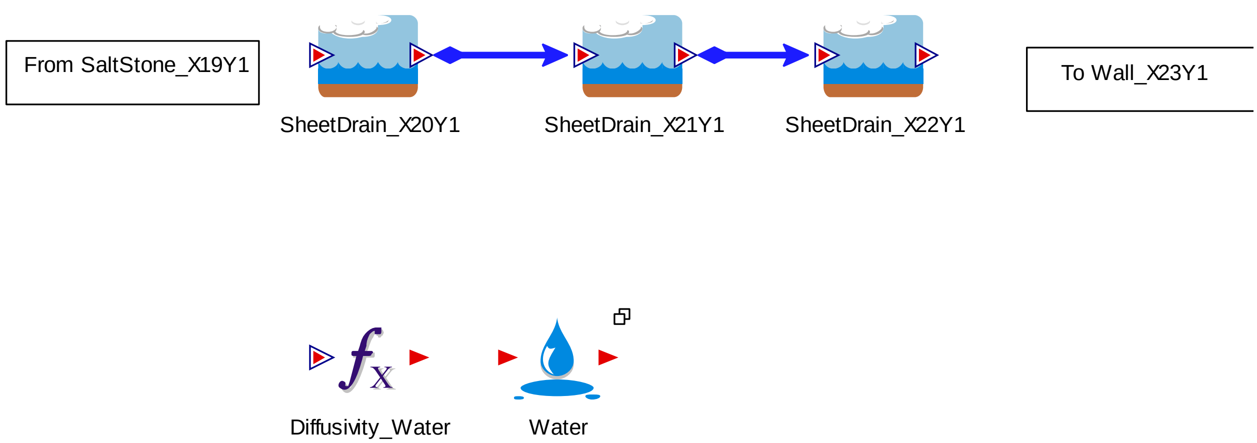

Figure 3.2-18: Contents of the *Wall* Container

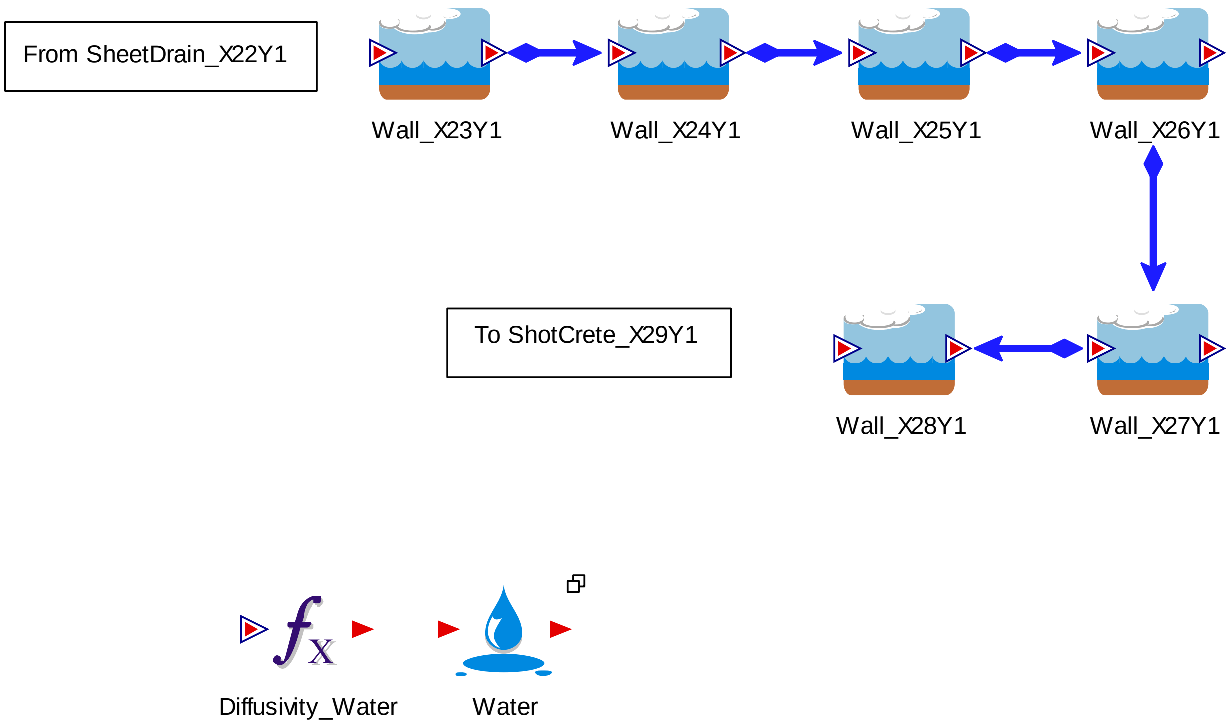

Figure 3.2-19: Contents of the *Shotcrete* Container

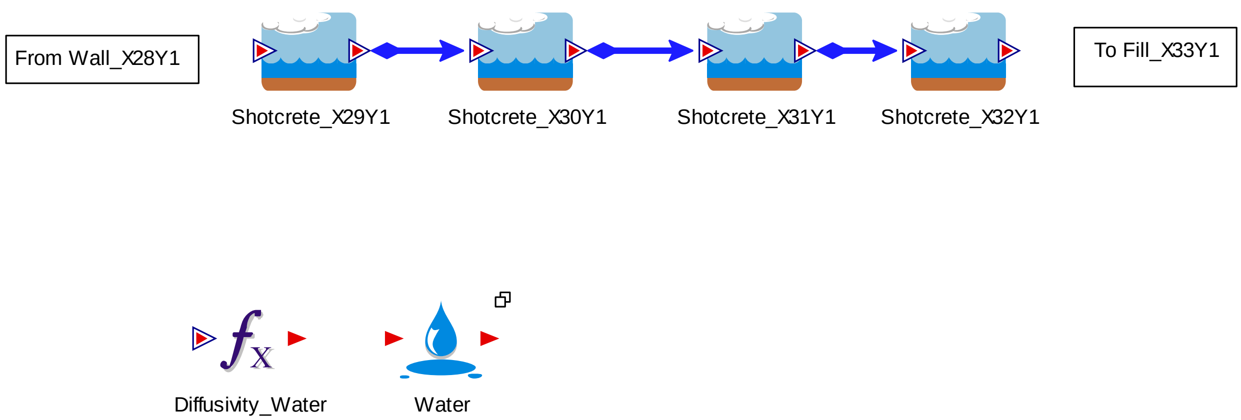

Figure 3.2-20: Contents of the *HDPE* Container

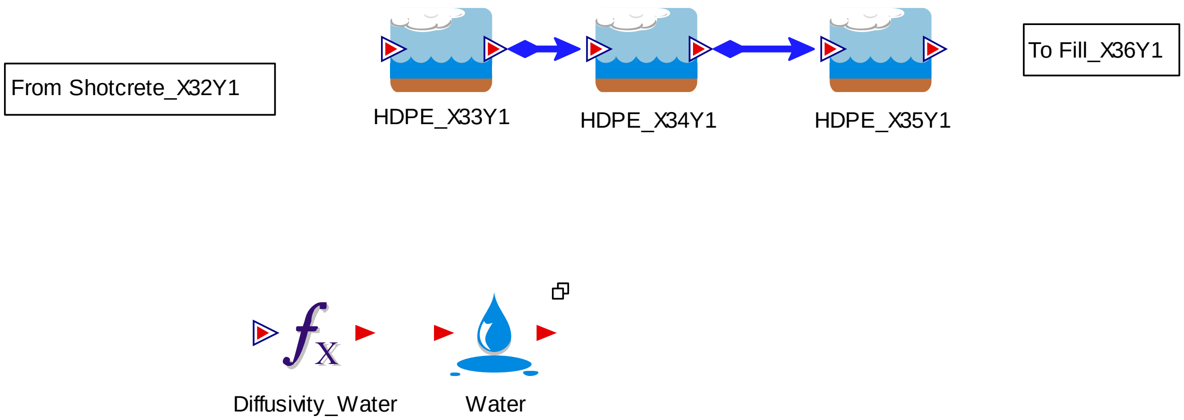

Figure 3.2-21: Contents of the *Fill* Container

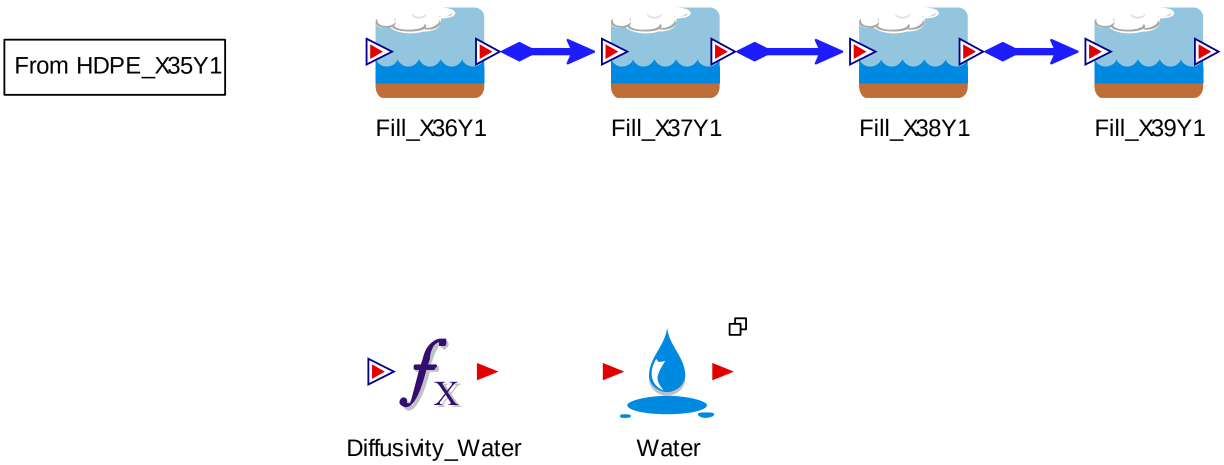

The containers *VaultFloor1*, *VaultFloor2*, *FastZone*, *SheetDrain*, and *WallFloor* contain 1-D strings of mixing cells that simulate vertical transport of radionuclides from *CellRow_20* through the floor and through the backfill. Note that the shotcrete cells in *CellRow_20* release their mass to either the wall floor cells or the backfill depending on the change in the vertical velocity at the shotcrete and floor boundaries. The walls are similarly evaluated. The cell structure for *VaultFloor1* and *VaultFloor2* is shown in Figure 3.2-22.

Figure 3.2-22: Contents of the *VaultFloor1* and *VaultFloor2* Containers

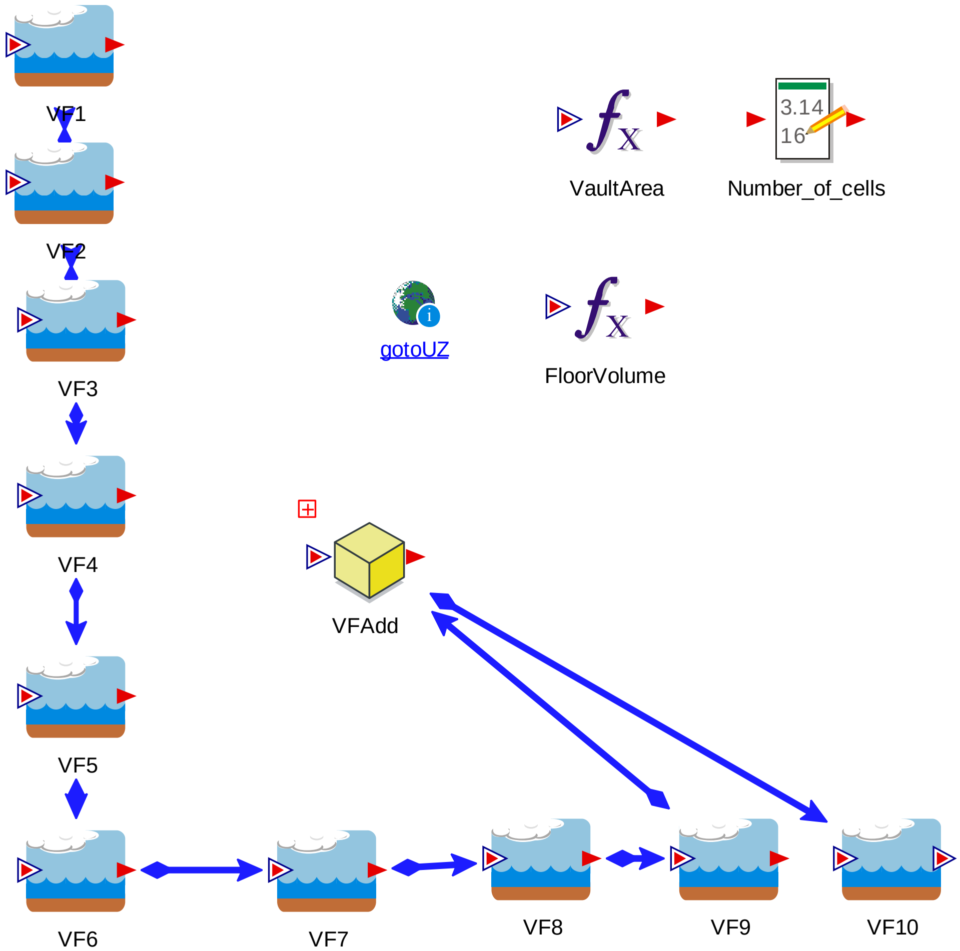

The container *VFAdd* contains a second set of 10 cells that brings the string to 20 cells. The containers for cells used to simulate transport through the floor segments under the fast flow zone (*FastZone*) and the sheet drain (*SheetDrain*) are similar. The container *WallFloor* includes two sets of cell pathways (Figure 3.2-23). The first set represents the floor under the wall. The second set represents alternate pathway through backfill that a fraction of the mass moving vertically through the wall (shotcrete) can use to bypass the floor when horizontal flow dominates at the wall floor interface. The fraction is based on the ratio of the vertical component of Darcy velocity in the floor below the wall (shotcrete) to the vertically averaged vertical component of Darcy velocity in the wall (shotcrete). Note that the data element *benchmarkingaid* which could be used to increase the length of the pathway is set to one (i.e., it is not used).

Figure 3.2-23: Contents of the *WallFloor* Container

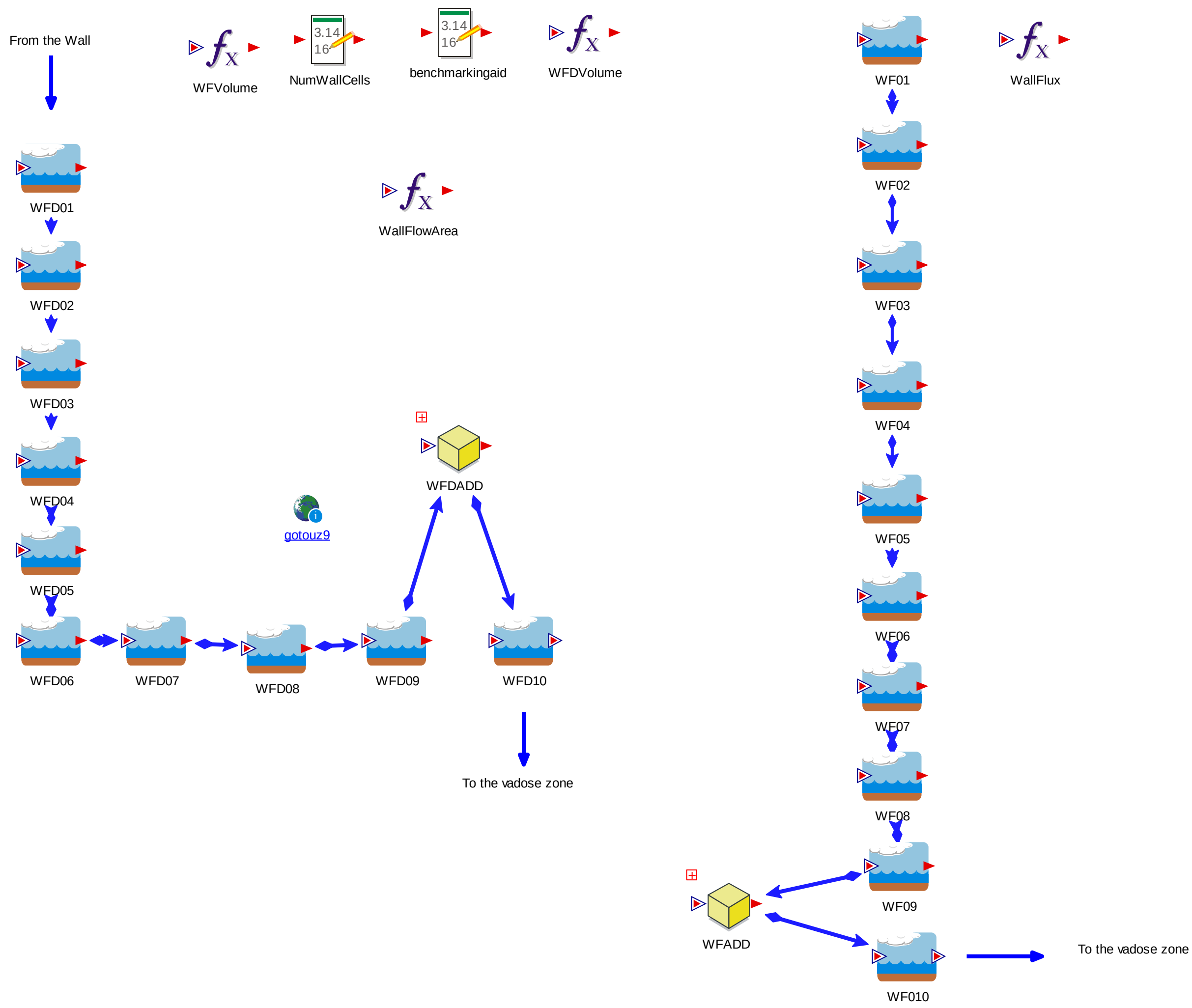

3.2.2 Unsaturated Zone

The unsaturated zone is simulated using a set of 10 or 20 cell pathway elements linked in series (see Figures 3.2-24 and 3.2-25). The unsaturated zone beneath Vault 1 is represented by 10 cells and the unsaturated zone beneath Vault 4 and the FDCs are represented by 20 cells. Either number of cells produces acceptable results as shown in the benchmarking analysis. The *MassToSaturatedZone* integrator element is used as a source term to the saturated zone pipe models. The benchmarking container contains time history elements that compare PORFLOW engineered barrier releases to releases from the present analysis. It should be noted that the time history comparisons are valid for Cases A (Base Case), C, and Alternative Sensitivity Case K, only. In addition, the time history comparisons are only valid when the *UnitInventory_Switch* is set to one (the source term for each element is set to 1 curie).

Figure 3.2-24: GoldSim Cell Pathway Elements Used to Simulate the Unsaturated Zone under Vault 1

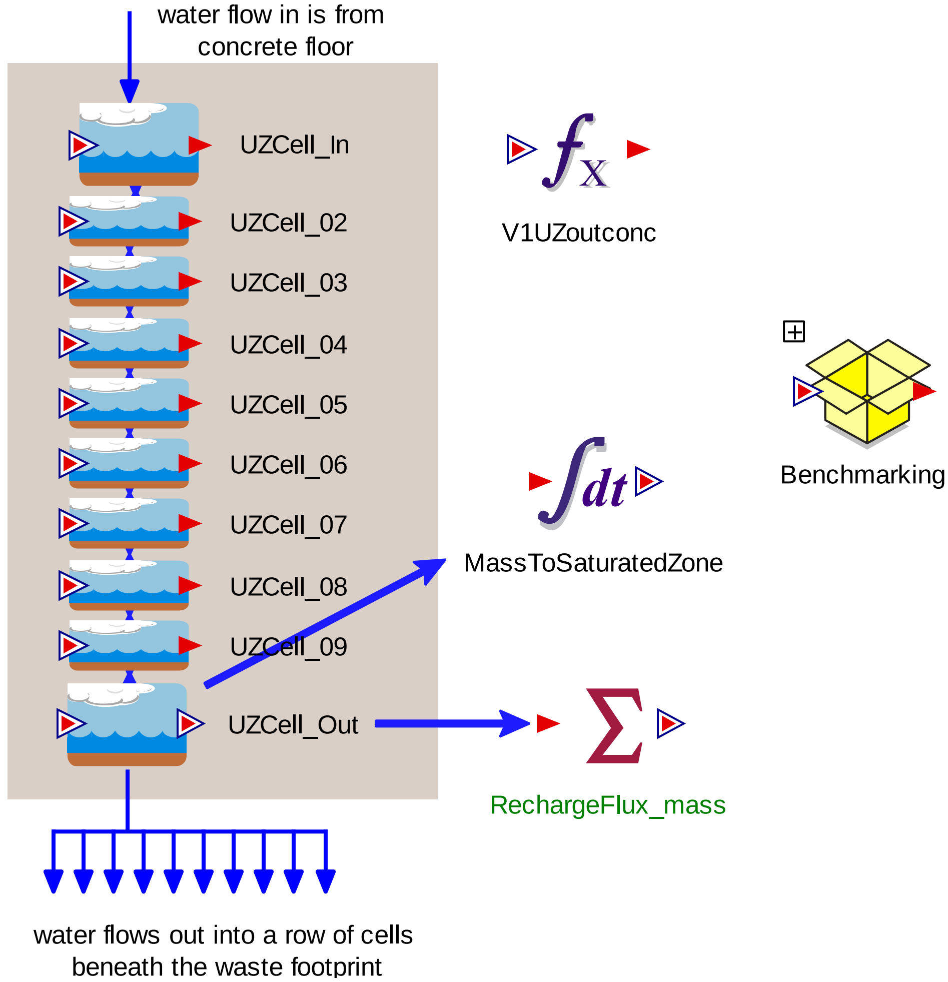

Figure 3.2-25: GoldSim Cell Pathway Elements Used to Simulate the Unsaturated Zone under Vault 4 and the FDCs

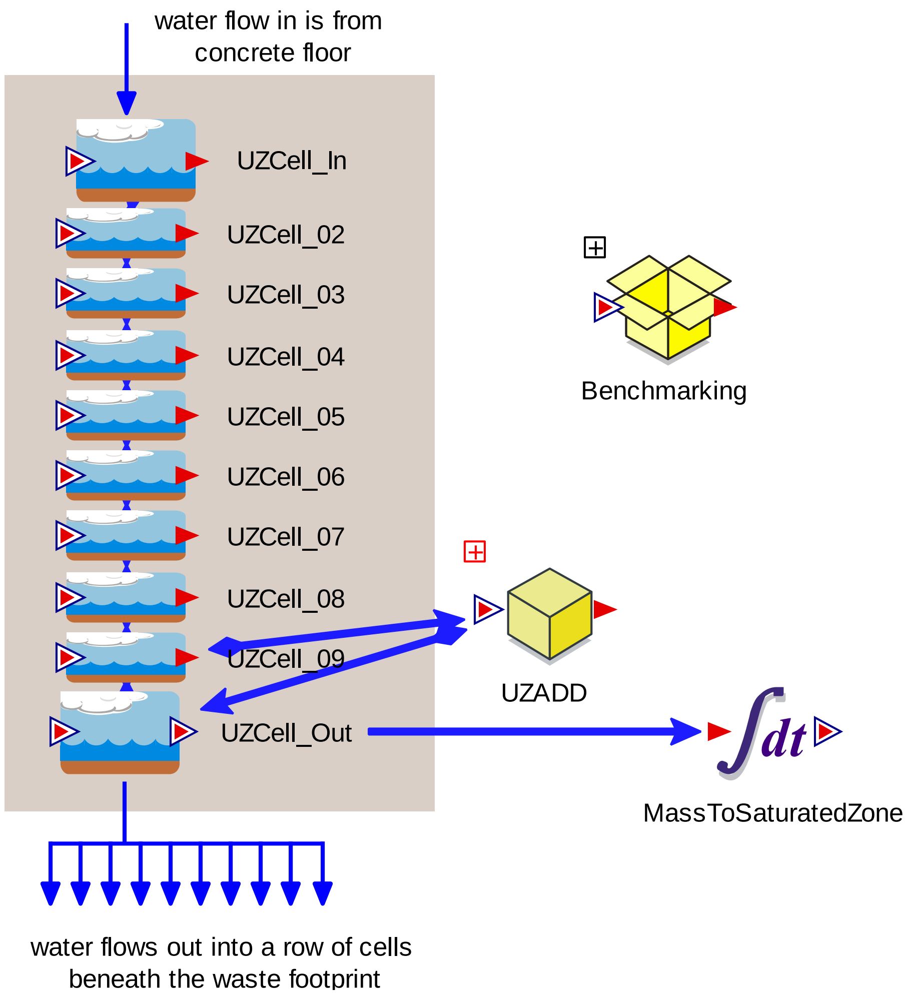

3.2.3 Saturated Zone

The saturated zone as simulated in the SDF GoldSim model is divided into two segments. The first segment is a series of cells representing the saturated zone beneath the footprint of the disposal unit structure. This segment is used to generate input to a cell representing the saturated zone just beyond the disposal unit, which is used to define concentrations for the Intruder analysis. The second segment is a pipe element representing transport from the disposal unit through the saturated zone to the 100-meter boundary.

3.2.3.1 Footprint Cells

The footprint cells represent the saturated zone found beneath the disposal unit footprint. A set of 10 cell pathway elements connected in series is used to approximate this zone (Figure 3.2-26). One-tenth of the mass released by the unsaturated zone cell *UZCell_Out* (Figures 3.2-24 and 3.2-25) is assigned to each of the footprint cells. The footprint cells are linked together in series (Figure 3.2-26) and a single volumetric flux rate defines the outflow from one cell to the next one. Note that because the volumetric water flux from *UZCell_Out* to

each footprint cell is not explicitly added to the outflow term for each footprint cell, GoldSim will indicate that there is a flow imbalance for these cells. This approximation assumes that the flow from the unsaturated zone is implicit to the volumetric flow rate approximation used for the footprint cell outflows. The outflow from *Footprint_Out* is used as input to a single cell used to generate the concentrations at 1-meter for the Intruder analysis.

Figure 3.2-26: GoldSim Cell Pathway Elements Used to Simulate the Saturated Zone under the Disposal Unit Footprint

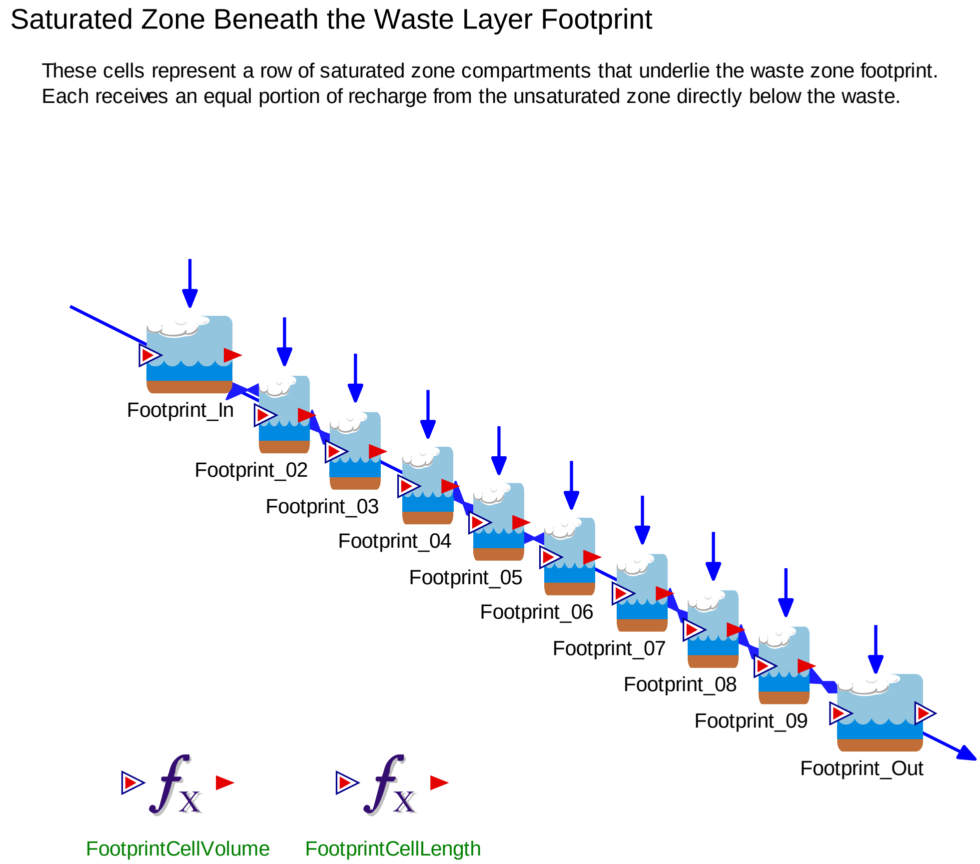

3.2.3.2 Saturated Zone Pipe Pathway Element

The total mass released over time from the cell pathway element *UZ_Out* as found in the *MassToSaturatedZone* integrator element is used as a source term to the pipe element *NearWellPipe* (Figure 3.2-27). The source is applied to the total width of the disposal unit (only half of the width is modeled) at the upgradient end of the pipe as shown in the pipe pathway properties element input screen (Figure 3.2-28).

Figure 3.2-27: GoldSim Cell Pathway and Pipe Elements Used to Simulate the Saturated Zone Transport

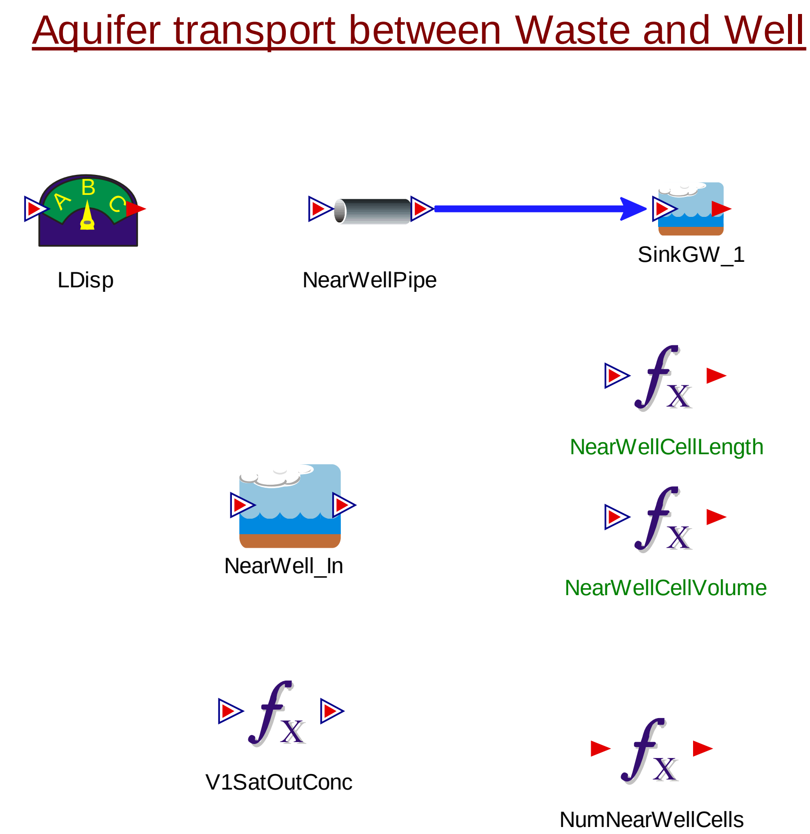

Figure 3.2-28: GoldSim Pipe Pathway Properties

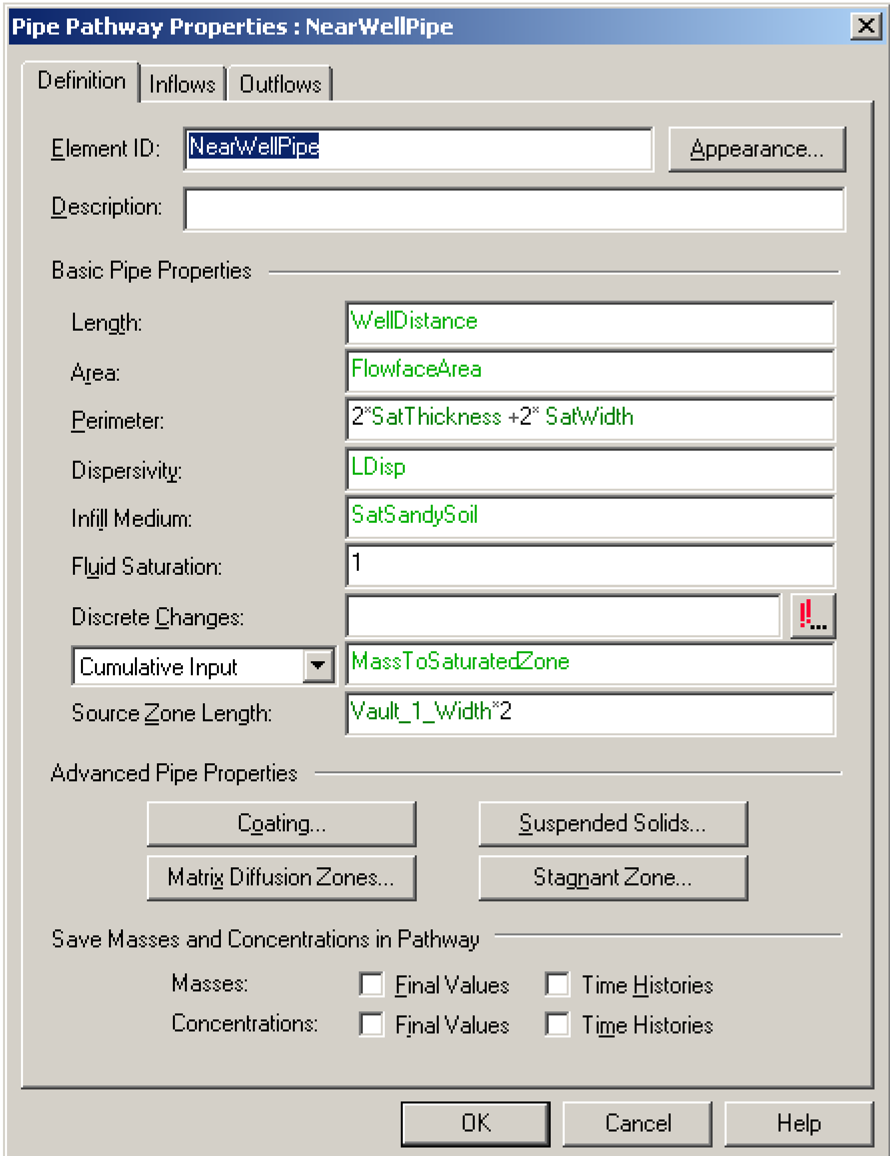

3.3 Advective Transport

The SDF GoldSim model solves for transport of dissolved radionuclides within the engineered barrier (the disposal unit structure) and the natural barrier (the unsaturated zone and saturated zone). The governing equation for advective-dispersive transport of a dissolved species in a unidirectional flow field can be written as follows:

$$\frac{\partial(\varphi RC)}{\partial t} = D\frac{\partial^2 C}{\partial l^2} - v\frac{\partial C}{\partial l} - \varphi R\lambda C \qquad (3.3\text{-}1)$$

where:

C = solute concentration (m/L^3)

R = retardation coefficient

φ = effective porosity

t = time (T)

D = hydrodynamic dispersion coefficient ($v\alpha + \varphi D_{eff}$ (L^2/T))

D_{eff} = effective diffusion coefficient (D_m/τ (L^2/T))

D_m = molecular (free water) diffusion coefficient

τ = tortuosity

v = Darcy velocity (L/T)

α = dispersivity (L)

λ = decay coefficient (T^{-1})

and

l = transport pathway coordinate (L)

The first term on the right hand side of Equation 3.3-1 represents the dispersive term and the second term the advective term. The hydrodynamic dispersion coefficient, D, can be broken down into two terms, the mechanical dispersion term, $v\alpha$, which is a function of flow, and a molecular diffusion term, φD_{eff}. The third term on the right hand side represents decay in a simplistic mode (without consideration of decay chains). The term on the left hand side of the equation is the storage or accumulation term.

The SDF GoldSim model simulates advective–dispersive transport in the saturated zone. In the engineered barrier, downward advection and the horizontal component of molecular diffusion are explicitly simulated. The flow rates, used in the SDF GoldSim model, are derived from results of the SDF PORFLOW simulations. For flow through the disposal unit structure and unsaturated zone (where simulated) spatially averaged velocities from PORFLOW flow runs are used directly. In the saturated zone the timing of concentration breakthrough curve peaks generated by PORFLOW (for a conservative tracer) and the stream trace lengths are used to determine the flow velocities along the stream traces.

3.4 Mechanical Dispersion

The SDF GoldSim model uses GoldSim pipe pathway elements to represent 1-D advective-transport pathways from the disposal units to the 100-meter boundary as depicted in Figures 3.1-2 through 3.1-5. The longitudinal dispersivity use in the pipe pathway elements is 10 meters, the same as used in the SDF PORFLOW simulations. Although the pipe pathway elements represent 1-D pathways, GoldSim allows the influence of transverse dispersion, both horizontal and vertical to be superimposed on the derived concentrations by using the plume function described in Section 3.1.4. The plume function generates a dilution factor that approximately accounts for the transverse dispersion. The transverse and vertical dispersivities used in the SDF GoldSim model are both 1.0 meter, the same values used in the SDF PORFLOW model.

3.5 Adsorption

Adsorption is a chemically controlled process that can inhibit the transport of dissolved species in the SDF GoldSim model. Adsorption is element specific, and is modeled as a linear process in the SDF GoldSim model with K_ds describing the ratio of the concentration in water to the mass of the species absorbed to the aquifer or cementitious material. The element specific K_d values for adsorption are allowed to change during a simulation based on changes in the chemical environment (Region II Reducing (middle reducing), Oxidizing Region II (middle oxidizing), or Oxidizing Region III (old oxidizing)). The chemical environment is determined by the number of pore volumes of water that has passed through a zone such as the saltstone grout or wall. The adsorption process is defined by linear isotherms. The K_ds used in the Base Case through E of the SDF GoldSim model, are taken from the Table 4.2-18 of the SDF PA. [SRS-CWDA-2009-00017]

For Alternative Sensitivity Case K, the K_ds for several elements have been updated as discussed in Section 4.5.1. In addition, the Tc-99 K_ds for the saltstone, floor, and wall K_ds have been replaced by shrinking core model time dependent functions where the K_ds vary depending on the degree of oxidized material in those zones. [SRR-CWDA-2011-00044, RAI PA-8]

The time dependent functions used in Alternative Sensitivity Case K PORFLOW runs and repeated in the SDF GoldSim model are based on the analytical approach of *The Role of Oxygen Diffusion in the Release of Technetium from Reducing Cementitious Waste Forms*. [ISBN: 1-55899-189-1] The results of this analysis provide an effective Tc-99 sorption coefficient reflecting varying oxidation through time. The derived sorption coefficient can then be used in a conventional liquid phase only PORFLOW simulation, thus implicitly accounting for both gas and liquid phase oxygen transport in fractured cementitious materials. The basis of the time dependent functions, as described in SRR-CWDA-2011-00044, RAI PA-8, is as follows.

Oxidation is assumed to occur as multiple 1-D moving fronts across the reducing material, emanating from multiple exposure faces. Fractions of oxidized and reduced material may be denoted by x_{Ox} and x_{Re}, respectively, such that

$$x_{Ox} + x_{\mathrm{Re}} = 1 \qquad \text{(Eq. 3.4-1)}$$

The total mass kilogram per mole *(M)* of a species in a porous medium with sorption is

$$M = Vnc + V(1-n)\rho_s c_s \qquad \text{(Eq. 3.4-2)}$$

where:

V	=	volume (cm^3 or mL)
n	=	porosity (%)
ρ_s	=	density (g/mL)
c	=	liquid concentration (mol/mL)
c_s	=	solid concentration (mol/mL)

For linear sorption:

$$c_s = K_d c \quad \text{(Eq. 3.4-3)}$$

where:

K_d = sorption coefficient

Equation 6 becomes:

$$\begin{aligned} M &= Vnc + V(1-n)\rho_s K_d c \\ &= Vnc\left[1 + \frac{(1-n)\rho_s K_d}{n}\right] \\ &= VncR \end{aligned} \quad \text{(Eq. 3.4-4)}$$

The retardation factor R is defined by:

$$R = 1 + \frac{(1-n)\rho_s K_d}{n} \quad \text{(Eq. 3.4-5)}$$

Therefore, the total species mass in the oxidized and reduced regions is:

$$VncR = x_{Ox} VncR_{Ox} + x_{\mathrm{Re}} VncR_{\mathrm{Re}} \quad \text{(Eq. 3.4-6)}$$

Where the liquid concentration has been assumed to be in equilibrium between the oxidized and reduced regions and R is the effective retardation for the composite of oxidized and reduced material. Equation 3.4-6 simplifies to:

$$R = x_{Ox} R_{Ox} + x_{\mathrm{Re}} R_{\mathrm{Re}} \quad \text{(Eq. 3.4-7)}$$

The composite sorption coefficient is derived as:

$$\begin{aligned} R - 1 &= x_{Ox} R_{Ox} + x_{\mathrm{Re}} R_{\mathrm{Re}} - (x_{Ox} + x_{\mathrm{Re}}) \\ \frac{(1-n)\rho_s K_d}{n} &= x_{Ox} \frac{(1-n)\rho_s K_{d,Ox}}{n} + x_{\mathrm{Re}} \frac{(1-n)\rho_s K_{d,\mathrm{Re}}}{n} \\ K_d &= x_{Ox} K_{d,Ox} + x_{\mathrm{Re}} K_{d,\mathrm{Re}} \end{aligned} \quad \text{(Eq. 3.4-8)}$$

As discussed in SRR-CWDA-2011-00044, a change in fracture spacing over time associated with the degradation of cementitious material can be described by the equation:

$$\log_{10}(B) = \begin{cases} \infty & t \le t_{0\%} \\ \dfrac{\log_{10}(B_{100\%}) - \log_{10}(B_{0\%})}{t_{100\%} - t_{0\%}}\left(t - t_{0\%}\right) + \log_{10}(B_{0\%}) & t_{0\%} < t < t_{100\%} \\ \log_{10}(BK_{100\%}) & t \ge t_{100\%} \end{cases} \quad \text{(Eq. 3.4-9)}$$

where:

B = fracture spacing

t = time

(Subscripts refer to degree of physical degradation)

Decreasing the fracture spacing increases the number of fractures, thus increasing the surface area of exposed surfaces on the saltstone. Counting both left and right boundaries, the number of exposure faces N for a material zone of dimension W (transverse to cracking) is:

$$N = 2\frac{W}{B} \quad \text{(Eq. 3.4-10)}$$

The intact matrix between exposure faces is assumed to have sufficiently low permeability that oxygen transport is by diffusion only within the matrix. Fractures are assumed to air-filled, except for thin liquid films on each exposure face, such that the concentration of dissolved oxygen is held constant at its saturation value (1.06 meq e-/L) at each face. The oxidation process is then independent of the flow through fractures (i.e., the system flow model). The oxidation front advances at a rate defined by the differential equation (ISBN: 1-55899-189-1):

$$r_{Ox}\rho_b \frac{d\delta}{dt} = \frac{nD_e c_{Ox}}{\delta} \quad \text{(Eq. 3.4-11)}$$

where:

r_{Ox} = reduction capacity of solid (meq e-/g)

ρ_b = bulk density of solid (g/mL)

δ = distance of oxidation front from the exposure face (cm)

t = time (s)

n = porosity (%)

D_e = effective diffusion coefficient (cm^2/s)

c_{Ox} = is the dissolved oxygen concentration at the exposure face (meq e-/mL)

The reduction capacity, as defined in the E_h-pH pore volume transitions discussion (above), is conservatively set to 0.206 meq e-/g. For the intact matrix, a constant diffusion coefficient of 1.0E-07cm^2/s is applied. The analytic solution to determine the oxidation front position from Equation 3.4-11 is:

$$\delta(t) = \left[\frac{2nD_e c_{Ox}}{r_{Ox}\rho_b} t \right]^{1/2} \quad \text{(Eq. 3.4-12)}$$

For exposure faces created at different discrete times, the cumulative oxidation thickness is the convolution:

$$\delta_T = N_1 \cdot \delta(t-\tau_1) + (N_2 - N_1) \cdot \delta(t-\tau_2) + (N_3 - N_2) \cdot \delta(t-\tau_3) + \quad \text{(Eq. 3.4-13)}$$

where N_i = total exposure faces through time τ_i. Equation 3.4-14 assumes that each new fracture exposes fresh material and each oxidation front advances independent of others. The fraction of material oxidized becomes:

$$x_{Ox} = \min\left[\frac{\delta_T}{W}, 1 \right] \quad \text{(Eq. 3.4-14)}$$

The effective sorption coefficient can then be determined from Equation 3.4-8. Assuming the log-linear fracture-spacing relationship given by Equation 3.4-9, RAI Figure PA-8.5 illustrates the resulting homogenized technetium K_d values for cementitious materials. For saltstone, this assumes $t_{0\%}$ = 5 year, $t_{100\%}$ = 10,000 year, $B_{0\%}$ = 10 meter, $B_{100\%}$ = 0.1 meter, $K_{d,Ox}$ = 10 mL/g, and $K_{d,Re}$ = 1,000 mL/g.

Figure 3.5-1: Effective Sorption Coefficients for Technetium in Partially Oxidized Cementitious Materials

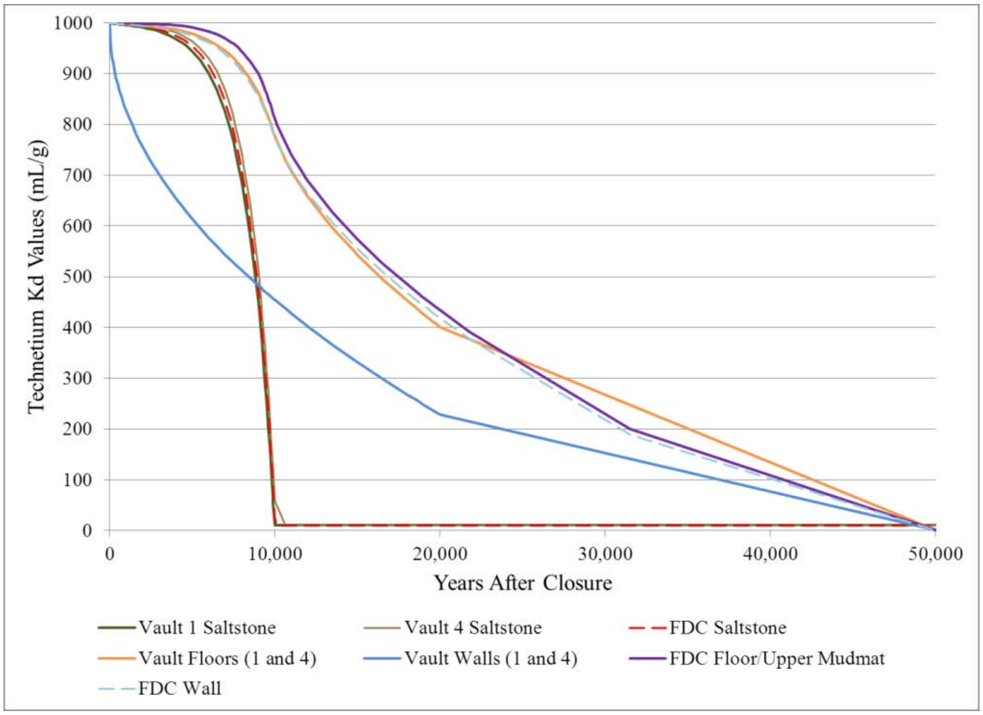

From SRR-CWDA-2011-00044, Rev. 1, Figure PA-8.5

Further discussion and numerical analysis of the shrinking core model is provided in SRR-CWDA-2011-00044 and SRNL-L4321-2011-00004.

4.0 TRANSPORT MODEL INPUTS

This section presents the input data used in the SDF GoldSim model. The organization of this section follows the organizational scheme used in the SDF GoldSim model.

4.1 General Inputs

The General Input Container in the SDF GoldSim model contains 1) commonly used constants, 2) the species list, and basic species data such as half-lives, 3) the reference fluid element and its basic properties such as solubilities, and 4) the input data controlling the temporal changes in transport parameters. The commonly used constants are not discussed in this section.

4.1.1 Species

The species evaluated in the SDF GoldSim model are listed in Table 4.1-1 along with their atomic weights, half-lives, daughter products and the daughter product stoichiometry.

Table 4.1-1: SDF GoldSim Model Species List

Species ID	Atomic Weight	Half-Life (yr)	Radioactive	Daughter 1 (Stoichiometry)	Daughter 2 (Stoichiometry)
Ac-227	227	2.18E+01	Y	N/A	N/A
Al-26	26	7.17E+05	Y	N/A	N/A
Am-241	241	4.32E+02	Y	Np-237 (1)	N/A
Am-242m	242	1.41E+02	Y	Pu-242 (0.173)	Pu-238 (0.827)
Am-243	243	7.37E+03	Y	Pu-239 (1)	N/A
C-14	14	5.70E+03	Y	N/A	N/A
Cf-249	249	3.51E+02	Y	Cm-245 (1)	N/A
Cf-251	251	8.98E+02	Y	Cm-247 (1)	N/A
Cl-36	36	3.01E+05	Y	N/A	N/A
Cm-243	243	2.91E+01	Y	Pu-239 (1)	N/A
Cm-244	244	1.81E+01	Y	Pu-240 (1)	N/A
Cm-245	245	8.50E+03	Y	Pu-241 (1)	N/A
Cm-246	246	4.76E+03	Y	Pu-242 (1)	N/A
Cm-247	247	1.56E+07	Y	Am-243 (1)	N/A
Cm-248	248	3.48E+05	Y	Pu-244 (1)	N/A
Co-60	60	5.27E+00	Y	N/A	N/A
Cs-135	135	2.30E+06	Y	N/A	N/A
Cs-137	137	3.00E+01	Y	N/A	N/A
Eu-152	152	1.35E+01	Y	Gd-152 (0.721)	N/A
Eu-154	154	8.59E+00	Y	N/A	N/A
Gd-152	152	1.08E+14	Y	N/A	N/A
H-3	3	1.23E+01	Y	N/A	N/A
I-129	129	1.57E+07	Y	N/A	N/A
K-40	40	1.25E+09	Y	N/A	N/A
Mo-93	93	4.00E+03	Y	Nb-93m (1)	N/A
Nb-93m	93	1.61E+01	Y	N/A	N/A
Nb-94	94	2.03E+04	Y	N/A	N/A
Ni-59	59	7.60E+04	Y	N/A	N/A
Ni-63	63	1.00E+02	Y	N/A	N/A
Np-237	237	2.14E+06	Y	U-233 (1)	N/A

Table 4.1-1: SDF GoldSim Model Species List (Continued)

Species ID	Atomic Weight	Half-Life (yr)	Radioactive	Daughter 1 (Stoichiometry)	Daughter 2 (Stoichiometry)
Pa-231	231	3.28E+04	Y	Ac-227 (1)	N/A
Pb-210	210	2.22E+01	Y	N/A	N/A
Pd-107	107	6.50E+06	Y	N/A	N/A
Pt-193	193	5.00E+01	Y	N/A	N/A
Pu-238	238	8.77E+01	Y	U-234 (1)	N/A
Pu-239	239	2.41E+04	Y	U-235 (1)	N/A
Pu-240	240	6.56E+03	Y	U-236 (1)	N/A
Pu-241	241	1.43E+01	Y	Am-241 (1)	N/A
Pu-242	242	3.75E+05	Y	U-238 (1)	N/A
Pu-244	244	8.00E+07	Y	Pu-240 (1)	N/A
Ra-226	226	1.60E+03	Y	Rn-222 (1)	N/A
Ra-228	228	5.75E+00	Y	N/A	N/A
Rn-222	222	1.05E-02	Y	Pb-210	N/A
Se-79	79	2.95E+05	Y	N/A	N/A
Sm-151	151	9.00E+01	Y	N/A	N/A
Sn-126	126	2.30E+05	Y	N/A	N/A
Sr-90	90	2.89E+01	Y	N/A	N/A
Tc-99	99	2.11E+05	Y	N/A	N/A
Th-229	229	7.34E+03	Y	N/A	N/A
Th-230	230	7.54E+04	Y	Ra-226 (1)	N/A
Th-232	232	1.41E+10	Y	Ra-228 (1)	N/A
U-232	232	6.89E+01	Y	N/A	N/A
U-233	233	1.59E+05	Y	Th-229 (1)	N/A
U-234	234	2.46E+05	Y	Th-230 (1)	N/A
U-235	235	7.04E+08	Y	Pa-231 (1)	N/A
U-236	236	2.34E+07	Y	Th-232 (1)	N/A
U-238	238	4.47E+09	Y	U-234 (1)	N/A
Zr-93	93	1.53E+06	Y	Nb-93m (1)	N/A

N/A = Not Applicable

4.1.2 Reference Fluid (Water)

There are two initial reference fluid (water) elements, one for Vaults 1 and 4 in the main model, and one for the sub model. Clones of these elements can be found in each container containing a string or strings of mixing-cells defining zones above the disposal unit floor. Each cloned reference fluid (water) elements can be assigned a different diffusion coefficient. In the SDF GoldSim model, the diffusion coefficients vary by the engineered barrier component.

4.1.3 Chronology

As an abstraction of the SDF PORFLOW model, much of the time-variant data is taken directly from the PORFLOW input data or from the SDF PORFLOW model outputs. Probably the most important time-variant data taken from the SDF PORFLOW model are the spatially averaged flow rates associated with different parts of the disposal unit structure.

For Cases A (Base Case) through E, there are 44 PORFLOW transition times for flow rate changes, implemented in the SDF GoldSim model. For Alternative Sensitivity Case K, there

are 59 PORFLOW transition times for flow rate changes. The transition times for flow rate changes are listed in Table 4.1-2. Transition times for changes in K_d values are explicitly solved for in the model.

Table 4.1-2: PORFLOW Time Periods by Configuration

Time Periods	Cases A-E (years)	Case K (years)	Time Periods (years)	Cases A-E (years)	Case K (years)
TI1	50	50	TI31	6,500	6,000
TI2	100	100	TI32	7,000	6,500
TI3	150	150	TI33	7,500	7,000
TI4	200	200	TI34	8,000	7,500
TI5	250	250	TI35	8,500	8,000
TI6	300	300	TI36	9,000	8,500
TI7	350	350	TI37	9,500	9,000
TI8	400	400	TI38	10,000	9,200
TI9	450	450	TI39	11,000	9,400
TI10	500	500	TI40	12,000	9,500
TI11	600	600	TI41	15,000	9,600
TI12	700	700	TI42	20,000	9,700
TI13	800	800	TI43	50,000	9,800
TI14	900	900	TI44	1.00E+07	9,900
TI15	1,000	1,000	TI45	N/A	10,000
TI16	1,200	1,200	TI46	N/A	11,000
TI17	1,400	1,400	TI47	N/A	12,000
TI18	1,600	1,600	TI48	N/A	13,500
TI19	1,800	1,800	TI49	N/A	15,000
TI20	2,000	2,000	TI50	N/A	16,500
TI21	2,300	2,300	TI51	N/A	18,000
TI22	2,600	2,600	TI52	N/A	18,800
TI23	2,900	2,900	TI53	N/A	18,900
TI24	3,200	3,200	TI54	N/A	19,013
TI25	3,600	3,500	TI55	N/A	19,500
TI26	4,000	3,600	TI56	N/A	19,700
TI27	4,500	4,000	TI57	N/A	20,000
TI28	5,000	4,500	TI58	N/A	50,000
TI29	5,500	5,000	TI59	N/A	100,000
TI30	6,000	5,500			

N/A = Not Applicable

4.2 SDF Engineered Barrier Inputs

The SDF source inputs for the disposal units include the inventories and geometries for Vault 1, Vault 4, and the FDCs. Additional information described in this section for the disposal unit components includes the diffusion coefficient values, and the disposal unit, configuration statistics. Material based properties such as K_ds, porosities, and bulk densities are described later in a separate section (Section 4.5).

4.2.1 Inventory

Note that except for Alternative Sensitivity Case K values, the inventory input section of the SDF GoldSim Model Version 3.002 has not been updated from the prior version described in the SDF PA.

4.2.1.1 SDF Inventory Deterministic Values

The development of the waste inventory in the SDF disposal units at time of closure is provided in *Estimated Inventory for the Saltstone Disposal Facility* (SRNS-J2100-2008-00004). Tables 4.2-1 through 4.2-3 provide the estimated radionuclide inventory in Vault 1, Vault 4, and the FDCs, respectively. In the SDF GoldSim model, the inventories provided in Tables 4.2-1 are doubled to account for the potential filling of the three empty cells in Vault 1. The FDC inventories presented in Table 4.2-3 are inventories per FDC. The total inventory for the FDCs would be 64 times those values. The uncertainty and variability associated with these values are presented in Section 4.2.1.2. All radionuclides have been pre-decayed to October 1, 2030 (expected date of SDF closure).

Table 4.2-1: Vault 1 Projected Radionuclide Inventory at Closure

Radionuclide	Projected Inventory at Closure (Ci)	Radionuclide	Projected Inventory at Closure (Ci)	Radionuclide	Projected Inventory at Closure (Ci)
Am-241	4.70E-04	Np-237	4.50E-03	Sn-126	1.00E+00
Ba-137m	4.10E+00	Pd-107	1.90E-03	Sr-90	6.90E-03
C-14	1.30E+00	Pt-193	3.70E-01	Tc-99	1.10E+02
Cl-36	7.60E-04	Pu-238	7.80E-03	Te-125m	3.80E-02
Co-60	8.20E-05	Pu-239	1.20E-02	Th-229	3.00E-01
Cs-137	4.30E+00	Pu-240	1.20E-02	Th-230	4.10E-01
Eu-152	1.80E-03	Pu-241	9.80E-03	U-233	2.80E-01
Eu-154	2.30E-04	Pu-242	9.00E-04	U-234	2.80E-01
H-3	6.10E+00	Ra-226	6.40E-07	U-235	3.20E-03
I-129	1.10E-01	Rh-106	1.50E-10	U-236	3.20E-03
K-40	7.60E-04	Ru-106	1.50E-10	U-238	7.40E-03
Nb-93m	2.50E-01	Sb-125	1.60E-01	Y-90	6.90E-03
Nb-94	2.50E-03	Sb-126	1.40E-01	Zr-93	2.50E-01
Ni-59	3.50E-02	Sb-126m	1.00E+00	**Total**	**1.30E+02**
Ni-63	7.80E-01	Se-79	3.00E-01		

From Table 3.3-1 from SRR-CWDA-2009-00017

Note: Due to the smaller number of radionuclides analyzed during disposal operations, the Vault 1 inventory contains fewer radionuclides than the other disposal units.

Table 4.2-2: Vault 4 Projected Radionuclide Inventory at Closure

Radionuclide	Projected Inventory at Closure (Ci)	Radionuclide	Projected Inventory at Closure (Ci)	Radionuclide	Projected Inventory at Closure (Ci)
Ac-227	1.60E-05	Eu-154	1.20E+01	Rh-106	9.10E-07
Al-26	3.40E-01	Eu-155	6.80E-01	Ru-106	9.10E-07
Am-241	1.30E+02	H-3	2.60E+02	Sb-125	5.70E+00
Am-242m	6.70E-02	I-129	2.80E-01	Sb-126	9.00E-01
Am-243	1.80E+00	K-40	3.00E-03	Sb-126m	6.40E+00
Ba-137m	2.80E+05	Na-22	1.50E-01	Se-79	4.60E+01
Bk-249	1.80E-28	Nb-93m	8.40E+00	Sm-151	4.20E+01
C-14	2.70E+01	Nb-94	8.70E-02	Sn-126	6.40E+00
Ce-144	1.80E-09	Ni-59	4.00E-01	Sr-90	2.40E+05
Cf-249	6.50E-13	Ni-63	2.20E+01	Tc-99	5.80E+02
Cf-251	1.20E+00	Np-237	6.10E-01	Te-125m	1.40E+00
Cf-252	1.80E-18	Pa-231	9.30E-05	Th-229	2.50E+01
Cl-36	3.00E-03	Pd-107	5.00E-02	Th-230	7.50E+00
Cm-242	6.70E-02	Pm-147	4.10E-01	Th-232	3.20E-04
Cm-243	2.10E-01	Pr-144	1.80E-09	U-232	4.40E-02
Cm-244	1.30E+02	Pt-193	1.00E+01	U-233	2.40E+01
Cm-245	9.20E-01	Pu-238	9.10E+03	U-234	2.60E+01
Cm-247	3.90E-06	Pu-239	3.80E+02	U-235	4.70E-01
Cm-248	1.20E-13	Pu-240	1.20E+02	U-236	7.70E-01
Co-60	4.60E-01	Pu-241	2.40E+03	U-238	5.90E-01
Cs-134	5.20E-01	Pu-242	8.10E-01	Y-90	2.40E+05
Cs-135	5.40E+00	Pu-244	1.60E-02	Zr-93	8.40E+00
Cs-137	3.00E+05	Ra-226	4.10E+00	**Total**	**1.10E+06**
Eu-152	9.70E-02	Ra-228	1.60E-06		

From Table 3.3-3 from SRR-CWDA-2009-00017

Table 4.2-3: FDC Projected Radionuclide Inventory (per FDC) at Closure

Radionuclide	Projected Inventory per Disposal Unit at Closure (Ci)	Radionuclide	Projected Inventory per Disposal Unit at Closure (Ci)	Radionuclide	Projected Inventory per Disposal Unit at Closure (Ci)
Ac-227	1.70E-07	Eu-154	1.80E+00	Rh-106	1.20E-06
Al-26	1.90E-01	Eu-155	1.30E-01	Ru-106	1.20E-06
Am-241	1.40E+00	H-3	3.00E+01	Sb-125	2.40E-01
Am-242m	5.90E-04	I-129	3.80E-01	Sb-126	1.20E+00
Am-243	3.70E-02	K-40	4.20E-04	Sb-126m	8.20E+00
Ba-137m	2.20E+01	Na-22	6.90E-02	Se-79	1.40E+00
Bk-249	1.80E-28	Nb-93m	3.70E-01	Sm-151	5.90E+01
C-14	2.00E+00	Nb-94	3.80E-03	Sn-126	8.20E+00
Ce-144	3.60E-10	Ni-59	8.40E-02	Sr-90	3.70E+01
Cf-249	6.70E-13	Ni-63	2.40E+00	Tc-99	5.40E+02
Cf-251	2.30E-14	Np-237	5.00E-02	Te-125m	5.80E-02
Cf-252	1.80E-18	Pa-231	9.80E-07	Th-229	3.90E-02
Cl-36	4.20E-04	Pd-107	5.60E-03	Th-230	1.90E-01
Cm-242	6.30E-19	Pm-147	7.70E-02	Th-232	1.40E-03
Cm-243	2.10E-04	Pr-144	3.60E-10	U-232	3.10E-04
Cm-244	9.50E-01	Pt-193	1.10E+00	U-233	3.70E-02
Cm-245	2.40E-04	Pu-238	1.70E+02	U-234	1.30E-01
Cm-247	7.10E-14	Pu-239	1.50E+01	U-235	3.00E-03
Cm-248	7.40E-14	Pu-240	4.10E+00	U-236	1.60E-02
Co-60	5.40E-02	Pu-241	4.20E+01	U-238	1.00E-01
Cs-134	1.50E-05	Pu-242	3.90E-03	Y-90	3.70E+01
Cs-135	1.30E-04	Pu-244	1.60E-05	Zr-93	3.70E-01
Cs-137	2.30E+01	Ra-226	7.80E-07	**Total**	**1.00E+03**
Eu-152	9.80E-02	Ra-228	8.70E-05		

From Table 3.3-5 from SRR-CWDA-2009-00017

Several inventory changes were also made for Alternative Sensitivity Case K. [SRR-CWDA-2011-00044] The changes are as follows:

Vault 1:

- No change

Vault 4:

- Pu-238 (from 9,300 curie to 1,000 curie)
- U-234 (from 26 curie to 10 curie)
- Th-230 (from 7.5 curie to 0.01 curie)
- Ra-226 (from 4.1 curie to 0.001 curie)

FDCs

- Th-230 (from 0.19 curie to 1.3E-04 curie)
- Ra-226 (from 7.8E-7 curie to 1.3E-05 curie)

4.2.1.2 Disposal Unit Inventory Distribution Values

In the SDF GoldSim model, the uncertainty in the SDF inventory values is considered by species. The minimum, maximum, median, and statistical mean values for the log-normal distributions are presented in Table 4.2-4 The values presented in Table 4.2-4 are used as multipliers to the baseline inventories presented in Tables 4.2-1 through 4.2-3.

Table 4.2-4: Radionuclide Inventory Uncertainty in the SDF GoldSim Model

Radionuclide	Minimum	Maximum	Geometric Mean	Geometric Standard Deviation	Median	Statistical Mean
C-14	0.1	10	1.0	1.1	1.0	1.005
Cs-137	1.0	10	1.0	1.1	1.07	1.081
Pu-239	0.1	10	1.0	1.1	1.0	1.005
Sr-90	0.001	1	1.0	1.1	0.94	0.928
U-238	0.0001	10	1.0	1.1	1.0	1.005
All others	0.1	10	1.0	1.1	1.0	1.005

Note: The Vault 1 geometric standard deviation is incorrectly set to 1.0001 as noted in the PA Appendix I.

4.2.1.3 Waste Tank to FDC Sampling

There is an option available in the SDF GoldSim model, which allows for the sampling of both Tank and Disposal Unit order. The volume of water (with dissolved inventory mass) from the first of 51 waste tanks on the list is released into the first of 64 FDCs on the list until either the waste tank is empty or the FDC is full. When a waste tank is emptied or FDC filled, the next waste tank or FDC is chosen from the list and the release of salt solution continues. Each FDC is assumed to hold a volume of saltstone that is comprised of 1.5E+06 gallons of salt solution. [SRR-LWP-2010-00070 Section 3.5] Table 4.2-5 contain the inventories for the waste tank to FDC analysis. [SRNS-J2100-2008-00004] Note that where waste tank inventories listed in Table 4.2-5 are listed as 0.0 curies for all species, the assumption for that waste tank inventory is that it will be sent to Vault 4. In addition, there are two waste tanks, Tank 25 and Tank 41, for which a fraction of the salt solution is sent to Vault 4. The fraction of the Tank 25 salt solution sent to Vault 4 is 0.5 and the fraction of salt solution from Tank 41 is 0.75.

The processed waste (salt solution) volume to be sent to the FDCs is presented in Table 4.2-6. The source of the data is SRNS-J2100-2008-00004, *Supporting Document Estimated Closure Inventory for the Saltstone Disposal Facility*. The salt solution volumes are taken from the supernate section of the "Remaining Cells" sheet in SRNS-J2100-2008-00004 and multiplied by five. The factor of five is based on the desire to fill almost all the FDCs for this analysis. Approximately 62.4 of the 64 FDCs are filled. For waste tanks where it is assumed the whole inventory is to be sent to Vault 4, the salt solution volumes are set at zero. For tanks where a fraction of the inventory is sent to the FDCs and the remainder to Vault 4, the product of the fraction going to the FDC (1-f) and five times the supernate solution volume provides the salt solution volume distributed to the FDCs.

Table 4.2-5: Tank to Disposal Cell Inventory

Species	T1 (Ci)	T2 (Ci)	T3 (Ci)	T4 (Ci)	T5 (Ci)	T6 (Ci)	T7 (Ci)	T8 (Ci)
Ac-227	7.34E-08	7.43E-08	7.43E-08	3.44E-08	1.20E-08	2.00E-09	1.63E-07	8.55E-08
Al-26	4.03E-01	1.50E-01	1.52E-01	2.52E-03	3.60E-03	5.94E-04	4.58E-02	3.12E-01
Am-241	2.58E+00	9.42E-01	9.55E-01	1.52E-02	2.32E-02	3.83E-03	2.96E-01	2.01E+00
Am-242m	1.39E-03	5.07E-04	5.14E-04	8.18E-06	1.25E-05	2.06E-06	1.59E-04	1.08E-03
Am-243	7.05E-03	2.58E-03	2.61E-03	4.16E-05	6.35E-05	1.05E-05	8.09E-04	5.51E-03
C-14	1.22E+00	1.21E+00	1.21E+00	1.01E+00	2.01E-01	4.02E-02	3.10E+00	2.17E+00
Cf-249	1.46E-12	5.35E-13	5.42E-13	8.63E-15	1.32E-14	2.18E-15	1.68E-13	1.14E-12
Cf-251	5.01E-14	1.83E-14	1.86E-14	2.95E-16	4.51E-16	7.44E-17	5.75E-15	3.92E-14
Cl-36	0.00E+00	0.00E+00	0.00E+00	0.00E+00	0.00E+00	0.00E+00	0.00E+00	0.00E+00
Cm-243	7.73E-04	2.83E-04	2.87E-04	4.56E-06	6.97E-06	1.15E-06	8.87E-05	6.05E-04
Cm-244	4.60E+00	1.68E+00	1.70E+00	2.71E-02	4.14E-02	6.84E-03	5.28E-01	3.60E+00
Cm-245	5.06E-04	1.85E-04	1.88E-04	2.99E-06	4.57E-06	7.53E-07	5.81E-05	3.96E-04
Cm-246	0	0	0	0	0	0	0	0
Cm-247	1.49E-13	5.45E-14	5.52E-14	8.79E-16	1.34E-15	2.22E-16	1.71E-14	1.17E-13
Cm-248	1.55E-13	5.68E-14	5.75E-14	9.16E-16	1.40E-15	2.31E-16	1.78E-14	1.21E-13
Co-60	6.47E-01	6.38E-01	6.38E-01	5.90E-01	1.17E-01	2.35E-02	1.81E+00	1.27E+00
Cs-135	2.72E-04	9.95E-05	1.01E-04	1.60E-06	2.45E-06	4.04E-07	3.12E-05	2.13E-04
Cs-137	8.25E+01	3.03E+01	3.07E+01	4.95E-01	7.42E-01	1.22E-01	9.44E+00	6.44E+01
Eu-152	6.72E-01	2.46E-01	2.49E-01	3.96E-03	6.06E-03	9.99E-04	7.71E-02	5.26E-01
Eu-154	2.46E+01	8.99E+00	9.11E+00	1.45E-01	2.22E-01	3.65E-02	2.82E+00	1.92E+01
Gd-152	0	0	0	0	0	0	0	0
H-3	6.28E+01	6.20E+01	6.20E+01	5.73E+01	1.14E+01	7.59E+00	5.86E+02	8.95E+01
I-129	5.17E-01	1.89E-01	1.92E-01	3.05E-03	4.66E-03	7.68E-04	5.93E-02	4.04E-01
K-40	0.00E+00	0.00E+00	0.00E+00	0.00E+00	0.00E+00	0.00E+00	0.00E+00	0.00E+00
Mo-93	0	0	0	0	0	0	0	0
Nb-93m	0.00E+00	0.00E+00	0.00E+00	0.00E+00	0.00E+00	0.00E+00	0.00E+00	0.00E+00
Nb-94	2.20E-05	8.03E-06	8.14E-06	1.30E-07	1.98E-07	3.26E-08	2.52E-06	1.72E-05
Ni-59	7.54E-02	2.76E-02	2.79E-02	4.45E-04	6.80E-04	1.12E-04	8.65E-03	5.90E-02
Ni-63	1.57E+00	1.55E+00	1.55E+00	1.43E+00	2.85E-01	5.71E-02	4.40E+00	3.08E+00
Np-237	2.67E-03	2.64E-03	2.64E-03	2.36E-03	8.79E-04	4.74E-05	7.50E-03	3.26E-03
Pa-231	2.04E-07	2.06E-07	2.06E-07	9.54E-08	3.34E-08	5.55E-09	4.52E-07	2.37E-07
Pb-210	0	0	0	0	0	0	0	0
Pd-107	0.00E+00	0.00E+00	0.00E+00	0.00E+00	0.00E+00	0.00E+00	0.00E+00	0.00E+00
Pt-193	0.00E+00	0.00E+00	0.00E+00	0.00E+00	0.00E+00	0.00E+00	0.00E+00	0.00E+00
Pu-238	5.16E+00	5.60E+00	5.60E+00	4.04E-01	2.64E-01	0.00E+00	3.35E+00	4.08E+00
Pu-239	4.13E-01	4.24E-01	4.24E-01	2.13E-01	4.41E-02	6.10E-03	7.86E-01	8.95E-01
Pu-240	7.55E-02	7.45E-02	7.45E-02	4.60E-02	1.05E-02	2.12E-03	2.12E-01	2.11E-01
Pu-241	6.28E-01	6.19E-01	6.19E-01	3.49E-01	6.32E-02	2.13E-02	1.76E+00	1.80E+00
Pu-242	8.28E-05	8.16E-05	8.16E-05	9.47E-06	3.11E-06	4.17E-06	2.32E-04	2.66E-04
Pu-244	3.78E-07	3.73E-07	3.73E-07	4.33E-08	1.42E-08	1.91E-08	1.06E-06	1.21E-06
Ra-226	4.54E-08	4.48E-08	4.48E-08	3.63E-08	7.14E-09	1.87E-09	1.27E-07	9.86E-08
Ra-228	0.00E+00	0.00E+00	0.00E+00	0.00E+00	0.00E+00	0.00E+00	0.00E+00	0.00E+00
Rn-222	0	0	0	0	0	0	0	0
Se-79	2.87E+00	1.05E+00	1.07E+00	1.70E-02	2.59E-02	4.27E-03	3.30E-01	2.25E+00

Table 4.2-5: Tank to Disposal Cell Inventory (continued)

Species	T1 (Ci)	T2 (Ci)	T3 (Ci)	T4 (Ci)	T5 (Ci)	T6 (Ci)	T7 (Ci)	T8 (Ci)
Sm-151	1.39E+02	5.08E+01	5.15E+01	8.19E-01	1.25E+00	2.07E-01	1.59E+01	1.09E+02
Sn-126	1.45E+01	5.32E+00	5.39E+00	8.57E-02	1.31E-01	2.16E-02	1.67E+00	1.14E+01
Sr-90	1.26E+02	1.10E+02	1.10E+02	4.46E+00	3.65E-01	6.02E-02	4.64E+00	3.17E+01
Tc-99	1.07E+03	3.90E+02	3.95E+02	6.29E+00	9.61E+00	1.59E+00	1.22E+02	8.34E+02
Th-229	4.98E-03	4.91E-03	4.91E-03	4.39E-03	1.64E-03	8.83E-05	1.40E-02	6.07E-03
Th-230	8.48E-03	8.36E-03	8.36E-03	6.77E-03	1.33E-03	3.50E-04	2.38E-02	1.84E-02
Th-232	0.00E+00	0.00E+00	0.00E+00	0.00E+00	0.00E+00	0.00E+00	0.00E+00	0.00E+00
U-232	1.08E-04	1.06E-04	1.06E-04	8.13E-05	1.96E-05	5.13E-06	3.02E-04	1.03E-04
U-233	4.75E-03	4.69E-03	4.69E-03	4.19E-03	1.56E-03	8.42E-05	1.33E-02	5.80E-03
U-234	5.88E-03	5.80E-03	5.80E-03	4.69E-03	9.25E-04	2.43E-04	1.65E-02	1.28E-02
U-235	2.38E-04	2.41E-04	2.41E-04	1.12E-04	3.90E-05	6.49E-06	5.28E-04	2.77E-04
U-236	1.21E-04	1.19E-04	1.19E-04	9.59E-05	1.91E-05	4.97E-06	3.38E-04	2.61E-04
U-238	7.00E-03	7.05E-03	7.05E-03	4.75E-03	9.25E-04	2.43E-04	1.65E-02	1.28E-02
Zr-93	0.00E+00	0.00E+00	0.00E+00	0.00E+00	0.00E+00	0.00E+00	0.00E+00	0.00E+00
Species	**T9 (Ci)**	**T10 (Ci)**	**T11 (Ci)**	**T12 (Ci)**	**T13 (Ci)**	**T14 (Ci)**	**T15 (Ci)**	**T16 (Ci)**
Ac-227	3.48E-08	1.34E-08	1.28E-10	4.08E-09	7.57E-08	1.63E-08	2.30E-09	0.00E+00
Al-26	1.57E-01	1.14E-02	7.67E-05	1.13E-01	1.17E+00	1.19E-01	4.85E-04	0.00E+00
Am-241	9.88E-01	6.43E-02	4.94E-04	7.26E-01	7.57E+00	7.64E-01	0.00E+00	0.00E+00
Am-242m	5.32E-04	3.46E-05	2.66E-07	3.91E-04	4.08E-03	4.12E-04	0.00E+00	0.00E+00
Am-243	2.70E-03	1.76E-04	1.35E-06	1.99E-03	2.07E-02	2.09E-03	0.00E+00	0.00E+00
C-14	1.29E+00	4.83E-01	9.19E-02	9.61E-01	4.97E+00	4.19E-01	1.65E-02	0.00E+00
Cf-249	5.61E-13	3.65E-14	2.81E-16	4.13E-13	4.30E-12	4.34E-13	0.00E+00	0.00E+00
Cf-251	1.92E-14	1.25E-15	9.61E-18	1.41E-14	1.47E-13	1.49E-14	0.00E+00	0.00E+00
Cl-36	0.00E+00	0.00E+00	0.00E+00	0.00E+00	0.00E+00	0.00E+00	0.00E+00	0.00E+00
Cm-243	2.97E-04	1.93E-05	1.48E-07	2.18E-04	2.27E-03	2.29E-04	0.00E+00	0.00E+00
Cm-244	1.76E+00	1.15E-01	8.82E-04	1.30E+00	1.35E+01	1.36E+00	0.00E+00	0.00E+00
Cm-245	1.94E-04	1.26E-05	9.72E-08	1.43E-04	1.49E-03	1.50E-04	0.00E+00	0.00E+00
Cm-246	0	0	0	0	0	0	0	0
Cm-247	5.71E-14	3.72E-15	2.86E-17	4.20E-14	4.38E-13	4.42E-14	0.00E+00	0.00E+00
Cm-248	5.95E-14	3.88E-15	2.98E-17	4.38E-14	4.56E-13	4.61E-14	0.00E+00	0.00E+00
Co-60	6.83E-01	2.55E-01	5.38E-02	5.58E-01	2.91E+00	2.28E-01	0.00E+00	0.00E+00
Cs-135	1.04E-04	6.79E-06	5.22E-08	7.67E-05	7.99E-04	8.07E-05	0.00E+00	0.00E+00
Cs-137	3.18E+01	2.14E+00	1.58E-02	2.32E+01	2.42E+02	2.45E+01	2.86E-02	0.00E+00
Eu-152	2.58E-01	1.68E-02	1.29E-04	1.89E-01	1.97E+00	1.99E-01	0.00E+00	0.00E+00
Eu-154	9.43E+00	6.14E-01	4.72E-03	6.93E+00	7.22E+01	7.29E+00	0.00E+00	0.00E+00
Gd-152	0	0	0	0	0	0	0	0
H-3	6.63E+01	2.47E+01	5.22E+00	5.41E+01	2.82E+02	2.21E+01	0.00E+00	0.00E+00
I-129	1.98E-01	1.29E-02	9.92E-05	1.46E-01	1.52E+00	1.53E-01	0.00E+00	0.00E+00
K-40	0.00E+00	0.00E+00	0.00E+00	0.00E+00	0.00E+00	0.00E+00	0.00E+00	0.00E+00
Mo-93	0	0	0	0	0	0	0	0
Nb-93m	0.00E+00	0.00E+00	0.00E+00	0.00E+00	0.00E+00	0.00E+00	0.00E+00	0.00E+00
Nb-94	8.42E-06	5.48E-07	4.21E-09	6.19E-06	6.45E-05	6.52E-06	0.00E+00	0.00E+00
Ni-59	2.89E-02	1.88E-03	1.45E-05	2.13E-02	2.22E-01	2.24E-02	0.00E+00	0.00E+00
Ni-63	1.66E+00	6.18E-01	1.31E-01	1.35E+00	7.05E+00	5.53E-01	0.00E+00	0.00E+00
Np-237	3.05E-03	1.14E-03	8.19E-06	6.30E-04	1.30E-02	2.93E-03	0.00E+00	0.00E+00
Pa-231	9.68E-08	3.72E-08	3.56E-10	1.13E-08	2.10E-07	4.53E-08	6.40E-09	0.00E+00

Table 4.2-5: Tank to Disposal Cell Inventory (continued)

Species	T9 (Ci)	T10 (Ci)	T11 (Ci)	T12 (Ci)	T13 (Ci)	T14 (Ci)	T15 (Ci)	T16 (Ci)
Pb-210	0	0	0	0	0	0	0	0
Pd-107	0.00E+00	0.00E+00	0.00E+00	0.00E+00	0.00E+00	0.00E+00	0.00E+00	0.00E+00
Pt-193	0.00E+00	0.00E+00	0.00E+00	0.00E+00	0.00E+00	0.00E+00	0.00E+00	0.00E+00
Pu-238	9.20E+00	3.53E+00	4.75E-01	5.00E+00	2.04E+01	1.63E+00	5.95E-01	0.00E+00
Pu-239	2.79E-01	1.07E-01	4.81E-03	9.01E-02	5.62E-01	1.77E-01	1.98E-02	0.00E+00
Pu-240	5.46E-02	2.04E-02	3.02E-03	4.43E-02	2.32E-01	4.56E-02	0.00E+00	0.00E+00
Pu-241	8.61E-01	3.21E-01	1.55E-01	1.01E+00	3.67E+00	2.07E-01	0.00E+00	0.00E+00
Pu-242	3.62E-05	1.35E-05	6.43E-06	6.41E-05	1.54E-04	8.35E-06	0.00E+00	0.00E+00
Pu-244	1.65E-07	6.17E-08	2.94E-08	2.93E-07	7.04E-07	3.82E-08	0.00E+00	0.00E+00
Ra-226	6.42E-09	2.40E-09	6.71E-11	1.54E-09	2.74E-08	1.49E-09	0.00E+00	0.00E+00
Ra-228	9.86E-05	3.68E-05	2.54E-07	2.59E-04	4.20E-04	1.36E-04	0.00E+00	0.00E+00
Rn-222	0	0	0	0	0	0	0	0
Se-79	1.10E+00	7.18E-02	5.52E-04	8.11E-01	8.45E+00	8.53E-01	0.00E+00	0.00E+00
Sm-151	5.33E+01	3.47E+00	2.67E-02	3.92E+01	4.08E+02	4.12E+01	0.00E+00	0.00E+00
Sn-126	5.57E+00	3.63E-01	2.79E-03	4.10E+00	4.27E+01	4.31E+00	0.00E+00	0.00E+00
Sr-90	1.11E+02	3.86E+01	7.77E-03	1.78E+01	1.19E+02	3.51E+01	1.28E+01	0.00E+00
Tc-99	4.09E+02	2.66E+01	2.05E-01	3.01E+02	3.13E+03	3.16E+02	0.00E+00	0.00E+00
Th-229	1.57E-02	5.85E-03	2.82E-05	5.66E-03	6.68E-02	3.73E-03	0.00E+00	0.00E+00
Th-230	3.04E-03	1.14E-03	3.18E-05	7.29E-04	1.30E-02	7.04E-04	0.00E+00	0.00E+00
Th-232	9.86E-05	3.68E-05	2.54E-07	2.59E-04	4.20E-04	1.36E-04	0.00E+00	0.00E+00
U-232	1.90E-05	7.09E-06	0.00E+00	1.89E-06	8.09E-05	2.93E-05	0.00E+00	0.00E+00
U-233	1.50E-02	5.58E-03	2.69E-05	5.40E-03	6.37E-02	3.56E-03	0.00E+00	0.00E+00
U-234	2.11E-03	7.88E-04	2.21E-05	5.06E-04	8.99E-03	4.88E-04	0.00E+00	0.00E+00
U-235	1.13E-04	4.35E-05	4.16E-07	1.33E-05	2.46E-04	5.29E-05	7.48E-06	0.00E+00
U-236	2.18E-04	8.12E-05	3.41E-06	4.01E-05	9.27E-04	4.20E-05	0.00E+00	0.00E+00
U-238	1.92E-03	7.44E-04	7.72E-07	1.80E-04	2.87E-03	1.05E-03	1.68E-04	0.00E+00
Zr-93	0.00E+00	0.00E+00	0.00E+00	0.00E+00	0.00E+00	0.00E+00	0.00E+00	0.00E+00

Species	T17 (Ci)	T18 (Ci)	T19 (Ci)	T20 (Ci)	T21 (Ci)	T22 (Ci)	T23 (Ci)	T24 (Ci)
Ac-227	0	0	0	0	1.39E-07	0.00E+00	0.00E+00	0.00E+00
Al-26	0	0	0	0	1.69E-04	0.00E+00	0.00E+00	0.00E+00
Am-241	0	0	0	0	1.09E-03	0.00E+00	0.00E+00	0.00E+00
Am-242m	0	0	0	0	5.87E-07	0.00E+00	0.00E+00	0.00E+00
Am-243	0	0	0	0	2.99E-06	0.00E+00	0.00E+00	0.00E+00
C-14	0	0	0	0	7.36E+00	0.00E+00	0.00E+00	0.00E+00
Cf-249	0	0	0	0	6.20E-16	0.00E+00	0.00E+00	0.00E+00
Cf-251	0	0	0	0	2.12E-17	0.00E+00	0.00E+00	0.00E+00
Cl-36	0	0	0	0	0.00E+00	0.00E+00	0.00E+00	0.00E+00
Cm-243	0	0	0	0	3.28E-07	0.00E+00	0.00E+00	0.00E+00
Cm-244	0	0	0	0	1.95E-03	0.00E+00	0.00E+00	0.00E+00
Cm-245	0	0	0	0	2.15E-07	0.00E+00	0.00E+00	0.00E+00
Cm-246	0	0	0	0	0	0	0	0
Cm-247	0	0	0	0	6.31E-17	0.00E+00	0.00E+00	0.00E+00
Cm-248	0	0	0	0	6.58E-17	0.00E+00	0.00E+00	0.00E+00
Co-60	0	0	0	0	4.31E+00	0.00E+00	0.00E+00	0.00E+00
Cs-135	0	0	0	0	1.15E-07	0.00E+00	0.00E+00	0.00E+00

Table 4.2-5: Tank to Disposal Cell Inventory (continued)

Species	T17 (Ci)	T18 (Ci)	T19 (Ci)	T20 (Ci)	T21 (Ci)	T22 (Ci)	T23 (Ci)	T24 (Ci)
Cs-137	0	0	0	0	3.49E-02	0.00E+00	0.00E+00	0.00E+00
Eu-152	0	0	0	0	2.85E-04	0.00E+00	0.00E+00	0.00E+00
Eu-154	0	0	0	0	1.04E-02	0.00E+00	0.00E+00	0.00E+00
Gd-152	0	0	0	0	0	0	0	0
H-3	0	0	0	0	4.18E+02	0.00E+00	0.00E+00	0.00E+00
I-129	0	0	0	0	2.42E-03	0.00E+00	0.00E+00	0.00E+00
K-40	0	0	0	0	0.00E+00	0.00E+00	0.00E+00	0.00E+00
Mo-93	0	0	0	0	0	0	0	0
Nb-93m	0	0	0	0	0.00E+00	0.00E+00	0.00E+00	0.00E+00
Nb-94	0	0	0	0	9.30E-09	0.00E+00	0.00E+00	0.00E+00
Ni-59	0	0	0	0	3.19E-05	0.00E+00	0.00E+00	0.00E+00
Ni-63	0	0	0	0	1.05E+01	0.00E+00	0.00E+00	0.00E+00
Np-237	0	0	0	0	1.33E-02	0.00E+00	0.00E+00	0.00E+00
Pa-231	0	0	0	0	3.87E-07	0.00E+00	0.00E+00	0.00E+00
Pb-210	0	0	0	0	0	0	0	0
Pd-107	0	0	0	0	0.00E+00	0.00E+00	0.00E+00	0.00E+00
Pt-193	0	0	0	0	0.00E+00	0.00E+00	0.00E+00	0.00E+00
Pu-238	0	0	0	0	3.43E+01	0.00E+00	0.00E+00	0.00E+00
Pu-239	0	0	0	0	5.13E-01	0.00E+00	0.00E+00	0.00E+00
Pu-240	0	0	0	0	1.74E-01	0.00E+00	0.00E+00	0.00E+00
Pu-241	0	0	0	0	2.98E+00	0.00E+00	0.00E+00	0.00E+00
Pu-242	0	0	0	0	1.95E-05	0.00E+00	0.00E+00	0.00E+00
Pu-244	0	0	0	0	8.93E-08	0.00E+00	0.00E+00	0.00E+00
Ra-226	0	0	0	0	8.67E-08	0.00E+00	0.00E+00	0.00E+00
Ra-228	0	0	0	0	1.14E-06	0.00E+00	0.00E+00	0.00E+00
Rn-222	0	0	0	0	0	0	0	0
Se-79	0	0	0	0	1.22E-03	0.00E+00	0.00E+00	0.00E+00
Sm-151	0	0	0	0	5.88E-02	0.00E+00	0.00E+00	0.00E+00
Sn-126	0	0	0	0	6.16E-03	0.00E+00	0.00E+00	0.00E+00
Sr-90	0	0	0	0	1.71E-02	0.00E+00	0.00E+00	0.00E+00
Tc-99	0	0	0	0	4.52E-01	0.00E+00	0.00E+00	0.00E+00
Th-229	0	0	0	0	2.80E-02	0.00E+00	0.00E+00	0.00E+00
Th-230	0	0	0	0	4.11E-02	0.00E+00	0.00E+00	0.00E+00
Th-232	0	0	0	0	1.14E-06	0.00E+00	0.00E+00	0.00E+00
U-232	0	0	0	0	0.00E+00	0.00E+00	0.00E+00	0.00E+00
U-233	0	0	0	0	2.67E-02	0.00E+00	0.00E+00	0.00E+00
U-234	0	0	0	0	2.85E-02	0.00E+00	0.00E+00	0.00E+00
U-235	0	0	0	0	4.52E-04	0.00E+00	0.00E+00	0.00E+00
U-236	0	0	0	0	5.23E-03	0.00E+00	0.00E+00	0.00E+00
U-238	0	0	0	0	2.68E-03	0.00E+00	0.00E+00	0.00E+00
Zr-93	0	0	0	0	0.00E+00	0.00E+00	0.00E+00	0.00E+00
Species	**T25 (Ci)**	**T26 (Ci)**	**T27 (Ci)**	**T28 (Ci)**	**T29 (Ci)**	**T30 (Ci)**	**T31 (Ci)**	**T32 (Ci)**
Ac-227	1.76E-08	1.56E-06	7.69E-07	1.05E-06	8.18E-08	1.37E-07	8.34E-08	8.17E-08
Al-26	3.70E-03	3.00E-01	1.58E-01	2.58E-01	8.10E-02	1.54E+00	6.29E-01	5.16E-01
Am-241	0.00E+00	1.93E+00	9.65E-01	1.62E+00	4.78E-01	9.90E+00	4.01E+00	3.32E+00

Table 4.2-5: Tank to Disposal Cell Inventory (continued)

Species	T25 (Ci)	T26 (Ci)	T27 (Ci)	T28 (Ci)	T29 (Ci)	T30 (Ci)	T31 (Ci)	T32 (Ci)
Am-242m	0.00E+00	1.04E-03	5.19E-04	8.72E-04	2.57E-04	5.33E-03	2.16E-03	1.79E-03
Am-243	0.00E+00	5.29E-03	2.64E-03	4.43E-03	1.31E-03	2.71E-02	1.10E-02	9.10E-03
C-14	1.26E-01	5.03E+00	2.64E+00	3.53E+00	3.46E+00	5.78E+00	3.33E+00	3.63E+00
Cf-249	0.00E+00	1.10E-12	5.48E-13	9.20E-13	2.72E-13	5.63E-12	2.28E-12	1.89E-12
Cf-251	0.00E+00	3.76E-14	1.88E-14	3.15E-14	9.29E-15	1.93E-13	7.79E-14	6.46E-14
Cl-36	0.00E+00	0.00E+00	0.00E+00	0.00E+00	0.00E+00	0.00E+00	0.00E+00	0.00E+00
Cm-243	0.00E+00	5.80E-04	2.90E-04	4.86E-04	1.43E-04	2.97E-03	1.20E-03	9.98E-04
Cm-244	0.00E+00	3.45E+00	1.72E+00	2.89E+00	8.53E-01	1.77E+01	7.15E+00	5.94E+00
Cm-245	0.00E+00	3.80E-04	1.90E-04	3.19E-04	9.40E-05	1.95E-03	7.88E-04	6.54E-04
Cm-246	0	0	0	0	0	0	0	0
Cm-247	0.00E+00	1.12E-13	5.58E-14	9.37E-14	2.76E-14	5.73E-13	2.32E-13	1.92E-13
Cm-248	0.00E+00	1.17E-13	5.81E-14	9.76E-14	2.88E-14	5.97E-13	2.42E-13	2.00E-13
Co-60	0.00E+00	2.95E+00	1.38E+00	1.93E+00	1.89E+00	3.35E+00	1.80E+00	2.12E+00
Cs-135	4.01E-05	2.04E-04	1.02E-04	1.71E-04	5.05E-05	1.05E-03	4.23E-04	3.51E-04
Cs-137	1.26E+01	6.17E+01	3.13E+01	5.22E+01	1.57E+01	3.16E+02	1.29E+02	1.06E+02
Eu-152	0.00E+00	5.04E-01	2.52E-01	4.23E-01	1.25E-01	2.58E+00	1.05E+00	8.67E-01
Eu-154	0.00E+00	1.84E+01	9.21E+00	1.55E+01	4.56E+00	9.45E+01	3.82E+01	3.17E+01
Gd-152	0	0	0	0	0	0	0	0
H-3	0.00E+00	2.17E+02	1.02E+02	1.87E+02	1.83E+02	3.25E+02	1.74E+02	2.06E+02
I-129	0.00E+00	3.88E-01	1.94E-01	3.25E-01	9.59E-02	1.99E+00	8.04E-01	6.67E-01
K-40	0.00E+00	0.00E+00	0.00E+00	0.00E+00	0.00E+00	0.00E+00	0.00E+00	0.00E+00
Mo-93	0	0	0	0	0	0	0	0
Nb-93m	0.00E+00	0.00E+00	0.00E+00	0.00E+00	0.00E+00	0.00E+00	0.00E+00	0.00E+00
Nb-94	0.00E+00	1.65E-05	8.22E-06	1.38E-05	4.07E-06	8.44E-05	3.42E-05	2.83E-05
Ni-59	0.00E+00	5.66E-02	2.82E-02	4.74E-02	1.40E-02	2.90E-01	1.17E-01	9.73E-02
Ni-63	0.00E+00	7.15E+00	3.36E+00	4.68E+00	4.58E+00	8.13E+00	4.36E+00	5.16E+00
Np-237	0.00E+00	8.80E-04	4.14E-04	5.77E-04	8.44E-03	6.80E-03	8.03E-03	4.31E-03
Pa-231	4.88E-08	4.32E-06	2.14E-06	2.92E-06	2.27E-07	3.80E-07	2.32E-07	2.27E-07
Pb-210	0	0	0	0	0	0	0	0
Pd-107	0.00E+00	0.00E+00	0.00E+00	0.00E+00	0.00E+00	0.00E+00	0.00E+00	0.00E+00
Pt-193	0.00E+00	0.00E+00	0.00E+00	0.00E+00	0.00E+00	0.00E+00	0.00E+00	0.00E+00
Pu-238	4.54E+00	7.93E+02	3.82E+02	5.28E+02	2.17E+01	1.02E+03	2.21E+01	6.48E+02
Pu-239	1.51E-01	1.24E+02	5.87E+01	8.17E+01	6.46E-01	9.20E+00	6.63E-01	5.79E+00
Pu-240	0.00E+00	2.78E+01	1.31E+01	1.82E+01	1.51E-01	6.78E+00	1.44E-01	4.30E+00
Pu-241	0.00E+00	5.85E+02	2.75E+02	3.84E+02	2.38E+00	4.17E+02	2.26E+00	2.64E+02

Table 4.2-5: Tank to Disposal Cell Inventory (continued)

Species	T25 (Ci)	T26 (Ci)	T27 (Ci)	T28 (Ci)	T29 (Ci)	T30 (Ci)	T31 (Ci)	T32 (Ci)
Pu-242	0.00E+00	5.53E-03	2.60E-03	3.63E-03	1.00E-04	1.43E-02	9.52E-05	9.06E-03
Pu-244	0.00E+00	2.53E-05	1.19E-05	1.66E-05	4.57E-07	6.53E-05	4.35E-07	4.14E-05
Ra-226	0.00E+00	5.19E-14	2.44E-14	3.40E-14	1.78E-08	8.89E-08	1.69E-08	5.64E-08
Ra-228	0.00E+00	0.00E+00	0.00E+00	0.00E+00	2.72E-04	0.00E+00	2.59E-04	0.00E+00
Rn-222	0	0	0	0	0	0	0	0
Se-79	0.00E+00	2.16E+00	1.08E+00	1.81E+00	5.33E-01	1.11E+01	4.47E+00	3.71E+00
Sm-151	0.00E+00	1.04E+02	5.20E+01	8.74E+01	2.58E+01	5.34E+02	2.16E+02	1.79E+02
Sn-126	0.00E+00	1.09E+01	5.44E+00	9.14E+00	2.70E+00	5.59E+01	2.26E+01	1.88E+01
Sr-90	9.77E+01	3.04E+01	2.24E+02	2.09E+02	1.90E+02	2.01E+02	2.67E+02	5.23E+01
Tc-99	0.00E+00	8.00E+02	3.99E+02	6.70E+02	1.98E+02	4.10E+03	1.66E+03	1.38E+03
Th-229	0.00E+00	5.61E-09	2.64E-09	3.67E-09	4.33E-02	1.27E-02	4.13E-02	8.03E-03
Th-230	0.00E+00	2.46E-08	1.16E-08	1.61E-08	8.41E-03	4.21E-02	8.01E-03	2.67E-02
Th-232	0.00E+00	0.00E+00	0.00E+00	0.00E+00	2.72E-04	0.00E+00	2.59E-04	0.00E+00
U-232	0.00E+00	1.72E-03	8.08E-04	1.13E-03	5.25E-05	0.00E+00	5.00E-05	0.00E+00
U-233	0.00E+00	5.35E-09	2.51E-09	3.50E-09	4.14E-02	1.21E-02	3.94E-02	7.67E-03
U-234	0.00E+00	1.71E-08	8.02E-09	1.12E-08	5.84E-03	2.92E-02	5.55E-03	1.85E-02
U-235	5.70E-05	5.05E-03	2.50E-03	3.42E-03	2.66E-04	4.45E-04	2.71E-04	2.65E-04
U-236	0.00E+00	6.52E-04	3.07E-04	4.27E-04	6.02E-04	6.56E-03	5.73E-04	4.16E-03
U-238	1.28E-03	6.06E-01	2.88E-01	4.00E-01	4.25E-03	7.90E-04	4.44E-03	1.25E-04
Zr-93	0.00E+00	0.00E+00	0.00E+00	0.00E+00	0.00E+00	0.00E+00	0.00E+00	0.00E+00

Species	T33 (Ci)	T34 (Ci)	T35 (Ci)	T36 (Ci)	T37 (Ci)	T38 (Ci)	T39 (Ci)	T40 (Ci)
Ac-227	6.21E-06	1.22E-06	2.05E-07	8.65E-08	1.14E-07	5.51E-07	4.22E-07	8.31E-07
Al-26	2.76E-01	8.14E-01	4.01E-01	1.16E+00	6.89E-01	2.38E-02	7.35E-02	2.85E-03
Am-241	1.77E+00	5.24E+00	2.58E+00	7.41E+00	4.40E+00	1.17E-01	4.74E-01	1.84E-02
Am-242m	9.51E-04	2.82E-03	1.39E-03	3.99E-03	2.37E-03	6.31E-05	2.55E-04	9.89E-06
Am-243	4.83E-03	1.43E-02	7.07E-03	2.03E-02	1.20E-02	3.21E-04	1.30E-03	5.03E-05
C-14	6.11E+00	6.49E+00	7.67E+00	3.74E+00	3.87E+00	4.07E+00	5.43E+00	2.47E+00
Cf-249	1.00E-12	2.98E-12	1.47E-12	4.21E-12	2.50E-12	6.66E-14	2.69E-13	1.04E-14
Cf-251	3.43E-14	1.02E-13	5.02E-14	1.44E-13	8.56E-14	2.28E-15	9.21E-15	3.57E-16
Cl-36	0.00E+00	0.00E+00	0.00E+00	0.00E+00	0.00E+00	0.00E+00	0.00E+00	0.00E+00
Cm-243	5.30E-04	1.57E-03	7.76E-04	2.23E-03	1.32E-03	3.52E-05	1.42E-04	5.52E-06
Cm-244	3.15E+00	9.35E+00	4.61E+00	1.32E+01	7.86E+00	2.09E-01	8.46E-01	3.28E-02
Cm-245	3.47E-04	1.03E-03	5.08E-04	1.46E-03	8.65E-04	2.31E-05	9.32E-05	3.61E-06
Cm-246	0	0	0	0	0	0	0	0

Table 4.2-5: Tank to Disposal Cell Inventory (continued)

Species	T33 (Ci)	T34 (Ci)	T35 (Ci)	T36 (Ci)	T37 (Ci)	T38 (Ci)	T39 (Ci)	T40 (Ci)
Cm-247	1.02E-13	3.03E-13	1.49E-13	4.29E-13	2.55E-13	6.78E-15	2.74E-14	1.06E-15
Cm-248	1.06E-13	3.16E-13	1.56E-13	4.47E-13	2.65E-13	7.07E-15	2.86E-14	1.11E-15
Co-60	3.54E+00	3.77E+00	4.49E+00	2.05E+00	2.13E+00	2.27E+00	3.18E+00	1.45E+00
Cs-135	1.86E-04	5.53E-04	2.73E-04	7.83E-04	4.65E-04	1.24E-05	5.00E-05	1.94E-06
Cs-137	5.65E+01	1.67E+02	8.25E+01	2.37E+02	1.41E+02	4.08E+00	1.51E+01	5.87E-01
Eu-152	4.61E-01	1.37E+00	6.74E-01	1.93E+00	1.15E+00	3.06E-02	1.24E-01	4.79E-03
Eu-154	1.68E+01	5.00E+01	2.47E+01	7.07E+01	4.20E+01	1.12E+00	4.52E+00	1.75E-01
Gd-152	0	0	0	0	0	0	0	0
H-3	8.04E+01	3.66E+02	4.36E+02	1.99E+02	2.07E+02	2.20E+02	3.09E+02	1.40E+02
I-129	3.54E-01	1.05E+00	5.18E-01	1.49E+00	8.83E-01	2.35E-02	9.51E-02	3.69E-03
K-40	0.00E+00	0.00E+00	0.00E+00	0.00E+00	0.00E+00	0.00E+00	0.00E+00	0.00E+00
Mo-93	0	0	0	0	0	0	0	0
Nb-93m	0.00E+00	0.00E+00	0.00E+00	0.00E+00	0.00E+00	0.00E+00	0.00E+00	0.00E+00
Nb-94	1.51E-05	4.46E-05	2.20E-05	6.32E-05	3.75E-05	1.00E-06	4.04E-06	1.57E-07
Ni-59	5.17E-02	1.53E-01	7.56E-02	2.17E-01	1.29E-01	3.43E-03	1.39E-02	5.38E-04
Ni-63	8.59E+00	9.15E+00	1.09E+01	4.97E+00	5.18E+00	5.51E+00	7.72E+00	3.51E+00
Np-237	5.15E-01	1.20E-01	7.78E-03	9.17E-03	4.33E-03	7.40E-02	2.30E-02	1.59E-01
Pa-231	1.73E-05	3.37E-06	5.68E-07	2.40E-07	3.16E-07	1.53E-06	1.17E-06	2.31E-06
Pb-210	0	0	0	0	0	0	0	0
Pd-107	0.00E+00	0.00E+00	0.00E+00	0.00E+00	0.00E+00	0.00E+00	0.00E+00	0.00E+00
Pt-193	0.00E+00	0.00E+00	0.00E+00	0.00E+00	0.00E+00	0.00E+00	0.00E+00	0.00E+00
Pu-238	3.69E+02	1.58E+00	1.38E+03	2.29E+01	6.59E+02	7.28E+02	7.78E+02	1.96E+02
Pu-239	2.00E+02	1.10E+01	1.14E+01	6.81E-01	6.09E+00	3.13E+00	9.85E+00	2.19E+01
Pu-240	3.51E+01	2.46E+00	8.70E+00	1.64E-01	4.31E+00	2.45E+00	6.12E+00	8.63E+00
Pu-241	9.34E+02	4.55E+01	6.05E+02	2.58E+00	2.65E+02	5.63E+02	6.33E+02	1.45E+02
Pu-242	2.03E-03	5.09E-04	1.95E-02	1.09E-04	9.10E-03	3.61E-02	1.30E-02	5.69E-03
Pu-244	9.29E-06	2.33E-06	8.93E-05	4.97E-07	4.16E-05	1.65E-04	5.96E-05	2.60E-05
Ra-226	3.26E-09	0.00E+00	1.16E-07	1.93E-08	5.66E-08	3.75E-07	2.71E-07	6.01E-08
Ra-228	0.00E+00	0.00E+00	0.00E+00	2.96E-04	0.00E+00	0.00E+00	0.00E+00	7.47E-04
Rn-222	0	0	0	0	0	0	0	0
Se-79	1.97E+00	5.85E+00	2.88E+00	8.27E+00	4.91E+00	1.31E-01	5.29E-01	2.05E-02
Sm-151	9.52E+01	2.82E+02	1.39E+02	4.00E+02	2.37E+02	6.32E+00	2.56E+01	9.91E-01
Sn-126	9.96E+00	2.96E+01	1.46E+01	4.18E+01	2.48E+01	6.62E-01	2.67E+00	1.04E-01
Sr-90	8.00E+01	1.16E+02	4.06E+01	3.01E+02	2.46E+02	1.51E+02	7.45E+00	2.89E-01
Tc-99	7.31E+02	2.17E+03	1.07E+03	3.07E+03	1.82E+03	4.85E+01	1.96E+02	7.60E+00

Table 4.2-5: Tank to Disposal Cell Inventory (continued)

Species	T33 (Ci)	T34 (Ci)	T35 (Ci)	T36 (Ci)	T37 (Ci)	T38 (Ci)	T39 (Ci)	T40 (Ci)
Th-229	5.46E-08	2.24E-01	1.45E-02	4.71E-02	8.06E-03	1.38E-01	4.28E-02	2.26E-02
Th-230	1.55E-03	4.00E-01	5.51E-02	9.14E-03	2.68E-02	1.78E-01	1.29E-01	2.85E-02
Th-232	0.00E+00	0.00E+00	0.00E+00	2.96E-04	0.00E+00	0.00E+00	0.00E+00	7.47E-04
U-232	1.06E-02	3.80E-03	0.00E+00	5.71E-05	0.00E+00	0.00E+00	0.00E+00	5.43E-04
U-233	5.20E-08	2.14E-01	1.38E-02	4.49E-02	7.69E-03	1.32E-01	4.08E-02	2.16E-02
U-234	1.07E-03	2.77E-01	3.82E-02	6.34E-03	1.86E-02	1.23E-01	8.92E-02	1.98E-02
U-235	2.02E-02	3.94E-03	6.64E-04	2.81E-04	3.69E-04	1.79E-03	1.37E-03	2.70E-03
U-236	1.12E-02	5.64E-03	1.13E-02	6.53E-04	4.17E-03	2.35E-02	1.53E-02	4.37E-03
U-238	2.92E+00	2.78E-01	3.92E-04	4.44E-03	2.44E-03	2.10E-03	1.93E-04	8.09E-02
Zr-93	0.00E+00	0.00E+00	0.00E+00	0.00E+00	0.00E+00	0.00E+00	0.00E+00	0.00E+00

Species	T41 (Ci)	T42 (Ci)	T43 (Ci)	T44 (Ci)	T45 (Ci)	T46 (Ci)	T47 (Ci)	T48 (Ci)
Ac-227	2.11E-08	2.44E-06	1.03E-06	1.20E-06	1.08E-06	1.09E-06	1.01E-06	2.43E-07
Al-26	4.45E-03	1.39E+00	2.22E-02	3.73E-01	2.86E-01	6.04E-01	3.69E-02	1.57E-03
Am-241	0.00E+00	8.96E+00	1.43E-01	2.36E+00	1.80E+00	3.85E+00	2.02E-01	1.01E-02
Am-242m	0.00E+00	4.83E-03	7.72E-05	1.27E-03	9.67E-04	2.07E-03	1.09E-04	5.45E-06
Am-243	0.00E+00	2.45E-02	3.92E-04	6.45E-03	4.91E-03	1.05E-02	5.52E-04	2.77E-05
C-14	1.51E-01	6.90E+00	7.62E+00	4.02E+00	3.65E+00	3.67E+00	3.39E+00	1.51E+00
Cf-249	0.00E+00	5.09E-12	8.14E-14	1.34E-12	1.02E-12	2.19E-12	1.15E-13	5.76E-15
Cf-251	0.00E+00	1.74E-13	2.79E-15	4.59E-14	3.49E-14	7.48E-14	3.92E-15	1.97E-16
Cl-36	0.00E+00	0.00E+00	0.00E+00	0.00E+00	0.00E+00	0.00E+00	0.00E+00	0.00E+00
Cm-243	0.00E+00	2.69E-03	4.30E-05	7.08E-04	5.39E-04	1.16E-03	6.06E-05	3.04E-06
Cm-244	0.00E+00	1.60E+01	2.56E-01	4.21E+00	3.20E+00	6.87E+00	3.60E-01	1.81E-02
Cm-245	0.00E+00	1.76E-03	2.82E-05	4.64E-04	3.53E-04	7.57E-04	3.97E-05	1.99E-06
Cm-246	0	0	0	0	0	0	0	0
Cm-247	0.00E+00	5.18E-13	8.29E-15	1.36E-13	1.04E-13	2.23E-13	1.17E-14	5.86E-16
Cm-248	0.00E+00	5.40E-13	8.64E-15	1.42E-13	1.08E-13	2.32E-13	1.22E-14	6.11E-16
Co-60	0.00E+00	4.04E+00	4.46E+00	2.22E+00	1.99E+00	2.00E+00	1.87E+00	8.86E-01
Cs-135	1.44E-05	9.46E-04	1.51E-05	2.49E-04	1.90E-04	4.06E-04	2.13E-05	1.07E-06
Cs-137	4.63E+00	2.86E+02	4.58E+00	7.58E+01	5.78E+01	1.23E+02	6.78E+00	3.24E-01
Eu-152	0.00E+00	2.34E+00	3.74E-02	6.15E-01	4.68E-01	1.00E+00	5.27E-02	2.64E-03
Eu-154	0.00E+00	8.55E+01	1.37E+00	2.25E+01	1.71E+01	3.67E+01	1.93E+00	9.67E-02
Gd-152	0	0	0	0	0	0	0	0
H-3	0.00E+00	3.92E+02	4.33E+02	2.15E+02	1.93E+02	1.95E+02	1.82E+02	8.60E+01
I-129	0.00E+00	1.80E+00	2.88E-02	4.73E-01	3.60E-01	7.72E-01	4.05E-02	2.03E-03

Table 4.2-5: Tank to Disposal Cell Inventory (continued)

Species	T41 (Ci)	T42 (Ci)	T43 (Ci)	T44 (Ci)	T45 (Ci)	T46 (Ci)	T47 (Ci)	T48 (Ci)
K-40	0.00E+00	0.00E+00	0.00E+00	0.00E+00	0.00E+00	0.00E+00	0.00E+00	0.00E+00
Mo-93	0	0	0	0	0	0	0	0
Nb-93m	0.00E+00	0.00E+00	0.00E+00	0.00E+00	0.00E+00	0.00E+00	0.00E+00	0.00E+00
Nb-94	0.00E+00	7.64E-05	1.22E-06	2.01E-05	1.53E-05	3.28E-05	1.72E-06	8.64E-08
Ni-59	0.00E+00	2.62E-01	4.20E-03	6.90E-02	5.26E-02	1.13E-01	5.91E-03	2.96E-04
Ni-63	0.00E+00	9.80E+00	1.08E+01	5.38E+00	4.82E+00	4.86E+00	4.54E+00	2.15E+00
Np-237	0.00E+00	1.56E-01	1.45E-01	6.63E-04	5.93E-04	5.99E-04	5.59E-04	1.36E-02
Pa-231	5.87E-08	6.79E-06	2.86E-06	3.34E-06	3.01E-06	3.04E-06	2.82E-06	6.76E-07
Pb-210	0	0	0	0	0	0	0	0
Pd-107	0.00E+00	0.00E+00	0.00E+00	0.00E+00	0.00E+00	0.00E+00	0.00E+00	0.00E+00
Pt-193	0.00E+00	0.00E+00	0.00E+00	0.00E+00	0.00E+00	0.00E+00	0.00E+00	0.00E+00
Pu-238	5.46E+00	1.06E+03	1.42E+03	6.05E+02	5.43E+02	5.48E+02	5.10E+02	4.74E+01
Pu-239	1.82E-01	3.83E+01	5.70E+00	9.38E+01	8.40E+01	8.48E+01	7.91E+01	2.72E-02
Pu-240	0.00E+00	1.37E+01	4.81E+00	2.09E+01	1.87E+01	1.89E+01	1.76E+01	9.86E-05
Pu-241	0.00E+00	2.11E+02	1.11E+03	4.41E+02	3.95E+02	3.98E+02	3.72E+02	7.57E-03
Pu-242	0.00E+00	1.26E-02	7.10E-02	4.17E-03	3.73E-03	3.76E-03	3.51E-03	0.00E+00
Pu-244	0.00E+00	5.74E-05	3.24E-04	1.90E-05	1.70E-05	1.72E-05	1.61E-05	0.00E+00
Ra-226	0.00E+00	1.02E-06	7.38E-07	3.91E-14	3.50E-14	3.53E-14	3.30E-14	4.34E-06
Ra-228	0.00E+00	8.76E-02	0.00E+00	0.00E+00	0.00E+00	0.00E+00	0.00E+00	1.84E-06
Rn-222	0	0	0	0	0	0	0	0
Se-79	0.00E+00	1.00E+01	1.60E-01	2.63E+00	2.00E+00	4.30E+00	2.25E-01	1.13E-02
Sm-151	0.00E+00	4.83E+02	7.73E+00	1.27E+02	9.68E+01	2.08E+02	1.09E+01	5.46E-01
Sn-126	0.00E+00	5.06E+01	8.09E-01	1.33E+01	1.01E+01	2.17E+01	1.14E+00	5.72E-02
Sr-90	1.18E+02	1.41E+02	2.25E+00	2.16E+02	2.25E+02	2.53E+02	1.52E+02	1.59E-01
Tc-99	0.00E+00	3.71E+03	5.93E+01	9.76E+02	7.43E+02	1.59E+03	8.35E+01	3.31E+01
Th-229	0.00E+00	9.58E-01	2.71E-01	4.22E-09	3.78E-09	3.81E-09	3.56E-09	3.19E-01
Th-230	0.00E+00	4.85E-01	3.50E-01	1.85E-08	1.66E-08	1.67E-08	1.56E-08	2.06E+00
Th-232	0.00E+00	8.76E-02	0.00E+00	0.00E+00	0.00E+00	0.00E+00	0.00E+00	1.84E-06
U-232	0.00E+00	2.25E-04	0.00E+00	1.29E-03	1.16E-03	1.17E-03	1.09E-03	0.00E+00
U-233	0.00E+00	9.14E-01	2.58E-01	4.03E-09	3.60E-09	3.64E-09	3.40E-09	3.05E-01
U-234	0.00E+00	3.36E-01	2.42E-01	1.29E-08	1.15E-08	1.16E-08	1.08E-08	1.43E+00
U-235	6.86E-05	7.93E-03	3.34E-03	3.91E-03	3.52E-03	3.55E-03	3.29E-03	7.90E-04
U-236	0.00E+00	4.50E-02	4.62E-02	4.91E-04	4.40E-04	4.44E-04	4.14E-04	5.81E-02
U-238	1.54E-03	1.39E-01	2.72E-04	4.59E-01	4.11E-01	4.15E-01	3.87E-01	7.76E-04
Zr-93	0.00E+00	0.00E+00	0.00E+00	0.00E+00	0.00E+00	0.00E+00	0.00E+00	0.00E+00

Table 4.2-5: Tank to Disposal Cell Inventory (Continued)

Species	T49 (Ci)	T50 (Ci)	T51 (Ci)	Species	T49 (Ci)	T50 (Ci)	T51 (Ci)
Ac-227	0.00E+00	0.00E+00	1.77E-07	**Np-237**	0.00E+00	0.00E+00	9.99E-03
Al-26	0.00E+00	0.00E+00	5.08E-03	**Pa-231**	0.00E+00	0.00E+00	4.90E-07
Am-241	0.00E+00	0.00E+00	3.28E-02	**Pb-210**	0	0	0
Am-242m	0.00E+00	0.00E+00	1.76E-05	**Pd-107**	0.00E+00	0.00E+00	0.00E+00
Am-243	0.00E+00	0.00E+00	6.21E-06	**Pt-193**	0.00E+00	0.00E+00	0.00E+00
C-14	0.00E+00	0.00E+00	2.80E+00	**Pu-238**	0.00E+00	0.00E+00	4.69E+02
Cf-249	0.00E+00	0.00E+00	1.86E-14	**Pu-239**	0.00E+00	0.00E+00	6.30E+00
Cf-251	0.00E+00	0.00E+00	6.37E-16	**Pu-240**	0.00E+00	0.00E+00	3.58E+00
Cl-36	0.00E+00	0.00E+00	0.00E+00	**Pu-241**	0.00E+00	0.00E+00	1.71E+02
Cm-243	0.00E+00	0.00E+00	9.84E-06	**Pu-242**	0.00E+00	0.00E+00	6.48E-03
Cm-244	0.00E+00	0.00E+00	5.85E-02	**Pu-244**	0.00E+00	0.00E+00	2.96E-05
Cm-245	0.00E+00	0.00E+00	6.44E-06	**Ra-226**	0.00E+00	0.00E+00	6.71E-08
Cm-246	0	0	0	**Ra-228**	0.00E+00	0.00E+00	2.95E-04
Cm-247	0.00E+00	0.00E+00	1.90E-15	**Rn-222**	0	0	0
Cm-248	0.00E+00	0.00E+00	1.97E-15	**Se-79**	0.00E+00	0.00E+00	3.66E-02
Co-60	0.00E+00	0.00E+00	1.64E+00	**Sm-151**	0.00E+00	0.00E+00	1.77E+00
Cs-135	0.00E+00	0.00E+00	3.46E-06	**Sn-126**	0.00E+00	0.00E+00	1.85E-01
Cs-137	0.00E+00	0.00E+00	1.05E+00	**Sr-90**	0.00E+00	0.00E+00	5.15E-01
Eu-152	0.00E+00	0.00E+00	8.55E-03	**Tc-99**	0.00E+00	0.00E+00	1.36E+01
Eu-154	0.00E+00	0.00E+00	3.13E-01	**Th-229**	0.00E+00	0.00E+00	2.79E-02
Gd-152	0	0	0	**Th-230**	0.00E+00	0.00E+00	3.18E-02
H-3	0.00E+00	0.00E+00	1.59E+02	**Th-232**	0.00E+00	0.00E+00	2.95E-04
I-129	0.00E+00	0.00E+00	6.57E-03	**U-232**	0.00E+00	0.00E+00	3.10E-05
K-40	0.00E+00	0.00E+00	0.00E+00	**U-233**	0.00E+00	0.00E+00	2.66E-02
Mo-93	0	0	0	**U-234**	0.00E+00	0.00E+00	2.21E-02
Nb-93m	0.00E+00	0.00E+00	0.00E+00	**U-235**	0.00E+00	0.00E+00	5.73E-04
Nb-94	0.00E+00	0.00E+00	2.79E-07	**U-236**	0.00E+00	0.00E+00	3.57E-03
Ni-59	0.00E+00	0.00E+00	9.59E-04	**U-238**	0.00E+00	0.00E+00	5.19E-03
Ni-63	0.00E+00	0.00E+00	3.98E+00	**Zr-93**	0.00E+00	0.00E+00	0.00E+00

Table 4.2-6: Waste Tank-Specific Salt Solution Volume to Disposal Cell

Tank ID	Volume (gallons)	Tank ID	Volume (gallons)	Tank ID	Volume (gallons)
T01	8.30E+05	**T18**	1.00E-40	**T35**	5.76E+06
T02	8.18E+05	**T19**	1.00E-40	**T36**	2.63E+06
T03	8.18E+05	**T20**	1.00E-40	**T37**	2.73E+06
T04	7.56E+05	**T21**	5.53E+06	**T38**	2.91E+06
T05	1.51E+05	**T22**	1.00E-40	**T39**	4.08E+06
T06	3.02E+04	**T23**	1.00E-40	**T40**	1.86E+06
T07	2.33E+06	**T24**	1.00E-40	**T41**	3.33E+05
T08	1.63E+06	**T25**	8.73E+05	**T42**	5.18E+06
T09	8.75E+05	**T26**	3.78E+06	**T43**	5.72E+06
T10	3.27E+05	**T27**	1.78E+06	**T44**	2.84E+06
T11	6.90E+04	**T28**	2.47E+06	**T45**	2.55E+06
T12	7.15E+05	**T29**	2.42E+06	**T46**	2.57E+06
T13	3.73E+06	**T30**	4.30E+06	**T47**	2.40E+06
T14	2.92E+05	**T31**	2.30E+06	**T48**	1.14E+06
T15	1.00E-40	**T32**	2.72E+06	**T49**	1.00E-40
T16	1.00E-40	**T33**	4.54E+06	**T50**	1.00E-40
T17	1.00E-40	**T34**	4.83E+06	**T51**	2.10E+06

4.2.2 Disposal Unit Geometry

There are three disposal unit types utilized at the SDF, Vault 1, Vault 4, and the FDCs. The disposal unit geometries are presented in Figures 3.2-10 through Figure 3.2-12 for Vault 1, Vault 4, and the FDCs, respectively. The associated dimensions of their components for Vault 1, Vault 4, and the FDCs, are presented in Tables 4.2-7, 4.2-8, and 4.2-9, respectively.

Table 4.2-7: Geometric Dimensions for the Vault 1 Model

Material Zone	Thickness	Material Type
Saltstone	24 feet	Saltstone
Floor Slab	2 feet	High Quality Concrete
Wall	18 inches	High Quality Concrete
Width	49.2 feet	N/A
Length	600 feet	N/A

Adapted from Table 4.4.1 and Table I4-7of SRR-CWDA-2009-00017

Table 4.2-8: Geometric Dimensions for the Vault 4 Model

Material Zone	Thickness	Material Type
Saltstone	24.75 feet	Saltstone
Floor Slab	2 feet	High Quality Concrete
Wall	18 inches	High Quality Concrete
Sheet Drain	2 inches	Polystyrene and Polypropylene
Width	98.4 feet	N/A
Length	600 feet	N/A

Adapted from Table 4.4.2 and Table I4-7of SRR-CWDA-2009-00017

Table 4.2-9: Geometric Dimensions for the FDC Model

Material Zone	Thickness	Material Type
Saltstone	20 feet	Saltstone
Floor Slab	8 inches	High Quality Concrete[a]
Upper Mud Mat	4 inches	High Quality Concrete[a]
HDPE-GCL	1 inch	HDPE-GCL[a]
Lower Mud Mat	4 inches	Low Quality Concrete[a]
Radial Orientation		
Wall	8 inches	High Quality Concrete
Shotcrete (not shown)	6 inches	Backfill
HDPE	1 inch	HDPE
Sheet Drain	2 inches	Chlorinated PVC
Radius	75 feet	N/A

Adapted from Table 4.4.3 of and Table I4-7 of SRR-CWDA-2009-00017

(a) In the simplified abstraction used in the SDF GoldSim model, the floor slab, upper mud mat, HDPE-GCL and lower mud mat zones are modeled as a single unit. The influence assumption of the individual zones is there to be captured in the flow fields.

4.2.3 Disposal Units Identifiers

The SDF is comprised of 66 disposal units, Vault 1, Vault 4 and 64 FDCs. The disposal unit identifiers as assigned in the SDF GoldSim model along with the associated SDF PORFLOW disposal unit identifiers are listed in Table 4.2-10. The disposal unit identifiers for the original SDF GoldSim model and the SDF PORFLOW differ, therefore a comparison of the identifiers is presented in Table 4.2-10. The disposal unit identifiers have been updated in his version of the SDF GoldSim model so that the GoldSim and PORFLOW model naming conventions are consistent. The disposal unit locations are presented in Figure 4.2-1.

Table 4.2-10: SDF Disposal Unit Identifiers

Disposal Unit Identifiers[2]	Disposal Unit Identifiers[1]	Disposal Unit Identifiers[2]	Disposal Unit Identifiers[1]	Disposal Unit Identifiers[2]	Disposal Unit Identifiers[1]
V2A	V2A	V10A	V10A	V15C	V16C
V2B	V2B	V10B	V10B	V15D	V16D
V5A	V5A	V10C	V10C	V16A	V17A
V5B	V5B	V10D	V10D	V16B	V17B
V5C	V5C	V11A	V11A	V16C	V17C
V5D	V5D	V11B	V11B	V16D	V17D
V6A	V6A	V11C	V11C	V17A	V18A
V6B	V6B	V11D	V11D	V17B	V18B
V6C	V6C	V12A	V12A	V17C	V18C
V6D	V6D	V12B	V12B	V17D	V18D
V7A	V7A	V12C	V12C	V18A	V19A
V7B	V7B	V12D	V12D	V18B	V19B
V7C	V7C	V3A	V13A	V18C	V19C
V7D	V7D	V3B	V13B	V18D	V19D
V8A	V8A	V13A	V14A	V19A	V20A
V8B	V8B	V13B	V14B	V19B	V20B
V8C	V8C	V13C	V14C	V20A	V21A
V8D	V8D	V13D	V14D	V20B	V21B
V9A	V9A	V14A	V15A	V20C	V21C
V9B	V9B	V14B	V15B	V20D	V21D
V9C	V9C	V15A	V16A	V1	V1
V9D	V9D	V15B	V16B	V4	V4

1 GoldSim prior to Version 3.002
2 PORFLOW
Note: The table cells tinted light orange contain the northern disposal units and the table cells tinted light green contain the southern disposal units
See Appendix A for additional information

Figure 4.2-1: Locations and Base Elevations of Disposal Units within SDF

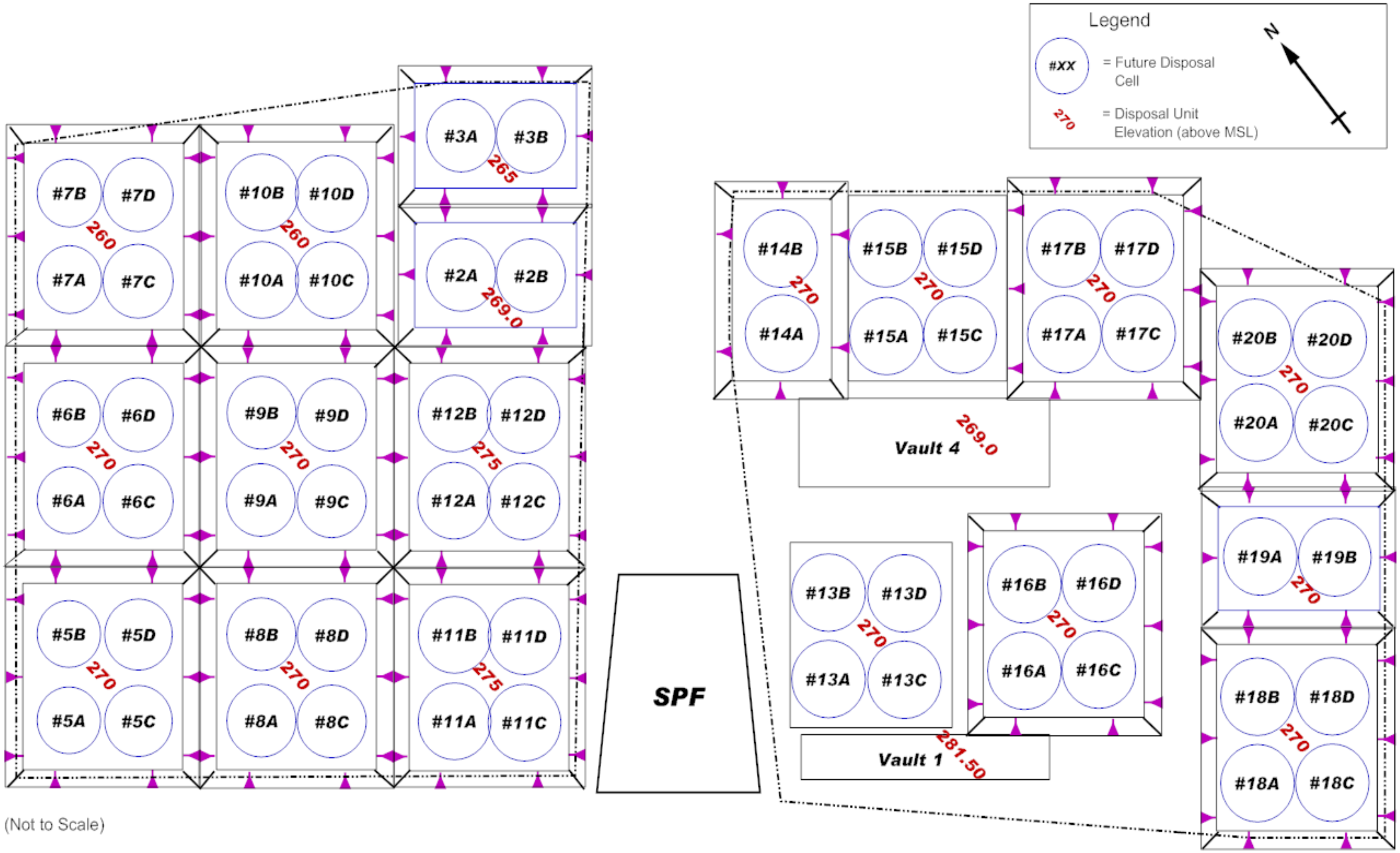

Note: Figure presents the anticipated FDC locations, numbering of the units are placeholders and may not match the final disposal unit nunbering. See Figure 4.2-20 of SRR-CWDA-2009-00017 (see Appendix A for additional information) .

4.2.4 SDF Model Configurations

The SDF PA considers five different cases (or scenarios). [SRR-CWDA-2009-00017] Case A, considered the Base Case, reflects the expected condition where intact disposal unit concrete and saltstone lead to a diffusion-dominated release, prior to the cover system and the disposal units becoming significantly degraded. Other cases were postulated for diagnostic purposes, to understand the range of possible disposal unit behavior better. Case B assumes that a fast flow path forms between saltstone and the Vault 4 wall and the walls of the FDCs at time zero, due to the presence of a sheet drain at the wall and connecting breaches through the roof and floor (including the upper and lower mud mats for the FDCs). This case is not applicable to Vault 1 because Vault 1 does not have sheet drain systems. Case C is similar to Case B with an additional fast flow path passing through the saltstone interior, possibly due to corrosion of support columns (in Vault 4 and the FDCs), or fissures in response to differential settlement. Case D is similar to the Base Case, except that an intact sheet drain creates a capillary break, precluding transport across the gap under unsaturated conditions. Because Vault 1 does not have sheet drain systems, this case is not applicable to Vault 1. Case E is similar to the Base Case in that no fast flow paths exist and the sheet drain system does not create a capillary break; however, the postulation for the saltstone is that it is severely degraded at time zero. These cases are summarized in Table 4.2-11. A complete description of the Base Case through E can be found in Section 4.4.2 of the SDF PA. [SRR-CWDA-2009-00017]

Table 4.2-11: Cases Postulated for SDF Vaults and FDCs

Case	Vault 1	Vault 4	FDCs
A	Base Case vault wall degraded, saltstone intact	Base Case vault wall degraded, saltstone intact	Base Case disposal unit wall intact, saltstone intact
B	N/A (no sheet drains)	Fast flow walls fast flow along walls from roof thru floor, vault wall degraded	Fast flow walls fast flow along walls from roof thru floor (including upper and lower mud mats)
C	Fast flow walls & crack fast flow along cracks from roof thru floor, vault wall degraded	Fast flow walls & crack fast flow along walls and cracks from roof thru floor vault wall degraded	Fast flow walls & columns fast flow along walls and columns from roof thru floor (including upper and lower mud mats)
D	N/A (no sheet drains)	Capillary break Base Case with capillary break at sheet drains	Capillary break Base Case with capillary break at sheet drains
E	Saltstone severely degraded vault wall degraded	Saltstone severely degraded vault wall degraded	Saltstone severely degraded disposal unit wall intact
K	Fast Flow Complete degradation of saltstone and other concrete structures within 10,000 yrs	Fast Flow Complete degradation of saltstone and other concrete structures within 10,000 yrs	Fast Flow Complete degradation of saltstone and other concrete structures within 10,000 yrs

From Table 4.4-4 of SRR-CWDA-2009-00017, and the response to RAI PA-8 in SRS-CWDA-2011-00044, Rev. 1

An additional case, Alternative Sensitivity Case K, was developed in response to the NRC's SDF RAIs and described in RAI PA-8 response. [SRS-CWDA-2011-00044] Alternative Sensitivity Case K assumes that that saltstone and other concrete structures are completely degraded within 10,000 years. Degraded saltstone is assumed to have a saturated hydraulic of 1.0E-06 cm/sec and an effective diffusion coefficient of 5.0E-06 cm^2/sec. Saltstone that is not degraded is assumed to have a saturated hydraulic of 1.0E-08 cm/sec and effective diffusion coefficient of 1.0E-07 cm^2/sec. Saturations were assumed 1.0 throughout the disposal unit structure. The E_h transition volume changed to 18 % of the Base Case value based on an arbitrary reduction by a factor of four, the reduction capacity of saltstone and applying a porosity correction. In addition, pH transition volume changed to 73 % of the Base Case value based on a porosity correction. Instead of changes in the step-function in technetium K_ds after a certain number of pore volumes of water has passed through a zone, K_ds were determined by a shrinking core model (see Section 3.5). In the shrinking core model, K_ds are based on the ratio of reducing environment to oxidized environment in the saltstone, wall, and floor as determined by evaluating the diffusive influx of oxygen into those zones over time. The oxygen diffusive flux rate increases over time do to the increasing number of fractures and associated increase in diffusive surface area. Other changes include the updating of K_d values for saltstone, disposal unit concrete, and soil, for specified radionuclides. The Vault 4 inventory was also updated for Pu-238, Ra-226, Th-230, and U-234. The FDC inventory was updated for Ra-226, Th-230. The dose methodology was also updated in Alternative Sensitivity Case K to include chicken and egg pathways, a leafy portion in the plant transfer factor, and 25-year buildup of radionuclides in irrigated soil and updated biotic transfer factors.

4.2.4.1 Disposal Unit Diffusion coefficients

Prior to complete degradation of the saltstone, matrix diffusion plays an important role in the transport of radionuclides into the wall and out to the backfill and accessible environment. The influence of molecular diffusion is defined by an effective matrix diffusion coefficient (D_e) which can be defined as:

$$D_e = \frac{D_m}{\tau} \qquad (4.2\text{-}1)$$

where:

D_m is the molecular diffusion coefficient (L^2/T) and τ is the tortuosity term. The initial (for time dependent coefficients) constant effective matrix diffusion coefficients used in the SDF GoldSim model are listed in Table 4.2-12. [WSRC-STI-2006-00198 Tables 5-12, 5-18, and 6-44, SRNL-STI-2009-00115]

The methodology used to describe the time dependent effective diffusion coefficient functions is described in SRNL-STI-2009-00115. The time dependent effective diffusion coefficients for the three disposal unit types are presented below in Tables 4.2-13 through 4.2-35.

Table 4.2-12: Effective Matrix Diffusion Coefficients by Medium

Medium	Initial or single-valued Effective Matrix Diffusion Coefficient (cm^2/s)					
	Base Case	**Case B**	**Case C**	**Case D**	**Case E**	**Case K**
Wall	5.0E-08[a]	5.0E-08[a]	5.0E-08[a]	5.0E-08[a]	5.0E-08[a]	5.0E-08[a]
Saltstone	1.0E-07[a]	1.0E-07[a]	1.0E-07[a]	1.0E-07[a]	1.0E-07[a]	1.0E-07[a]
Backfill	5.3E-06	5.3E-06	5.3E-06	5.3E-06	5.3E-06	5.3E-06
Shotcrete	5.3E-06	5.3E-06	5.3E-06	5.3E-06	5.3E-06	5.3E-06
HDPE	4.75E-10[a]	4.75E-10[a]	4.75E-10[a]	4.75E-10[a]	4.75E-10[a]	4.75E-10[a]
Sheet Drain	1.0E-07	9.4E-06	9.4E-06	1.0E-13	1.0E-07	1.0E-07
Fast Path	1.0E-07	1.0E-07	8.0E-06	1.0E-07	1.0E-07	1.0E-07
Degraded Diffusion Coefficient	5.01E-06	5.01E-06	5.01E-06	5.01E-06	5.01E-06	5.01E-06

a – Initial value for time-variant degradation.

Table 4.2-13: Vault 1 Wall Effective Matrix Diffusion Coefficients for Case A, B, and D

Time (years)	D_{eff}	Time (years)	D_{eff}	Time (years)	D_{eff}
0	5.00E-08	1,000	5.38E-08	6,000	6.17E-08
50	5.02E-08	1,200	5.41E-08	6,500	6.24E-08
100	5.06E-08	1,400	5.45E-08	7,000	6.31E-08
150	5.09E-08	1,600	5.49E-08	7,500	6.38E-08
200	5.11E-08	1,800	5.53E-08	8,000	6.45E-08
250	5.14E-08	2,000	5.57E-08	8,500	6.51E-08
300	5.16E-08	2,300	5.62E-08	9,000	6.58E-08
350	5.18E-08	2,600	5.67E-08	9,500	6.64E-08
400	5.20E-08	2,900	5.72E-08	10,000	6.71E-08
450	5.22E-08	3,200	5.77E-08	11,000	6.80E-08
500	5.24E-08	3,600	5.83E-08	12,000	6.93E-08
600	5.26E-08	4,000	5.89E-08	15,000	7.18E-08
700	5.30E-08	4,500	5.96E-08	20,000	7.68E-08
800	5.33E-08	5,000	6.03E-08	50,000	1.01E-07
900	5.35E-08	5,500	6.10E-08	100,000	2.14E-07

Table 4.2-14: Vault 1 Wall Effective Matrix Diffusion Coefficients for Case C

Time (years)	D_{eff}	Time (years)	D_{eff}	Time (years)	D_{eff}
0	5.00E-08	1,000	5.38E-08	6,000	6.17E-08
50	5.02E-08	1,200	5.41E-08	6,500	6.24E-08
100	5.06E-08	1,400	5.45E-08	7,000	6.31E-08
150	5.09E-08	1,600	5.49E-08	7,500	6.38E-08
200	5.11E-08	1,800	5.53E-08	8,000	6.45E-08
250	5.14E-08	2,000	5.57E-08	8,500	6.51E-08
300	5.16E-08	2,300	5.62E-08	9,000	6.58E-08
350	5.18E-08	2,600	5.67E-08	9,500	6.64E-08
400	5.20E-08	2,900	5.72E-08	10,000	6.71E-08
450	5.22E-08	3,200	5.77E-08	11,000	6.80E-08
500	5.24E-08	3,600	5.83E-08	12,000	6.93E-08
600	5.26E-08	4,000	5.89E-08	15,000	7.18E-08
700	5.30E-08	4,500	5.96E-08	20,000	7.68E-08
800	5.33E-08	5,000	6.03E-08	50,000	1.01E-07
900	5.35E-08	5,500	6.10E-08	100,000	2.14E-07

Table 4.2-15: Vault 1 Wall Effective Matrix Diffusion Coefficients for Case E

Time (years)	D_{eff}	Time (years)	D_{eff}	Time (years)	D_{eff}
0	5.00E-08	1,400	5.45E-08	8,000	6.45E-08
50	5.02E-08	1,600	5.49E-08	8,500	6.51E-08
100	5.06E-08	1,800	5.53E-08	9,000	6.58E-08
150	5.09E-08	2,000	5.57E-08	9,500	6.64E-08
200	5.11E-08	2,300	5.62E-08	10,000	6.71E-08
250	5.14E-08	2,600	5.67E-08	11,000	6.80E-08
300	5.16E-08	2,900	5.72E-08	11,626	6.91E-08
350	5.18E-08	3,200	5.77E-08	12,000	6.97E-08
400	5.20E-08	3,600	5.83E-08	13,669	7.10E-08
450	5.22E-08	4,000	5.89E-08	15,000	7.28E-08
500	5.24E-08	4,500	5.96E-08	20,000	7.68E-08
600	5.26E-08	5,000	6.03E-08	20,012	8.00E-08
700	5.30E-08	5,500	6.10E-08	20,205	8.01E-08
800	5.33E-08	6,000	6.17E-08	22,690	8.18E-08
900	5.35E-08	6,500	6.24E-08	40,000	1.02E-07
1000	5.38E-08	7,000	6.31E-08		
1200	5.41E-08	7,500	6.38E-08		

Table 4.2-16: Vault 1 Saltstone Effective Matrix Diffusion Coefficients for Case K

Time (years)	D_{eff}	Time (years)	D_{eff}	Time (years)	D_{eff}
0	1.00E-07	1,800	1.94E-07	8,000	2.17E-06
50	1.01E-07	2,000	2.10E-07	8,227	2.39E-06
100	1.03E-07	2,300	2.32E-07	8,297	2.53E-06
150	1.05E-07	2,600	2.60E-07	8,500	2.67E-06
200	1.07E-07	2,900	2.93E-07	9,000	3.07E-06
250	1.09E-07	3,200	3.30E-07	9,200	3.52E-06
300	1.11E-07	3,500	3.71E-07	9,400	3.81E-06
350	1.13E-07	3,600	4.00E-07	9,500	4.03E-06
400	1.15E-07	4,000	4.41E-07	9,545	4.15E-06
450	1.18E-07	4,500	5.26E-07	9,600	4.22E-06
500	1.20E-07	4,646	5.96E-07	9,700	4.38E-06
600	1.24E-07	5,000	6.60E-07	9,800	4.54E-06
700	1.28E-07	5,500	7.80E-07	9,882	4.69E-06
800	1.34E-07	6,000	9.48E-07	9,900	4.79E-06
900	1.39E-07	6,500	1.15E-06	10,000	4.92E-06
1000	1.45E-07	7,000	1.40E-06	14,196	5.01E-06
1200	1.53E-07	7,251	1.62E-06	20,000	5.01E-06
1400	1.66E-07	7,500	1.79E-06	100,000	5.01E-06
1600	1.79E-07	7,740	1.97E-06		

Table 4.2-17: Vault 4 Wall Effective Matrix Diffusion Coefficients for the Base Case

Time (years)	D_{eff}	Time (years)	D_{eff}	Time (years)	D_{eff}
0	5.00E-08	1,200	5.41E-08	7,000	6.31E-08
50	5.02E-08	1,400	5.45E-08	7,500	6.38E-08
100	5.06E-08	1,600	5.49E-08	8,000	6.45E-08
150	5.09E-08	1,800	5.53E-08	8,500	6.51E-08
200	5.11E-08	2,000	5.57E-08	9,000	6.58E-08
250	5.14E-08	2,300	5.62E-08	9,500	6.64E-08
300	5.16E-08	2,600	5.67E-08	10,000	6.71E-08
350	5.18E-08	2,900	5.72E-08	11,000	6.80E-08
400	5.20E-08	3,200	5.77E-08	12,000	6.93E-08
450	5.22E-08	3,600	5.83E-08	15,000	7.18E-08
500	5.24E-08	4,000	5.89E-08	15,519	7.40E-08
600	5.26E-08	4,500	5.96E-08	16,018	7.46E-08
700	5.30E-08	5,000	6.03E-08	16,547	7.53E-08
800	5.33E-08	5,500	6.10E-08	20,000	7.78E-08
900	5.35E-08	6,000	6.17E-08	50,000	1.01E-07
1,000	5.38E-08	6,500	6.24E-08	100,000	2.14E-07

Table 4.2-18: Vault 4 Wall Effective Matrix Diffusion Coefficients for Case B

Time (years)	D_{eff}	Time (years)	D_{eff}	Time (years)	D_{eff}
0	5.00E-08	1,200	5.41E-08	6,000	6.17E-08
50	5.02E-08	1,400	5.45E-08	6,500	6.24E-08
100	5.06E-08	1,600	5.49E-08	7,000	6.31E-08
150	5.09E-08	1,800	5.53E-08	7,500	6.38E-08
200	5.11E-08	2,000	5.57E-08	8,000	6.45E-08
250	5.14E-08	2,300	5.62E-08	8,500	6.51E-08
300	5.16E-08	2,600	5.67E-08	9,000	6.58E-08
350	5.18E-08	2,900	5.72E-08	9,500	6.64E-08
400	5.20E-08	3,200	5.77E-08	10,000	6.71E-08
450	5.22E-08	3,600	5.83E-08	11,000	6.80E-08
500	5.24E-08	3,987	5.89E-08	12,000	6.93E-08
600	5.26E-08	4,000	5.92E-08	15,000	7.18E-08
700	5.30E-08	4,500	5.96E-08	16,507	7.46E-08
800	5.33E-08	5,000	6.03E-08	20,000	7.78E-08
900	5.35E-08	5,016	6.07E-08	50,000	1.01E-07
1,000	5.38E-08	5,500	6.10E-08	100,000	2.14E-07

Table 4.2-19: Vault 4 Wall Effective Matrix Diffusion Coefficients for Case C

Time (years)	D_{eff}	Time (years)	D_{eff}	Time (years)	D_{eff}
0	5.00E-08	1,200	5.41E-08	6,000	6.17E-08
50	5.02E-08	1,400	5.45E-08	6,500	6.24E-08
100	5.06E-08	1,600	5.49E-08	7,000	6.31E-08
150	5.09E-08	1,800	5.53E-08	7,500	6.38E-08
200	5.11E-08	2,000	5.57E-08	8,000	6.45E-08
250	5.14E-08	2,300	5.62E-08	8,500	6.51E-08
300	5.16E-08	2,600	5.67E-08	9,000	6.58E-08
350	5.18E-08	2,900	5.72E-08	9,500	6.64E-08
400	5.20E-08	3,069	5.76E-08	10,000	6.71E-08
450	5.22E-08	3,200	5.78E-08	11,000	6.80E-08
500	5.24E-08	3,363	5.81E-08	11,151	6.88E-08
600	5.26E-08	3,600	5.84E-08	12,000	6.94E-08
700	5.30E-08	4,000	5.89E-08	15,000	7.18E-08
800	5.33E-08	4,500	5.96E-08	20,000	7.68E-08
900	5.35E-08	5,000	6.03E-08	50,000	1.01E-07
1,000	5.38E-08	5,500	6.10E-08	100,000	2.14E-07

Table 4.2-20: Vault 4 Wall Effective Matrix Diffusion Coefficients for Case D

Time (years)	D_{eff}	Time (years)	D_{eff}	Time (years)	D_{eff}
0	1.00E-07	1,800	1.94E-07	8,000	2.17E-06
50	1.01E-07	2,000	2.10E-07	8,227	2.39E-06
100	1.03E-07	2,300	2.32E-07	8,297	2.53E-06
150	1.05E-07	2,600	2.60E-07	8,500	2.67E-06
200	1.07E-07	2,900	2.93E-07	9,000	3.07E-06
250	1.09E-07	3,200	3.30E-07	9,200	3.52E-06
300	1.11E-07	3,500	3.71E-07	9,400	3.81E-06
350	1.13E-07	3,600	4.00E-07	9,500	4.03E-06
400	1.15E-07	4,000	4.41E-07	9,545	4.15E-06
450	1.18E-07	4,500	5.26E-07	9,600	4.22E-06
500	1.20E-07	4,646	5.96E-07	9,700	4.38E-06
600	1.24E-07	5,000	6.60E-07	9,800	4.54E-06
700	1.28E-07	5,500	7.80E-07	9,882	4.69E-06
800	1.34E-07	6,000	9.48E-07	9,900	4.79E-06
900	1.39E-07	6,500	1.15E-06	10,000	4.92E-06
1,000	1.45E-07	7,000	1.40E-06	14,196	5.01E-06
1,200	1.53E-07	7,251	1.62E-06	20,000	5.01E-06
1,400	1.66E-07	7,500	1.79E-06	100,000	5.01E-06
1,600	1.79E-07	7,740	1.97E-06		

Table 4.2-21: Vault 4 Wall Effective Matrix Diffusion Coefficients for Case E

Time (years)	D_{eff}	Time (years)	D_{eff}	Time (years)	D_{eff}
0	5.00E-08	1,400	5.45E-08	6,500	6.24E-08
50	5.02E-08	1,600	5.49E-08	7,000	6.31E-08
100	5.06E-08	1,800	5.53E-08	7,500	6.38E-08
150	5.09E-08	2,000	5.57E-08	8,000	6.45E-08
200	5.11E-08	2,300	5.62E-08	8,500	6.51E-08
250	5.14E-08	2,600	5.67E-08	9,000	6.58E-08
300	5.16E-08	2,900	5.72E-08	9,500	6.64E-08
350	5.18E-08	3,200	5.77E-08	10,000	6.71E-08
400	5.20E-08	3,600	5.83E-08	11,000	6.80E-08
450	5.22E-08	4,000	5.89E-08	12,000	6.93E-08
500	5.24E-08	4,500	5.96E-08	12,839	7.04E-08
600	5.26E-08	4,594	6.00E-08	15,000	7.23E-08
700	5.30E-08	5,000	6.04E-08	20,000	7.68E-08
800	5.33E-08	5,134	6.08E-08	25,004	8.32E-08
900	5.35E-08	5,500	6.11E-08	39,421	9.65E-08
1,000	5.38E-08	5,836	6.16E-08	40,000	1.17E-07
1,200	5.41E-08	6,000	6.20E-08	100,000	2.14E-07

Table 4.2-22: Vault 4 Saltstone Effective Matrix Diffusion Coefficients for Case K

Time (years)	D_{eff}	Time (years)	D_{eff}	Time (years)	D_{eff}
0	1.00E-07	1,600	1.79E-07	7,500	1.87E-06
50	1.01E-07	1,800	1.94E-07	7,635	1.93E-06
100	1.03E-07	2,000	2.10E-07	8,000	2.13E-06
150	1.05E-07	2,300	2.32E-07	8,141	2.35E-06
200	1.07E-07	2,600	2.60E-07	8,500	2.59E-06
250	1.09E-07	2,900	2.93E-07	9,000	3.07E-06
300	1.11E-07	3,200	3.30E-07	9,200	3.52E-06
350	1.13E-07	3,500	3.71E-07	9,219	3.68E-06
400	1.15E-07	3,600	4.00E-07	9,400	3.81E-06
450	1.18E-07	4,000	4.41E-07	9,500	4.03E-06
500	1.20E-07	4,500	5.26E-07	9,600	4.19E-06
600	1.24E-07	4,615	5.93E-07	9,700	4.38E-06
700	1.28E-07	5,000	6.56E-07	9,800	4.54E-06
800	1.34E-07	5,500	7.80E-07	9,900	4.73E-06
900	1.39E-07	6,000	9.48E-07	10,000	4.92E-06
1,000	1.45E-07	6,500	1.15E-06	14,844	5.01E-06
1,200	1.53E-07	7,000	1.40E-06	20,000	5.01E-06
1,400	1.66E-07	7,467	1.69E-06	100,0000	5.01E-06

Table 4.2-23: FDC Wall Effective Matrix Diffusion Coefficients for the Base Case

Time (years)	D_{eff}	Time (years)	D_{eff}	Time (years)	D_{eff}
0	5.00E-08	1,200	6.42E-08	7,000	1.25E-07
50	5.06E-08	1,400	6.59E-08	7,500	1.33E-07
100	5.16E-08	1,600	6.76E-08	8,000	1.42E-07
150	5.26E-08	1,800	6.93E-08	8,500	1.51E-07
200	5.34E-08	2,000	7.10E-08	9,000	1.62E-07
250	5.42E-08	2,300	7.32E-08	9,500	1.74E-07
300	5.49E-08	2,600	7.59E-08	10,000	1.88E-07
350	5.56E-08	2,900	7.85E-08	11,000	2.16E-07
400	5.63E-08	3,200	8.12E-08	12,000	2.57E-07
450	5.69E-08	3,600	8.46E-08	14,928	4.49E-07
500	5.75E-08	4,000	8.85E-08	15,000	8.01E-07
600	5.84E-08	4,500	9.31E-08	16,344	1.12E-06
700	5.96E-08	5,000	9.86E-08	16,753	2.22E-06
800	6.07E-08	5,500	1.04E-07	20,000	4.54E-06
900	6.18E-08	6,000	1.11E-07	100,000	4.54E-06
1,000	6.28E-08	6,500	1.17E-07		

Table 4.2-24: FDC Wall Effective Matrix Diffusion Coefficients for Case B

Time (years)	D_{eff}	Time (years)	D_{eff}	Time (years)	D_{eff}
0	5.00E-08	1,200	6.42E-08	7,000	1.25E-07
50	5.06E-08	1,400	6.59E-08	7,500	1.33E-07
100	5.16E-08	1,600	6.76E-08	8,000	1.42E-07
150	5.26E-08	1,800	6.93E-08	8,500	1.51E-07
200	5.34E-08	2,000	7.10E-08	9,000	1.62E-07
250	5.42E-08	2,300	7.32E-08	9,500	1.74E-07
300	5.49E-08	2,600	7.59E-08	10,000	1.88E-07
350	5.56E-08	2,900	7.85E-08	11,000	2.16E-07
400	5.63E-08	3,200	8.12E-08	12,000	2.57E-07
450	5.69E-08	3,600	8.46E-08	15,000	4.58E-07
500	5.75E-08	4,000	8.85E-08	15,784	9.54E-07
600	5.84E-08	4,500	9.31E-08	16,027	1.14E-06
700	5.96E-08	5,000	9.86E-08	16,985	2.14E-06
800	6.07E-08	5,500	1.04E-07	20,000	4.67E-06
900	6.18E-08	6,000	1.11E-07	100,000	5.00E-06
1,000	6.28E-08	6,500	1.17E-07		

Table 4.2-25: FDC Wall Effective Matrix Diffusion Coefficients for Case C

Time (years)	D_{eff}	Time (years)	D_{eff}	Time (years)	D_{eff}
0	5.00E-08	1,200	6.42E-08	7,000	1.25E-07
50	5.06E-08	1,400	6.59E-08	7,500	1.33E-07
100	5.16E-08	1,600	6.76E-08	8,000	1.42E-07
150	5.26E-08	1,800	6.93E-08	8,500	1.51E-07
200	5.34E-08	2,000	7.10E-08	9,000	1.62E-07
250	5.42E-08	2,300	7.32E-08	9,500	1.74E-07
300	5.49E-08	2,600	7.59E-08	10,000	1.88E-07
350	5.56E-08	2,900	7.85E-08	11,000	2.16E-07
400	5.63E-08	3,200	8.12E-08	12,000	2.57E-07
450	5.69E-08	3,600	8.46E-08	15,000	4.58E-07
500	5.75E-08	4,000	8.85E-08	15,803	9.57E-07
600	5.84E-08	4,500	9.31E-08	16,052	1.15E-06
700	5.96E-08	5,000	9.86E-08	17,224	2.39E-06
800	6.07E-08	5,500	1.04E-07	20,000	4.79E-06
900	6.18E-08	6,000	1.11E-07	50,000	5.00E-06
1,000	6.28E-08	6,500	1.17E-07	100,000	5.00E-06

Table 4.2-26: FDC Wall Effective Matrix Diffusion Coefficients for Case D

Time (years)	D_{eff}	Time (years)	D_{eff}	Time (years)	D_{eff}
0	5.00E-08	1,200	6.42E-08	7,000	1.25E-07
50	5.06E-08	1,400	6.59E-08	7,500	1.33E-07
100	5.16E-08	1,600	6.76E-08	8,000	1.42E-07
150	5.26E-08	1,800	6.93E-08	8,500	1.51E-07
200	5.34E-08	2,000	7.10E-08	9,000	1.62E-07
250	5.42E-08	2,300	7.32E-08	9,500	1.74E-07
300	5.49E-08	2,600	7.59E-08	10,000	1.88E-07
350	5.56E-08	2,900	7.85E-08	11,000	2.16E-07
400	5.63E-08	3,200	8.12E-08	12,000	2.57E-07
450	5.69E-08	3,600	8.46E-08	15,000	4.58E-07
500	5.75E-08	4,000	8.85E-08	15,803	9.57E-07
600	5.84E-08	4,500	9.31E-08	16,052	1.15E-06
700	5.96E-08	5,000	9.86E-08	17,224	2.39E-06
800	6.07E-08	5,500	1.04E-07	20,000	4.79E-06
900	6.18E-08	6,000	1.11E-07	50,000	5.00E-06
1,000	6.28E-08	6,500	1.17E-07	100,000	5.00E-06

Table 4.2-27: FDC Wall Effective Matrix Diffusion Coefficients for Case E

Time (years)	D_{eff}	Time (years)	D_{eff}	Time (years)	D_{eff}
0	1.00E-07	1,200	6.42E-08	7,000	1.25E-07
50	5.06E-08	1,400	6.59E-08	7,500	1.33E-07
100	5.16E-08	1,600	6.76E-08	8,000	1.42E-07
150	5.26E-08	1,800	6.93E-08	8,500	1.51E-07
200	5.34E-08	2,000	7.10E-08	9,000	1.62E-07
250	5.42E-08	2,300	7.32E-08	9,500	1.74E-07
300	5.49E-08	2,600	7.59E-08	10,000	1.88E-07
350	5.56E-08	2,900	7.85E-08	11,000	2.16E-07
400	5.63E-08	3,200	8.12E-08	12,000	2.57E-07
450	5.69E-08	3,600	8.46E-08	14,716	4.26E-07
500	5.75E-08	4,000	8.85E-08	15,000	7.64E-07
600	5.84E-08	4,500	9.31E-08	15,631	9.26E-07
700	5.96E-08	5,000	9.86E-08	15,841	1.08E-06
800	6.07E-08	5,500	1.04E-07	20,000	3.93E-06
900	6.18E-08	6,000	1.11E-07		
1,000	6.28E-08	6,500	1.17E-07		

Table 4.2-28: FDC Wall Effective Matrix Diffusion Coefficients for Case K

Time (years)	D_{eff}	Time (years)	D_{eff}	Time (years)	D_{eff}
0	5.00E-08	1,800	1.09E-07	8,000	1.98E-06
50	5.04E-08	2,000	1.20E-07	8,091	2.03E-06
100	5.17E-08	2,300	1.34E-07	8,232	2.14E-06
150	5.26E-08	2,600	1.54E-07	8,462	2.33E-06
200	5.39E-08	2,900	1.77E-07	8,500	2.48E-06
250	5.52E-08	3,200	2.03E-07	9,000	2.82E-06
300	5.64E-08	3,500	2.33E-07	9,200	3.30E-06
350	5.77E-08	3,600	2.56E-07	9,385	3.62E-06
400	5.93E-08	4,000	2.87E-07	9,400	3.77E-06
450	6.06E-08	4,500	3.55E-07	9,500	3.87E-06
500	6.18E-08	5,000	4.47E-07	9,600	4.06E-06
600	6.41E-08	5,500	5.61E-07	9,688	4.25E-06
700	6.72E-08	6,000	7.07E-07	9,700	4.34E-06
800	7.04E-08	6,500	8.91E-07	9,800	4.47E-06
900	7.36E-08	7,000	1.12E-06	9,900	4.66E-06
1,000	7.71E-08	7,361	1.36E-06	10,000	4.88E-06
1,200	8.28E-08	7,500	1.53E-06	20,000	5.01E-06
1,400	9.07E-08	7,756	1.68E-06		
1,600	9.96E-08	7,970	1.87E-06		

Table 4.2-29: FDC Saltstone Effective Matrix Diffusion Coefficients for Case K

Time (years)	D_{eff}	Time (years)	D_{eff}	Time (years)	D_{eff}
0	1.00E-07	1,800	1.94E-07	8,000	2.27E-06
50	1.01E-07	2,000	2.10E-07	8,091	2.33E-06
100	1.03E-07	2,300	2.32E-07	8,232	2.44E-06
150	1.05E-07	2,600	2.60E-07	8,462	2.62E-06
200	1.07E-07	2,900	2.93E-07	8,500	2.76E-06
250	1.09E-07	3,200	3.30E-07	9,000	3.07E-06
300	1.11E-07	3,500	3.71E-07	9,200	3.52E-06
350	1.13E-07	3,600	4.00E-07	9,385	3.81E-06
400	1.15E-07	4,000	4.41E-07	9,400	3.93E-06
450	1.18E-07	4,500	5.26E-07	9,500	4.03E-06
500	1.20E-07	5,000	6.41E-07	9,600	4.19E-06
600	1.24E-07	5,500	7.80E-07	9,688	4.34E-06
700	1.28E-07	6,000	9.48E-07	9,700	4.44E-06
800	1.34E-07	6,500	1.15E-06	9,800	4.54E-06
900	1.39E-07	7,000	1.40E-06	9,900	4.73E-06
1,000	1.45E-07	7,361	1.66E-06	10,000	4.92E-06
1,200	1.53E-07	7,500	1.83E-06	20,000	5.01E-06
1,400	1.66E-07	7,756	1.98E-06		
1,600	1.79E-07	7,970	2.17E-06		

Table 4.2-30: FDC HDPE Effective Matrix Diffusion Coefficients for the Base Case

Time (years)	D_{eff}	Time (years)	D_{eff}	Time (years)	D_{eff}
0	4.75E-10	1,200	9.65E-09	7,000	5.90E-08
50	4.77E-10	1,400	1.14E-08	7,500	6.33E-08
100	7.02E-10	1,600	1.32E-08	8,000	6.77E-08
150	1.12E-09	1,800	1.49E-08	8,500	7.21E-08
200	1.58E-09	2,000	1.66E-08	9,000	7.64E-08
250	2.02E-09	2,300	1.88E-08	9,500	8.08E-08
300	2.45E-09	2,600	2.14E-08	10,000	8.52E-08
350	2.89E-09	2,900	2.41E-08	11,000	9.17E-08
400	3.32E-09	3,200	2.67E-08	12,000	1.00E-07
450	3.76E-09	3,600	2.97E-08	14,928	1.18E-07
500	4.20E-09	4,000	3.32E-08	15,000	1.31E-07
600	4.85E-09	4,500	3.72E-08	16,344	1.37E-07
700	5.73E-09	5,000	4.15E-08	16,753	1.45E-07
800	6.60E-09	5,500	4.59E-08	20,000	1.61E-07
900	7.47E-09	6,000	5.03E-08	100,000	6.54E-07
1,000	8.34E-09	6,500	5.46E-08		

Table 4.2-31: FDC HDPE Effective Matrix Diffusion Coefficients for Case B

Time (years)	D_{eff}	Time (years)	D_{eff}	Time (years)	D_{eff}
0	4.75E-10	1,200	9.65E-09	7,000	5.90E-08
50	4.77E-10	1,400	1.14E-08	7,500	6.33E-08
100	7.02E-10	1,600	1.32E-08	8,000	6.77E-08
150	1.12E-09	1,800	1.49E-08	8,500	7.21E-08
200	1.58E-09	2,000	1.66E-08	9,000	7.64E-08
250	2.02E-09	2,300	1.88E-08	9,500	8.08E-08
300	2.45E-09	2,600	2.14E-08	10,000	8.52E-08
350	2.89E-09	2,900	2.41E-08	11,000	9.17E-08
400	3.32E-09	3,200	2.67E-08	12,000	1.00E-07
450	3.76E-09	3,600	2.97E-08	15,000	1.18E-07
500	4.20E-09	4,000	3.32E-08	15,784	1.34E-07
600	4.85E-09	4,500	3.72E-08	16,027	1.39E-07
700	5.73E-09	5,000	4.15E-08	16,985	1.44E-07
800	6.60E-09	5,500	4.59E-08	20,000	1.62E-07
900	7.47E-09	6,000	5.03E-08	100,000	6.54E-07
1,000	8.34E-09	6,500	5.46E-08		

Table 4.2-32: FDC HDPE Effective Matrix Diffusion Coefficients for Case C

Time (years)	D_{eff}	Time (years)	D_{eff}	Time (years)	D_{eff}
0	4.75E-10	1,200	9.65E-09	7,000	5.90E-08
50	4.77E-10	1,400	1.14E-08	7,500	6.33E-08
100	7.02E-10	1,600	1.32E-08	8,000	6.77E-08
150	1.12E-09	1,800	1.49E-08	8,500	7.21E-08
200	1.58E-09	2,000	1.66E-08	9,000	7.64E-08
250	2.02E-09	2,300	1.88E-08	9,500	8.08E-08
300	2.45E-09	2,600	2.14E-08	10,000	8.52E-08
350	2.89E-09	2,900	2.41E-08	11,000	9.17E-08
400	3.32E-09	3,200	2.67E-08	12,000	1.00E-07
450	3.76E-09	3,600	2.97E-08	15,000	1.18E-07
500	4.20E-09	4,000	3.32E-08	15,803	1.35E-07
600	4.85E-09	4,500	3.72E-08	16,052	1.39E-07
700	5.73E-09	5,000	4.15E-08	17,224	1.45E-07
800	6.60E-09	5,500	4.59E-08	20,000	1.63E-07
900	7.47E-09	6,000	5.03E-08	100,000	6.54E-07
1,000	8.34E-09	6,500	5.46E-08		

Table 4.2-33: FDC HDPE Effective Matrix Diffusion Coefficients for Case D

Time (years)	D_{eff}	Time (years)	D_{eff}	Time (years)	D_{eff}
0	4.75E-10	1,200	9.65E-09	7,000	5.90E-08
50	4.77E-10	1,400	1.14E-08	7,500	6.33E-08
100	7.02E-10	1,600	1.32E-08	8,000	6.77E-08
150	1.12E-09	1,800	1.49E-08	8,500	7.21E-08
200	1.58E-09	2,000	1.66E-08	9,000	7.64E-08
250	2.02E-09	2,300	1.88E-08	9,500	8.08E-08
300	2.45E-09	2,600	2.14E-08	10,000	8.52E-08
350	2.89E-09	2,900	2.41E-08	11,000	9.17E-08
400	3.32E-09	3,200	2.67E-08	12,000	1.00E-07
450	3.76E-09	3,600	2.97E-08	15,000	1.18E-07
500	4.20E-09	4,000	3.32E-08	15,803	1.35E-07
600	4.85E-09	4,500	3.72E-08	16,052	1.39E-07
700	5.73E-09	5,000	4.15E-08	17,224	1.45E-07
800	6.60E-09	5,500	4.59E-08	20,000	1.63E-07
900	7.47E-09	6,000	5.03E-08	100,000	6.54E-07
1,000	8.34E-09	6,500	5.46E-08		

Table 4.2-34: FDC HDPE Effective Matrix Diffusion Coefficients for Case E

Time (years)	D_{eff}	Time (years)	D_{eff}	Time (years)	D_{eff}
0	4.75E-10	1,200	9.65E-09	7,000	5.90E-08
50	4.77E-10	1,400	1.14E-08	7,500	6.33E-08
100	7.02E-10	1,600	1.32E-08	8,000	6.77E-08
150	1.12E-09	1,800	1.49E-08	8,500	7.21E-08
200	1.58E-09	2,000	1.66E-08	9,000	7.64E-08
250	2.02E-09	2,300	1.88E-08	9,500	8.08E-08
300	2.45E-09	2,600	2.14E-08	10,000	8.52E-08
350	2.89E-09	2,900	2.41E-08	11,000	9.17E-08
400	3.32E-09	3,200	2.67E-08	12,000	1.00E-07
450	3.76E-09	3,600	2.97E-08	14,716	1.17E-07
500	4.20E-09	4,000	3.32E-08	15,000	1.30E-07
600	4.85E-09	4,500	3.72E-08	15,631	1.34E-07
700	5.73E-09	5,000	4.15E-08	15,841	1.37E-07
800	6.60E-09	5,500	4.59E-08	20,000	1.57E-07
900	7.47E-09	6,000	5.03E-08	100,000	6.54E-07
1,000	8.34E-09	6,500	5.46E-08		

Table 4.2-35: FDC HDPE Effective Matrix Diffusion Coefficients for Case K

Time (years)	D_{eff}	Time (years)	D_{eff}	Time (years)	D_{eff}
0	4.70E-10	2,900	2.41E-08	9,500	8.25E-08
50	4.76E-10	3,200	2.67E-08	9,600	8.34E-08
100	7.01E-10	3,500	2.93E-08	9,688	8.44E-08
150	1.12E-09	3,600	3.10E-08	9,700	8.47E-08
200	1.58E-09	4,000	3.33E-08	9,800	8.53E-08
250	2.01E-09	4,500	3.71E-08	9,900	8.59E-08
300	2.45E-09	5,000	4.15E-08	10,000	8.69E-08
350	2.89E-09	5,500	4.60E-08	10,129	8.78E-08
400	3.33E-09	6,000	5.01E-08	11,000	9.23E-08
450	3.77E-09	6,500	5.45E-08	11,784	9.96E-08
500	4.19E-09	7,000	5.90E-08	11,795	1.03E-07
600	4.85E-09	7,361	6.28E-08	12,000	1.04E-07
700	5.74E-09	7,500	6.50E-08	13,500	1.11E-07
800	6.60E-09	7,756	6.66E-08	15,000	1.24E-07
900	7.48E-09	7,970	6.88E-08	16,500	1.38E-07
1,000	8.34E-09	8,091	7.04E-08	18,000	1.51E-07
1,200	9.64E-09	8,232	7.14E-08	18,800	1.61E-07
1,400	1.14E-08	8,462	7.29E-08	18,900	1.65E-07
1,600	1.32E-08	8,500	7.42E-08	19,013	1.66E-07
1,800	1.49E-08	9,000	7.64E-08	19,500	1.68E-07
2,000	1.67E-08	9,200	7.96E-08	19,700	1.71E-07
2,300	1.88E-08	9,385	8.12E-08	20,000	1.74E-07
2,600	2.14E-08	9,400	8.21E-08		

4.2.5 Flow Rates

The SDF vertical components of Darcy velocity used in the SDF GoldSim model to describe vertical advective transport through the disposal units are based on spatially averaged (in the horizontal plane) PORFLOW generated downward components of Darcy velocities. Total fluxes through specific engineered barrier components (saltstone, wall, and floor) are used to determine transition times at which changes in sorption coefficients are initiated. In setting up the SDF GoldSim model, several simplifications were made with respect to the flow and its continuity. Only the vertical components of the flow fields are considered. In addition, saturations level assumptions in the disposal unit are 1.0. The Darcy velocities, for the components of the disposal units are derived from PORFLOW outputs using Visual Basic macros in Excel. The spreadsheet files used to generate the Base Case through E, and K flow fields for the SDF GoldSim model are listed in Tables 4.2-36 through 4.2-41 respectively.

Note that for the Base Case and Alternative Sensitivity Case K, there are additional sets of files listed for the Vault 4 unsaturated zone flow fields. The *.tab files were generated directly by PORFLOW and are based on spatially averaging of all the unsaturated zone elements beneath the engineered barrier. When the completely averaged values generated releases which were more compatible with PORFLOW results, the "*.tab" files were used instead of the vertically differentiated flow fields. Note that the 2-D aspects of the unsaturated zone flow fields dictate whether the completely (horizontal and vertically) averaged values are appropriate. Spatially averaged volumetric fluxes generated by the SDF PORFLOW model were used in the transition time calculations. Note the fluxes represent an averaging over a complete segment of the structure, for example, both the modeled walls in Vault 4, as opposed to the two spatially separated walls. The use of averaged fluxes in conjunction with the complete volume of both walls is consistent with the methodology used in the SDF PORFLOW modeling.

Table 4.2-36: The Base Case PORFLOW Flow Fields for Disposal Units

Data	Disposal Unit Type	GoldSim Element	Source File
Grout Zone 1 Darcy Velocity	Vault 1	*V1_CaseA_Grout1*	FlowFieldFilesV1CaseA_Run2.xls
Grout Zone 2 Darcy Velocity	Vault 1	*V1_CaseA_Grout2*	FlowFieldFilesV1CaseA_Run2.xls
Grout Fast Zone Darcy Velocity	Vault 1	*V1_CaseA_GroutFast*	FlowFieldFilesV1CaseA_Run2.xls
Single-Valued Wall Darcy Velocity	Vault 1	*V1_CaseA_Wall*	FlowFieldFilesV1CaseA_Run2.xls
Depth Dependent Wall Darcy Velocity	Vault 1	*V1_CaseA_Wall_vec*	FlowFieldFilesV1CaseA_Run2.xls
Backfill Darcy Velocity	Vault 1	*V1_CaseA_Dirt*	FlowFieldFilesV1CaseA_Run2.xls
Unsaturated Zone Darcy Velocity	Vault 1	*V1_CaseA_UZ*	FlowFieldFilesV1CaseA_Run2.xls
Grout Zone 1 Darcy Velocity	Vault 4	*V4_CaseA_Grout1*	FlowFieldFilesV4CaseA_Run1c.xls
Grout Zone 2 Darcy Velocity	Vault 4	*V4_CaseA_Grout2*	FlowFieldFilesV4CaseA_Run1c.xls
Grout Fast Zone Darcy Velocity	Vault 4	*V4_CaseA_GroutFast*	FlowFieldFilesV4CaseA_Run1c.xls
Sheet Drain Zone 1 Darcy Velocity	Vault 4	*V4_CaseA_ SheetDrain1*	FlowFieldFilesV4CaseA_Run1c.xls
Sheet Drain Zone 2 Darcy Velocity	Vault 4	*V4_CaseA_ SheetDrain2*	FlowFieldFilesV4CaseA_Run1c.xls
Wall 1 Darcy Velocity	Vault 4	*V4_CaseA_Wall*	FlowFieldFilesV4CaseA_Run1c.xls
Single-Valued Wall 2 Darcy Velocity	Vault 4	*V4_CaseA_Wall*	FlowFieldFilesV4CaseA_Run1c.xls
Depth Dependent Wall 2 Darcy Velocity	Vault 4	*V4_CaseA_Wall_vec*	FlowFieldFilesV4CaseA_Run1c.xls
Backfill Darcy Velocity	Vault 4	*V4_CaseA_Dirt*	FlowFieldFilesV4CaseA_Run1c.xls
Spatially Averaged Unsaturated Zone Darcy Velocity	Vault 4	*V4_CaseA_UZ*	flowratesV4CaseA.tab
Vertically Discretized Unsaturated Zone Darcy Velocity	Vault 4	*V4_CaseA_UZ_1*	FlowFieldFilesV4CaseA_Run1c.xls
Grout Zone 1 Darcy Velocity	FDCs	*V2_CaseA_Grout1*	FlowFieldFilesV2CaseA_Run1c.xls
Grout Zone 2 Darcy Velocity	FDCs	*V2_CaseA_Grout2*	FlowFieldFilesV2CaseA_Run4.xls
Grout Fast Zone Darcy Velocity	FDCs	*V2_CaseA_GroutFast*	FlowFieldFilesV2CaseA_Run4.xls
Sheet Drain Darcy Velocity	FDCs	*V2_CaseA_ SheetDrain1*	FlowFieldFilesV2CaseA_Run4.xls
Single-Valued Wall Darcy Velocity	FDCs	*V2_CaseA_Wall*	FlowFieldFilesV2CaseA_Run4.xls
Depth Dependent Wall Darcy Velocity	FDCs	*V2_CaseA_Wall_vec*	FlowFieldFilesV2CaseA_Run4.xls
Shot Crete Darcy Velocity	FDCs	*V2_CaseA_ShotCrete*	FlowFieldFilesV2CaseA_Run4.xls
HDPE Darcy Velocity	FDCs	*V2_CaseA_HDPE*	FlowFieldFilesV2CaseA_Run4.xls
Backfill Darcy Velocity	FDCs	*V2_CaseA_Dirt*	FlowFieldFilesV2CaseA_Run4.xls
Vertically Discretized Unsaturated Zone Darcy Velocity	FDCs	*V2_CaseA_UZ*	FlowFieldFilesV2CaseA_Run4.xls

Table 4.2-37: Case B PORFLOW Flow Fields for Disposal Units

Data	Disposal Unit Type	GoldSim Element	Source File
Grout Zone 1 Darcy Velocity	Vault 1	*V1_CaseA_Grout1*	FlowFieldFilesV1CaseA_Run2.xls
Grout Zone 2 Darcy Velocity	Vault 1	*V1_CaseA_Grout2*	FlowFieldFilesV1CaseA_Run2.xls
Grout Fast Zone Darcy Velocity	Vault 1	*V1_CaseA_GroutFast*	FlowFieldFilesV1CaseA_Run2.xls
Single-Valued Wall Darcy Velocity	Vault 1	*V1_CaseA_Wall*	FlowFieldFilesV1CaseA_Run2.xls
Depth Dependent Wall Darcy Velocity	Vault 1	*V1_CaseA_Wall_vec*	FlowFieldFilesV1CaseA_Run2.xls
Backfill Darcy Velocity	Vault 1	*V1_CaseA_Dirt*	FlowFieldFilesV1CaseA_Run2.xls
Unsaturated Zone Darcy Velocity	Vault 1	*V1_CaseA_UZ*	FlowFieldFilesV1CaseA_Run2.xls
Grout Zone 1 Darcy Velocity	Vault 4	*V4_CaseB_Grout1*	FlowFieldFilesV4CaseB_Run1c.xls
Grout Zone 2 Darcy Velocity	Vault 4	*V4_CaseB_Grout2*	FlowFieldFilesV4CaseB_Run1c.xls
Grout Fast Zone Darcy Velocity	Vault 4	*V4_CaseB_GroutFast*	FlowFieldFilesV4CaseB_Run1c.xls
Sheet Drain Zone 1 Darcy Velocity	Vault 4	*V4_CaseB_ SheetDrain1*	FlowFieldFilesV4CaseB_Run1c.xls
Sheet Drain Zone 2 Darcy Velocity	Vault 4	*V4_CaseB_ SheetDrain2*	FlowFieldFilesV4CaseB_Run1c.xls
Wall 1 Darcy Velocity	Vault 4	*V4_CaseB_Wall*	FlowFieldFilesV4CaseB_Run1c.xls
Single-Valued Wall 2 Darcy Velocity	Vault 4	*V4_CaseB_Wall*	FlowFieldFilesV4CaseB_Run1c.xls
Depth Dependent Wall 2 Darcy Velocity	Vault 4	*V4_CaseB_Wall_vec*	FlowFieldFilesV4CaseB_Run1c.xls
Backfill Darcy Velocity	Vault 4	*V4_CaseB_Dirt*	FlowFieldFilesV4CaseB_Run1c.xls
Vertically Discretized Unsaturated Zone Darcy Velocity	Vault 4	*V4_CaseB_UZ*	FlowFieldFilesV4CaseB_Run1c.xls
Grout Zone 1 Darcy Velocity	FDCs	*V2_CaseB_Grout1*	FlowFieldFilesV2CaseB_Run1c.xls
Grout Zone 2 Darcy Velocity	FDCs	*V2_CaseB_Grout2*	FlowFieldFilesV2CaseB_Run4.xls
Grout Fast Zone Darcy Velocity	FDCs	*V2_CaseB_GroutFast*	FlowFieldFilesV2CaseB_Run4.xls
Sheet Drain Darcy Velocity	FDCs	*V2_CaseB_ SheetDrain1*	FlowFieldFilesV2CaseB_Run4.xls
Single-Valued Wall Darcy Velocity	FDCs	*V2_CaseB_Wall*	FlowFieldFilesV2CaseB_Run4.xls
Depth Dependent Wall Darcy Velocity	FDCs	*V2_CaseB_Wall_vec*	FlowFieldFilesV2CaseB_Run4.xls
Shot Crete Darcy Velocity	FDCs	*V2_CaseB_ShotCrete*	FlowFieldFilesV2CaseB_Run4.xls
HDPE Darcy Velocity	FDCs	*V2_CaseB_HDPE*	FlowFieldFilesV2CaseB_Run4.xls
Backfill Darcy Velocity	FDCs	*V2_CaseB_Dirt*	FlowFieldFilesV2CaseB_Run4.xls
Vertically Discretized Unsaturated Zone Darcy Velocity	FDCs	*V2_CaseB_UZ*	FlowFieldFilesV2CaseB_Run4.xls

Table 4.2-38: Case C PORFLOW Flow Fields for Disposal Units

Data	Disposal Unit Type	GoldSim Element	Source File
Grout Zone 1 Darcy Velocity	Vault 1	*V1_CaseC_Grout1*	FlowFieldFilesV1CaseC_Run2.xls
Grout Zone 2 Darcy Velocity	Vault 1	*V1_CaseC_Grout2*	FlowFieldFilesV1CaseC_Run2.xls
Grout Fast Zone Darcy Velocity	Vault 1	*V1_CaseC_GroutFast*	FlowFieldFilesV1CaseC_Run2.xls
Single-Valued Wall Darcy Velocity	Vault 1	*V1_CaseC_Wall*	FlowFieldFilesV1CaseC_Run2.xls
Depth Dependent Wall Darcy Velocity	Vault 1	*V1_CaseC_Wall_vec*	FlowFieldFilesV1CaseC_Run2.xls
Backfill Darcy Velocity	Vault 1	*V1_CaseC_Dirt*	FlowFieldFilesV1CaseC_Run2.xls
Unsaturated Zone Darcy Velocity	Vault 1	*V1_CaseC_UZ*	FlowFieldFilesV1CaseC_Run2.xls
Grout Zone 1 Darcy Velocity	Vault 4	*V4_CaseC_Grout1*	FlowFieldFilesV4CaseC_Run1c.xls
Grout Zone 2 Darcy Velocity	Vault 4	*V4_CaseC_Grout2*	FlowFieldFilesV4CaseC_Run1c.xls
Grout Fast Zone Darcy Velocity	Vault 4	*V4_CaseC_GroutFast*	FlowFieldFilesV4CaseC_Run1c.xls
Sheet Drain Zone 1 Darcy Velocity	Vault 4	*V4_CaseC_ SheetDrain1*	FlowFieldFilesV4CaseC_Run1c.xls
Sheet Drain Zone 2 Darcy Velocity	Vault 4	*V4_CaseC_ SheetDrain2*	FlowFieldFilesV4CaseC_Run1c.xls
Wall 1 Darcy Velocity	Vault 4	*V4_CaseC_Wall*	FlowFieldFilesV4CaseC_Run1c.xls
Single-Valued Wall 2 Darcy Velocity	Vault 4	*V4_CaseC_Wall*	FlowFieldFilesV4CaseC_Run1c.xls
Depth Dependent Wall 2 Darcy Velocity	Vault 4	*V4_CaseC_Wall_vec*	FlowFieldFilesV4CaseC_Run1c.xls
Backfill Darcy Velocity	Vault 4	*V4_CaseC_Dirt*	FlowFieldFilesV4CaseC_Run1c.xls
Vertically Discretized Unsaturated Zone Darcy Velocity	Vault 4	*V4_CaseC_UZ*	FlowFieldFilesV4CaseC_Run1c.xls
Grout Zone 1 Darcy Velocity	FDCs	*V2_CaseC_Grout1*	FlowFieldFilesV2CaseC_Run1c.xls
Grout Zone 2 Darcy Velocity	FDCs	*V2_CaseC_Grout2*	FlowFieldFilesV2CaseC_Run4.xls
Grout Fast Zone Darcy Velocity	FDCs	*V2_CaseC_GroutFast*	FlowFieldFilesV2CaseC_Run4.xls
Sheet Drain Darcy Velocity	FDCs	*V2_CaseC_ SheetDrain1*	FlowFieldFilesV2CaseC_Run4.xls
Single-Valued Wall Darcy Velocity	FDCs	*V2_CaseC_Wall*	FlowFieldFilesV2CaseC_Run4.xls
Depth Dependent Wall Darcy Velocity	FDCs	*V2_CaseC_Wall_vec*	FlowFieldFilesV2CaseC_Run4.xls
Shot Crete Darcy Velocity	FDCs	*V2_CaseC_ShotCrete*	FlowFieldFilesV2CaseC_Run4.xls
HDPE Darcy Velocity	FDCs	*V2_CaseC_HDPE*	FlowFieldFilesV2CaseC_Run4.xls
Backfill Darcy Velocity	FDCs	*V2_CaseC_Dirt*	FlowFieldFilesV2CaseC_Run4.xls
Vertically Discretized Unsaturated Zone Darcy Velocity	FDCs	*V2_CaseC_UZ*	FlowFieldFilesV2CaseC_Run4.xls

Table 4.2-39: Case D PORFLOW Flow Fields for Disposal Units

Data	Disposal Unit Type	GoldSim Element	Source File
Grout Zone 1 Darcy Velocity	Vault 1	*V1_CaseA_Grout1*	FlowFieldFilesV1CaseA_Run2.xls
Grout Zone 2 Darcy Velocity	Vault 1	*V1_CaseA_Grout2*	FlowFieldFilesV1CaseA_Run2.xls
Grout Fast Zone Darcy Velocity	Vault 1	*V1_CaseA_GroutFast*	FlowFieldFilesV1CaseA_Run2.xls
Single-Valued Wall Darcy Velocity	Vault 1	*V1_CaseA_Wall*	FlowFieldFilesV1CaseA_Run2.xls
Depth Dependent Wall Darcy Velocity	Vault 1	*V1_CaseA_Wall_vec*	FlowFieldFilesV1CaseA_Run2.xls
Backfill Darcy Velocity	Vault 1	*V1_CaseA_Dirt*	FlowFieldFilesV1CaseA_Run2.xls
Unsaturated Zone Darcy Velocity	Vault 1	*V1_CaseA_UZ*	FlowFieldFilesV1CaseA_Run2.xls
Grout Zone 1 Darcy Velocity	Vault 4	*V4_CaseD_Grout1*	FlowFieldFilesV4CaseD_Run1c.xls
Grout Zone 2 Darcy Velocity	Vault 4	*V4_CaseD_Grout2*	FlowFieldFilesV4CaseD_Run1c.xls
Grout Fast Zone Darcy Velocity	Vault 4	*V4_CaseD_GroutFast*	FlowFieldFilesV4CaseD_Run1c.xls
Sheet Drain Zone 1 Darcy Velocity	Vault 4	*V4_CaseD_ SheetDrain1*	FlowFieldFilesV4CaseD_Run1c.xls
Sheet Drain Zone 2 Darcy Velocity	Vault 4	*V4_CaseD_ SheetDrain2*	FlowFieldFilesV4CaseD_Run1c.xls
Wall 1 Darcy Velocity	Vault 4	*V4_CaseD_Wall*	FlowFieldFilesV4CaseD_Run1c.xls
Single-Valued Wall 2 Darcy Velocity	Vault 4	*V4_CaseD_Wall*	FlowFieldFilesV4CaseD_Run1c.xls
Depth Dependent Wall 2 Darcy Velocity	Vault 4	*V4_CaseD_Wall_vec*	FlowFieldFilesV4CaseD_Run1c.xls
Backfill Darcy Velocity	Vault 4	*V4_CaseD_Dirt*	FlowFieldFilesV4CaseD_Run1c.xls
Vertically Discretized Unsaturated Zone Darcy Velocity	Vault 4	*V4_CaseD_UZ*	FlowFieldFilesV4CaseD_Run1c.xls
Grout Zone 1 Darcy Velocity	FDCs	*V2_CaseD_Grout1*	FlowFieldFilesV2CaseD_Run1c.xls
Grout Zone 2 Darcy Velocity	FDCs	*V2_CaseD_Grout2*	FlowFieldFilesV2CaseD_Run4.xls
Grout Fast Zone Darcy Velocity	FDCs	*V2_CaseD_GroutFast*	FlowFieldFilesV2CaseD_Run4.xls
Sheet Drain Darcy Velocity	FDCs	*V2_CaseD_ SheetDrain1*	FlowFieldFilesV2CaseD_Run4.xls
Single-Valued Wall Darcy Velocity	FDCs	*V2_CaseD_Wall*	FlowFieldFilesV2CaseD_Run4.xls
Depth Dependent Wall Darcy Velocity	FDCs	*V2_CaseD_Wall_vec*	FlowFieldFilesV2CaseD_Run4.xls
Shot Crete Darcy Velocity	FDCs	*V2_CaseD_ShotCrete*	FlowFieldFilesV2CaseD_Run4.xls
HDPE Darcy Velocity	FDCs	*V2_CaseD_HDPE*	FlowFieldFilesV2CaseD_Run4.xls
Backfill Darcy Velocity	FDCs	*V2_CaseD_Dirt*	FlowFieldFilesV2CaseD_Run4.xls
Vertically Discretized Unsaturated Zone Darcy Velocity	FDCs	*V2_CaseD_UZ*	FlowFieldFilesV2CaseD_Run4.xls

Table 4.2-40: Case E PORFLOW Flow Fields for Disposal Units

Data	Disposal Unit Type	GoldSim Element	Source File
Grout Zone 1 Darcy Velocity	Vault 1	*V1_CaseE_Grout1*	FlowFieldFilesV1CaseE_Run2.xls
Grout Zone 2 Darcy Velocity	Vault 1	*V1_CaseE_Grout2*	FlowFieldFilesV1CaseE_Run2.xls
Grout Fast Zone Darcy Velocity	Vault 1	*V1_CaseE_GroutFast*	FlowFieldFilesV1CaseE_Run2.xls
Single-Valued Wall Darcy Velocity	Vault 1	*V1_CaseE_Wall*	FlowFieldFilesV1CaseE_Run2.xls
Depth Dependent Wall Darcy Velocity	Vault 1	*V1_CaseE_Wall_vec*	FlowFieldFilesV1CaseE_Run2.xls
Backfill Darcy Velocity	Vault 1	*V1_CaseE_Dirt*	FlowFieldFilesV1CaseE_Run2.xls
Unsaturated Zone Darcy Velocity	Vault 1	*V1_CaseE_UZ*	FlowFieldFilesV1CaseE_Run2.xls
Grout Zone 1 Darcy Velocity	Vault 4	*V4_CaseE_Grout1*	FlowFieldFilesV4CaseE_Run1c.xls
Grout Zone 2 Darcy Velocity	Vault 4	*V4_CaseE_Grout2*	FlowFieldFilesV4CaseE_Run1c.xls
Grout Fast Zone Darcy Velocity	Vault 4	*V4_CaseE_GroutFast*	FlowFieldFilesV4CaseE_Run1c.xls
Sheet Drain Zone 1 Darcy Velocity	Vault 4	*V4_CaseE_ SheetDrain1*	FlowFieldFilesV4CaseE_Run1c.xls
Sheet Drain Zone 2 Darcy Velocity	Vault 4	*V4_CaseE_ SheetDrain2*	FlowFieldFilesV4CaseE_Run1c.xls
Wall 1 Darcy Velocity	Vault 4	*V4_CaseE_Wall*	FlowFieldFilesV4CaseE_Run1c.xls
Single-Valued Wall 2 Darcy Velocity	Vault 4	*V4_CaseE_Wall*	FlowFieldFilesV4CaseE_Run1c.xls
Depth Dependent Wall 2 Darcy Velocity	Vault 4	*V4_CaseE_Wall_vec*	FlowFieldFilesV4CaseE_Run1c.xls
Backfill Darcy Velocity	Vault 4	*V4_CaseE_Dirt*	FlowFieldFilesV4CaseE_Run1c.xls
Vertically Discretized Unsaturated Zone Darcy Velocity	Vault 4	*V4_CaseE_UZ*	FlowFieldFilesV4CaseE_Run1c.xls
Grout Zone 1 Darcy Velocity	FDCs	*V2_CaseE_Grout1*	FlowFieldFilesV2CaseE_Run1c.xls
Grout Zone 2 Darcy Velocity	FDCs	*V2_CaseE_Grout2*	FlowFieldFilesV2CaseE_Run4.xls
Grout Fast Zone Darcy Velocity	FDCs	*V2_CaseE_GroutFast*	FlowFieldFilesV2CaseE_Run4.xls
Sheet Drain Darcy Velocity	FDCs	*V2_CaseE_ SheetDrain1*	FlowFieldFilesV2CaseE_Run4.xls
Single-Valued Wall Darcy Velocity	FDCs	*V2_CaseE_Wall*	FlowFieldFilesV2CaseE_Run4.xls
Depth Dependent Wall Darcy Velocity	FDCs	*V2_CaseE_Wall_vec*	FlowFieldFilesV2CaseE_Run4.xls
Shot Crete Darcy Velocity	FDCs	*V2_CaseE_ShotCrete*	FlowFieldFilesV2CaseE_Run4.xls
HDPE Darcy Velocity	FDCs	*V2_CaseE_HDPE*	FlowFieldFilesV2CaseE_Run4.xls
Backfill Darcy Velocity	FDCs	*V2_CaseE_Dirt*	FlowFieldFilesV2CaseE_Run4.xls
Vertically Discretized Unsaturated Zone Darcy Velocity	FDCs	*V2_CaseE_UZ*	FlowFieldFilesV2CaseE_Run4.xls

Table 4.2-41: Case K PORFLOW Flow Fields for Disposal Units

Data	Disposal Unit Type	GoldSim Element	Source File
Grout Zone 1 Darcy Velocity	Vault 1	*V1_CaseK_Grout1*	FlowFieldFilesV1CaseK_Run3.xls
Grout Zone 2 Darcy Velocity	Vault 1	*V1_CaseK_Grout2*	FlowFieldFilesV1CaseK_Run3.xls
Grout Fast Zone Darcy Velocity	Vault 1	*V1_CaseK_GroutFast*	FlowFieldFilesV1CaseK_Run3.xls
Single-Valued Wall Darcy Velocity	Vault 1	*V1_CaseK_Wall*	FlowFieldFilesV1CaseK_Run3.xls
Depth Dependent Wall Darcy Velocity	Vault 1	*V1_CaseK_Wall_vec*	FlowFieldFilesV1CaseK_Run3.xls
Backfill Darcy Velocity	Vault 1	*V1_CaseK_Dirt*	FlowFieldFilesV1CaseK_Run3.xls
Unsaturated Zone Darcy Velocity	Vault 1	*V1_CaseK_UZ*	FlowFieldFilesV1CaseK_Run3xls
Grout Zone 1 Darcy Velocity	Vault 4	*V4_CaseK_Grout1*	FlowFieldFilesV4CaseK_Run2.xls
Grout Zone 2 Darcy Velocity	Vault 4	*V4_CaseK_Grout2*	FlowFieldFilesV4CaseK_Run2.xls
Grout Fast Zone Darcy Velocity	Vault 4	*V4_CaseK_GroutFast*	FlowFieldFilesV4CaseK_Run2.xls
Sheet Drain Zone 1 Darcy Velocity	Vault 4	*V4_CaseK_ SheetDrain1*	FlowFieldFilesV4CaseK_Run2.xls
Sheet Drain Zone 2 Darcy Velocity	Vault 4	*V4_CaseK_ SheetDrain2*	FlowFieldFilesV4CaseK_Run2.xls
Wall 1 Darcy Velocity	Vault 4	*V4_CaseK_Wall*	FlowFieldFilesV4CaseK_Run2.xls
Single-Valued Wall 2 Darcy Velocity	Vault 4	*V4_CaseK_Wall*	FlowFieldFilesV4CaseK_Run2.xls
Depth Dependent Wall 2 Darcy Velocity	Vault 4	*V4_CaseK_Wall_vec*	FlowFieldFilesV4CaseK_Run2.xls
Backfill Darcy Velocity	Vault 4	*V4_CaseK_Dirt*	FlowFieldFilesV4CaseK_Run2.xls
Spatially Averaged Unsaturated Zone Darcy Velocity	Vault 4	*V4_CaseK_UZ*	flowratesV4CaseK.tab
Vertically Discretized Unsaturated Zone Darcy Velocity	Vault 4	*V4_CaseK_UZ_1*	FlowFieldFilesV4CaseK_Run2.xls
Grout Zone 1 Darcy Velocity	FDCs	*V2_CaseK_Grout1*	FlowFieldFilesV2CaseK_Main6.xls
Grout Zone 2 Darcy Velocity	FDCs	*V2_CaseK_Grout2*	FlowFieldFilesV2CaseK_Main6.xls
Grout Fast Zone Darcy Velocity	FDCs	*V2_CaseK_GroutFast*	FlowFieldFilesV2CaseK_Main6.xls
Sheet Drain Darcy Velocity	FDCs	*V2_CaseK_ SheetDrain1*	FlowFieldFilesV2CaseK_Main6.xls
Single-Valued Wall Darcy Velocity	FDCs	*V2_CaseK_Wall*	FlowFieldFilesV2CaseK_Main6.xls
Depth Dependent Wall Darcy Velocity	FDCs	*V2_CaseK_Wall_vec*	FlowFieldFilesV2CaseK_Main6.xls
Shot Crete Darcy Velocity	FDCs	*V2_CaseK_ShotCrete*	FlowFieldFilesV2CaseK_Main6.xls
HDPE Darcy Velocity	FDCs	*V2_CaseK_HDPE*	FlowFieldFilesV2CaseK_Main6.xls
Backfill Darcy Velocity	FDCs	*V2_CaseK_Dirt*	FlowFieldFilesV2CaseK_Main6.xls
Vertically Discretized Unsaturated Zone Darcy Velocity	FDCs	*V2_CaseK_UZ*	FlowFieldFilesV2CaseK_Main6.xls

4.2.5.1 Transition Times

As noted in Section 4.2.1.5, the SDF GoldSim model solves for chemical transition times based upon the volumes of disposal unit specific zone segments and time-dependent total flux-rates generated by the SDF PORFLOW model. The K_d values for the material properties of the saltstone, the wall, and the floor are time-dependent in the SDF GoldSim model. The chemical transition times are used to determine the chemistry-dependent K_ds based on the present redox stage. [SRR-CWDA-2009-00017 Section 4.2] The redox stages considered by the model include Region II Reducing (middle reducing), Region II Oxidizing

(middle oxidizing), and Region III Oxidizing (old oxidizing). The specific state at any given time is determined by the number of pore volumes of water that have passed through the segment of the disposal unit over time.

Note that all sorbing species, except for Alternative Sensitivity Case K Tc-99 values, are simulated using these step-function changes in the K_ds. Alternative Sensitivity Case K Tc-99 K_ds are assumed to vary over time as discussed in Section 3.5. In stochastic simulations, the number of pore volumes used to define transition times in saltstone are derived from triangular distributions (mean values are used for deterministic simulations). The parameters defining the stochastic distributions for saltstone transition-time pore volumes are listed in Table 4.2-42. The number of pore volumes used to define transition times in concrete (the wall and floor) are also derived from triangular distributions. The parameters defining the stochastic distributions for pore volumes used to define transition times in concrete are listed in Table 4.2-43. Deterministic simulations utilize the mean values of the pore-volume distributions. The transition times as derived by the GoldSim and PORFLOW models are presented in Tables 4.2-44 through 4.2-46, for Vault 1, Vault 2, and the FDCs, respectively.

Table 4.2-42: Distribution Parameters for Pore Volumes Used to Determine Transition Times in Saltstone

Transition Time effected	Pore Volumes	
	Base Case	Case K
Transition from middle age reducing to middle age oxidizing (mean values)	2,806	505
Transition from middle age to old age oxidizing (mean values)	10,422	7,608
Transition from middle age reducing to middle age oxidizing (minimum values)	1,403	415
Transition from middle age to old age oxidizing (minimum values)	5,211	5,606
Transition from middle age reducing to middle age oxidizing (maximum values)	4,209	1,653
Transition from middle age to old age oxidizing (maximum values)	15,633	11,213

Table 4.2-43: Distribution Parameters for Pore Volumes Used to Determine Transition Times in Concrete

Transition Time effected	Pore Volumes	
	Base Case	Case K
Transition from middle age reducing to middle age oxidizing (mean values)	3,230	3,230
Transition from middle age to old age oxidizing (mean values)	4,206	4,206
Transition from middle age reducing to middle age oxidizing (minimum values)	1,615	2,476
Transition from middle age to old age oxidizing (minimum values)	2,103	3,223
Transition from middle age reducing to middle age oxidizing (maximum values)	4,845	4,953
Transition from middle age to old age oxidizing (maximum values)	6,309	6,446

Table 4.2-44: Vault 1 Transition Times

Transition	Case-Specific Time of Occurrence for GoldSim/PORFLOW (years after closure)	
	Base Case	Case K
Floor concrete transitions from middle age reducing to middle age oxidizing	20,000+/40,000+	7,700/7,740
Floor concrete transitions from middle age to old age oxidizing	20,000+/40,000+	8,400/8,227
Wall concrete transitions from middle age reducing to middle age oxidizing	20,000+/20,781	8,300/8,297
Wall concrete transitions from middle age to old age oxidizing	20,000+/21,043	9,500/9,545
Saltstone transitions from middle age reducing to middle age oxidizing	20,000+/50,000+	14,100/14,196
Saltstone transitions from middle age to old age oxidizing	20,000+/50,000+	20,000+/20,000+

[SRR-CWDA-2009-00017 Table 4.4-7 and the Base Case and Alternative Sensitivity Case K PORFLOW result files]
+ = Transition times occur beyond the time indicated.

Table 4.2-45: Vault 4 Transition Times

Transition	Case-Specific Time of Occurrence for GoldSim/PORFLOW (years after closure)	
	Base Case	Case K
Floor concrete transitions from middle age reducing to middle age oxidizing	20,000+/40,000+	7,600/7,635
Floor concrete transitions from middle age to old age oxidizing	20,000+/40,000+	8,100/8,141
Wall concrete transitions from middle age reducing to middle age oxidizing	15,500/15,519	9,200/9,219
Wall concrete transitions from middle age to old age oxidizing	16,000/16,018	10,600/10,671
Saltstone transitions from middle age reducing to middle age oxidizing	20,000+/40,000+	14,800/14,844
Saltstone transitions from middle age to old age oxidizing	20,000+/40,000+	20,000+/20,000+

[SRR-CWDA-2009-00017 Table 4.4-7 and the Base Case and Alternative Sensitivity Case K PORFLOW result files]
+ = Transition times occur beyond the time indicated.

Table 4.2-46: FDC Transition Times

Transition	Case-Specific Time of Occurrence for GoldSim/PORFLOW (years after closure)	
	Base Case	Case K
Floor concrete transitions from middle age reducing to middle age oxidizing	20,000+/22,498	7,900/7,970
Floor concrete transitions from middle age to old age oxidizing	20,000+/23,274	8,400/8,462
Wall concrete transitions from middle age reducing to middle age oxidizing	16,300/16,344	7,700/7,756
Wall concrete transitions from middle age to old age oxidizing	16,700/16,753	8,200/8,232
Saltstone transitions from middle age reducing to middle age oxidizing	20,000+/50,000+	20,000+/20,000+
Saltstone transitions from middle age to old age oxidizing	20,000+/50,000+	20,000+/20,000+

[SRR-CWDA-2009-00017 Table 4.4-7 and the Base Case and Alternative Sensitivity Case K PORFLOW result files]
+ = Transition times occur beyond the time indicated.

4.3 The Vadose Zone

The transport of radionuclides from disposal units to the 100-meter boundary is strongly controlled by the flow rates through the vadose and saturated zones and the geometry of the vadose and saturated zones.

4.3.1 Vadose Zone Flow Rates

The vadose zone flow rates used in the SDF GoldSim model, disposal unit calculations are generated from PORFLOW flow model outputs. These flow rates are generated using the same spreadsheet files described for the engineered barrier in Section 4.2.1.5.

4.3.2 Vadose Zone Geometry

For the disposal units, the vadose zone thicknesses are assigned based disposal unit type. Vault 1 is assigned a vadose zone thickness of 50 feet, Vault 4 is assigned a vadose zone thickness of 40 feet, and the FDCs are assigned a vadose zone thickness of 42 feet. Note that the values for Vaults 1 and 4 differ slightly from SDF PA (SRR-CWDA-2009-00017 Table 4.2-13) values and the FDC value is the average between the high and low values for the FDCs. These values are the same as used in the PA sensitivity and uncertainty analyses. The stochastic distribution for the vadose zone thicknesses is based on a triangular distribution with these values of 50 feet, 40 feet, and 42 feet, representing the most likely values for Vault 1, Vault 4, and the FDCs, respectively. The minimum values for the three distributions are defined by the sum of each most likely value and -5 meters, and the maximum values are defined by the sum of each most likely value and 5 meters.

The areal extent of the vadose zone is defined by the footprints of the disposal units as determined from the widths and lengths for Vaults 1 and 4 and by the radius for the FDCs as listed in Tables 4.2-7, 4.2-8, and 4.2-9, respectively.

4.4 Saturated Zone Inputs

For disposal unit releases, the saturated zone, modeling domain begins at the upgradient edge of the unit and extends to the 100-meter boundary depicted in Figure 3.1-2. Data input specific to the saturated zone includes: 1) data that describes the flow fields controlling the transport of mass released from the disposal units and 2) data describing the geometry of the saturated zone and the spatial relationships between the sources (Vault 1, Vault 4, and the FDCs) and the 100-meter boundary.

4.4.1 Saturated Zone Darcy Velocity

Groundwater flow in the saturated zone is approximated as a unidirectional flow field of constant Darcy velocity. The flow velocity is derived from a PORFLOW simulation of the release of a conservative tracer and the arrival time of peak values in the associated breakthrough curves generated at the 100-meter boundary. The particle's path length to the 100-meter boundary from a stream trace simulation and the time it took for the peak value of the breakthrough curves to reach the boundary were translated into averaged transport velocities. Darcy velocities were in turn derived from the transport velocities and the saturated zone porosity used in the SDF GoldSim model as follows:

$$DarcyVelocity = TransportVelocity \times Porosity \ . \qquad (4.4\text{-}1)$$

The disposal unit-specific average Darcy velocities in the saturated zone are presented in Table 4.4-1 and are located in the GoldSim data elements *MeanSatZoneDarcyVel_V1*, *MeanSatZoneDarcyVel_V4*, and *MeanSatZoneDarcyVel_FDC* found in the container *\Transport\WaterTransport*.

Table 4.4-1: Mean Darcy Velocity (m/yr) from Disposal Units

Disposal Unit ID (north)	Mean Darcy Velocity (m/yr)	Disposal Unit ID (south)	Mean Darcy Velocity (m/yr)
V2A	10.16	V13A	6.37
V2B	10.16	V13B	10.53
V5A	9.15	V13C	12.47
V5B	7.62	V13D	9.98
V5C	12.20	V14A	11.59
V5D	12.96	V14B	8.54
V6A	6.86	V15A	14.48
V6B	6.86	V15B	9.15
V6C	9.91	V15C	13.72
V6D	9.91	V15D	10.21
V7A	3.92	V16A	16.01
V7B	4.36	V16B	14.48
V7C	6.97	V16C	15.24
V7D	5.66	V16D	12.20
V8A	8.13	V17A	18.29
V8B	7.45	V17B	13.21
V8C	9.49	V17C	17.28
V8D	9.49	V17D	13.21
V9A	5.66	V18A	21.34
V9B	4.79	V18B	21.34
V9C	6.53	V18C	15.24
V9D	6.97	V18D	15.24
V10A	7.84	V19A	19.82
V10B	5.23	V19B	13.72
V10C	7.84	V20A	20.33
V10D	5.23	V20B	12.2
V11A	5.13	V20C	14.23
V11B	5.46	V20D	10.16
V11C	7.38	V1	9.85
V11D	6.74	V4	10.45
V12A	4.88		
V12B	4.27		
V12C	5.18		
V12D	3.96		
V3A	6.86		
V3B	6.86		

From the MS Office Excel workbook: "SZVelocities.xls" and its source BreakthroughCurves.ppt See Appendix A for additional information.

4.4.2 Saturated Zone Geometry and Other Spatial Relationships

For solute transport from SDF disposal units, the saturated zone-modeling domain in the SDF GoldSim model begins at the upgradient edge of the disposal unit and extends to the 100-meter boundary. PORFLOW generated stream traces used to outline the 1-D travel pathways over which solute transport from the disposal units to the 100-meter boundary takes place in the SDF GoldSim model are depicted in Figures 3.1-3 for Vault 1, 3.1-4 for Vault 4 and 3.1-5 for the FDCs. Note that for clarity only half of the FDC stream traces are plotted in Figure 3.1-5. The stream traces were generated using particle tracking, with several particles initiated along the perimeter of Vaults 1 and 4, and one particle in the center of the FDCs. The dots along the stream traces represent the particles location at 5-year intervals.

In addition to total pathway lengths, saturated thickness and saturated zone width are needed to define the geometry of the pipe element representing the saturated zone. In addition, dispersivity values are needed to determine how much the released radionuclides spread within the saturated zone. This spreading is an important mechanism contributing to the dilution of the release, as the radionuclides are transported downgradient.

4.4.2.1 Saturated Zone Geometry

4.4.2.1.1 Saturated Zone Pathway Lengths

The saturated zone, transport pathway lengths were provided by the SDF PORFLOW model and are based on the PORFLOW stream trace analysis. These distances are used to define the total length of the saturated zone cell network. The pathway length for each disposal unit is presented in Table 4.4-2.

Table 4.4-2: Distance Traveled from Disposal Units to 100-Meter Boundary

Disposal Unit ID (north)	Distance to 100-meter Boundary (ft)	Disposal Unit ID (south)	Distance to 100-meter Boundary (ft)
V2A	800	V13A	1,920
V2B	800	V13B	1,520
V5A	480	V13C	1,800
V5B	400	V13D	1,440
V5C	640	V14A	760
V5D	680	V14B	560
V6A	360	V15A	760
V6B	360	V15B	480
V6C	520	V15C	720
V6D	520	V15D	536
V7A	360	V16A	1,680
V7B	400	V16B	1,520
V7C	640	V16C	1,600
V7D	520	V16D	1,280
V8A	960	V17A	720
V8B	880	V17B	520
V8C	1120	V17C	680
V8D	1120	V17D	520
V9A	1040	V18A	1,120
V9B	880	V18B	1,120
V9C	1200	V18C	800
V9D	1280	V18D	800
V10A	720	V19A	1,040
V10B	480	V19B	720
V10C	720	V20A	800
V10D	480	V20B	480
V11A	1,280	V20C	560
V11B	1,360	V20D	400
V11C	1,840	V1	1,680
V11D	1,680	V4	960
V12A	1,280		
V12B	1,120		
V12C	1,360		
V12D	1,040		
V3A	360		
V3B	360		

See Appendix A for additional information

4.4.2.1.2 Saturated Zone Thickness

Mass released from the disposal units enters the saturated zone dissolved in recharge water from the vadose zone and mixes with the groundwater flowing through the saturated zone. The concentrations of radionuclides at the 100-meter boundary are a direct function of the volume of water flowing through the saturated zone and the mass flux released from the unsaturated zone. The volume of water flowing through the saturated zone is defined as the product of the Darcy velocity (see Section 4.4.1) and the cross-sectional area of the pipe element perpendicular to flow. The cross-sectional area of the pipe element perpendicular to flow is in turn defined as the product of the saturated thickness and the saturated width. In the SDF GoldSim model, the saturated thickness is based on mixing zone thickness estimated from cross-sectional diagrams of results from the SDF PORFLOW model results. The deterministic value (and mean value for stochastic simulations) used in the model is 20 meters. The 20-meter value was chosen based on observation of cross sections of PORFLOW generated plumes for a conservative species such as the plot presented in Figure 4.4-1. This value is an update from the original value of 12 meters used in the SDF PA analyses (SDF PA Section 5.6.3.8.1). The stochastic distribution used for the saturated zone thickness is defined as a truncated normal distribution with a minimum of 12 meter and a maximum of 28 meter. The standard deviation is 2.8 meters or 5/3 (1-2/3) of the value used in the original SDF PA analyses (SRR-CWDA-2009-00017 Section 5.6.3.8.1).

4.4.2.1.3 Saturated Zone Width

As noted above, the cross-sectional area of the pipe-elements perpendicular to flow is defined as the product of the saturated zone width and the saturated zone thickness. The saturated zone widths for Vaults 1 and 4 are defined as the widths of the vaults (600 feet) and the saturated zone widths for the FDCs are defined as the diameter of the FDCs (150 feet) as presented in Tables 4.2-7, Tables 4.2-8, and Tables 4.2-9. Uncertainty is not considered for the disposal unit because the unit geometry is known.

4.4.2.1.4 Saturated Zone Dispersivity

For consistency with the SDF PORFLOW modeling effort, the longitudinal dispersivity used in the SDF GoldSim model is 10 meters and the horizontal transverse and vertical dispersivities are set to 1 meter, the same as used in the SDF PORFLOW model.

Figure 4.4-1: Areal Views and Cross-Sections of a PORFLOW Generated Plume for a Conservative Species Released from Vault 1

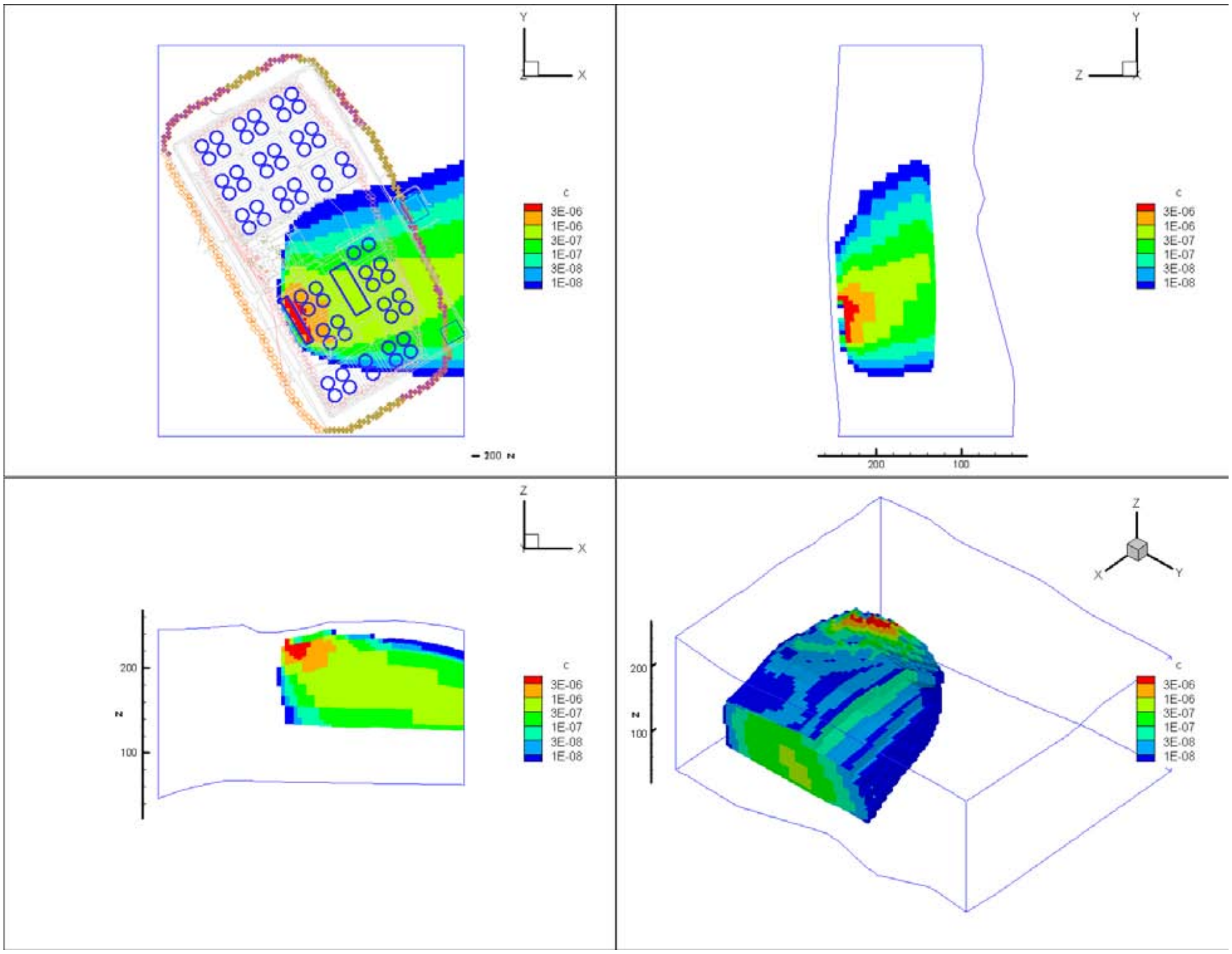

4.4.2.2 Sectors

4.4.2.2.1 Sector Locations

To minimize the model's computational effort and storage needs, the GoldSim results are evaluated for only a subset of 100-meter boundary locations utilized in the PORFLOW analysis. As with PORFLOW, results are presented in terms of dose for each sector. Sector locations are shown in Figure 3.1-2. The final dose results are based on the peak dose from all sectors at any given time. The 100-meter boundary doses for each sector are based on a superposition of the concentrations from releases from the different disposal units, at the boundary. Using a combined concentration is equivalent to superposition of doses due to the linearity of the governing equations. The concentrations are derived at the center of each sector.

4.4.2.2.2 Well Centerline and Offset distances

The GoldSim plume function is used to approximate a 3-D system based on the 1-D pipe-element radionuclide transport analysis (see Section 3.1.4). To utilize the GoldSim plume function, observation well centerline distances and offsets are needed. The centerline distances used in GoldSim (see Table 4.4-2) were generated by measuring the distances along stream traces from the disposal unit to the point where the stream traces cross the 100-meter boundary (Figures 3.1-2 through 3.1-5. The offset distance is the length of the normal from the stream trace to the center of the sector (Figure 3.1-2). The centerline distances for the disposal units are listed in Table 4.4-2 and the offset distances for the northern and southern disposal units are presented in Table 4.4-3 and Table 4.4-4, respectively.

Table 4.4-3: Offset Distance from Northern Disposal Units Steam Traces to Sector Centers

	Sector G (ft)	Sector H (ft)	Sector I (ft)	Sector J (ft)	Sector K (ft)	Sector L (ft)
V2A	1,671	1,378	1,275	982	465	258
V2B	1,809	1,516	1,430	1,154	620	86
V5A	0	724	1,206	1,516	N/A	N/A
V5B	207	517	999	1,327	N/A	N/A
V5C	0	706	1,171	1,516	N/A	N/A
V5D	207	517	982	1,327	N/A	N/A
V6A	465	258	724	1,103	N/A	N/A
V6B	655	69	551	930	N/A	N/A
V6C	500	241	706	1,051	N/A	N/A
V6D	724	310	465	879	N/A	N/A
V7A	1,034	551	172	603	N/A	N/A
V7B	1,206	413	86	379	N/A	N/A
V7C	1,103	689	52	482	N/A	N/A
V7D	1,275	724	327	172	N/A	N/A
V8A	0	500	1,154	0	N/A	N/A
V8B	207	689	965	0	N/A	N/A
V8C	34	465	965	0	N/A	N/A
V8D	258	465	930	0	N/A	N/A
V9A	655	69	551	896	1068	1,413
V9B	861	121	207	603	948	1,275
V9C	1,051	293	379	775	861	1,275
V9D	1,240	792	534	86	465	1,085
V10A	N/A	N/A	689	293	258	965
V10B	N/A	N/A	810	431	121	965
V10C	N/A	N/A	913	569	0	706
V10D	N/A	N/A	982	655	121	603
V11A	207	517	982	1,327	N/A	N/A
V11B	465	362	844	1,085	N/A	N/A
V11C	362	241	724	1,171	N/A	N/A
V11D	741	0	431	810	999	N/A
V12A	N/A	N/A	N/A	551	0	724
V12B	N/A	N/A	N/A	844	310	431
V12C	N/A	N/A	N/A	999	465	258
V12D	N/A	N/A	N/A	1,103	603	103
V3A	N/A	N/A	N/A	982	482	258
V3B	N/A	N/A	N/A	1,154	689	69

N/A = Not Applicable

Table 4.4-4: Offset Distance from Southern Disposal Units Stream Traces to Sector Centers

	Sector A (ft)	Sector B (ft)	Sector C (ft)	Sector D (ft)	Sector E (ft)	Sector F (ft)
V13A	176	197	507	958	1,430	1,705
V13B	169	211	521	972	1,444	1,719
V13C	493	120	190	648	1,127	1,444
V13D	423	70	247	704	1,183	1,486
V14A	106	486	810	1,247	1,712	N/A
V14B	148	528	845	1,296	1,747	N/A
V15A	218	162	472	930	1,388	N/A
V15B	162	218	535	986	1,458	N/A
V15C	380	21	296	754	1,226	N/A
V15D	352	21	338	789	1,268	N/A
V16A	944	585	275	183	676	1,050
V16B	909	549	247	204	711	1,064
V16C	1,183	831	528	92	423	852
V16D	1,113	824	444	7	500	916
V17A	747	373	70	380	881	N/A
V17B	669	303	7	451	951	N/A
V17C	909	549	247	204	711	N/A
V17D	719	472	204	225	740	N/A
V18A	1,768	1,430	1,127	676	169	338
V18B	1,655	1,317	1,007	564	56	458
V18C	1,888	1,543	1,240	789	282	211
V18D	1,768	1,430	1,127	676	169	338
V19A	1,493	1,148	845	402	106	620
V19B	1,592	1,254	958	507	7	514
V20A	1,317	986	690	240	275	N/A
V20B	1,162	838	549	99	275	N/A
V20C	1,416	1,064	761	310	197	N/A
V20D	1,303	965	669	211	0	N/A
V1	0	0	0	458	951	1,148
V4	0	0	0	775	1,254	1,338

N/A = Not Applicable

4.5 Material Properties

The material properties that are discussed in this section include the K_ds, which describe the affinity of specific radionuclides to sorbing onto the different materials used in constructing the disposal units or found naturally at the sight. They also include the site-specific physical parameters such as porosity and bulk density.

4.5.1 Adsorption

In the GoldSim SDF Model, within the disposal units, the saltstone and concrete structures play a role in retarding contaminant transport of species subject to sorption. Sorption also takes place in the vadose zone and saturated zone soils beneath the disposal units. The effectiveness of each zone in retarding the transport of different species is associated with K_d values, which vary for different elements and are depend on the time-variant chemical states of the structure. Table 4.5-1 contains the median K_d values for the cementitious zones, such as the walls and the floor for the Base Case through E. The values are posted for the different reducing/oxidized regions. The K_d values for the cementitious zones are also used for the saltstone in the Base Case through E. Note that the elements listed in Table 4.5-1 are a subset of the elements listed in SRR-CWDA-2009-00017 Table 4.2-18, and represent only the radionuclides evaluated in the SDF GoldSim model. In addition, several of the K_ds listed in Table 4.5-1 are assigned a value of 1.00E-09 mL/g as opposed to a value of zero in SRR-CWDA-2009-00017 Table 4.2-18. For practical purposes, there is no difference. Table 4.5-2 contains a list of the updated median K_d values used in the cementitious zone for Alternative Sensitivity Case K. For elements where the Alternative Sensitivity Case K K_d values for saltstone differ from the cementitious zone values, the updated K_d values are listed in Table 4.5-3. Table 4.5-4 contains the median K_d values used in the backfill, vadose zone, and saturated zone, for the Base Case through E. A list of the median K_d values for the backfill, vadose zone, and saturated zone, that are updated in Alternative Sensitivity Case K is presented in Table 4.5-5.

The median K_d distributions for the K_d values used in the SDF GoldSim modeling are based on the approach described in SRNL-STI-2009-00473. This report recommends lognormal distribution with maximum and minimum values based on the material under consideration. The shape of the lognormal distribution is based on the GSD, which differs by the material under consideration and the magnitude of the median value for the K_d. Table 4.5-3 provides the parameters for the lognormal distributions used in the SDF GoldSim model.

Table 4.5-1: Recommended K_d Values for Cementitious Materials in mL/g

Element	Reducing Cementitious Media			Oxidizing Cementitious Media		
	Young Age	Middle Age	Old Age	Young Age	Middle Age	Old Age
Ac	5.00E+03	5.00E+03	1.00E+03	6.00E+03	6.00E+03	6.00E+02
Al	5.00E+03	5.00E+03	1.00E+03	6.00E+03	6.00E+03	6.00E+02
Am	5.00E+03	5.00E+03	1.00E+03	6.00E+03	6.00E+03	6.00E+02
Cd	5.00E+03	5.00E+03	1.00E+03	4.00E+03	4.00E+03	1.00E+03
Cf	5.00E+03	5.00E+03	1.00E+03	6.00E+03	6.00E+03	6.00E+02
Cl	2.00E+01	2.00E+01	2.00E+00	2.00E+01	2.00E+01	2.00E+00
Cm	5.00E+03	5.00E+03	1.00E+03	6.00E+03	6.00E+03	6.00E+02
Co	5.00E+03	5.00E+03	1.00E+03	4.00E+03	4.00E+03	1.00E+03
Cr	5.00E+03	5.00E+03	1.00E+03	2.00E+01	2.00E+01	2.00E+00
Cs	1.00E-09	2.00E+00	1.00E+01	2.00E+00	2.00E+01	1.00E+01
Cu	1.00E+00	1.00E+00	1.00E-01	1.00E+00	1.00E+00	1.00E-01
Eu	5.00E+03	5.00E+03	1.00E+03	6.00E+03	6.00E+03	6.00E+02
F	2.00E+01	2.00E+01	2.00E+00	2.00E+01	2.00E+01	2.00E+00
Fe	5.00E+03	5.00E+03	1.00E+03	6.00E+03	6.00E+03	6.00E+02
Gd	5.00E+03	5.00E+03	1.00E+03	6.00E+03	6.00E+03	6.00E+02
H	1.00E-09	0.00E+00	0.00E+00	1.00E-09	1.00E-09	1.00E-09
Hg	1.00E+03	1.00E+03	3.00E+02	3.00E+02	3.00E+02	3.00E+02
I	5.00E+00	9.00E+00	0.00E+00	8.00E+00	1.50E+01	4.00E+00
K	0.00E+00	2.00E+00	1.00E+01	2.00E+00	2.00E+01	1.00E+01
Nb	1.00E+03	1.00E+03	5.00E+02	1.00E+03	1.00E+03	5.00E+02
Ni	5.00E+03	5.00E+03	1.00E+03	4.00E+03	4.00E+03	1.00E+03
NO2	1.00E-09	0.00E+00	0.00E+00	1.00E-09	1.00E-09	0.00E+00
NO3	1.00E-09	0.00E+00	0.00E+00	1.00E-09	1.00E-09	0.00E+00
Np	4.00E+03	4.00E+03	3.00E+03	1.60E+03	1.60E+03	2.50E+02
Pa	5.00E+03	5.00E+03	5.00E+02	1.60E+03	1.60E+03	2.50E+02
Pb	5.00E+02	5.00E+02	2.50E+02	5.00E+02	5.00E+02	2.50E+02
Pd	5.00E+03	5.00E+03	1.00E+03	4.00E+03	4.00E+03	1.00E+03
Pt	0.00E+00	0.00E+00	0.00E+00	0.00E+00	0.00E+00	0.00E+00
Pu	1.00E+04	1.00E+04	1.00E+04	1.00E+04	1.00E+04	1.00E+03
Ra	5.00E-01	3.00E+00	2.00E+01	1.00E+02	1.00E+02	7.00E+01
Rn	1.00E-09	0.00E+00	0.00E+00	1.00E-09	1.00E-09	0.00E+00
Sb	5.00E+03	5.00E+03	1.00E+03	1.00E+02	1.00E+02	2.00E+00
Se	3.00E+02	3.00E+02	3.00E+02	3.00E+02	3.00E+02	1.50E+02
Sm	5.00E+03	5.00E+03	1.00E+03	6.00E+03	6.00E+03	6.00E+02
Sn	5.00E+03	5.00E+03	2.00E+03	4.00E+03	4.00E+03	2.00E+03
Sr	5.00E-01	3.00E+00	2.00E+01	3.00E+00	3.00E+01	1.50E+01
Tc	5.00E+03	1.00E+03	5.00E+03	8.00E-01	8.00E-01	5.00E-01
Th	5.00E+03	5.00E+03	5.00E+02	5.00E+03	5.00E+03	5.00E+02
U	2.50E+03	2.50E+03	2.50E+03	2.50E+02	2.50E+02	7.00E+01
Zr	5.00E+03	5.00E+03	5.00E+02	5.00E+03	5.00E+03	5.00E+02

[Adapted From SRR-CWDA-2009-00017 Table 4.2-18]

Table 4.5-2: Saltstone PA versus Case K K_d Values for Cementitious Materials

Element	Ox/Re	Age	PA K_d (mL/g)	PA Value Reference	Current K_d (mL/g)	Reference for Current Value	Location in Reference
Ac	Re	Young	5,000	Table 4.2-18	7,000	SRNL-STI-2009-00473	Table 18
Ac	Re	Middle	5,000	Table 4.2-18	7,000	SRNL-STI-2009-00473	Table 18
Ac	Re	Old	1,000	Table 4.2-18	1,000	SRNL-STI-2009-00473	Table 18
Al	Re	Young	5,000	Table 4.2-18	7,000	SRNL-STI-2009-00473	Table 18
Al	Re	Middle	5,000	Table 4.2-18	7,000	SRNL-STI-2009-00473	Table 18
Al	Re	Old	1,000	Table 4.2-18	1,000	SRNL-STI-2009-00473	Table 18
Am	Re	Young	5,000	Table 4.2-18	7,000	SRNL-STI-2009-00473	Table 18
Am	Re	Middle	5,000	Table 4.2-18	7,000	SRNL-STI-2009-00473	Table 18
Am	Re	Old	1,000	Table 4.2-18	1,000	SRNL-STI-2009-00473	Table 18
C	Re	Young	20	Table 4.2-18	3,000	SRNL-STI-2009-00473	Table 18
C	Re	Middle	10	Table 4.2-18	3,000	SRNL-STI-2009-00473	Table 18
C	Re	Old	0	Table 4.2-18	300	SRNL-STI-2009-00473	Table 18
Cf	Re	Young	5,000	Table 4.2-18	7,000	SRNL-STI-2009-00473	Table 18
Cf	Re	Middle	5,000	Table 4.2-18	7,000	SRNL-STI-2009-00473	Table 18
Cf	Re	Old	1,000	Table 4.2-18	1,000	SRNL-STI-2009-00473	Table 18
Cl	Re	Young	20	Table 4.2-18	10	SRNL-STI-2009-00473	Table 18
Cl	Re	Middle	20	Table 4.2-18	10	SRNL-STI-2009-00473	Table 18
Cl	Re	Old	2	Table 4.2-18	1.0	SRNL-STI-2009-00473	Table 18
Cm	Re	Young	5,000	Table 4.2-18	7,000	SRNL-STI-2009-00473	Table 18
Cm	Re	Middle	5,000	Table 4.2-18	7,000	SRNL-STI-2009-00473	Table 18
Cm	Re	Old	1,000	Table 4.2-18	1,000	SRNL-STI-2009-00473	Table 18
Cs	Re	Young	0	Table 4.2-18	2.0	SRNL-STI-2009-00473	Table 18
Cs	Re	Middle	2	Table 4.2-18	20	SRNL-STI-2009-00473	Table 18
Cs	Re	Old	10	Table 4.2-18	10	SRNL-STI-2009-00473	Table 18
Eu	Re	Young	5,000	Table 4.2-18	7,000	SRNL-STI-2009-00473	Table 18
Eu	Re	Middle	5,000	Table 4.2-18	7,000	SRNL-STI-2009-00473	Table 18
Eu	Re	Old	1,000	Table 4.2-18	1,000	SRNL-STI-2009-00473	Table 18
I	Re	Young	5	Table 4.2-18	5.0	SRNL-STI-2009-00473	Table 18
I	Re	Middle	9	Table 4.2-18	9.0	SRNL-STI-2009-00473	Table 18
I	Re	Old	0	Table 4.2-18	4.0	SRNL-STI-2009-00473	Table 18
K	Re	Young	0	Table 4.2-18	2.0	SRNL-STI-2009-00473	Table 18
K	Re	Middle	2	Table 4.2-18	20	SRNL-STI-2009-00473	Table 18

Table 4.5-2: Saltstone PA versus Case K K_d Values for Cementitious Materials (Continued)

Element	Ox/Re	Age	PA K_d (mL/g)	PA Value Reference	Current K_d (mL/g)	Reference for Current Value	Location in Reference
K	Re	Old	10	Table 4.2-18	10	SRNL-STI-2009-00473	Table 18
Ni	Re	Young	5,000	Table 4.2-18	4,000	SRNL-STI-2009-00473	Table 18
Ni	Re	Middle	5,000	Table 4.2-18	4,000	SRNL-STI-2009-00473	Table 18
Ni	Re	Old	1,000	Table 4.2-18	400	SRNL-STI-2009-00473	Table 18
Np	Re	Young	4,000	Table 4.2-18	10,000	SRNL-STI-2009-00473	Table 18
Np	Re	Middle	4,000	Table 4.2-18	10,000	SRNL-STI-2009-00473	Table 18
Np	Re	Old	3,000	Table 4.2-18	5,000	SRNL-STI-2009-00473	Table 18
Pa	Re	Young	5,000	Table 4.2-18	10,000	SRNL-STI-2009-00473	Table 18
Pa	Re	Middle	5,000	Table 4.2-18	10,000	SRNL-STI-2009-00473	Table 18
Pa	Re	Old	500	Table 4.2-18	5,000	SRNL-STI-2009-00473	Table 18
Pb	Re	Young	500	Table 4.2-18	5,000	SRNL-STI-2009-00473	Table 18
Pb	Re	Middle	500	Table 4.2-18	5,000	SRNL-STI-2009-00473	Table 18
Pb	Re	Old	250	Table 4.2-18	1,000	SRNL-STI-2009-00473	Table 18
Pt	Re	Young	0	Table 4.2-18	5,000	SRNL-STI-2009-00473	Table 18
Pt	Re	Middle	0	Table 4.2-18	5,000	SRNL-STI-2009-00473	Table 18
Pt	Re	Old	0	Table 4.2-18	1,000	SRNL-STI-2009-00473	Table 18
Pu	Re	Young	10,000	Table 4.2-18	10,000	SRNL-STI-2009-00473	Table 18
Pu	Re	Middle	10,000	Table 4.2-18	10,000	SRNL-STI-2009-00473	Table 18
Pu	Re	Old	10,000	Table 4.2-18	2,000	SRNL-STI-2009-00473	Table 18
Ra	Re	Young	0.5	Table 4.2-18	100	SRNL-STI-2009-00473	Table 18
Ra	Re	Middle	3	Table 4.2-18	100	SRNL-STI-2009-00473	Table 18
Ra	Re	Old	20	Table 4.2-18	70	SRNL-STI-2009-00473	Table 18
Sb	Re	Young	5,000	Table 4.2-18	1,000	SRNL-STI-2009-00473	Table 18
Sb	Re	Middle	5,000	Table 4.2-18	1,000	SRNL-STI-2009-00473	Table 18
Sb	Re	Old	1,000	Table 4.2-18	100	SRNL-STI-2009-00473	Table 18
Se	Re	Young	300	Table 4.2-18	300	SRNL-STI-2009-00473	Table 18
Se	Re	Middle	300	Table 4.2-18	300	SRNL-STI-2009-00473	Table 18
Se	Re	Old	300	Table 4.2-18	150	SRNL-STI-2009-00473	Table 18
Sm	Re	Young	5,000	Table 4.2-18	7,000	SRNL-STI-2009-00473	Table 18
Sm	Re	Middle	5,000	Table 4.2-18	7,000	SRNL-STI-2009-00473	Table 18
Sm	Re	Old	1,000	Table 4.2-18	1,000	SRNL-STI-2009-00473	Table 18
Sn	Re	Young	5,000	Table 4.2-18	5,000	SRNL-STI-2009-00473	Table 18

Table 4.5-2: Saltstone PA versus Case K K_d Values for Cementitious Materials (Continued)

Element	Ox/Re	Age	PA K_d (mL/g)	PA Value Reference	Current K_d (mL/g)	Reference for Current Value	Location in Reference
Sn	Re	Middle	5,000	Table 4.2-18	5,000	SRNL-STI-2009-00473	Table 18
Sn	Re	Old	2,000	Table 4.2-18	500	SRNL-STI-2009-00473	Table 18
Sr	Re	Young	0.5	Table 4.2-18	15	SRNL-STI-2010-00667	Table 2
Sr	Re	Middle	3	Table 4.2-18	15	SRNL-STI-2010-00667	Table 2
Sr	Re	Old	20	Table 4.2-18	5.0	SRNL-STI-2009-00473	Table 18
Tc[a]	Re	Young	5,000	Table 4.2-18	1,000	SRNL-STI-2010-00667	Table 2
Tc[a]	Re	Middle	5,000	Table 4.2-18	1,000	SRNL-STI-2010-00667	Table 2
Tc[a]	Re	Old	5,000	Table 4.2-18	1,000	SRNL-STI-2009-00473	Table 18
C	Ox	Young	20	Table 4.2-18	3,000	SRNL-STI-2009-00473	Table 17
C	Ox	Middle	10	Table 4.2-18	3,000	SRNL-STI-2009-00473	Table 17
C	Ox	Old	0	Table 4.2-18	300	SRNL-STI-2009-00473	Table 17
Cl	Ox	Young	20	Table 4.2-18	10	SRNL-STI-2009-00473	Table 17
Cl	Ox	Middle	20	Table 4.2-18	10	SRNL-STI-2009-00473	Table 17
Cl	Ox	Old	2	Table 4.2-18	1.0	SRNL-STI-2009-00473	Table 17
Co	Ox	Young	4,000	Table 4.2-18	4,000	SRNL-STI-2009-00473	Table 17
Co	Ox	Middle	4,000	Table 4.2-18	4,000	SRNL-STI-2009-00473	Table 17
Co	Ox	Old	1,000	Table 4.2-18	400	SRNL-STI-2009-00473	Table 17
Ni	Ox	Young	4,000	Table 4.2-18	4,000	SRNL-STI-2009-00473	Table 17
Ni	Ox	Middle	4,000	Table 4.2-18	4,000	SRNL-STI-2009-00473	Table 17
Ni	Ox	Old	1,000	Table 4.2-18	400	SRNL-STI-2009-00473	Table 17
Np	Ox	Young	1,600	Table 4.2-18	10,000	SRNL-STI-2009-00473	Table 17
Np	Ox	Middle	1,600	Table 4.2-18	10,000	SRNL-STI-2009-00473	Table 17
Np	Ox	Old	250	Table 4.2-18	5,000	SRNL-STI-2009-00473	Table 17
Pa	Ox	Young	1,600	Table 4.2-18	10,000	SRNL-STI-2009-00473	Table 17
Pa	Ox	Middle	1,600	Table 4.2-18	10,000	SRNL-STI-2009-00473	Table 17
Pa	Ox	Old	250	Table 4.2-18	5,000	SRNL-STI-2009-00473	Table 17
Pb	Ox	Young	500	Table 4.2-18	300	SRNL-STI-2009-00473	Table 17
Pb	Ox	Middle	500	Table 4.2-18	300	SRNL-STI-2009-00473	Table 17
Pb	Ox	Old	250	Table 4.2-18	100	SRNL-STI-2009-00473	Table 17
Pd	Ox	Young	4,000	Table 4.2-18	4,000	SRNL-STI-2009-00473	Table 17
Pd	Ox	Middle	4,000	Table 4.2-18	4,000	SRNL-STI-2009-00473	Table 17
Pd	Ox	Old	1,000	Table 4.2-18	400	SRNL-STI-2009-00473	Table 17

Table 4.5-2: Saltstone PA versus Case K K_d Values for Cementitious Materials (Continued)

Element	Ox/Re	Age	PA K_d (mL/g)	PA Value Reference	Current K_d (mL/g)	Reference for Current Value	Location in Reference
Pt	Ox	Young	0	Table 4.2-18	4,000	SRNL-STI-2009-00473	Table 17
Pt	Ox	Middle	0	Table 4.2-18	4,000	SRNL-STI-2009-00473	Table 17
Pt	Ox	Old	0	Table 4.2-18	400	SRNL-STI-2009-00473	Table 17
Pu	Ox	Young	10,000	Table 4.2-18	10,000	SRNL-STI-2009-00473	Table 17
Pu	Ox	Middle	10,000	Table 4.2-18	10,000	SRNL-STI-2009-00473	Table 17
Pu	Ox	Old	1,000	Table 4.2-18	2,000	SRNL-STI-2009-00473	Table 17
Sb	Ox	Young	100	Table 4.2-18	1,000	SRNL-STI-2009-00473	Table 17
Sb	Ox	Middle	100	Table 4.2-18	1,000	SRNL-STI-2009-00473	Table 17
Sb	Ox	Old	2	Table 4.2-18	100	SRNL-STI-2009-00473	Table 17
Se	Ox	Young	300	Table 4.2-18	300	SRNL-STI-2009-00473	Table 17
Se	Ox	Middle	300	Table 4.2-18	300	SRNL-STI-2009-00473	Table 17
Se[b]	Ox	Old	150	Table 4.2-18	150	SRNL-STI-2009-00473	Table 17
Sr	Ox	Young	3	Table 4.2-18	15	SRNL-STI-2010-00667	Table 1
Sr	Ox	Middle	30	Table 4.2-18	15	SRNL-STI-2010-00667	Table 1
Sr	Ox	Old	15	Table 4.2-18	5.0	SRNL-STI-2009-00473	Table 17
Tc[a]	Ox	Young	0.8	Table 4.2-18	0.8	SRNL-STI-2010-00667	Table 1
Tc[a]	Ox	Middle	0.8	Table 4.2-18	0.8	SRNL-STI-2010-00667	Table 1
Tc[a]	Ox	Old	0.5	Table 4.2-18	0.5	SRNL-STI-2009-00473	Table 17
Th	Ox	Young	5,000	Table 4.2-18	10,000	SRNL-STI-2009-00473	Table 17
Th	Ox	Middle	5,000	Table 4.2-18	10,000	SRNL-STI-2009-00473	Table 17
Th	Ox	Old	500	Table 4.2-18	2,000	SRNL-STI-2009-00473	Table 17
U	Ox	Young	250	Table 4.2-18	1,000	SRNL-STI-2010-00493	Table 8
U	Ox	Middle	250	Table 4.2-18	1,000	SRNL-STI-2010-00493	Table 8
U	Ox	Old	70	Table 4.2-18	100	SRNL-STI-2010-00493	Table 8
Zr	Ox	Young	5,000	Table 4.2-18	10,000	SRNL-STI-2009-00473	Table 17
Zr	Ox	Middle	5,000	Table 4.2-18	10,000	SRNL-STI-2009-00473	Table 17
Zr	Ox	Old	500	Table 4.2-18	2,000	SRNL-STI-2009-00473	Table 17

Notes: (a) For the Alternative Sensitivity Case K analysis, the technetium values are used as bounding values for shrinking core model calculations. (b) For old aged oxidized cementitious materials, a different K_d value was applied for Se-79 in the Alternative Sensitivity Case K analysis. Instead of using the value of 150 (as shown in Table 3), a value of 30 was applied, which reduces the retardation of selenium and increases its water concentration which will increase the dose from selenium.

Table 4.5-3: Saltstone Specific K_d Values

Element	Ox/Re	Age	PA K_d (mL/g)	PA Value Reference	Current K_d (mL/g)	Reference for Current Value	Location in Reference
Ba	Re	Young	0.5	Table 4.2-18	6,000	SRNL-STI-2010-00667	Table 2
Ba	Re	Middle	3	Table 4.2-18	6,000	SRNL-STI-2010-00667	Table 2
Sr	Re	Young	0.5	Table 4.2-18	1,000	SRNL-STI-2010-00667	Table 2
Sr	Re	Middle	3	Table 4.2-18	1,000	SRNL-STI-2010-00667	Table 2
Tc[a]	Re	Young	5,000	Table 4.2-18	1,000	SRNL-STI-2010-00667	Table 2
Tc[a]	Re	Middle	5,000	Table 4.2-18	1,000	SRNL-STI-2010-00667	Table 2
Ba	Ox	Young	100	Table 4.2-18	6,000	SRNL-STI-2010-00667	Table 1
Ba	Ox	Middle	100	Table 4.2-18	6,000	SRNL-STI-2010-00667	Table 1
Sr	Ox	Young	3	Table 4.2-18	1,000	SRNL-STI-2010-00667	Table 1
Sr	Ox	Middle	30	Table 4.2-18	1,000	SRNL-STI-2010-00667	Table 1
Tc[a]	Ox	Young	0.8	Table 4.2-18	10	SRNL-STI-2010-00667	Table 1
Tc[a]	Ox	Middle	0.8	Table 4.2-18	10	SRNL-STI-2010-00667	Table 1

(a) For the Alternative Sensitivity Case K analysis, the technetium values are used as bounding values for shrinking core model calculations.

Table 4.5-4: Recommended K_d Values for Backfill and the Vadose Zone

Element	Soils Media			
	Backfill Soil (mL/g)*	Ref.	Vadose Zone Soil (mL/g)**	Ref.
Ac	8,500	a	1,100	a
Al	1,300	b	1,300	b
Am	8,500	a	1,100	a
C	0	a	0	a
Cd	10	b	4	b
Cf	8,500	a	1,100	a
Cl	0	a	0	a
Cm	8,500	a	1,100	a
Co	30	a	7	a
Cr	10	b	4	b
Cs	250	a	50	a
Cu	70	b	50	b
Eu	8,500	a	1,100	a
F	0	b	0	b
Fe	400	b	200	b
Gd	8,500	a	1,100	a
H	0	a	0	a
Hg	1,000	b	800	b
I	0.6	a	0	a
K	60	b	10	b
Mo	120	N/A	6	N/A
Nb	0	a	0	a
Ni	30	a	7	a
NO2	0	c	0	c
NO3	0	c	0	c
Np	35	a	0.6	a
Pa	35	a	0.6	a
Pb	5,000	a	2,000	a
Pd	30	b	7	b
Pt	0	c	0	c
Pu	5,900	a	270	a
Ra	17	a	5	a
Rn	0	a	0	a
Sb	2,500	b	2,500	b
Se	1,000	a	1,000	a
Sm	8,500	a	1,100	a
Sn	5,000	a	2,000	a
Sr	17	a	5	a
Tc	1.8	d	0.6	d
Th	2,000	a	900	a
U	300	a	200	a
Zr	2,000	a	900	a

* Backfill soil represented by clayey sediment.
** Vadose zone soil represented by sandy sediment.
(a) WSRC-TR-2006-00004
(b) SRNL-RPA-2007-00006
(c) Assigned a value of zero
(d) SRNL-TR-2009-00019
(e) SRS-REG-2007-00036

The K_d values for backfill and the vadose zone presented in Table 4.2-5 are valid for the Base Case through E. Table 4.2-5 presents the K_d values that are different for Alternative Sensitivity Case K along with a comparison between Alternative Sensitivity Case K and the Base Case through E values.

Table 4.5-5: Updated K_d Values for Backfill and the Vadose Zone

Element	Material	PA K_d (mL/g)	PA Value Reference	Current K_d (mL/g)	Reference for Current Value	Location in Reference
Ba	Clay (Backfill Soil)	17	Table 4.2-15	101	SRNL-STI-2011-00011	Table 2-2
C	Clay (Backfill Soil)	0	Table 4.2-15	400	SRNL-STI-2009-00473	Table 16
Ce	Clay (Backfill Soil)	1,500	Table 4.2-15	8,500	SRNL-STI-2009-00473	Table 16
Cl	Clay (Backfill Soil)	0	Table 4.2-15	8.0	SRNL-STI-2010-00493	Table 9
Co	Clay (Backfill Soil)	30	Table 4.2-15	100	SRNL-STI-2009-00473	Table 16
Cs	Clay (Backfill Soil)	250	Table 4.2-15	50	SRNL-STI-2009-00473	Table 16
I	Clay (Backfill Soil)	0.6	Table 4.2-15	0.9	SRNL-STI-2009-00473	Table 16
K	Clay (Backfill Soil)	60	Table 4.2-15	25	SRNL-STI-2009-00473	Table 16
Np	Clay (Backfill Soil)	35	Table 4.2-15	9.0	SRNL-STI-2009-00473	Table 16
Pa	Clay (Backfill Soil)	35	Table 4.2-15	9.0	SRNL-STI-2009-00473	Table 16
Pt	Clay (Backfill Soil)	0	Table 4.2-15	30	SRNL-STI-2009-00473	Table 16
Pu	Clay (Backfill Soil)	5,900	Table 4.2-15	5,950	SRNL-STI-2009-00473	Table 16
Ra	Clay (Backfill Soil)	17	Table 4.2-15	185	SRNL-STI-2011-00011	Table 2-2
U	Clay (Backfill Soil)	300	Table 4.2-15	400	SRNL-STI-2010-00493	Table 8
C	Sand (Vadose Zone Soil)	0	Table 4.2-15	10	SRNL-STI-2009-00473	Table 16
Cl	Sand (Vadose Zone Soil)	0	Table 4.2-15	1.0	SRNL-STI-2010-00493	Table 9
Co	Sand (Vadose Zone Soil)	7	Table 4.2-15	40	SRNL-STI-2009-00473	Table 16
Cs	Sand (Vadose Zone Soil)	50	Table 4.2-15	10	SRNL-STI-2009-00473	Table 16
I	Sand (Vadose Zone Soil)	0	Table 4.2-15	0.3	SRNL-STI-2009-00473	Table 16
K	Sand (Vadose Zone Soil)	10	Table 4.2-15	5.0	SRNL-STI-2009-00473	Table 16
Np	Sand (Vadose Zone Soil)	0.6	Table 4.2-15	3.0	SRNL-STI-2009-00473	Table 16
Pa	Sand (Vadose Zone Soil)	0.6	Table 4.2-15	3.0	SRNL-STI-2009-00473	Table 16
Pt	Sand (Vadose Zone Soil)	0	Table 4.2-15	7.0	SRNL-STI-2009-00473	Table 16
Pu	Sand (Vadose Zone Soil)	270	Table 4.2-15	290	SRNL-STI-2009-00473	Table 16
Ra	Sand (Vadose Zone Soil)	5	Table 4.2-15	25	SRNL-STI-2011-00011	Table 2-2
U	Sand (Vadose Zone Soil)	200	Table 4.2-15	300	SRNL-STI-2010-00493	Table 8

Prior to the release of SRNL-STI-2010-00667, K_d values assigned to cementitious materials (SDF PA Section 4.2.3.2.4) are also assigned to saltstone. New site-specific studies have yielded saltstone-specific recommended K_d values for three elements: barium, strontium, and technetium. These values are documented in Table 4.5-3. Note that the Alternative Sensitivity Case K run uses these updated technetium values as the bounding values for the shrinking core model calculations.

Table 4.5-6: K_d Variability in the SDF GoldSim Model

Material Zone	Min	Max	Lognormal GSD	
Clayey Soils[b]	0.5 × GM[a]	1.5 × GM	GM < 4.0 mL/g	GM = 4.0 mL/g or greater
			1.001 mL/g	0.25 × GM
Sandy Soils[c]	0.25 × GM	1.75 × GM	GM < 2.7 mL/g	GM = 2.7 mL/g or greater
			1.001 mL/g	0.375 × GM
Cementitious Materials	0.25 × GM	1.75 × GM	GM < 2.7 mL/g	GM = 2.7 mL/g or greater
			1.001 mL/g	0.375 × GM

[a] GM = Geometric Mean of the lognormal distribution defined as the baseline value presented in Tables 4.5-1 through 4.5-3for cementitious materials and Tables 4.5-4 and 4.5-5 for soils.
[b] Backfill Layer
[c] Vadose Zone and Saturated Zone

4.5.2 Physical Properties

The physical parameters describing the material that the water flows through include the porosity, bulk density, and saturations for each component or material type.

4.5.2.1 Engineered Barrier

The engineered barrier includes the components of the disposal units. The physical parameters include the porosity, bulk density, particle density, and saturations for each component or material type. The saturation is assumed to 1.0 in the engineered barrier. The other physical parameters are listed in Table 4.5-7 for the components of the engineered barrier.

Table 4.5-7: Disposal Unit Material Properties

Material	Porosity η (%)	Dry Bulk Density ρ_b (g/cm^3)	Particle Density ρ_p (g/cm^3)
Concrete (floor and walls) - Vaults 1 and 4	12	2.24	2.55
Concrete (floor and walls) - FDCs	11	2.22	2.49
Saltstone	58	1.01	2.40
Sheet Drain - Cases A, D, E, and K	58	1.01	2.40
Sheet Drain - Cases B and C	30	1.82	2.60
Fast Path - Cases A, B, D, E, and K	58	1.01	2.40
Fast Path - Case C (Vaults 1 and 4)	30	1.86	2.66
Fast Path - Case C (FDCs)	38	1.65	2.66
Shotcrete and Backfill	35	1.71	2.63
HDPE	30	1.50	2.14

[SRR-CWDA-2009-00017 Table 4.4-10]

4.5.2.2 Natural Barrier

The natural barrier includes the vadose zone and the saturated zone. The physical parameters include the porosity, bulk density, and saturations (for the vadose zone). The physical parameters for the vadose and saturated zones are presented in Table 4.5-8.

Table 4.5-8: Estimated Vadose Zone Material Properties of Interest

Material	Average Total Porosity (%)	Average Dry Bulk Density (g/cm^3)	Average Particle Density (g/cm^3)	Saturation
Vadose Zone	39[a]	1.62	2.66	0.75[b]
Saturated Zone	25	1.04	1.39	1.0

[SRR-CWDA-2009-00017 Table 4.2-19, WSRC-STI-2006-00198 Section 5.6.1 Table 5-14]

a Incorrectly set to 0.38 in the original SDF model and not fixed in this version (this slight error will be updated in future versions).

b Value found in Version 2.009 of the SDF GoldSim model (will be updated in future versions).

See Appendix A for additional information

5.0 MODEL BENCHMARKING

The disposal unit SDF PORFLOW models are 2-D (Vaults 1 and 4) or radial (FDCs) flow and transport models that take advantage of the disposal unit symmetries to rigorously simulate the potential release of radionuclides from disposal units located at the SDF and the transport of the released species to downgradient locations. The SDF GoldSim model is an abstraction of the SDF PORFLOW model designed for use in performing sensitivity and uncertainty analyses that would be prohibitive using a more rigorous but computationally intensive model like the SDF PORFLOW model. In the abstraction, vertical flow is assumed to dominate the advective component of the radionuclide transport process. Therefore, only the vertical component of flow is considered and the Darcy velocities are spatially averaged in the horizontal plane. Since the 2-D of flow is important in evaluating the number of pore volumes that circulate through different components of the disposal units, the transition times are evaluated using total flux terms from PORFLOW as opposed to the Darcy velocities. Because molecular dispersion is an important process in transporting radionuclides from the saltstone, through the walls and into the accessible environment, horizontal transport by molecular diffusion is also considered. Darcy velocities from the SDF PORFLOW model, used as input to the SDF GoldSim model, control the transport of radionuclides through a simplified assemblage of the main structural features found in the disposal units. In the saturated zone, a complex 3-D flow field produced by PORFLOW is represented by 1-D flow along stream traces, produced by PORFLOW, emanating from the center of the footprint of each disposal unit. In the saturated zone the timing of concentration breakthrough curve peaks generated by PORFLOW (for a conservative tracer) and the stream trace lengths were used to determine spatially averaged flow velocities along the stream traces.

Before performing sensitivity and uncertainty analyses using the GoldSim based model, it is necessary to show that results from the PORFLOW and GoldSim based models have a sufficient degree of agreement. In doing so, the results of the SDF GoldSim model's stochastic simulations can be assumed reflective of results the SDF PORFLOW model would generate, with a like set of parameters. In other words, it is important that the GoldSim abstraction successfully approximate the basic features of the SDF PORFLOW model. Because of the simplifications associated with the abstraction, a perfect match between GoldSim and PORFLOW results is not expected, but basic features of breakthrough curves should be similar.

In the benchmarking effort, PORFLOW/GoldSim comparisons were performed in three phases. The first phase focused on how well the abstraction model approximates the PORFLOW generated radionuclide releases from the disposal units. The radionuclide releases to the saturated zone are used for this comparison, and are referred to below as "vadose zone mass release." Note that for the benchmarking analysis, the inventories for all radionuclide species are set to 1 curie. The second phase focused on how well the abstraction model approximates the radionuclide transport behavior in the saturated zone. The radionuclide concentrations at specified sectors along the 100-meter boundary are used to evaluate the similarity in the dilution/attenuation processes in the saturated zone. The sectors used for the comparison were B and G from the southern and northern disposal units. The locations of the sectors are shown in Figure 3.1-2 and the concentrations are evaluated at the center of the sector. The third phase focused on how well the timing and magnitude of the time histories matched. This third step is

used to verify that the physical and radiological processes controlling radionuclide transport were translated to the dose results. Comparisons are made to the maximum total dose to the MOP based on the radionuclide concentrations at 100 meters computed by PORFLOW and the GoldSim model. The maximum total dose to the MOP is the highest dose reported at each time step regardless of sector.

The benchmarking evaluation was conducted for the Base Case and Alternative Sensitivity Case K results. This version of the model was developed to evaluate Alternative Sensitivity Case K for a response to NRC's RAIs. The other alternative configuration results (Case B through Case E), discussed in Section 4.2.4 and summarized in Table 4.2-11 will be benchmarked later.

5.1 Base Case (Case A)

The Base Case represents what is considered the most likely scenario for the time-based degradation of the disposal unit components, including saltstone and other cementitious material. For the FDCs, shotcrete, the vertical HDPE liners, and changes to the flow fields as they degrade are also simulated. The FDC floor is also modeled in a simplified manner as a single concrete medium. As indicated in the summary Table 4.2-11, Base Case lacks a fast flow path through the saltstone and floor.

5.1.1 Mass Releases to the Saturated Zone

To build confidence in the SDF GoldSim model, mass fluxes entering the saturated zone below the disposal units were collected from both the SDF PORFLOW model and the SDF GoldSim model for comparisons.

5.1.1.1 Vault 1

A comparison of PORFLOW and GoldSim mass releases of Ra-226 presented in Figure 5.1-1 indicates that the SDF GoldSim model can produce a good approximation of PORFLOW releases of Ra-226 from Vault 1. Ra-226 was chosen as a benchmarking species because it represents a major dose contributor in the Base Case model. It is also a good example of a species that is part of a decay chain. Ra-226 is generated through ingrowth from two chains:

1. Pu-238→U-234→Th-230→Ra-226
2. Cm-238→Pu-242→U-238→U-234→Th-230→Ra-226

The benchmarking species chosen was Tc-99 because its transport is strongly controlled by saltstone and concrete middle reduced state K_ds, in addition to it being a major dose contributor in the results from the Base Case model. Figure 5.1-2 shows the SDF GoldSim model does an adequate job of reproducing the trends in the release of Tc-99 to the saturated zone from Vault 1. The early GoldSim release is higher than the PORFLOW release and the later release matches well, except where the time-dependent PORFLOW K_ds changes occur. Note that in the SDF GoldSim model the middle oxidized state, Tc-99 K_d for the wall is set to 80 L/mg to approximate the effects of oxygen diffusion in the PORFLOW time-dependent K_d model. Only the wall K_d was adjusted because PORFLOW output showed that the oxygen diffusion had little influence on the floor and saltstone. The benchmarking species I-129 was chosen because its transport is either slightly sorbed or unsorbed along its transport pathway. The results for the Base Case model shows I-129 as a major dose contributor.

Figure 5.1-3 shows that there is a good match between the PORFLOW results and the GoldSim results for I-129 releases from Vault 1. The initial GoldSim estimate of the I-129 break though, which includes the peak of the breakthrough curve, is conservatively high compared to the POFLOW results. At the end of the 20,000-year simulation, the GoldSim releases dissipate faster than the PORFLOW results. The benchmarking species Cs-135 was chosen because it is a major contributor in Alternative Sensitivity Case K. Figure 5.1-4 shows there is a good match between the PORFLOW results and the GoldSim results. Figure 5.1-5 presents the Np-237 releases from the two models. Trends for Np-237 have moderately higher results for the first 16,000 years indicating a good match. Note that Np-237 is generated through ingrowth from the Cf-249→Cm-245→Pu-241→Am-241→ Np-237 chain.

Figure 5.1-1: Vault 1 Ra-226 Release to the Saturated Zone

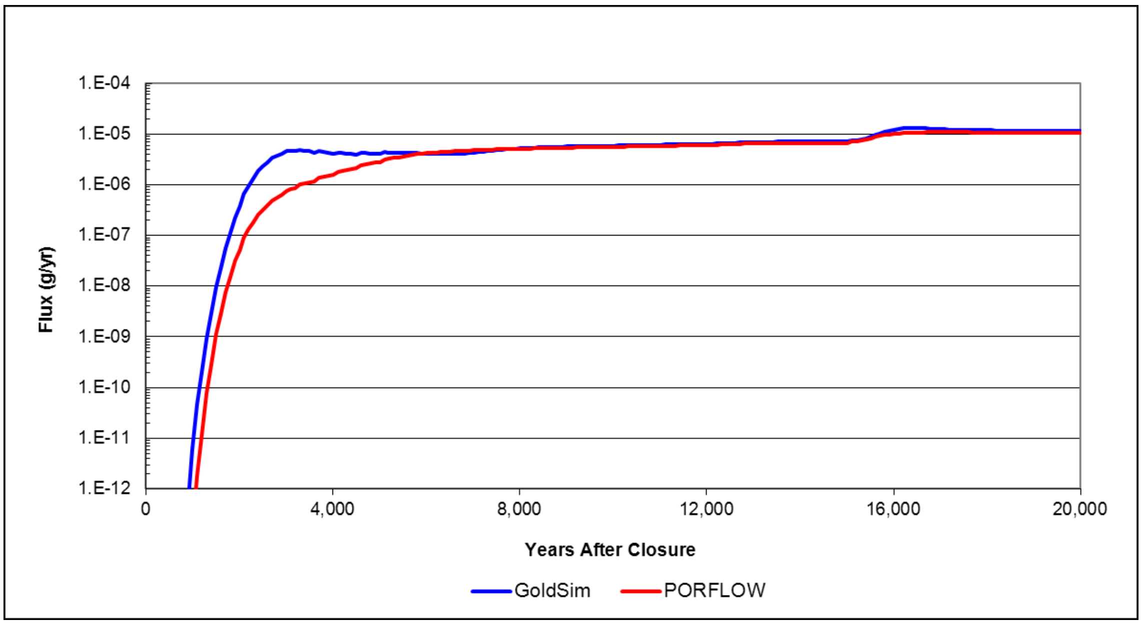

Figure 5.1-2: Vault 1 Tc-99 Release to the Saturated Zone

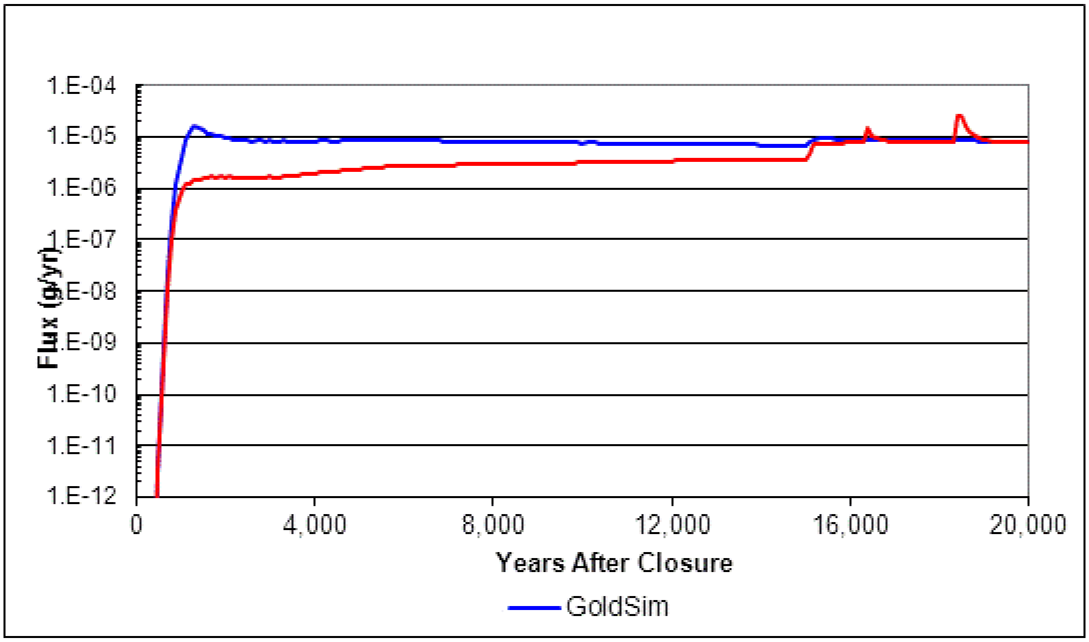

Figure 5.1-3: Vault 1 I-129 Release to the Saturated Zone

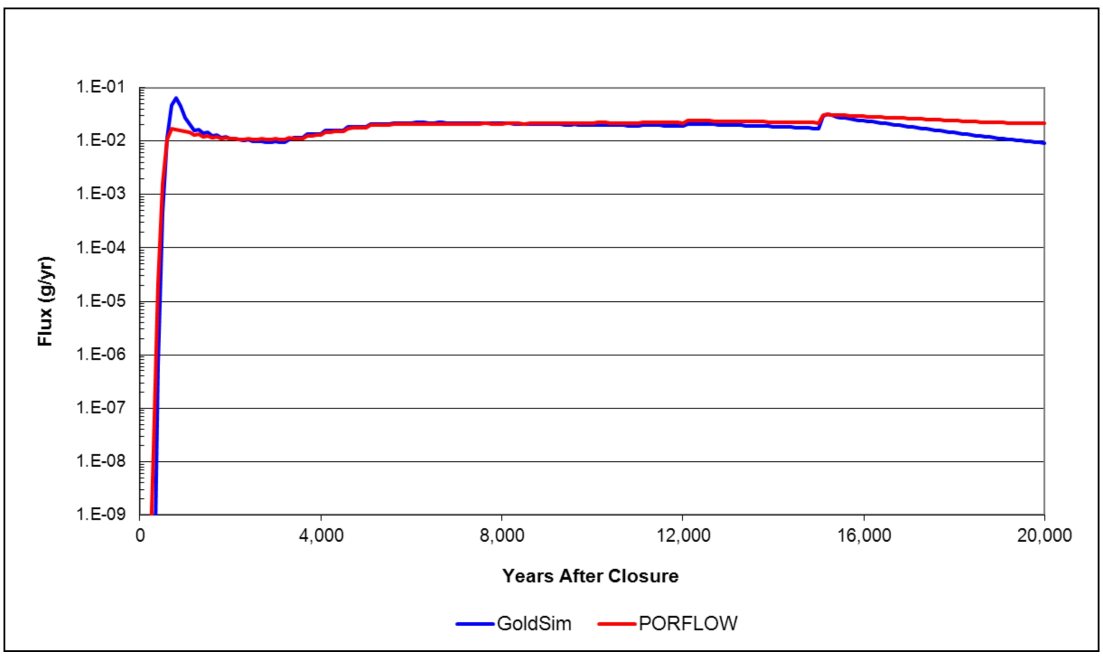

Figure 5.1-4: Vault 1 Cs-135 Release to the Saturated Zone

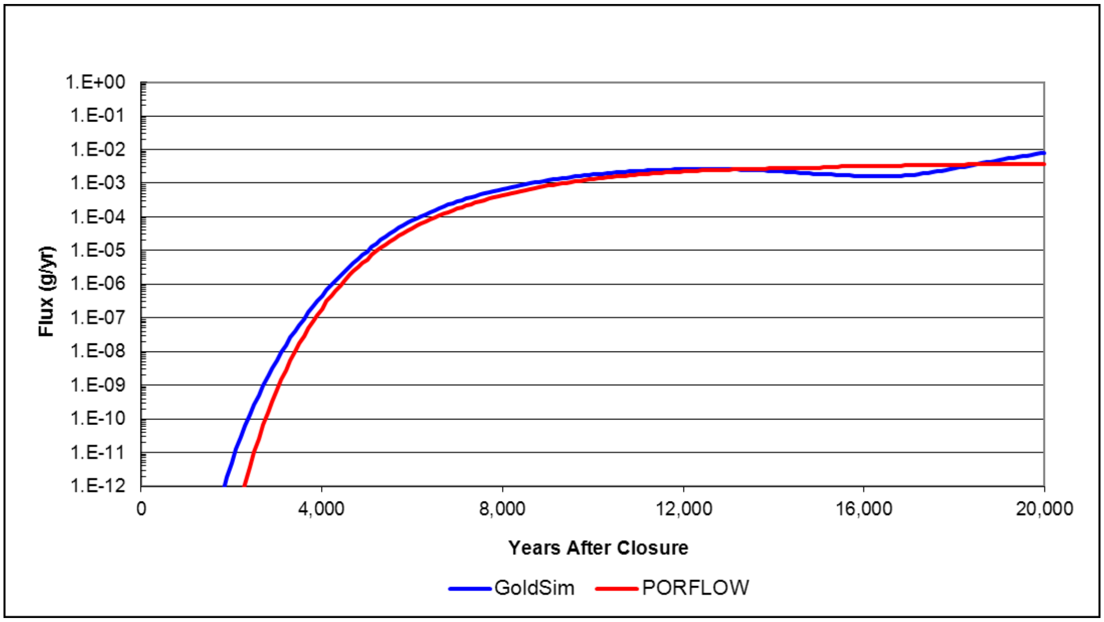

Figure 5.1-5: Vault 1 Np-237 Release to the Saturated Zone

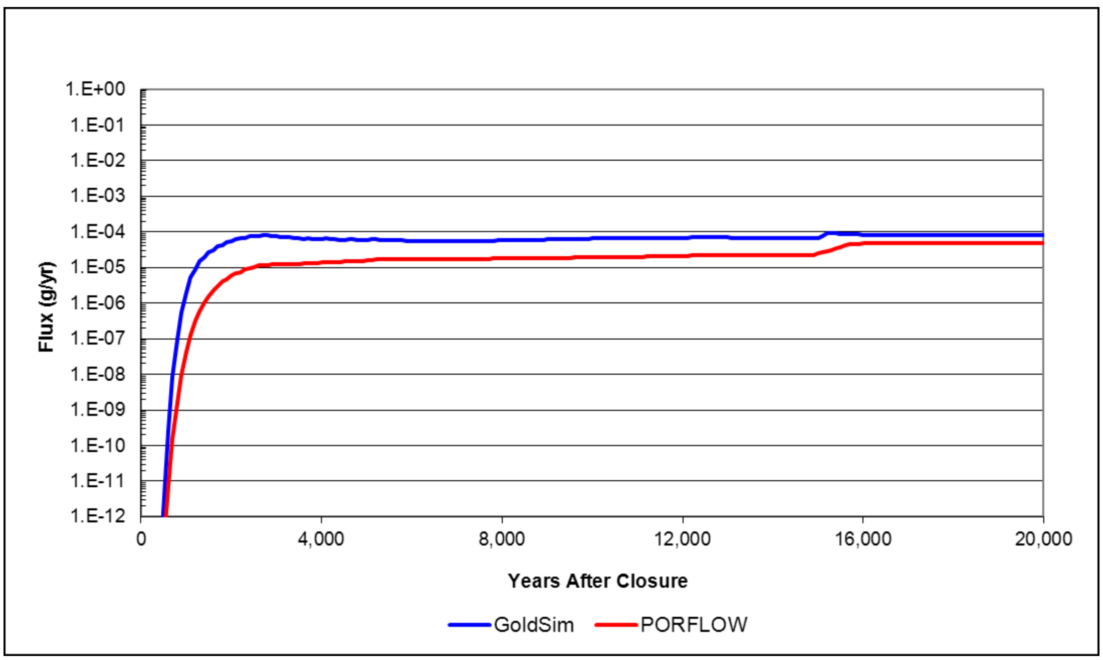

5.1.1.2 Vault 4

A comparison of PORFLOW and GoldSim mass releases of Ra-226 presented in Figure 5.1-6 indicate that the SDF GoldSim model can produce the same general trends as SDF PORFLOW model in addition to similar release rates from Vault 4. As can be seen in Figure 5.1-7, the SDF GoldSim model does is acceptable at reproducing the trends in the release of Tc-99 to the saturated zone from Vault 4. The early-year GoldSim release is higher than the PORFLOW release. In later years, the GoldSim release matches are lower with the PORFLOW results reflecting the oxygen diffusion controlled K_d influences transport in the walls. The peak releases are relatively similar between the two models. Figure 5.1-8 shows that there is a good match between the PORFLOW results and the GoldSim results for I-129 releases for Vault 4. As with Vault 1, the early year breakthrough is higher in the GoldSim breakthrough profile. Figure 5.1-9 shows that there is an adequate match between the PORFLOW and GoldSim Cs-135 results with PORFLOW breakthrough coming slightly earlier and the GoldSim results being higher. Figure 5.1-10 presents the Np-237 releases from the two models. For Np-237, the trend match is good with moderately higher results for the first 10,000 years.

Figure 5.1-6: Vault 4 Ra-226 Release to the Saturated Zone

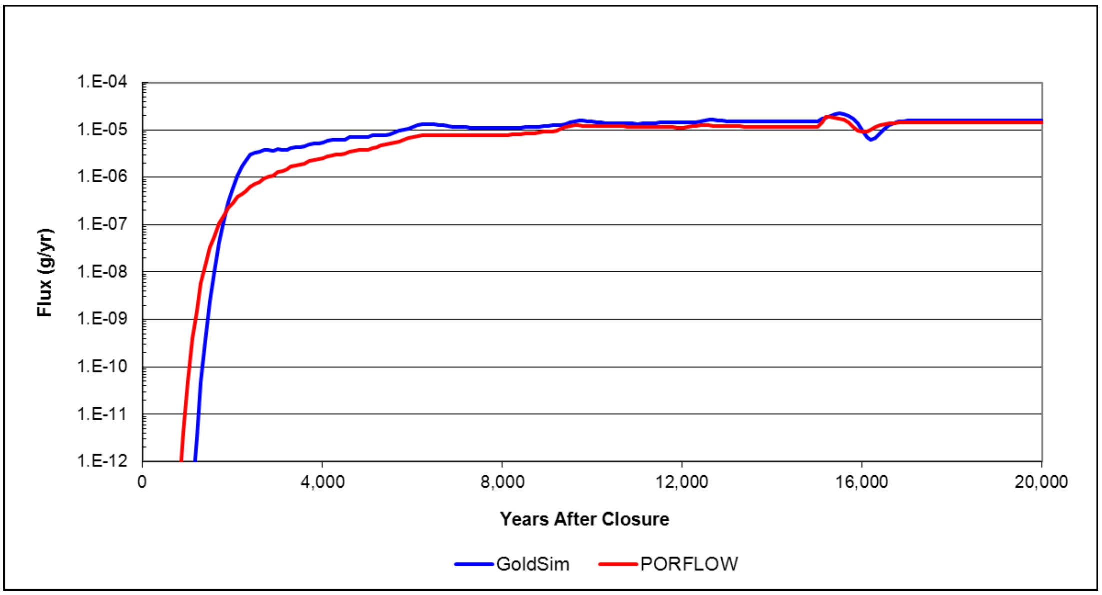

Figure 5.1-7: Vault 4 Tc-99 Release to the Saturated Zone

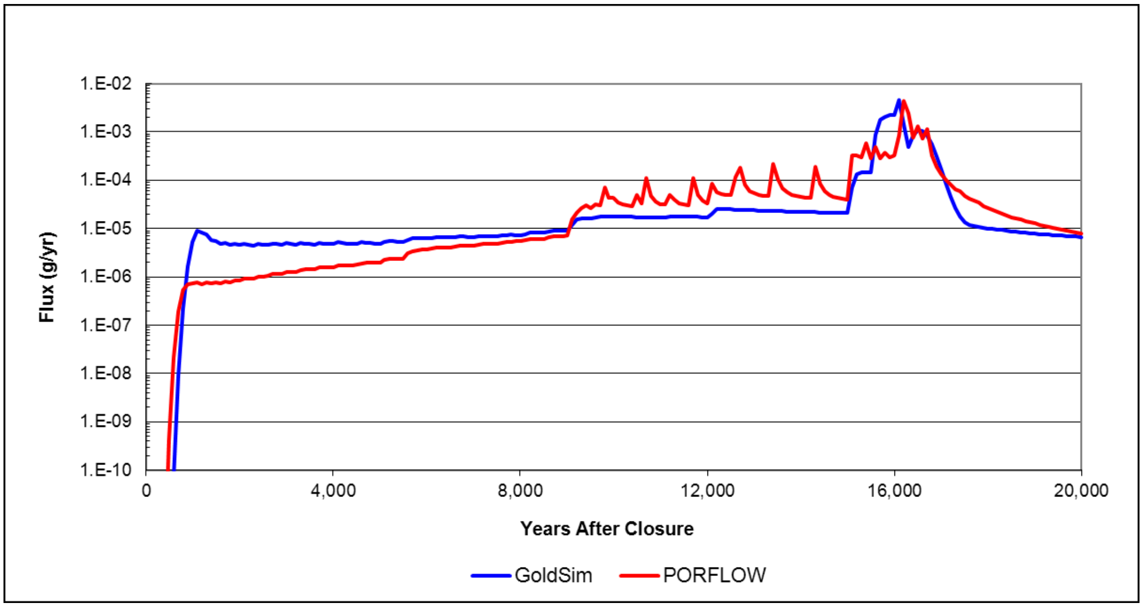

Figure 5.1-8: Vault 4 I-129 Release to the Saturated Zone

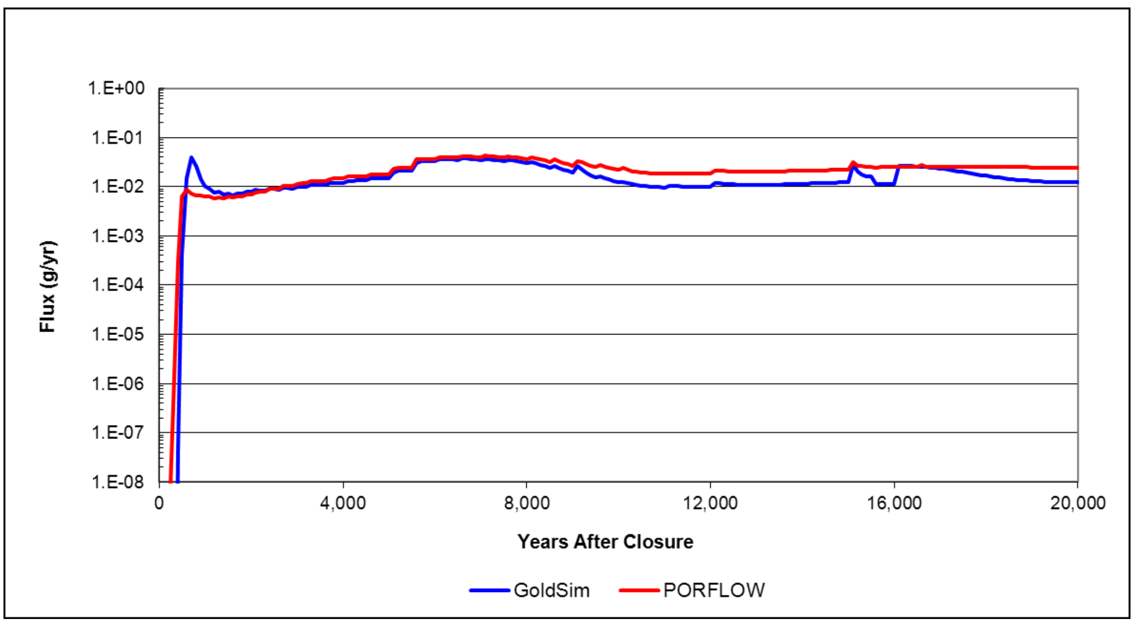

Figure 5.1-9: Vault 4 Cs-135 Release to the Saturated Zone

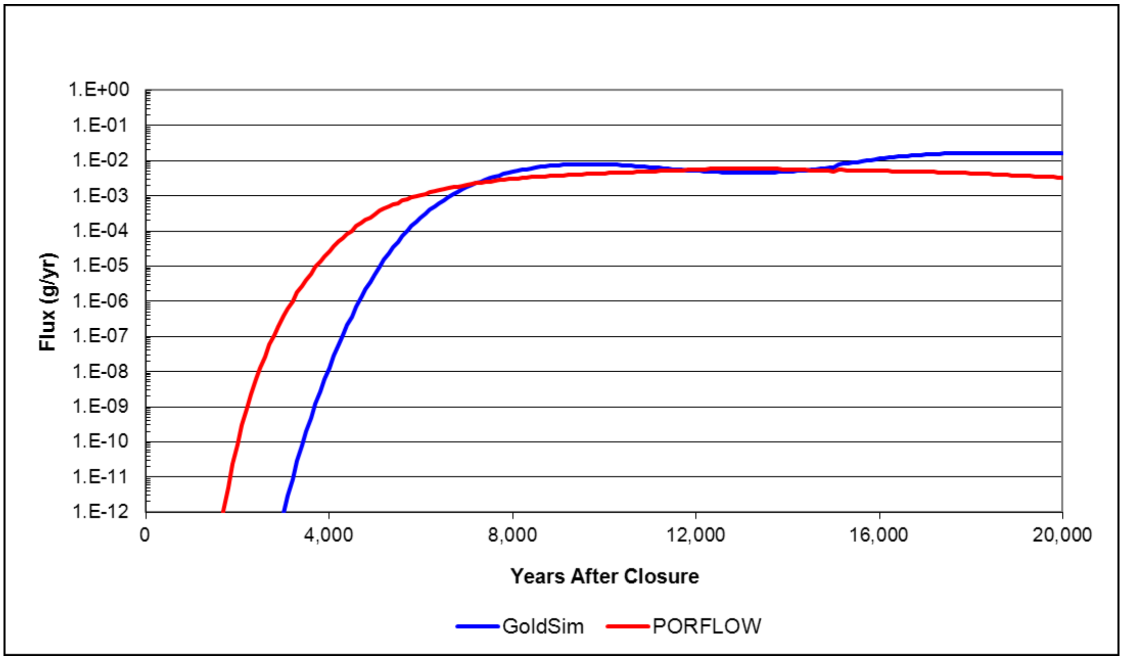

Figure 5.1-10: Vault 4 Np-237 Release to the Saturated Zone

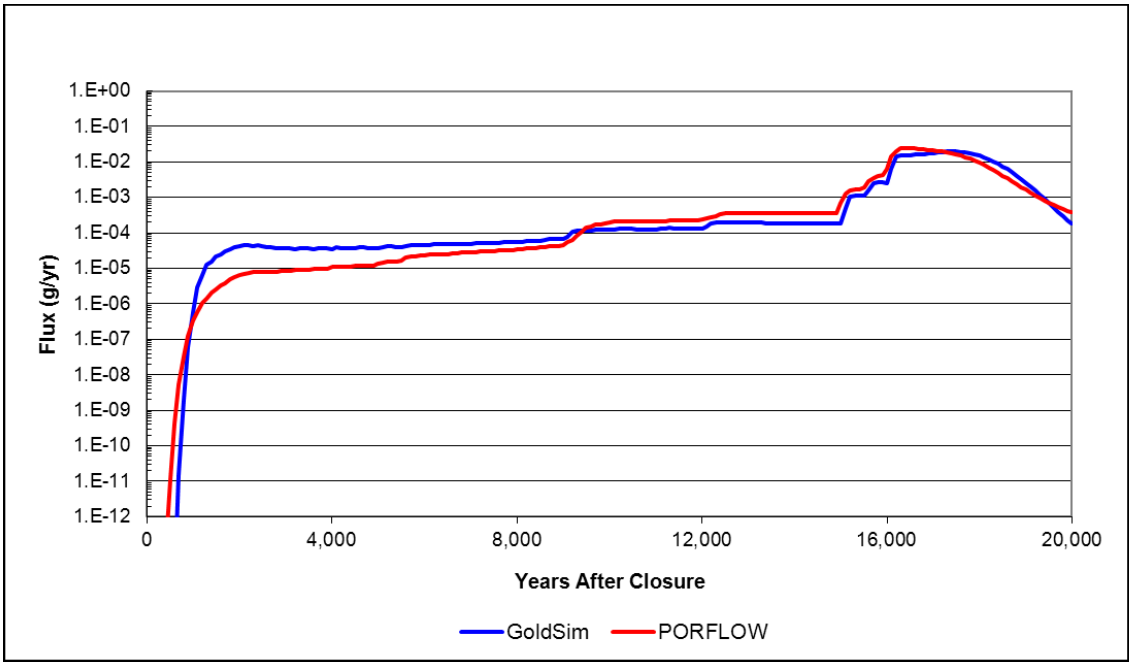

5.1.1.3 FDCs

A comparison of PORFLOW and GoldSim mass releases of Ra-226 presented in Figure 5.1-11 shows that the SDF GoldSim model and PORFLOW releases of Ra-226 from the FDCs are similar. As can be seen in Figure 5.1-12, the SDF GoldSim model does an adequate job of reproducing the trends in the release of Tc-99 to the saturated zone from the FDCs. The early-year GoldSim release prior to seeing the effects from the time-dependent PORFLOW K_d are quite similar. The later year PORFLOW results reflect the oxygen diffusion based K_d influence in the walls. The peak releases are quite similar between the two models. Figure 5.1-13 shows that there is a good match between the PORFLOW results and the GoldSim results for I-129 releases from the FDCs. Figure 5.1-14 shows that there is a good match between the PORFLOW Cs-135 results and the GoldSim results except in early years, with the PORFLOW breakthrough coming earlier and the GoldSim and PORFLOW results converging over time. Figure 5.1-15 presents the Np-237 releases from the two models. For Np-237, the match of the trends is good, with higher GoldSim releases at the initial breakthrough.

Figure 5.1-11: FDC Ra-226 Release to the Saturated Zone

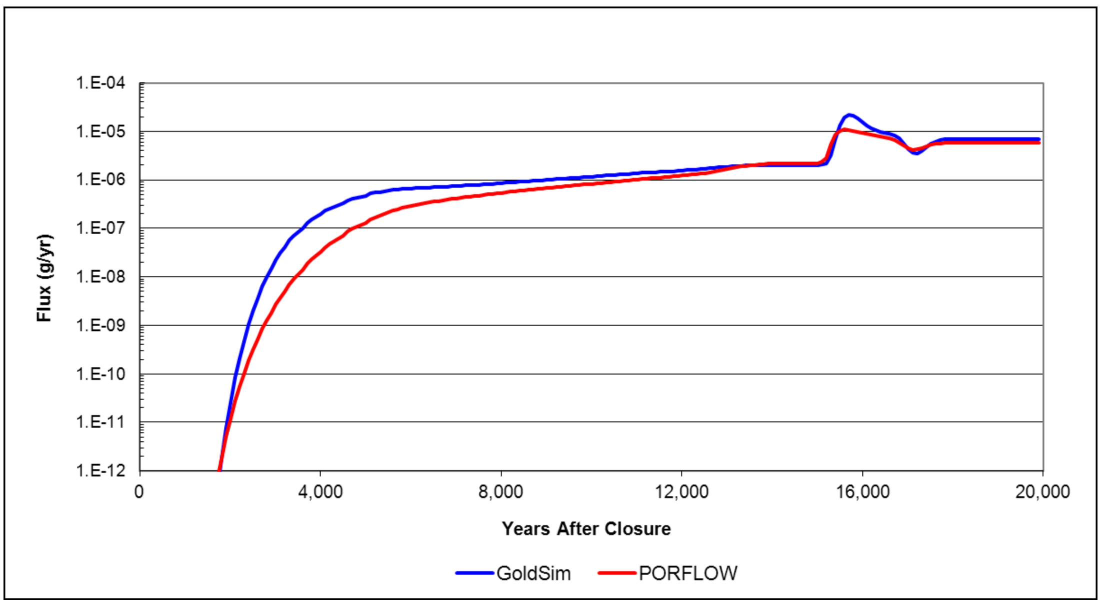

Figure 5.1-12: FDC Tc-99 Release to the Saturated Zone

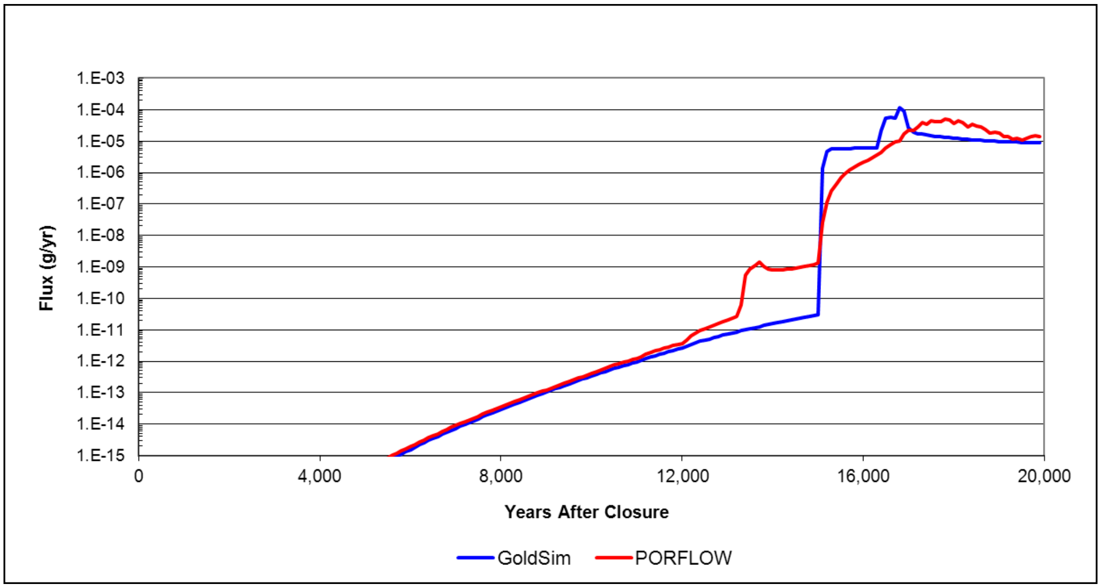

Figure 5.1-13: FDC I-129 Release to the Saturated Zone

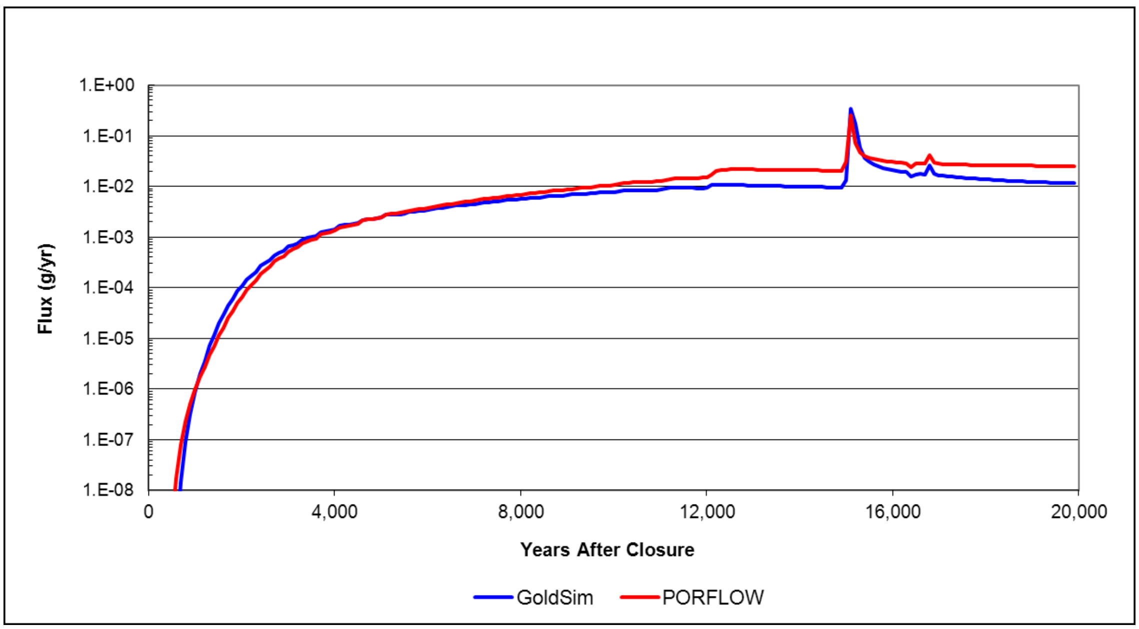

Figure 5.1-14: FDC Cs-135 Release to the Saturated Zone

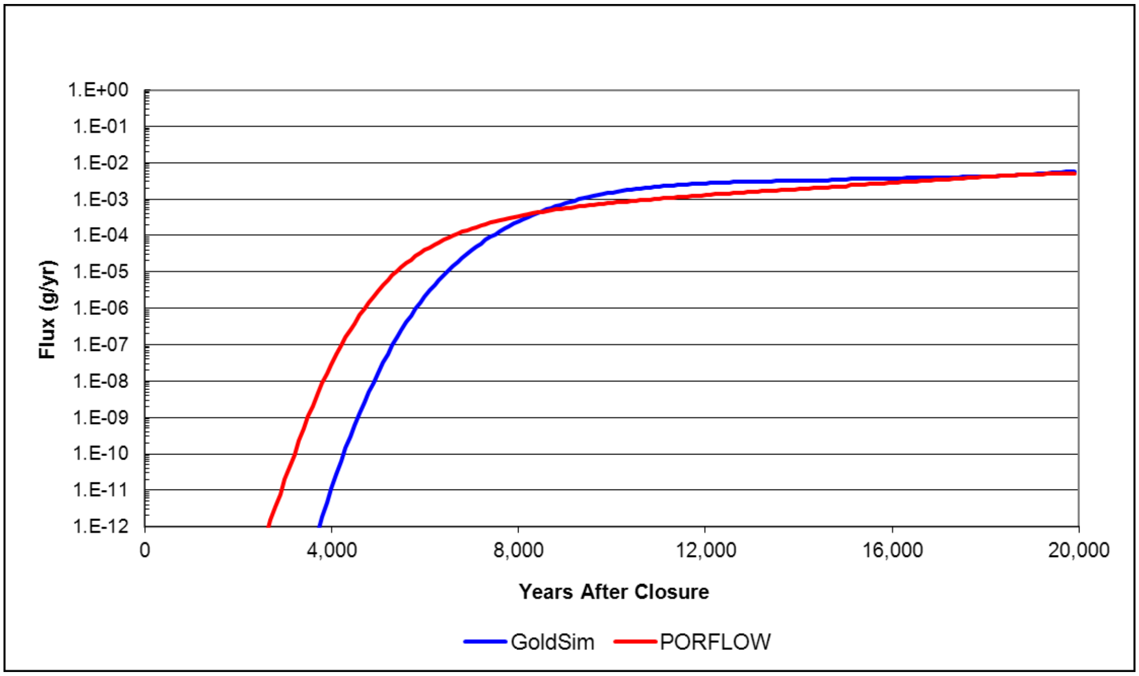

Figure 5.1-15: FDC Np-237 Release to the Saturated Zone

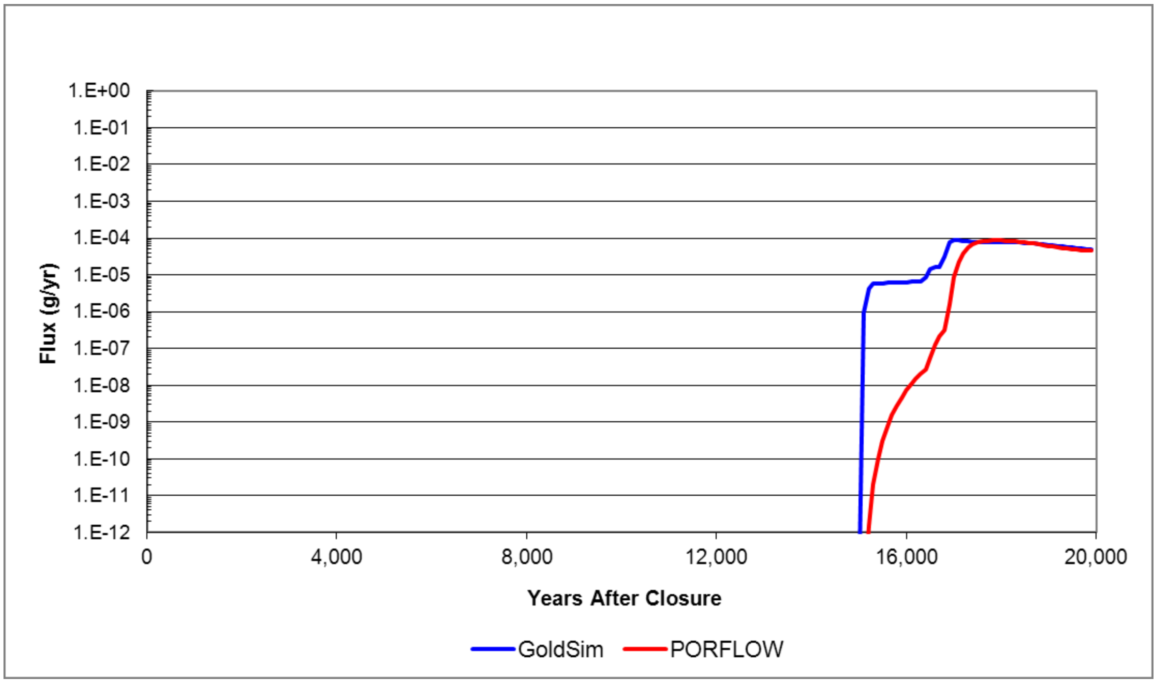

5.1.2 100-Meter Well Locations

The second phase of the benchmarking process is focused on how well the abstracted model approximates the radionuclide transport behavior in the saturated zone. The radionuclide concentrations in picocuries per liter, at two sectors, were examined for this task. The sectors used for the comparison were the southern Sector B and the northern Sector G. The locations of the sectors are shown in Figure 3.1-2. For this exercise, four species (Ra-226, Tc-99, I-129, and Np-237) were examined in the Phase 1 analysis.

5.1.2.1 Sector B

An examination of PORFLOW and SDF GoldSim model generated Ra-226 concentrations presented in Figure 5.1-16 indicates that the SDF GoldSim model can provide a computationally efficient approximation of 100-meter boundary Ra-226 concentrations produced by the migration of Ra-226 from the SDF to Sector B. There is a good consistency in the trends observed in the two Ra-226 breakthrough curves throughout the 20,000-year simulation. The slightly earlier breakthrough in the PORFLOW results reflects the similar pattern in the Vault 4 releases. The GoldSim also conservatively overestimates the concentrations, which is reflective of the Vault 4 and FDC releases prior to 16,000 years and the FDC releases after that time. Comparing the Vault 4 releases presented in Figure 5.1-6 with the 100-meter boundary results for Sector B presented in Figure 5.1-16 indicates that dilution in the saturated zone as simulated by the SDF GoldSim model has a similar effect to dilution simulated by the SDF PORFLOW model with the SDF GoldSim model showing a slight lesser degree of dilution.

As can be seen in Figure 5.1-17, the SDF GoldSim model also does a good job of reproducing the PORFLOW trends in the Tc-99 breakthrough curve at the 100-meter boundary. As with Ra-226, the GoldSim and PORFLOW simulations show similar degrees of dilution of the Tc-99 releases as the radionuclide is transported through the saturated zone to the 100-meter boundary (Figure 5.1-7, Figure 5.1-12, and Figure 5.1-17). Figure 5.1-18 shows that there is a very good correlation between the I-129 100-meter concentration levels generated by PORFLOW and their concentration levels simulated by the SDF GoldSim model. The 100-meter I-129 concentrations are dominated by the Vault 4 releases in early years and the FDC releases in later years. The GoldSim based I-129 concentrations are higher at the initial breakthrough, but the curves are quite similar thereafter.

Figure 5.1-19 shows that there is a good correlation between Np-237 100-meter concentrations generated by PORFLOW and the 100-meter concentrations given by the SDF GoldSim model for most of the 20,000-year simulation and the peak values are honored. By comparing Figures 5.1-10 and 5.1-19, it can be seen that the 100-meter concentrations are dominated by the Vault 4 releases. Note that there is a slightly smaller degree of dilution in the saturated zone concentrations generated by the SDF GoldSim model.

Figure 5.1-16: Ra-226 Concentration at Sector B (Base Case)

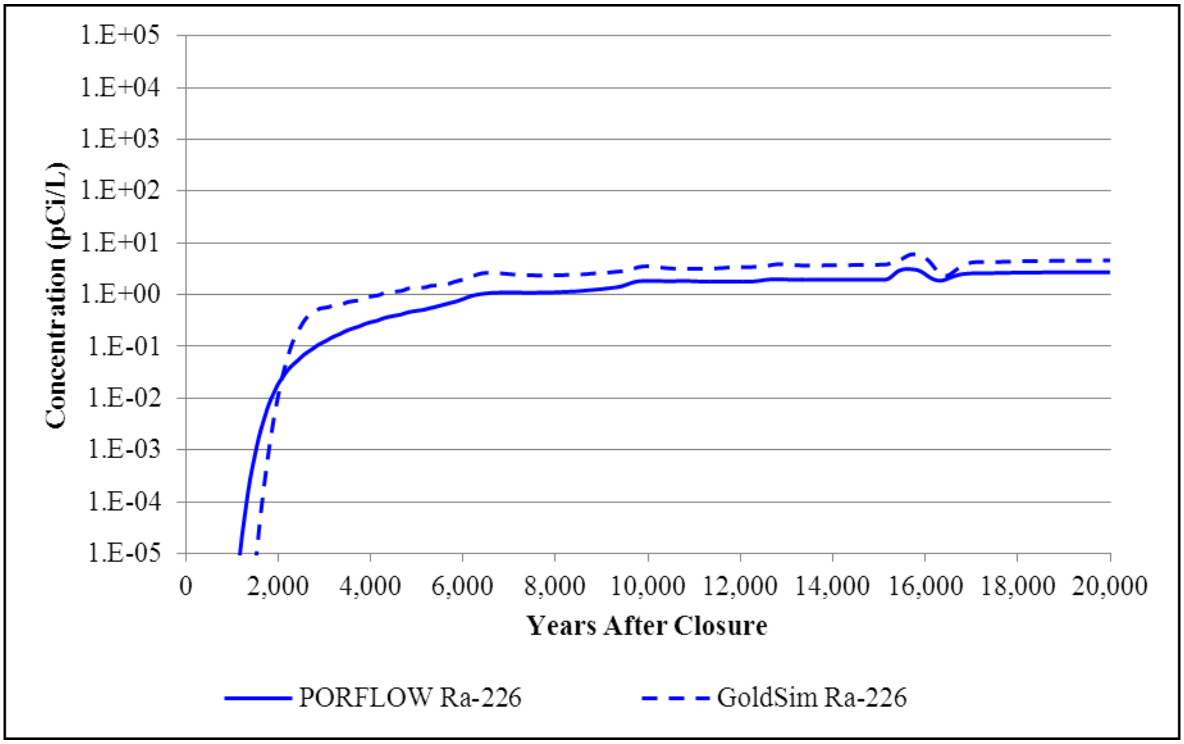

Figure 5.1-17: Tc-99 Concentration at Sector B (Base Case)

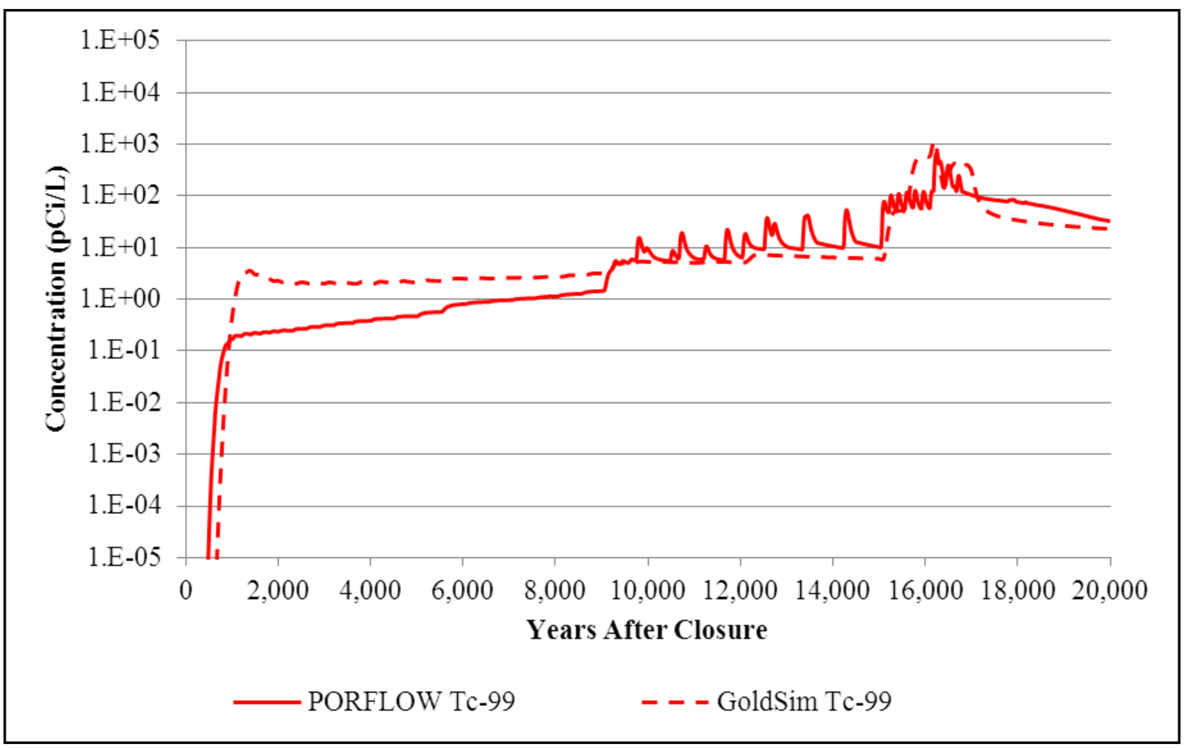

Figure 5.1-18: I-129 Concentration at Sector B (Base Case)

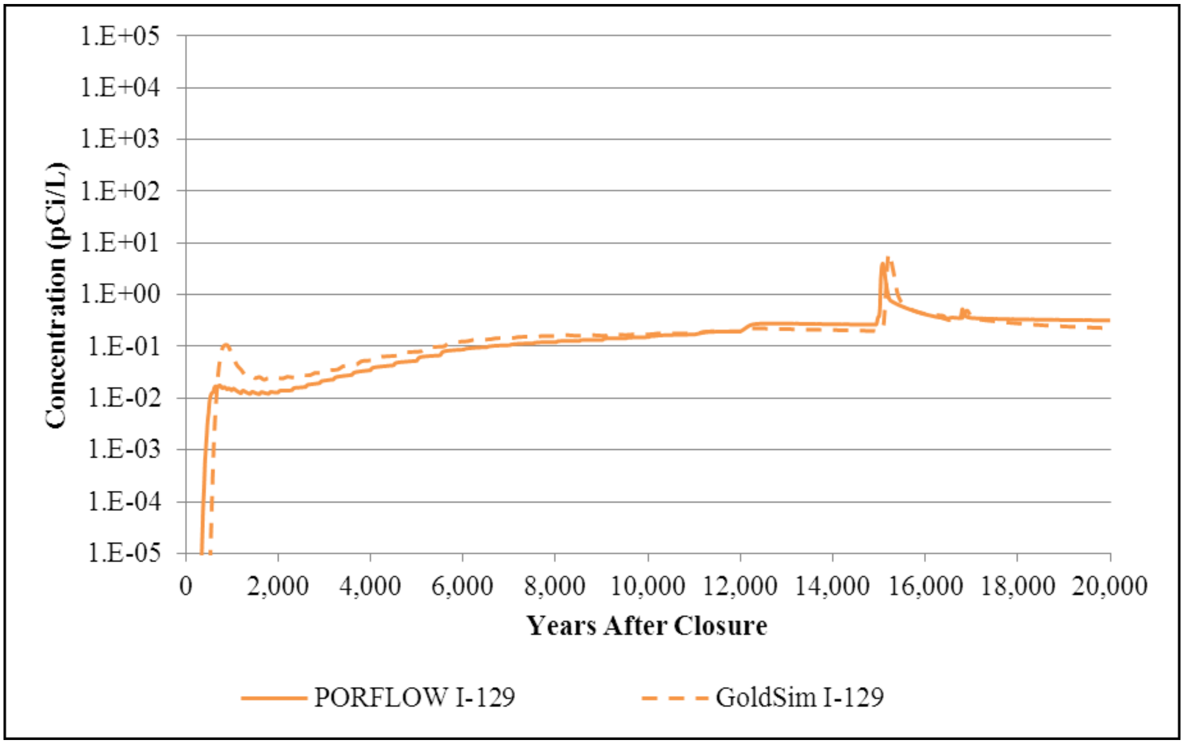

Figure 5.1-19: Np-237 Concentration at Sector B (Base Case)

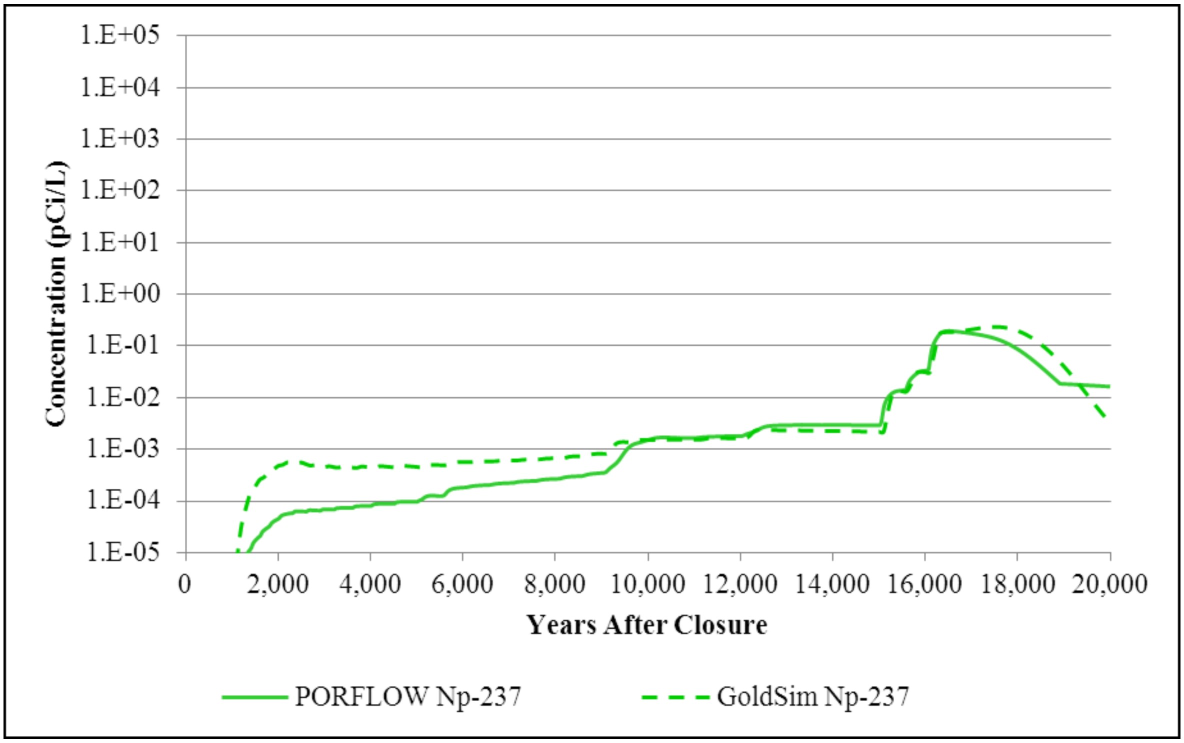

5.1.2.2 Sector G

As with the Sector B analysis, an examination of PORFLOW and SDF GoldSim model generated Ra-226 concentrations in Sector G presented in Figure 5.1-20 indicate that the SDF GoldSim model can provide a computationally efficient approximation of 100-meter boundary Ra-226 concentrations produced by the migration of Ra-226 from the SDF. There is good consistency between the trends observed in the two Ra-226 breakthrough curves throughout the 20,000-year simulation with the SDF GoldSim model showing a slightly higher peak value. By comparing Figures 5.1-11 and 5.1-20, it can be seen that the SDF GoldSim model reproduces the saturated zone, transport dilution effects, seen in the PORFLOW results, quite well. It can also be seen that the Sector G results are controlled by the FDC releases as expected

As can be seen in Figure 5.1-21, the SDF GoldSim model does an adequate job of reproducing the PORFLOW trends in the Tc-99 breakthrough curve at the 100-meter boundary after 15,000 years. In earlier years when the concentration is low, the SDF GoldSim model under predicts the concentrations. The differences are due to the northerly flow of groundwater in the Gordon Aquifer, which is not simulated in the SDF GoldSim model. The SDF GoldSim model disregards the Gordon Aquifer because concentrations in the Gordon Aquifer have very little influence on peak dose. Figure 5.1-22 shows that there is a very good correlation between the I-129 100-meter concentration levels generated by PORFLOW and I-129 concentration levels simulated by the SDF GoldSim model. The 100-meter I-129 concentrations reflect the FDC releases and the dilution factors between the GoldSim and PORFLOW models are again shown to be quite consistent (Figures 5.1-13 and 5.1-22).

Figure 5.1-23 shows that the GoldSim Np-237 breakthrough is earlier than the SDF PORFLOW model in Sector G, but there is a good correlation between Np-237 100-meter concentrations after 18,000 years. Comparing Figures 5.1-15 and 5.1-23 shows that the dilution factors for both models are quite similar.

Figure 5.1-20: Ra-226 Concentration at Sector G (Base Case)

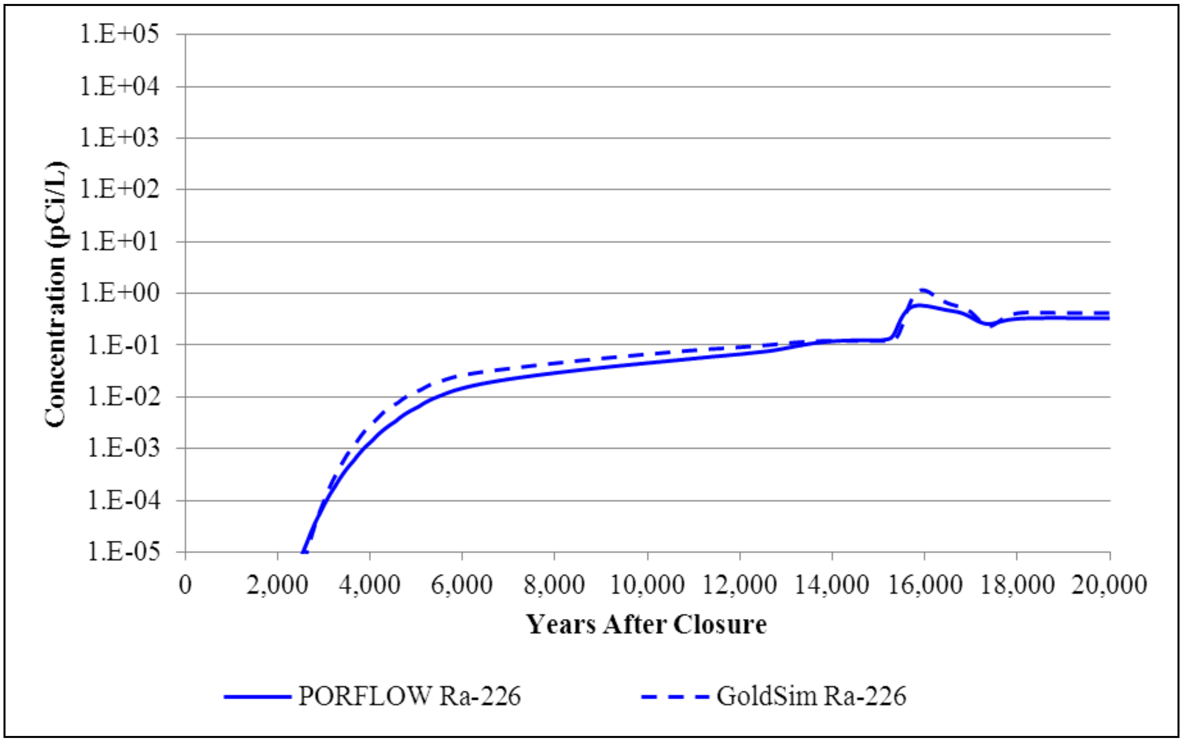

Figure 5.1-21: Tc-99 Concentration at Sector G (Base Case)

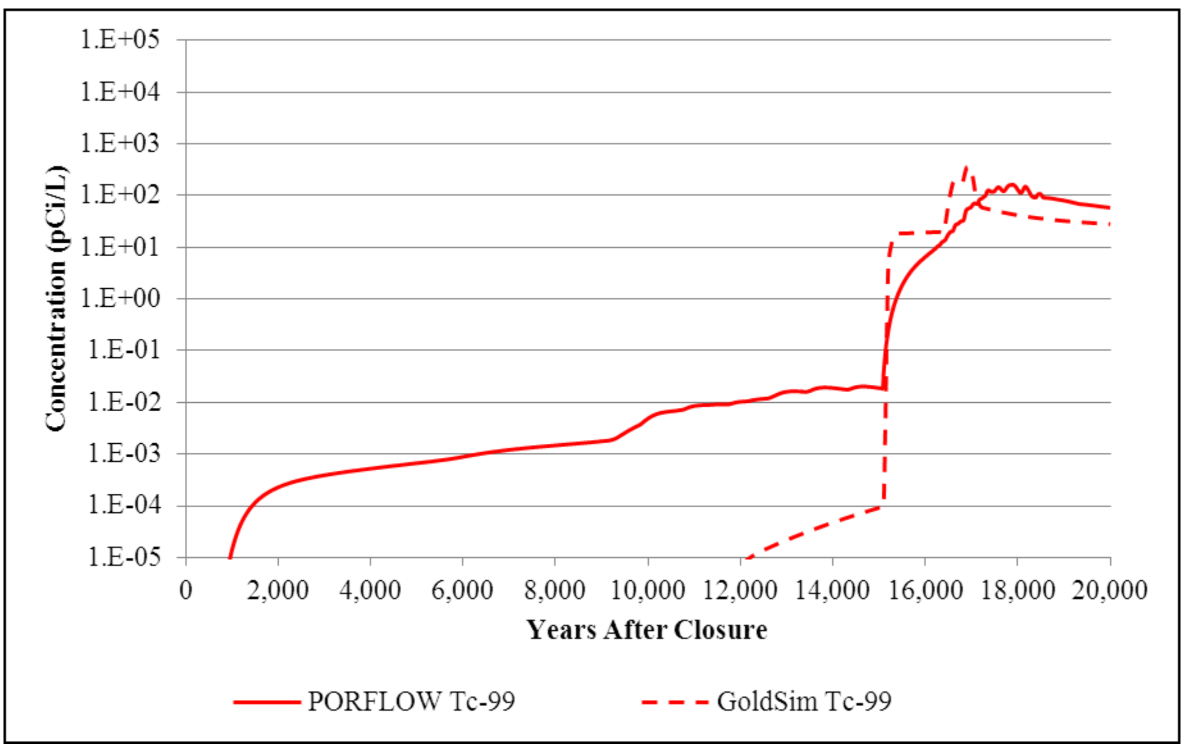

Figure 5.1-22: I-129 Concentration at Sector G (Base Case)

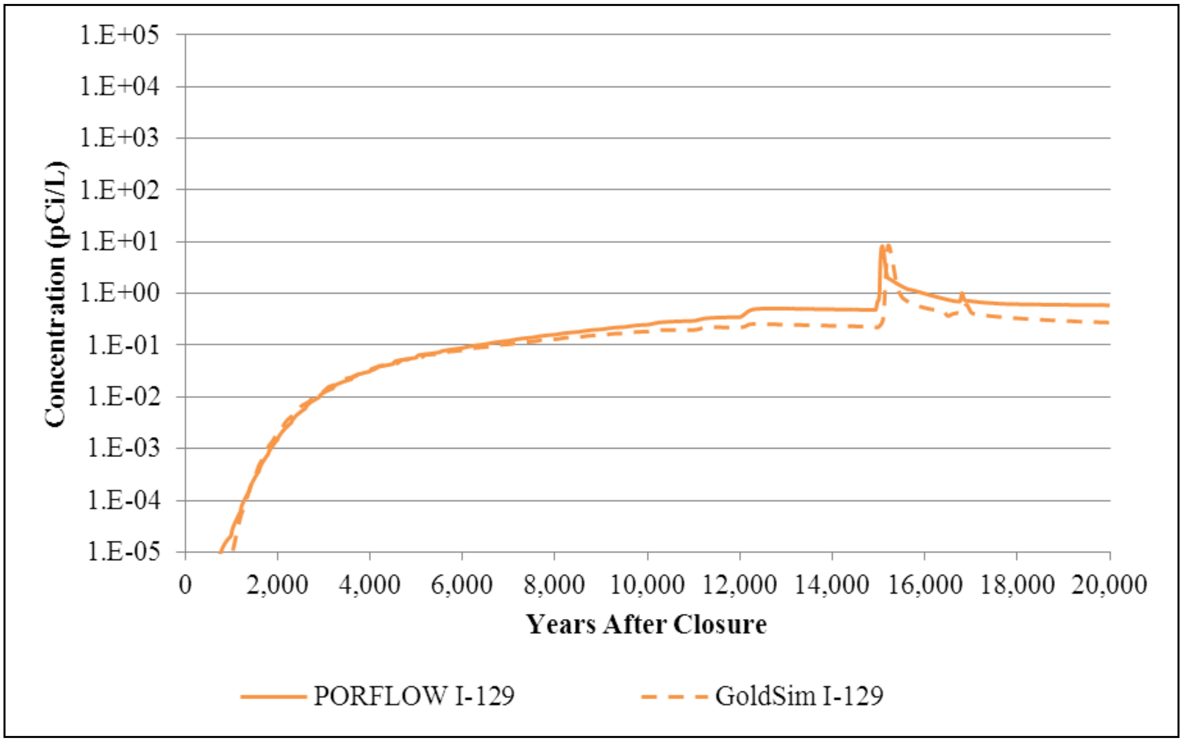

Figure 5.1-23: Np-237 Concentration at Sector G (Base Case)

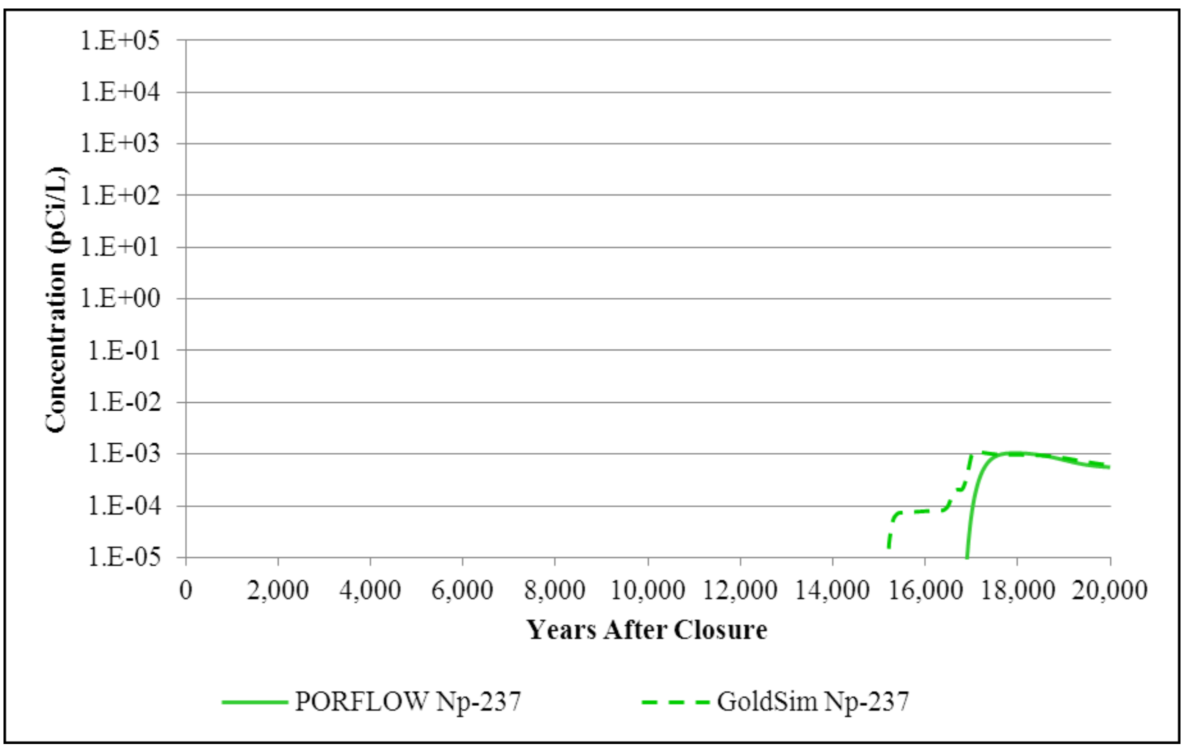

5.1.3 Total Dose Time Histories

An additional check on the appropriateness of the SDF GoldSim model as a surrogate for the SDF PORFLOW model, is a comparison between the maximum total doses generated using PORFLOW and the SDF GoldSim model. The Base Case comparison between PORFLOW and GoldSim results (Figure 5.1-24) shows that the SDF GoldSim model is higher, but approximates the general trends quite well.

Figure 5.1-24: Comparison between PORFLOW and GoldSim Total Max Dose Results, Base Case

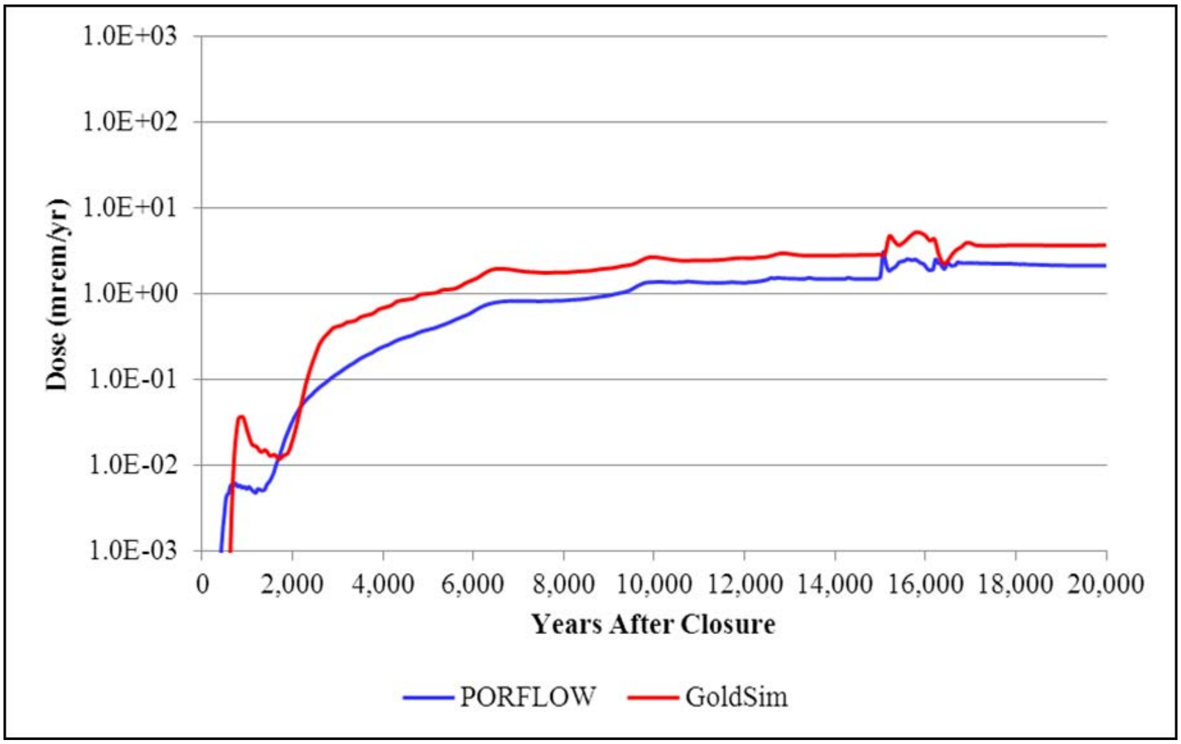

5.2 Alternate Scenario (Case K)

The alternate scenario (Alternative Sensitivity Case K) was designed to answer questions presented to the U.S. Department of Energy (DOE) by the NRC. Alternative Sensitivity Case K was developed in response to the NRC's SDF PA RAIs and was described in response RAI PA-8. [SRS-CWDA-2011-00044] The basic changes with respect to the base that are implemented in Alternative Sensitivity Case K are listed in Table 2.2-2.

5.2.1 Mass Releases to the Saturated Zone

To build confidence in the SDF GoldSim model, the SDF PORFLOW model and the SDF GoldSim model generated mass fluxes entering the saturated zone below Vault 1, Vault 4, and the FDCs were compared.

5.2.1.1 Vault 1

A comparison of PORFLOW and GoldSim mass releases of Ra-226 presented in Figure 5.2-1 indicates that the SDF GoldSim model can produce a very good approximation of

PORFLOW releases of Ra-226 from Vault 1. As can be seen in Figure 5.2-2, the SDF GoldSim model does an adequate job of reproducing the trends in the release of Tc-99 to the saturated zone from Vault 1. The GoldSim release tends to be less dispersed during the time-span between 8,000 and 18,000 years. Note that the time-dependent Tc-99 K_d curves generated by the shrinking core model (see Section 3.5) are used in both the GoldSim and PORFLOW models. [SRR-CWDA-2011-00044 RAI PA-8] Figure 5.2-3 shows that there is a very good match between the PORFLOW results and the GoldSim results for I-129 releases Vault 1. Figure 5.2-4 shows that there is also a good match between the PORFLOW results and the GoldSim results for Cs-135. Figure 5.2-5 presents the Np-237 releases from the two models. For Np-237, the models produce a good match of the trends for the first 7,000 years. Later, the SDF GoldSim model, conservatively over estimates the Np-237 releases until 19,000 years into the simulation when the results match up again.

Figure 5.2-1: Vault 1 Ra-226 Release to the Saturated Zone

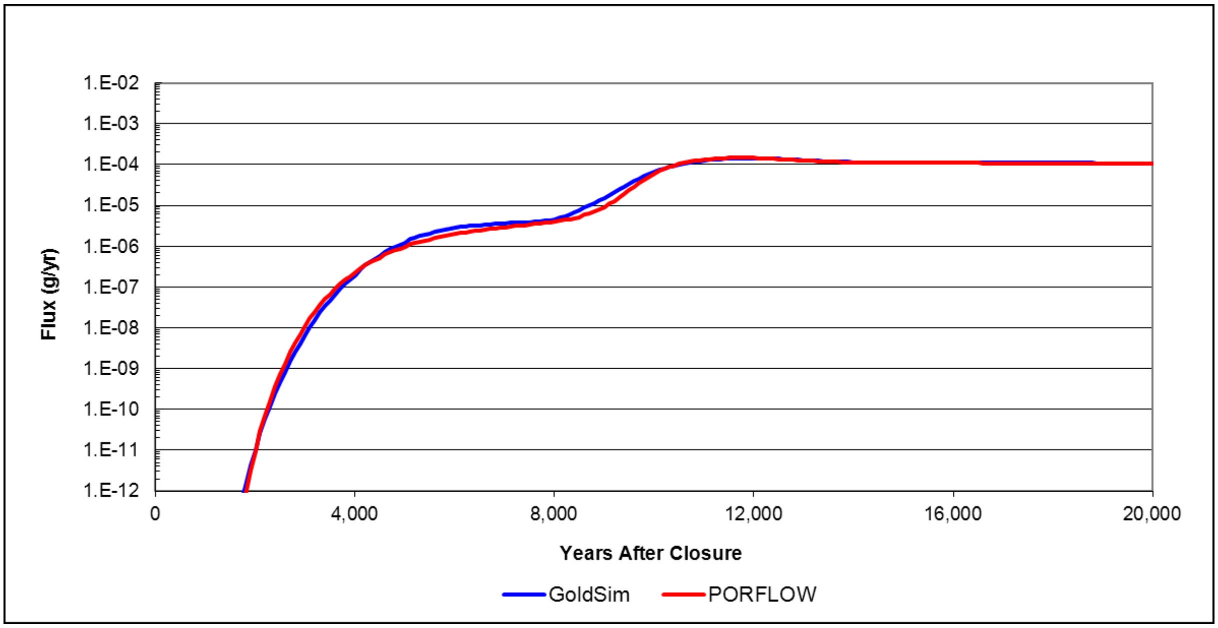

Figure 5.2-2: Vault 1 Tc-99 Release to the Saturated Zone

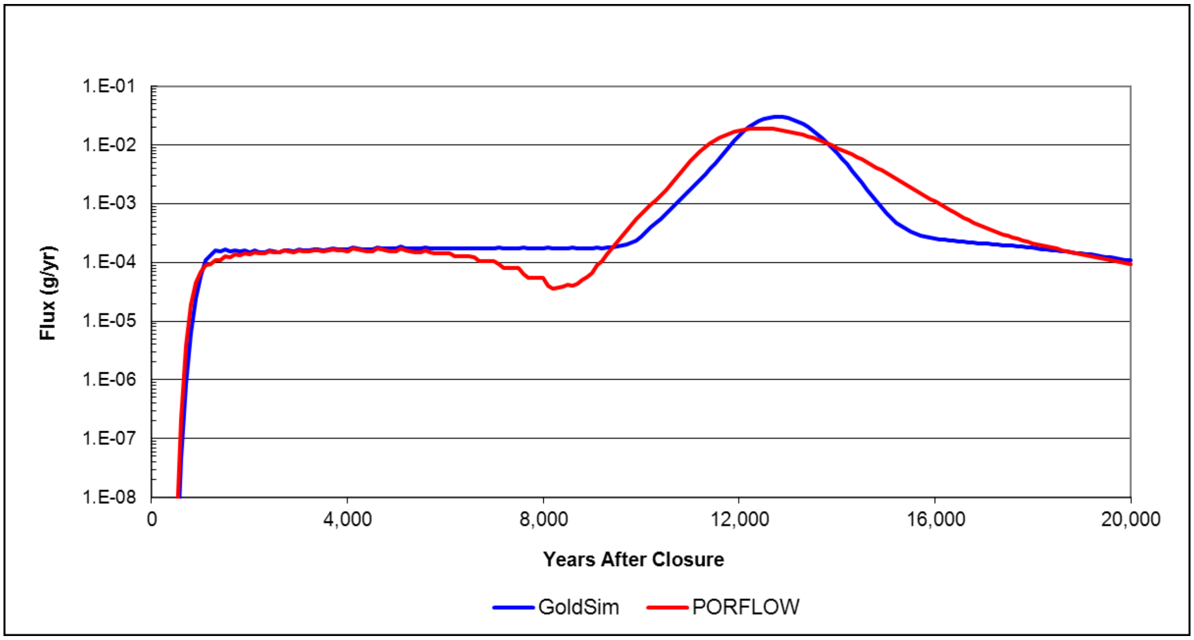

Figure 5.2-3: Vault 1 I-129 Release to the Saturated Zone

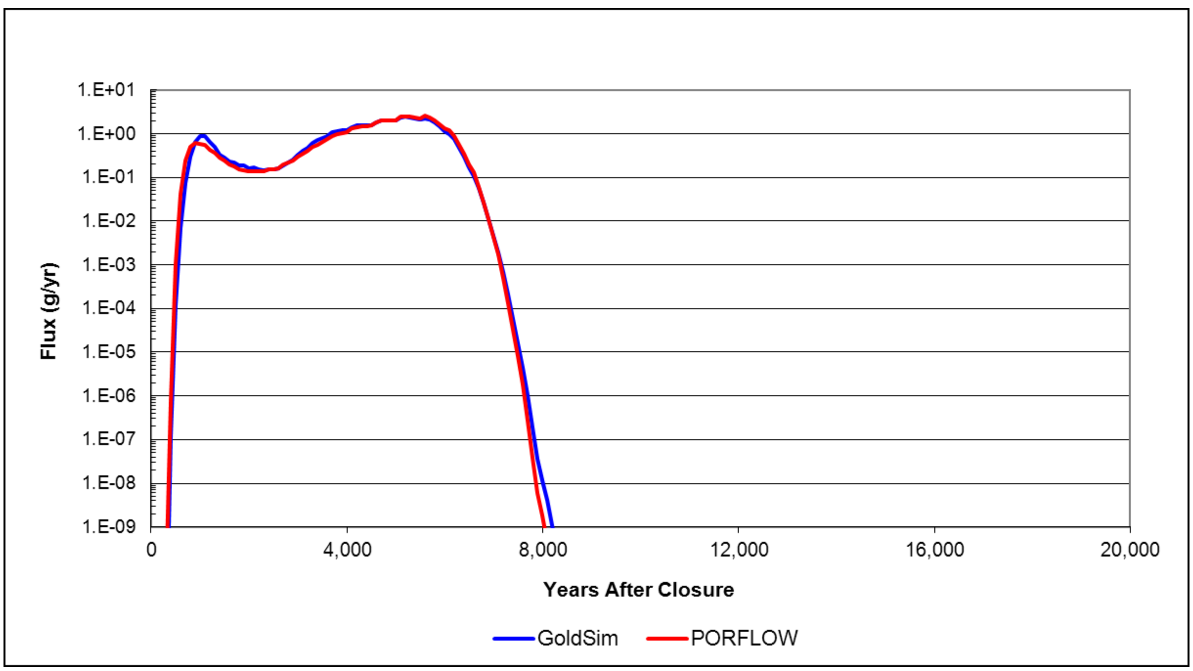

Figure 5.2-4: Vault 1 Cs-135 Release to the Saturated Zone

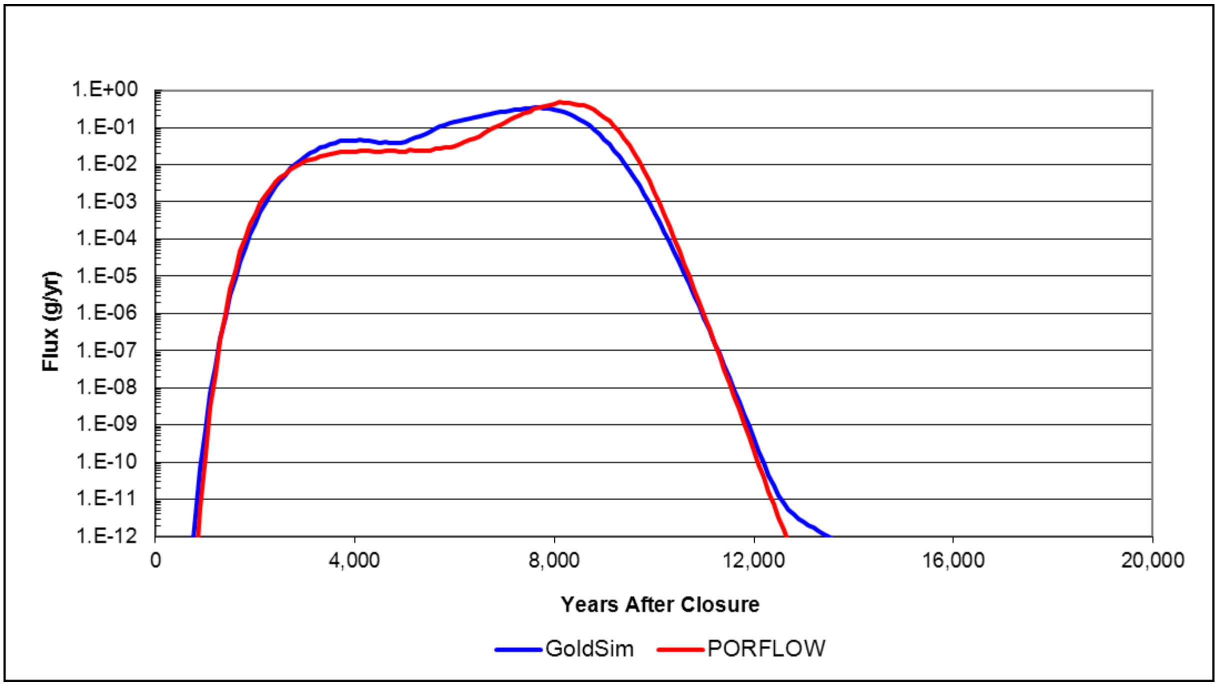

Figure 5.2-5: Vault 1 Np-237 Release to the Saturated Zone

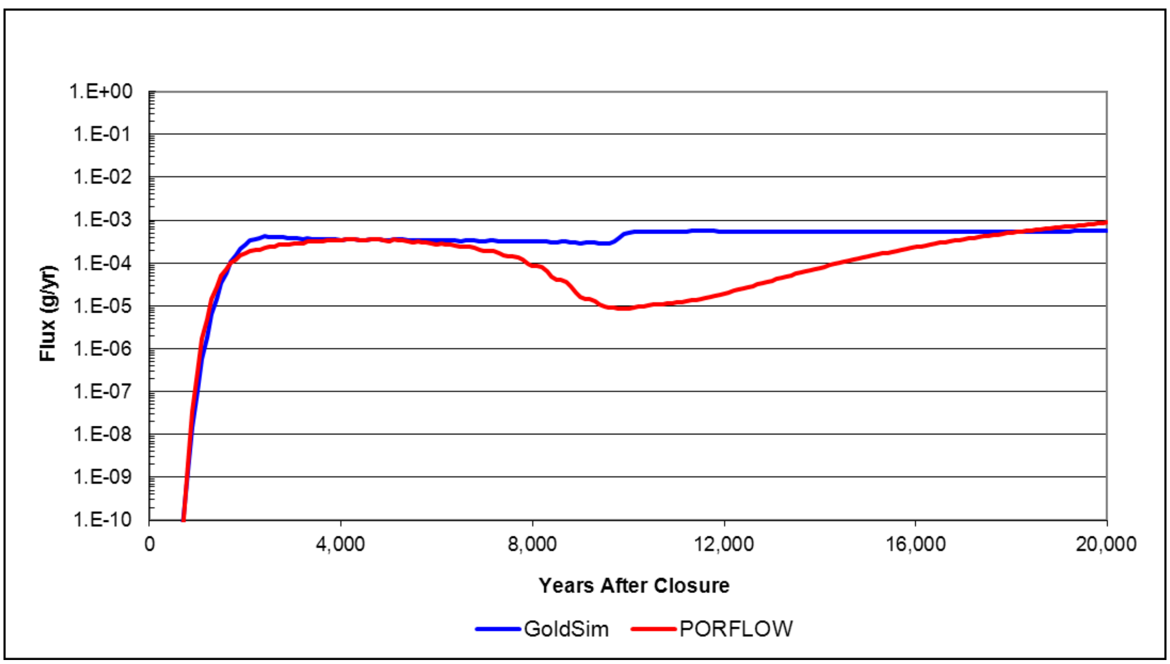

5.2.1.2 Vault 4

A comparison of PORFLOW and GoldSim mass releases of Ra-226 presented in Figure 5.2-6 indicates that the SDF GoldSim model can produce the same general trends as PORFLOW releases of Ra-226 and similar release rates from Vault 4. The only difference is in early time when the Ra-226 breakthrough is later for the GoldSim simulation than for the PORFLOW simulation. As can be seen in Figure 5.2-7, the SDF GoldSim model does an adequate job of reproducing the trends in the release of Tc-99 to the saturated zone from Vault 4. The peak is slightly higher and more dispersed in the SDF PORFLOW model. Figure 5.2-8 shows that there is a good match between the PORFLOW results and the GoldSim results for I-129 releases Vault 4. Figure 5.2-9 shows that the general trends of the Cs-135 GoldSim and PORFLOW model releases are similar but the SDF PORFLOW model shows a little more dispersed breakthrough pattern. Figure 5.2-10 presents the Np-237 releases from the two models. For Np-237, the match of the trends is good with moderately higher GoldSim generated releases between 8,000 and 14,000 years and moderately higher PORFLOW generated releases between 14,000 and 20,000 years.

Figure 5.2-6: Vault 4 Ra-226 Release to the Saturated Zone

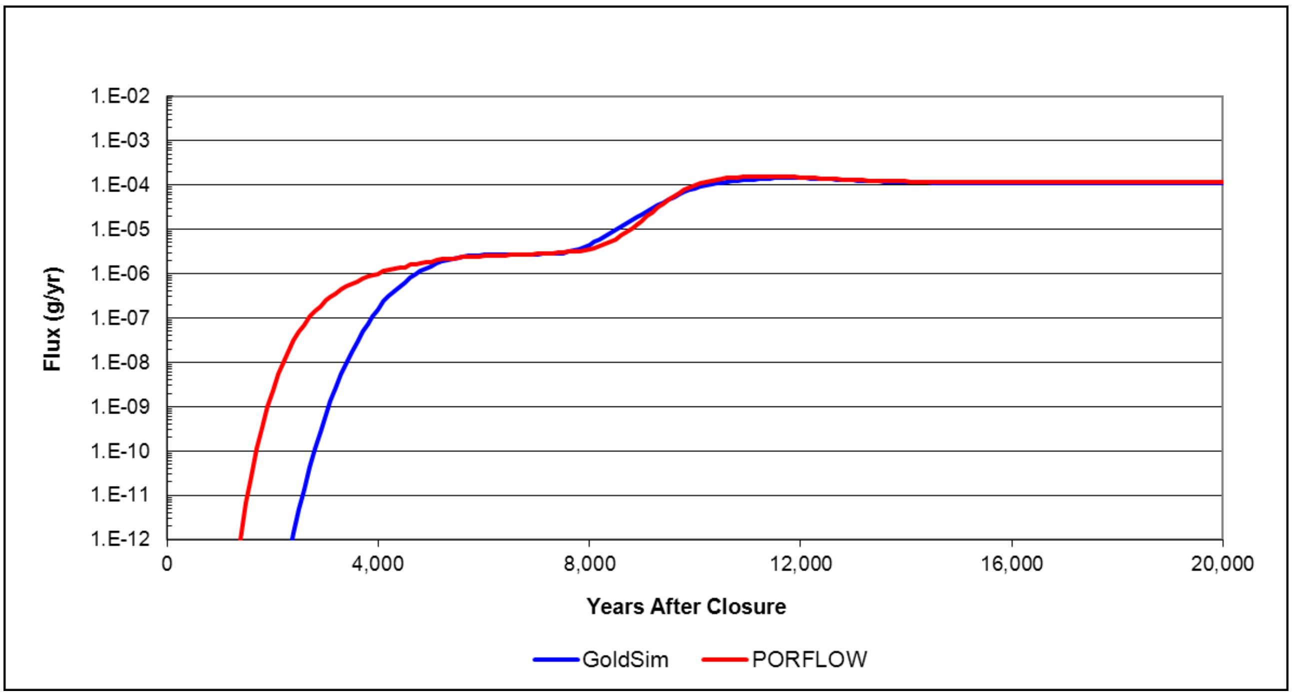

Figure 5.2-7: Vault 4 Tc-99 Release to the Saturated Zone

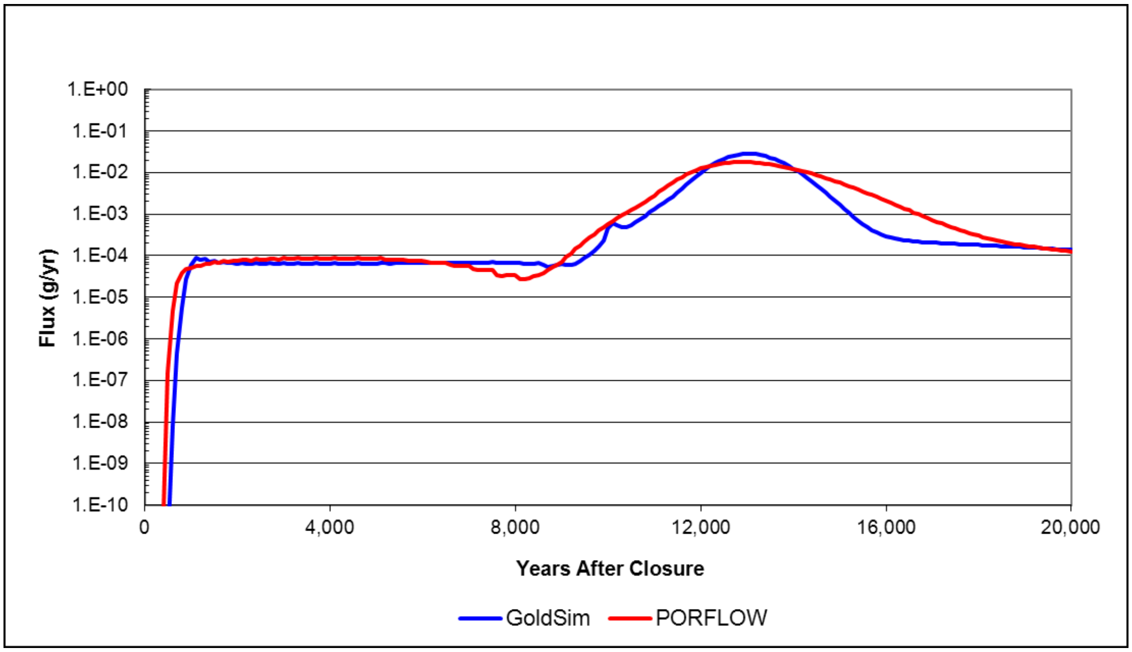

Figure 5.2-8: Vault 4 I-129 Release to the Saturated Zone

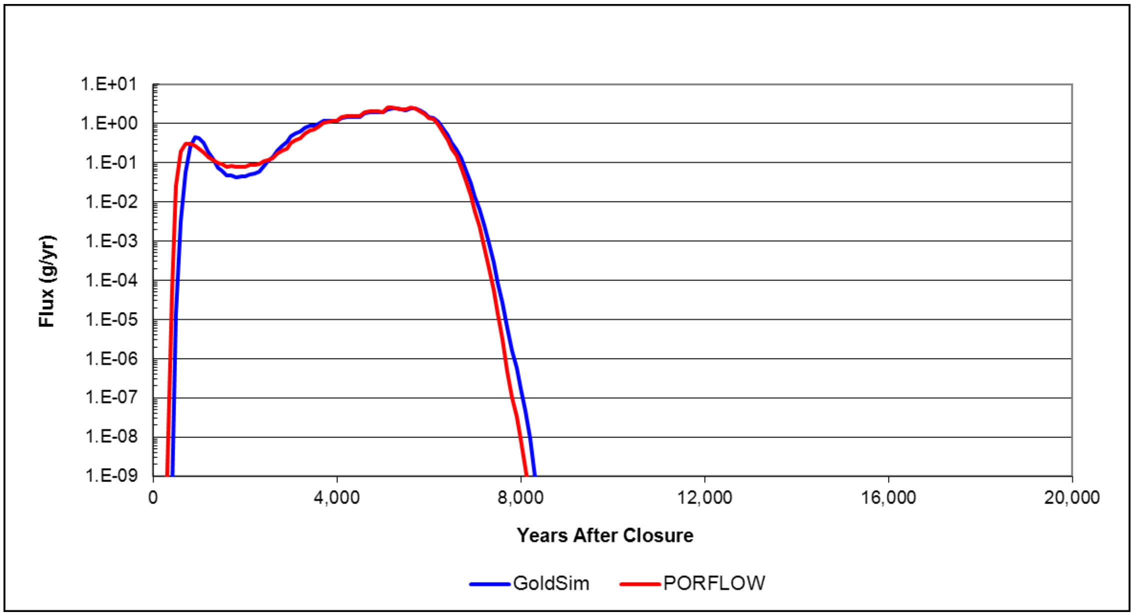

Figure 5.2-9: Vault 4 Cs-135 Release to the Saturated Zone

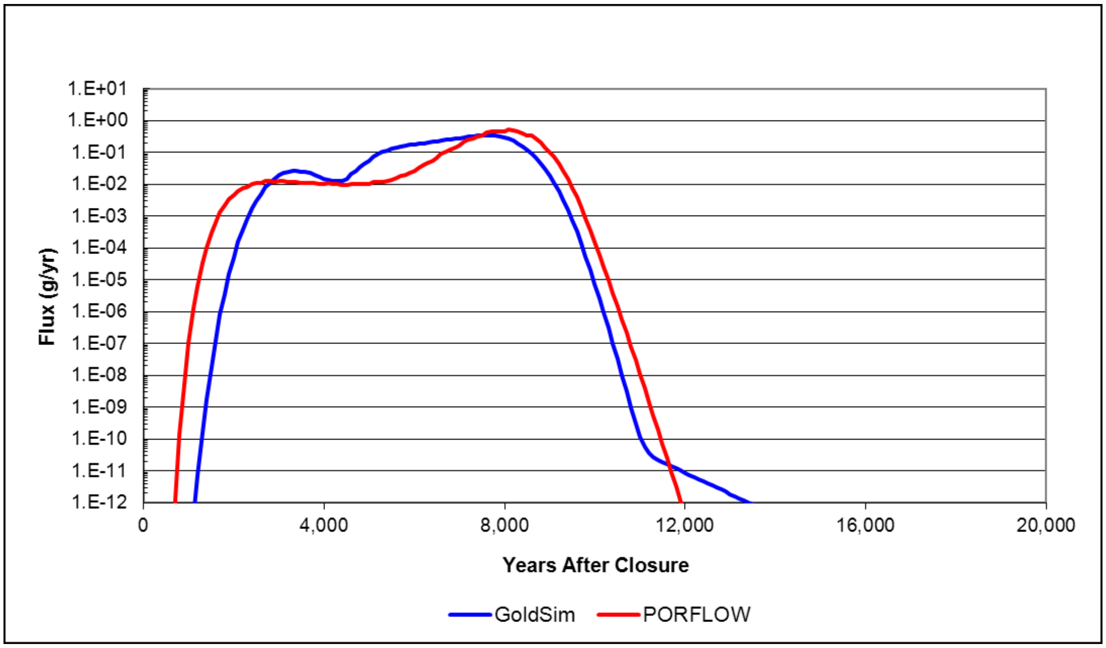

Figure 5.2-10: Vault 4 Np-237 Release to the Saturated Zone

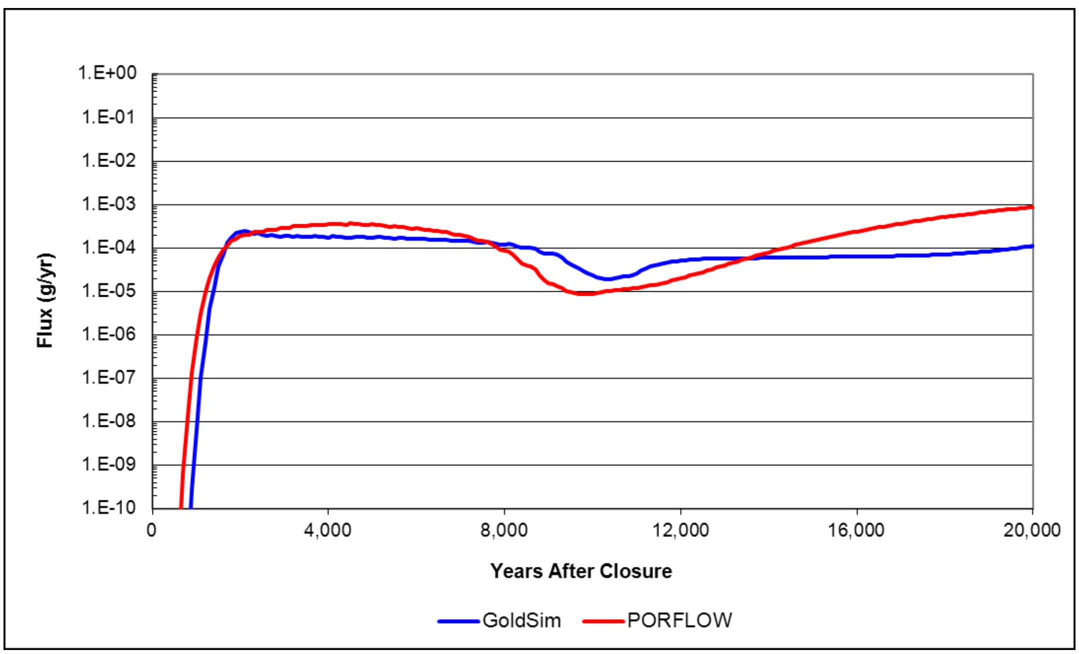

5.2.1.3 FDCs

A comparison of PORFLOW and GoldSim mass releases of Ra-226 presented in Figure 5.2-11 shows that the SDF GoldSim model does an adequate job of reproducing the trends in the release of Ra-226 from the FDCs. The release of Ra-226 is inclined to be more dispersed, and lower in the PORFLOW releases. As can be seen in Figure 5.2-12, the SDF GoldSim model does a good job of reproducing the trends in the release of Tc-99 to the saturated zone from the FDCs. Prior to 10,000 years, the match is quite good, and after 10,000 years, the SDF PORFLOW model shows a more dispersed release curve. Figure 5.2-13 shows that there is an adequate match between the PORFLOW results and the GoldSim results for I-129 releases from the FDCs. In later years, the release from the SDF PORFLOW model decreases at a slower rate. This slower rate of release in PORFLOW results is reflective of one of the major differences in the two models, the fact that the simplified abstraction used in the SDF GoldSim model does not consider vertical diffusion and PORFLOW does. Figure 5.2-14 shows that there is an adequate match between the PORFLOW Cs-135 results and the GoldSim results, with the differences between the PORFLOW breakthrough and the GoldSim breakthrough curves reflecting the difference in the handling of vertical diffusion. Figure 5.2-15 presents the Np-237 releases from the two models. For Np-237, the match of the trends is fair, with the initial breakthrough of the GoldSim releases sooner and the PORFLOW releases higher later.

Figure 5.2-11: FDC Ra-226 Release to the Saturated Zone

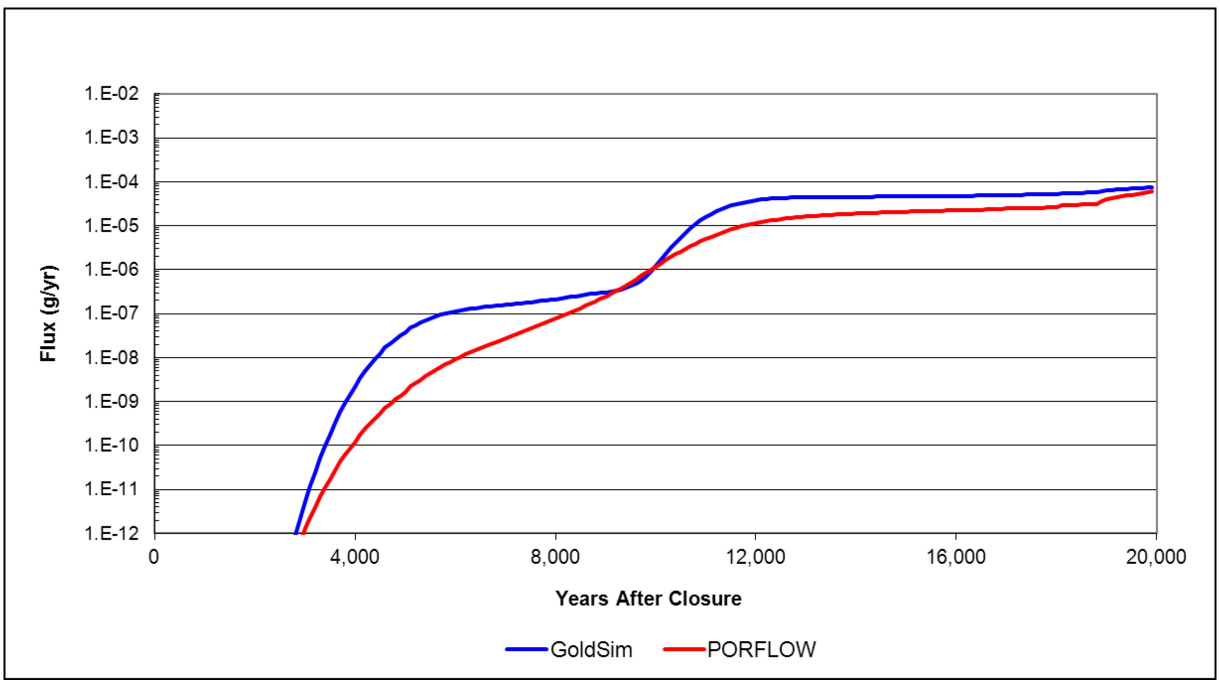

Figure 5.2-12: FDC Tc-99 Release to the Saturated Zone

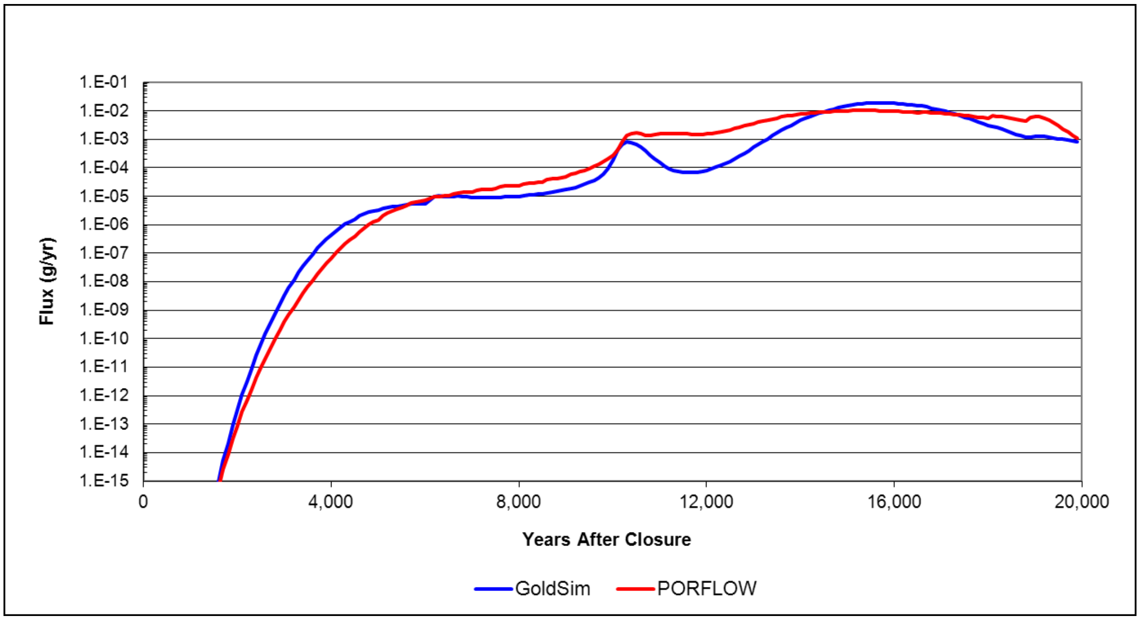

Figure 5.2-13: FDC I-129 Release to the Saturated Zone

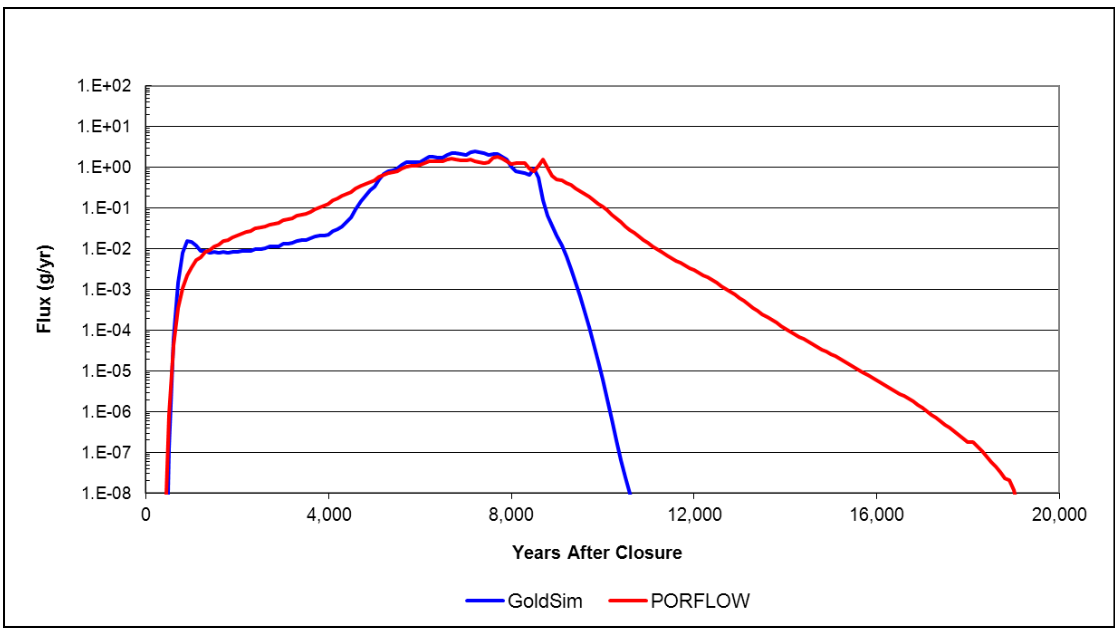

Figure 5.2-14: FDC Cs-135 Release to the Saturated Zone

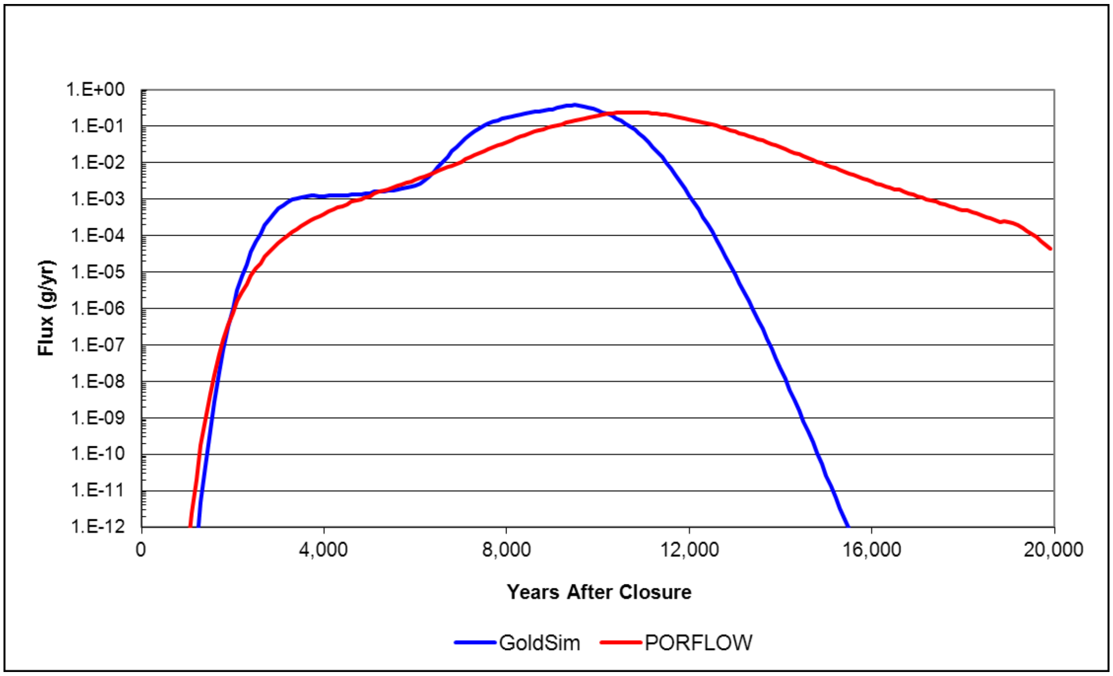

Figure 5.2-15: FDC Np-237 Release to the Saturated Zone

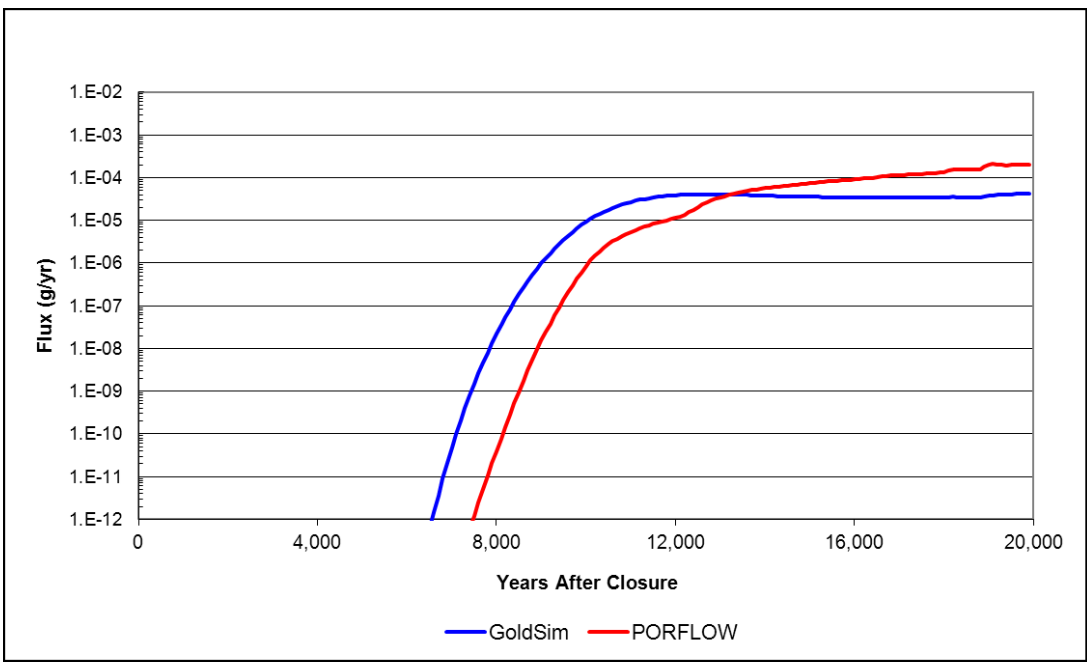

5.2.2 100-Meter Well Locations

The second phase of the benchmarking process is focused on how well the abstracted model approximates the radionuclide transport behavior in the saturated zone. As with the Base Case, the radionuclide concentrations in picocurie per liter, at two sectors, were examined for this task. The sectors used for the comparison were the southern Sector B and the northern Sector G. The locations of the observation wells are shown in Figure 3.1-2. For this exercise, five species (Ra-226, Tc-99, I-129, Cs-135, and Np-237) were compared.

5.2.2.1 Sector B

An examination of PORFLOW and SDF GoldSim model generated Ra-226 concentrations presented in Figure 5.2-16 indicates that the SDF GoldSim model produces a similar approximation of 100-meter boundary Ra-226 concentrations to the results generated by PORFLOW. There is good consistency in the trends observed in the two Ra-226 breakthrough curves throughout the 20,000-year simulation. The slightly earlier breakthrough in the PORFLOW results reflects a similar pattern in the Vault 4 releases (see Figure 5.2-6). Comparing the Vault 4 release results (presented in Figure 5.2-6) with the 100-meter boundary results for Sector B (Figure 5.2-16), shows that the influence of dilution in the two models is similar, with the SDF GoldSim model showing a slightly lesser degree of dilution.

As can be seen in Figure 5.2-17, the SDF GoldSim model also does a good job of reproducing the PORFLOW trends in the Tc-99 breakthrough curve at the 100-meter boundary. As with Ra-226, the GoldSim and PORFLOW simulations show similar degrees of dilution for the Tc-99 releases as the radionuclide is transported through the saturated zone to the 100-meter boundary (Figure 5.2-7, Figure 5.2-12, and Figure 5.2-17). Figure 5.2-18 shows that there is a very good correlation between the I-129 100-meter concentration levels generated by PORFLOW and their concentration levels simulated by the SDF GoldSim model until 9,000 years when the GoldSim breakthrough curve decreases at a faster rate (see the discussion in Section 5.2.1.3).

Figure 5.2-19 shows there is an adequate correlation between Cs-135 100-meter concentrations generated by PORFLOW, and the 100-meter concentrations generated by the SDF GoldSim model until 10,000 years when the releases decrease more rapidly in the SDF GoldSim model results. Figure 5.2-20 shows that there is a good correlation between Np-237 100-meter concentrations generated by SDF PORFLOW model and the 100-meter concentrations given by the SDF GoldSim model for most of the 20,000-year simulation.

Figure 5.2-16: Ra-226 Concentration at Sector B (Case K)

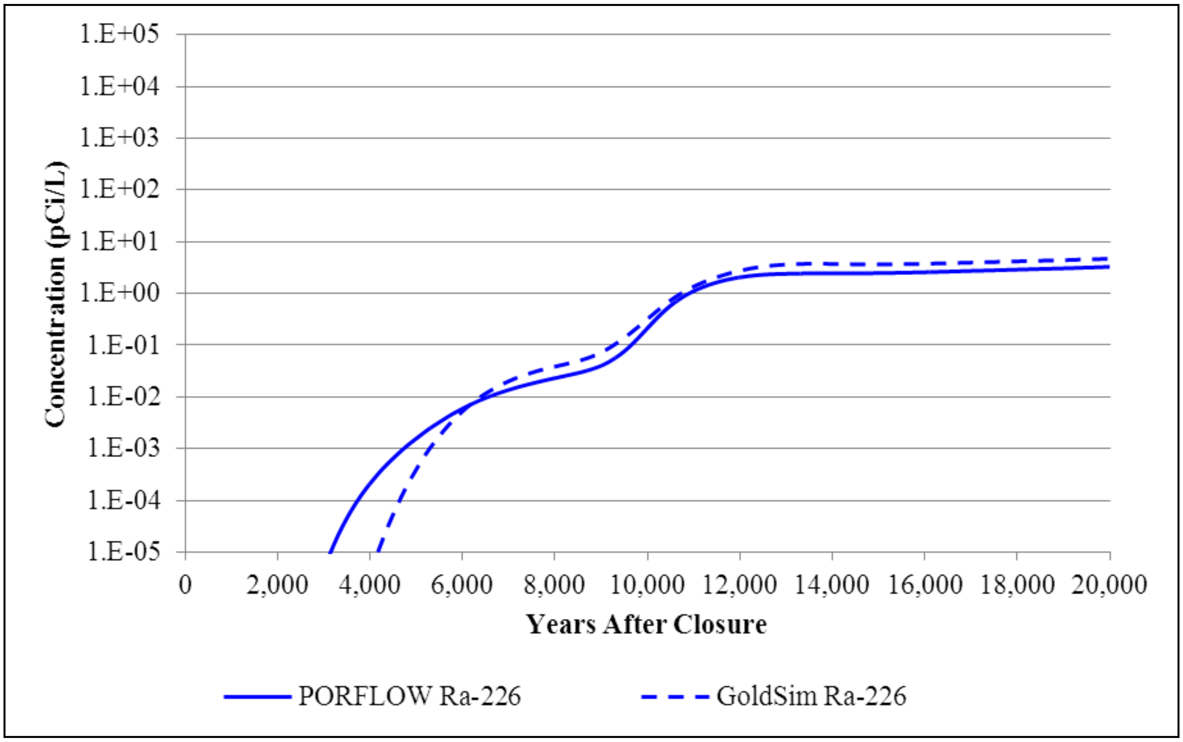

Figure 5.2-17: Tc-99 Concentration at Sector B (Case K)

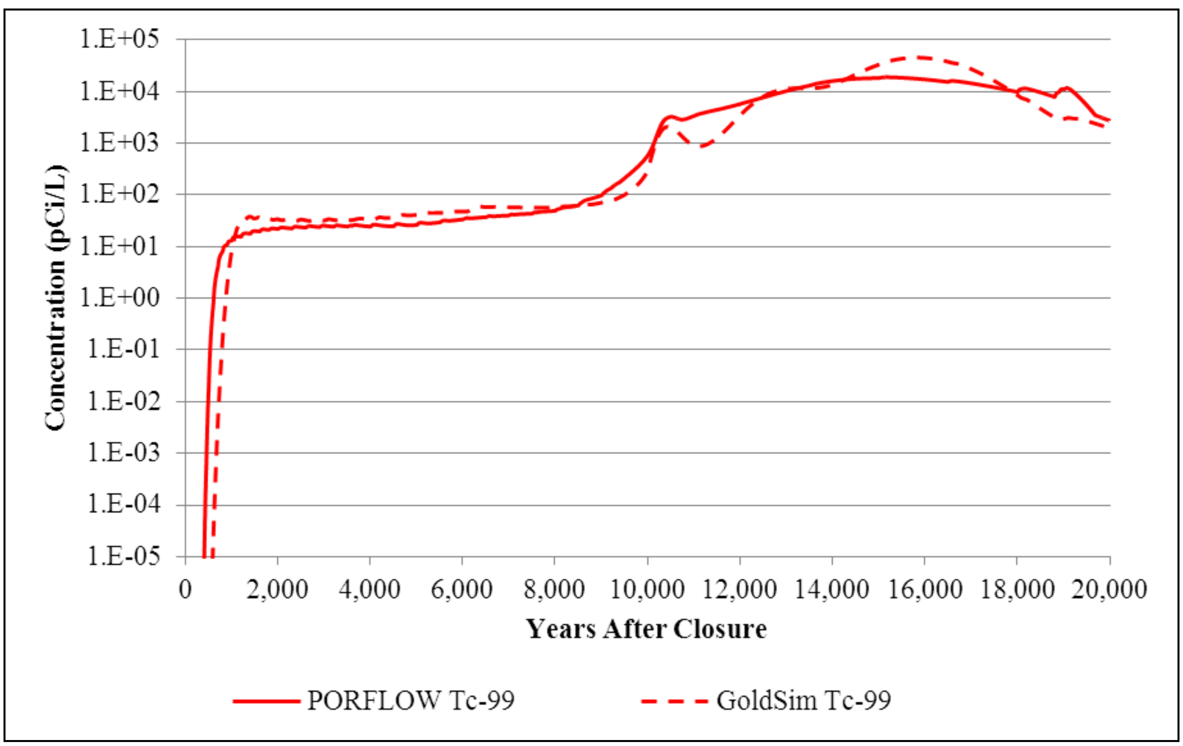

Figure 5.2-18: I-129 Concentration at Sector B (Case K)

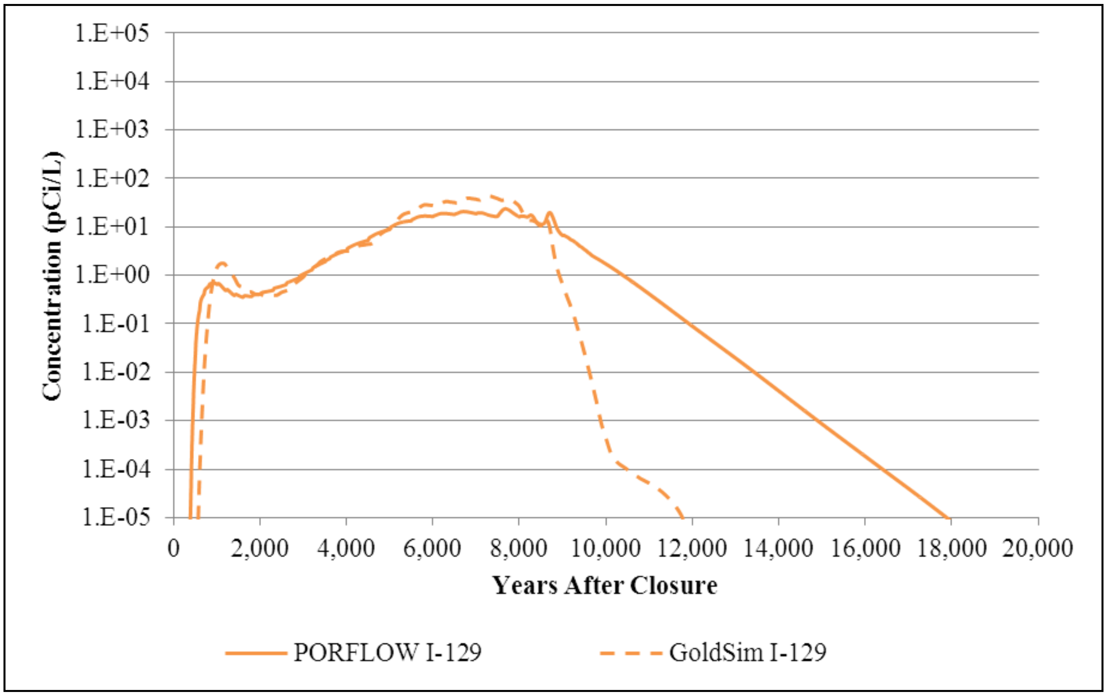

Figure 5.2-19: Cs-135 Concentration at Sector B (Case K)

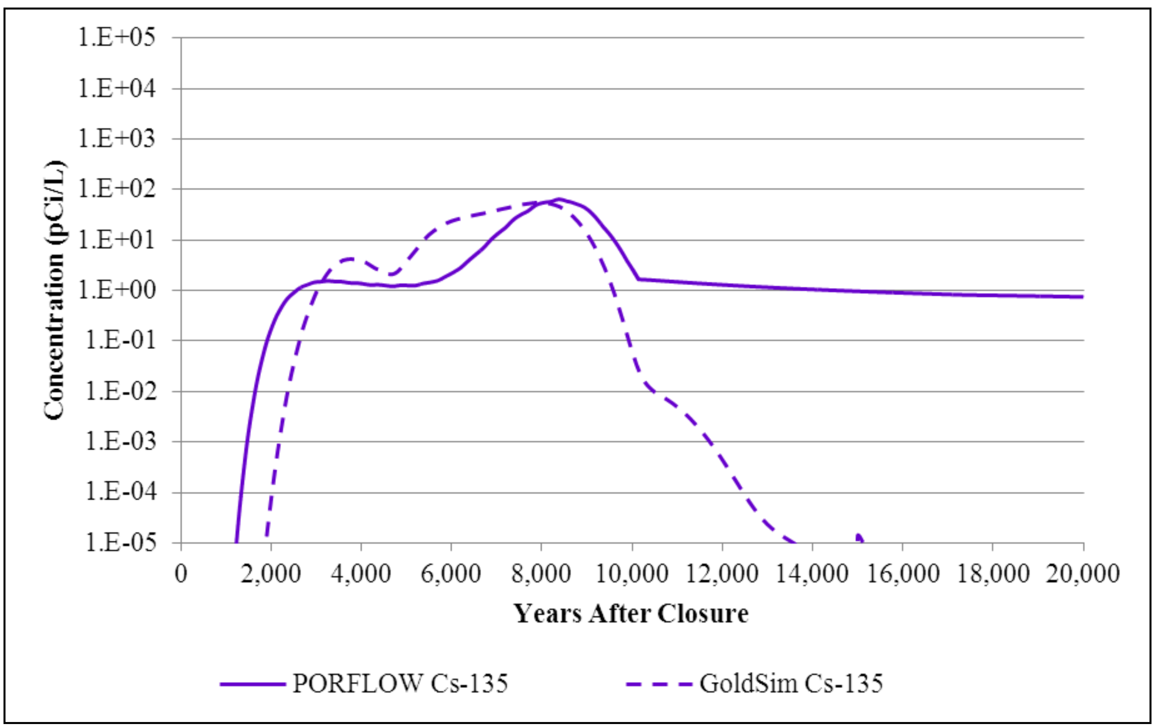

Figure 5.2-20: Np-237 Concentration at Sector B (Case K)

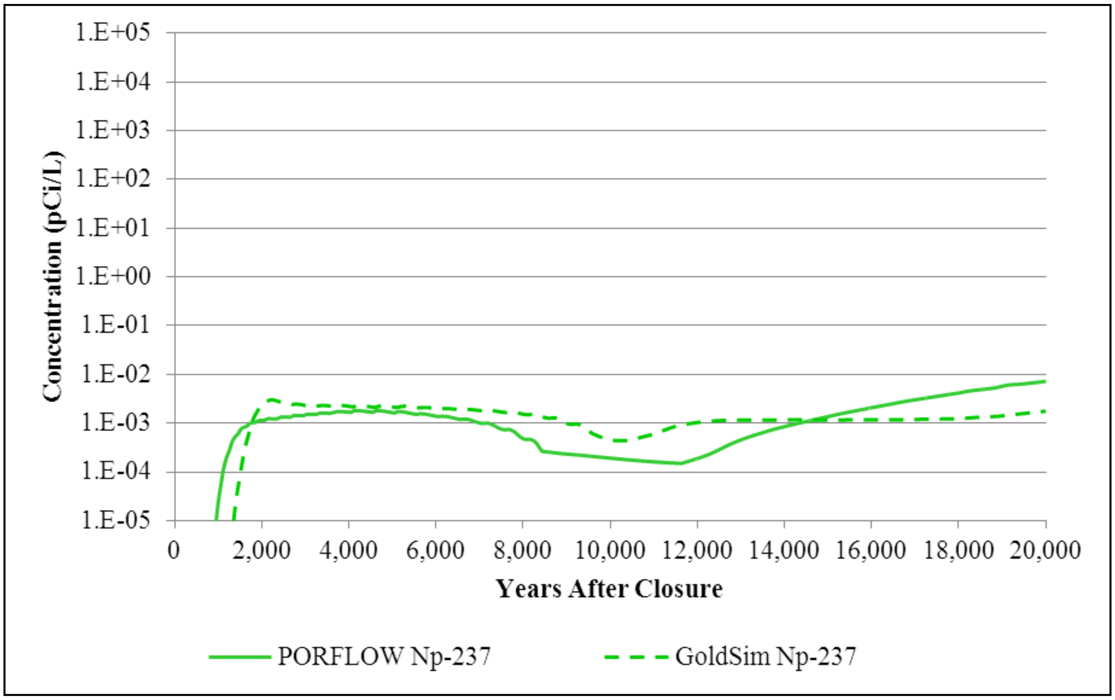

5.2.2.2 Sector G

An examination of PORFLOW and SDF GoldSim model generated Ra-226 concentrations in Sector G presented in Figure 5.2-21 indicate that the SDF GoldSim model can provide a computationally efficient approximation of 100-meter boundary Ra-226 concentrations produced by the migration of Ra-226 from the SDF. There is a fair consistency between the trends observed in the two Ra-226 breakthrough curves throughout the 20,000-year simulation with the SDF GoldSim model showing slightly higher releases. By comparing Figures 5.2-11 and 5.2-21, it can be seen that the GoldSim model reproduces the saturated zone, transport dilution effects, seen in the SDF PORFLOW model results, fairly well.

As can be seen in Figure 5.2-22, the SDF GoldSim model also does a good job of reproducing the SDF PORFLOW model trends in the Tc-99 breakthrough curve at the 100-meter. In earlier years when the concentration is low, the SDF GoldSim model under predicts the concentrations. The early differences are due to the northerly flow of groundwater in the Gordon Aquifer, which is not simulated in the SDF GoldSim model. As previously noted, the SDF GoldSim model disregards the Gordon Aquifer because concentrations in the Gordon Aquifer have very little influence on peak dose. Comparing Figure 5.2-12 to Figure 5.2-22 shows the SDF GoldSim model captures the dilution effects of the SDF PORFLOW model quite well. Figure 5.2-23 shows that there is a good correlation between the I-129 100-meter concentration levels generated by SDF PORFLOW and GoldSim models until the tails of the releases decrease at different rates due to the influence of vertical diffusion as discussed in Section 5.2.1.3. As with other species, dilution effects of the SDF GoldSim and PORFLOW models are quite similar (see Figures 5.2-13 and 5.2-23).

Figure 5.2-24 shows that the GoldSim Cs-135 breakthrough is earlier than the SDF PORFLOW model's in Sector G, and there is an adequate correlation between Np-237 100-meter concentrations until the releases start to dissipate at 10,000 years. Comparing Figures 5.2-14 and 5.2-24 shows that the degree of dilution imposed by both models is similar. Figure 5.2-25 shows that the GoldSim Np-237 breakthrough is earlier than the SDF PORFLOW model's in Sector G, but there is an adequate correlation between Np-237 100-meter concentrations with SDF PORFLOW model being higher. Comparing Figures 5.2-15 and 5.2-25 shows that the influence of dilution simulated by both models is similar.

Figure 5.2-21: Ra-226 Concentration at Sector G (Case K)

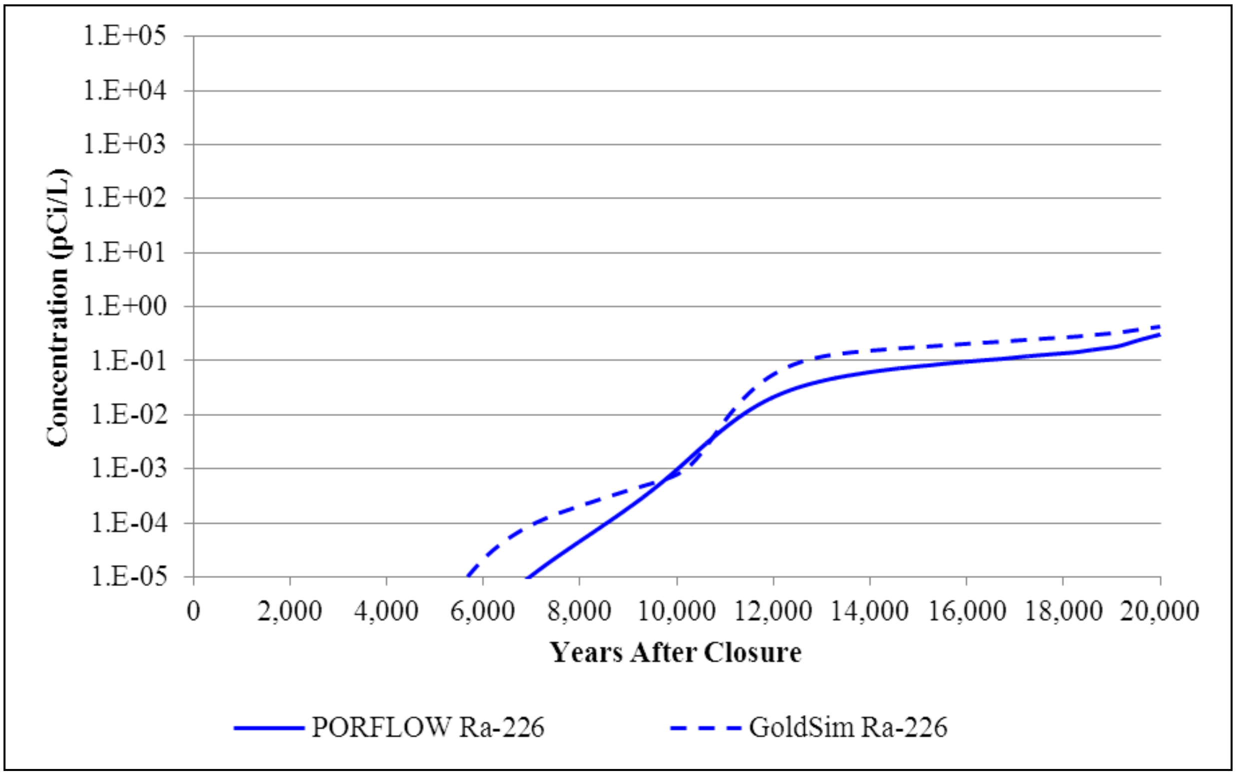

Figure 5.2-22: Tc-99 Concentration at Sector G (Case K)

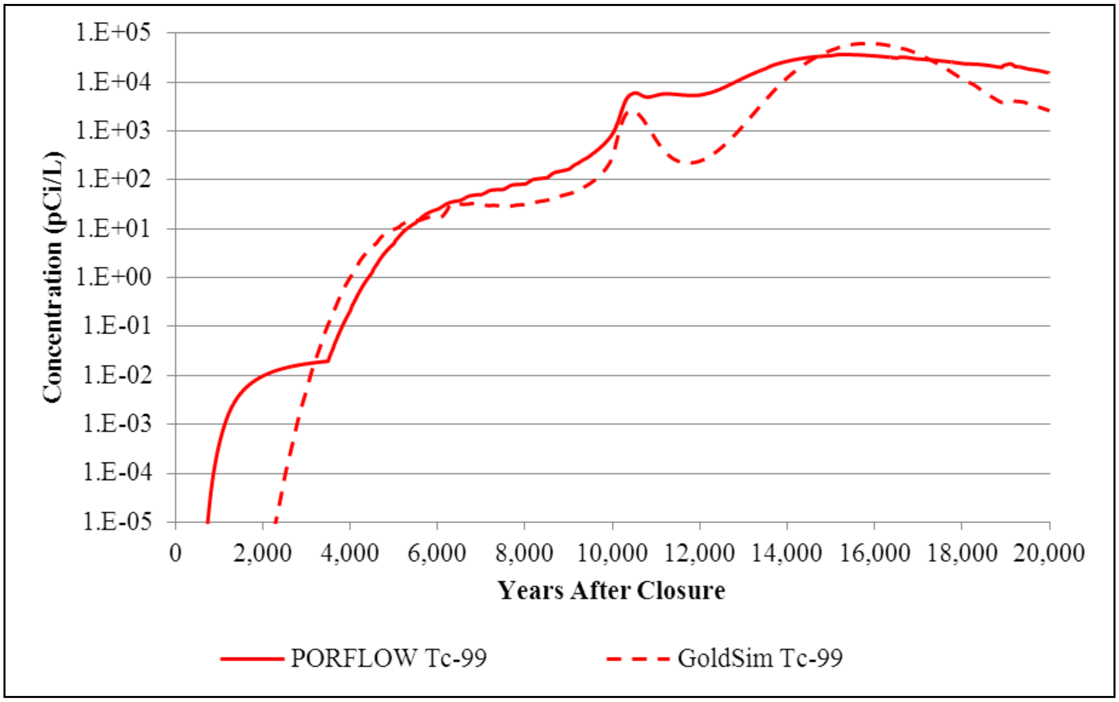

Figure 5.2-23: I-129 Concentration at Sector G (Case K)

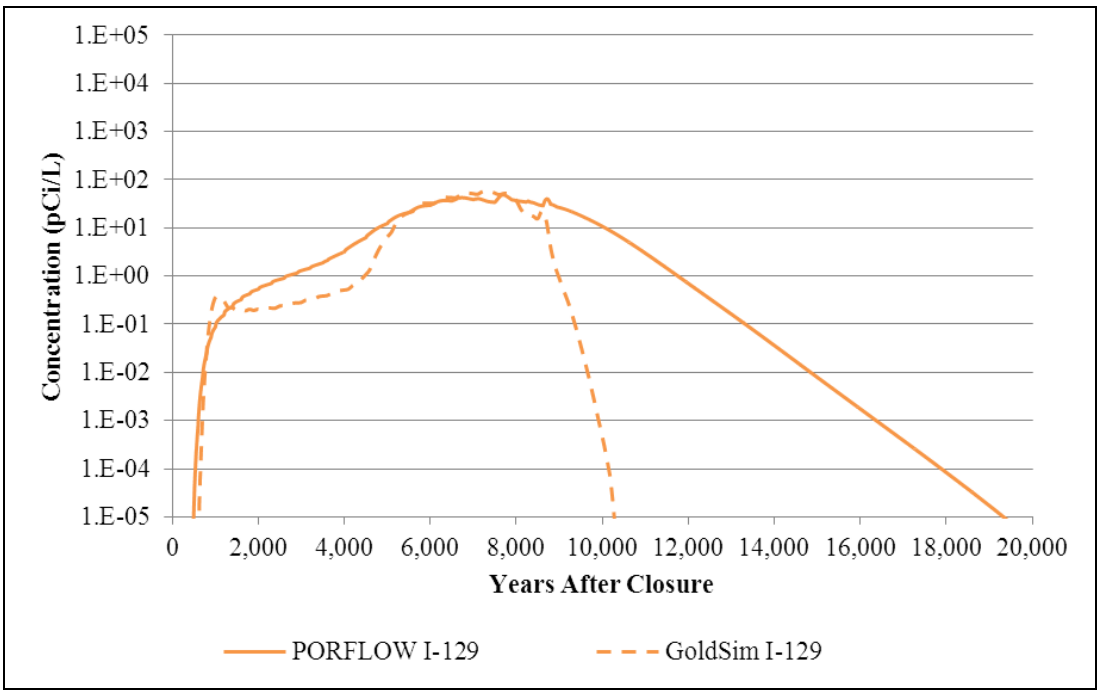

Figure 5.2-24: Cs-135 Concentration at Sector G (Case K)

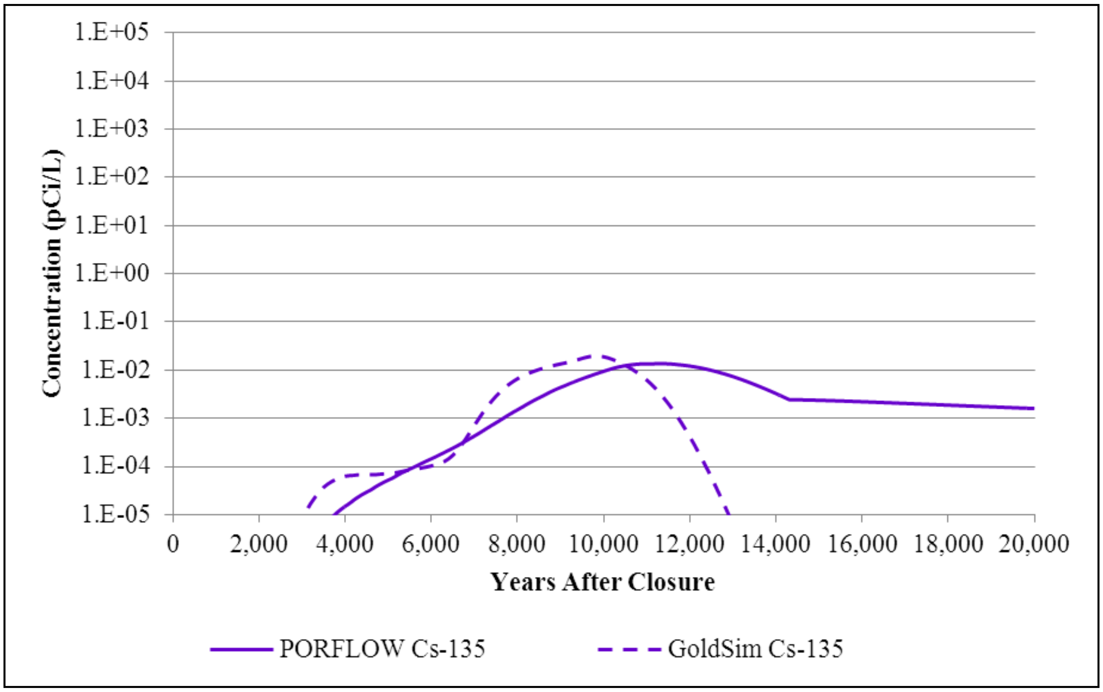

Figure 5.2-25: Np-237 Concentration at Sector G (Case K)

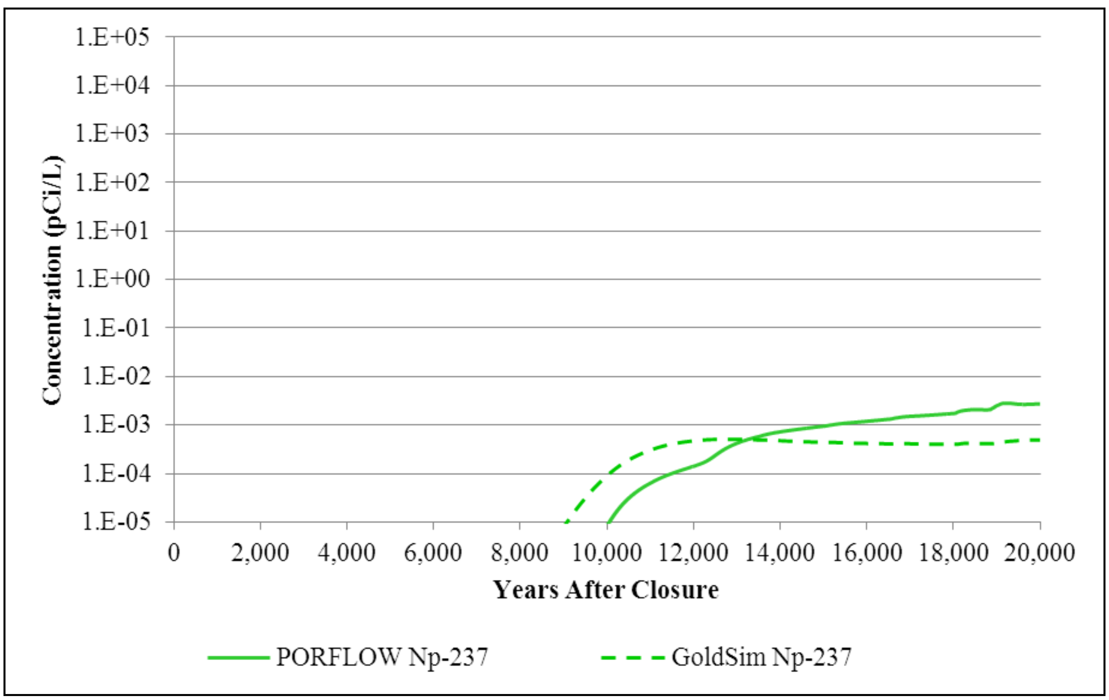

5.2.3 Total Dose Time Histories

An additional check on the appropriateness of the SDF GoldSim model as a surrogate for the SDF PORFLOW model, is a comparison between maximum total doses generated using the PORFLOW and the SDF GoldSim model. The SDF PORFLOW and GoldSim model total dose comparison for Alternative Sensitivity Case K (Figure 5.2-26) shows the SDF GoldSim model approximates the general trends of the SDF PORFLOW model well. The influence of vertical diffusion (as discussed in Section 5.2-1) causes the SDF GoldSim model breakthrough curve to have a steeper profile.

Figure 5.2-26: Comparison between PORFLOW and GoldSim Max Total Dose Results, Case K

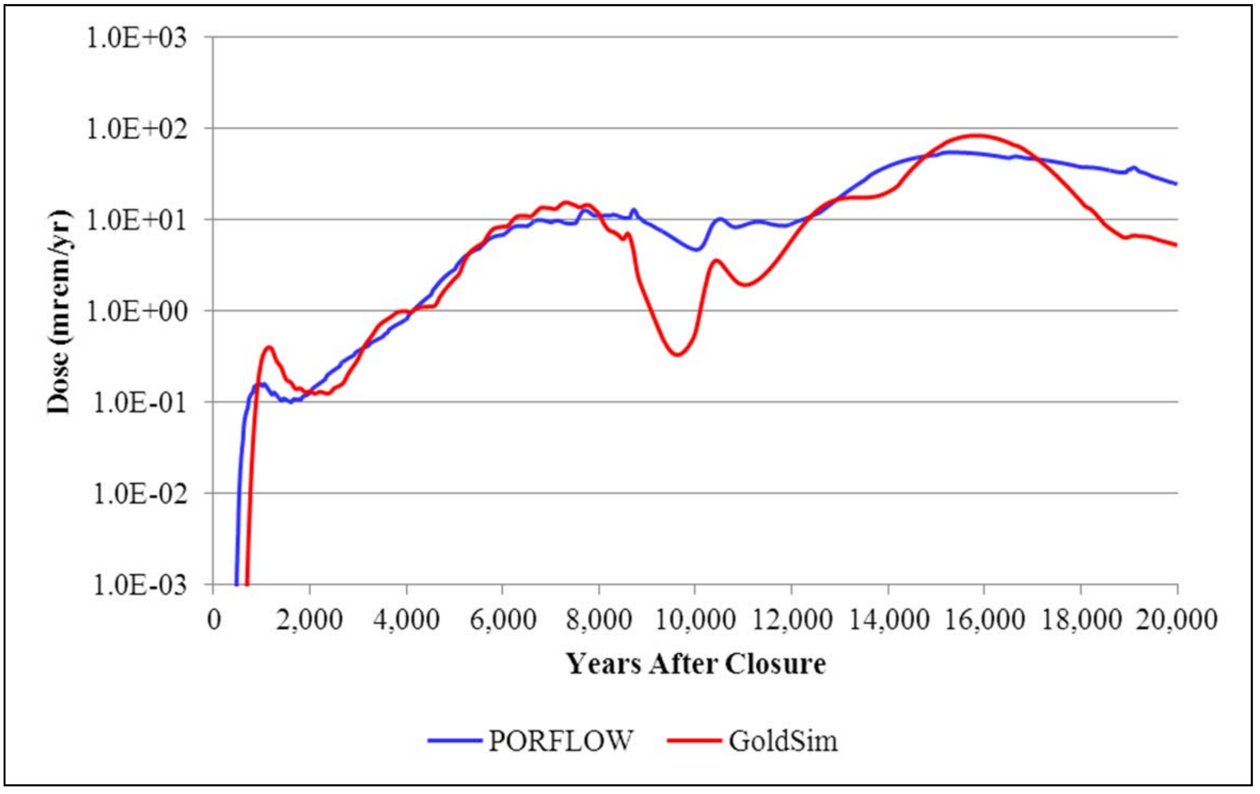

6.0 REFERENCES

GTG-2010 (Copyright*), GoldSim Contaminant Transport Module*, GoldSim Technology Group LLC, Issaquah, WA, December 2010.

GTG-2010c, (Copyright), *GoldSim User's Guide, Version 10.1. Volumes 1 & 2*, GoldSim Technology Group LLC, Issaquah, WA, December 2010.

ISBN: 1-55899-189-1, (Copyright), Smith, R.W., et al., *The Role of Oxygen Diffusion in the Release of Technetium from Reducing Cementitious Waste Forms*, Material Resource Society Scientific Basis for Nuclear Waste Management XVI Symposium, April 1993.

SRNL-L4321-2011-00004, Flach, G., *Oxidation of Fractured Cementitious Materials in Performance Assessments*, Savannah River Site, Aiken, SC, Rev. 0, March 24, 2011.

SRNL-RPA-2007-00006, Kaplan, D. I., *Distribution Coefficients for Various Elements of Concern to the Tank Waste Performance Assessment*, Savannah River Site, Aiken, SC, July 10, 2007.

SRNL-STI-2009-00114, Flach, G. P., et al., *Approximate Solutions for Diffusional Release from Saltstone Vaults*, Savannah River Site, Aiken, SC, Rev. 0, February 2009.

SRNL-STI-2009-00115, Flach, G. P., et al., *Numerical Flow and Transport Simulations Supporting the Saltstone Facility Performance Assessment*, Savannah River Site, Aiken, SC, Rev. 1, June 2009.

SRNL-STI-2009-00473, Kaplan, D. I., *Geochemical Data Package for Performance Assessment Calculations Related to the Savannah River Site*, Savannah River Site Aiken, SC, Rev. 2, March 15, 2010.

SRNL-STI-2010-00667, Almond, P. M. and Kaplan, D. I., *Distribution Coefficients (K_d) Generated from a Core Sample Collected from the Saltstone Disposal Facility*, Savannah River Site, Aiken, SC, Rev. 0, April 29, 2011.

SRNL-TR-2009-00019, Kaplan, D. I., *Tc and Pu Distribution Coefficients, Kd Values, for the Saltstone Facility Performance Assessment*, Savannah River Site, Aiken, SC, January 16, 2009.

SRNS-J2100-2008-00004, Dean, B., *Estimated Inventory for the Saltstone Disposal Facility*, , Savannah River Site, Aiken, SC, Rev. 2, June 22, 2009.

SRR-CWDA-2009-00017, *Performance Assessment for the Saltstone Disposal Facility at the Savannah River Site,* Savannah River Site, Aiken, SC, Rev. 0, October 29, 2009.

SRR-CWDA-2010-00093, *H-Area Tank Farm Stochastic Fate and Transport Model,* Savannah River Site, Aiken, SC, Rev. 1, September 2010.

SRR-CWDA-2011-00044, *Comment Response Matrix for Nuclear Regulatory Commission RAI-2009-02 Second Request for Additional Information (RAI) on the Saltstone Disposal Facility Performance Assessment (SRR-CWDA-2009-00017, Revision 0, dated October 29, 2009)*, Savannah River Site, Aiken, SC, Rev. 1, March 31, 2010.

SRR-CWDA-2011-00166, Hommel, S., *Software Acceptance Testing for GoldSim© Version 10.50 SP2*, Savannah River Site, Aiken, SC, Rev. 0, October 2011.

SRR-CWDA-2011-00189, *SRS Saltstone v3.002.gsm*, Savannah River Site, Aiken, SC, January 2012.

SRR-LWP-2010-00070, Le, T., et al., *Salt Batch Plan-2010 in Support of System Plan R-16*, Savannah River Site, Aiken, SC, Rev. 0, November 8, 2010.

SRS-REG-2007-00036, *Documentation of Personal Communication Between Kaplan, D. I. to Newman, J. L.*, Savannah River Site, Aiken, SC, Rev. 0, September 9, 2007.

WSRC-STI-2006-00198, Phifer, M. A., et al., *Hydraulic Property Data Package for the E-Area and Z-Area Soils, Cementitious Materials, and Waste Zones*, Savannah River Site, Aiken, SC, Rev. 0, September 2006.

WSRC-TR-2006-00004, Kaplan, D. I., *Geochemical Data Package for Performance Assessment Calculations Related to Savannah River Site*, Savannah River Site, Aiken, SC, Rev. 0, February 2006.

APPENDIX A

SDF PORFLOW Model Generated Breakthrough Curves used to Determine Darcy Velocity

The Figures A.0-1 through A.0-20 show SDF PORFLOW model generated breakthrough curves at the 100-meter boundary for releases emanating from Vaults 1 and 4 in addition to each grouping of FDCs depicted in Figure 4.2-1. The releases for FDCs initialized at the center of each grouping of two or four disposal units within the SDF (see Figure 4.2-1 and Table 4.2-10 to identify the individual FDCs). The timing of the peaks of the breakthrough curves, the distances presented in Table 4.4-2, and the saturated zone porosity (Table 4.5-8) were used to generate the Darcy velocities presented in Table 4.4-1 as follows:

$$V_{Darcy} = \frac{D_{boundary}\phi}{T_{peak}}$$

where:

V_{Darcy} is the Darcy velocity in meter per year, $D_{boundary}$ is the distance to the 100-meter boundary in meters, and T_{peak}, is the time of the peak on the breakthrough curve in years.

Note: The x-axis for each graph (Figure A.0-1 through A.0-20) is the measure of time in years, and the y-axis is concentration in kilograms per liter.

Figure A.0-1: Concentration Breakthrough Curve for a Conservative Constituent Release at Vault 1

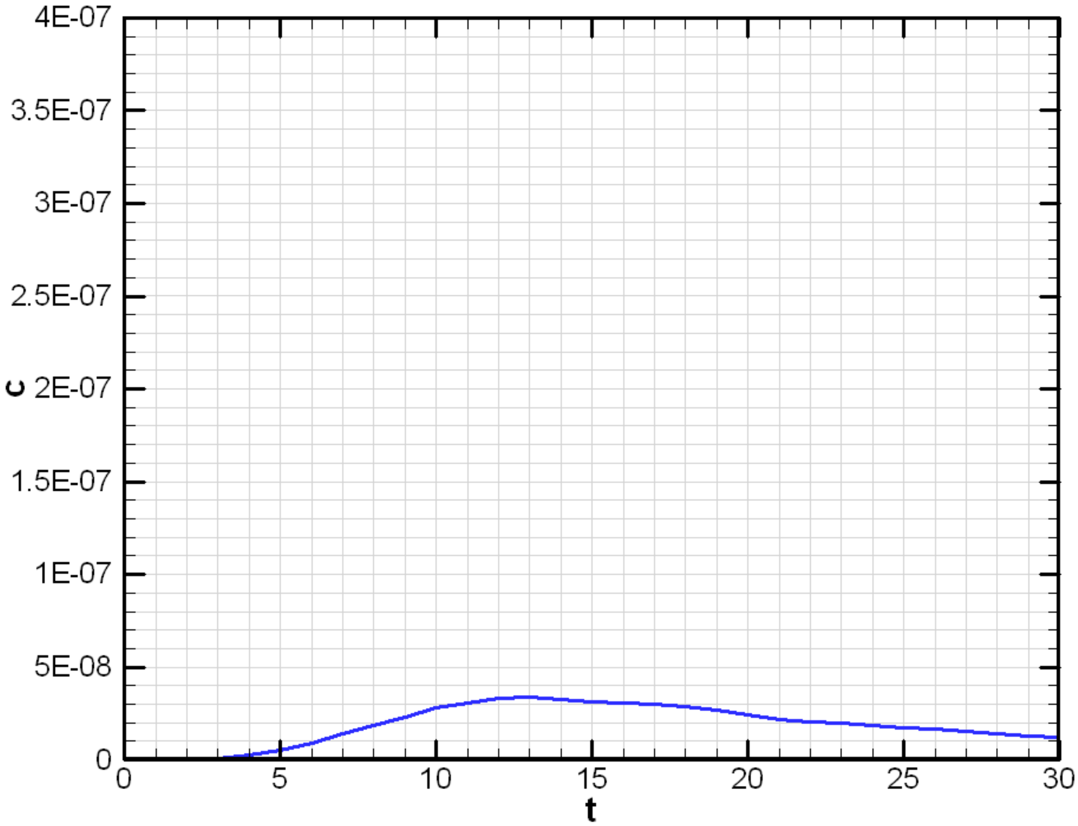

Figure A.0-2: Concentration Breakthrough Curve for a Conservative Constituent Release at Vault 4

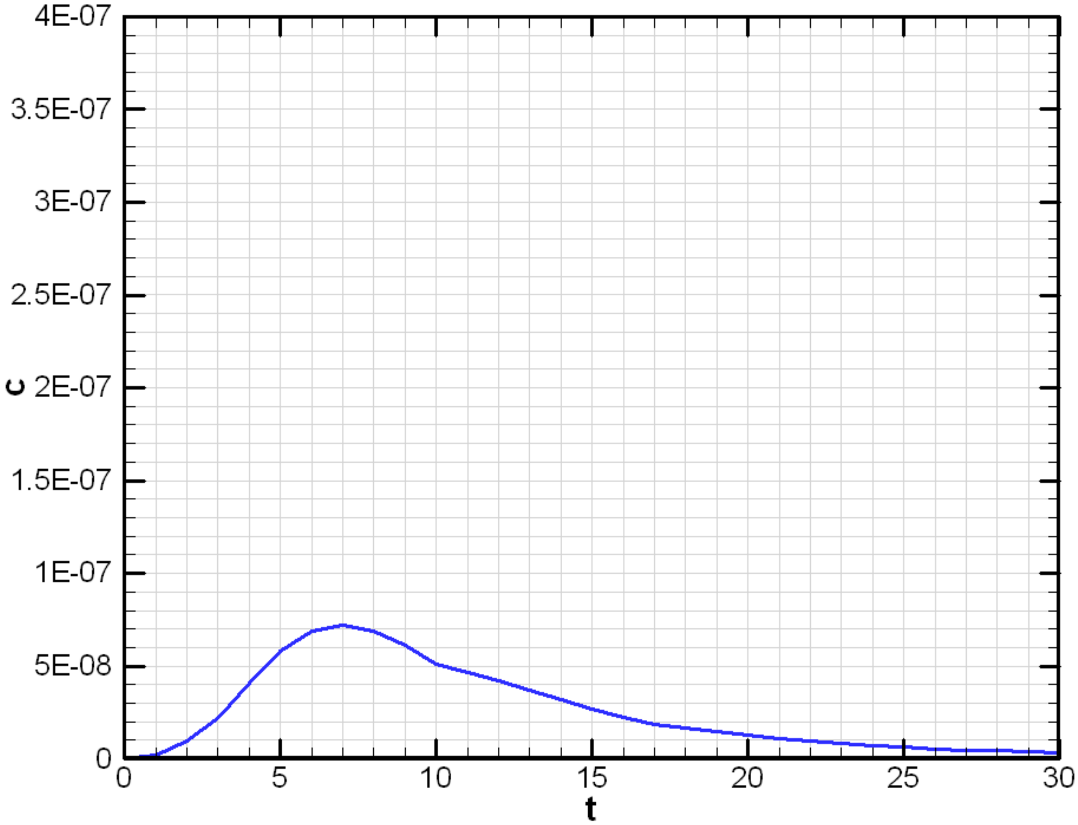

Figure A.0-3: Concentration Breakthrough Curve for a Conservative Constituent Release at the Center of FDC Group 2

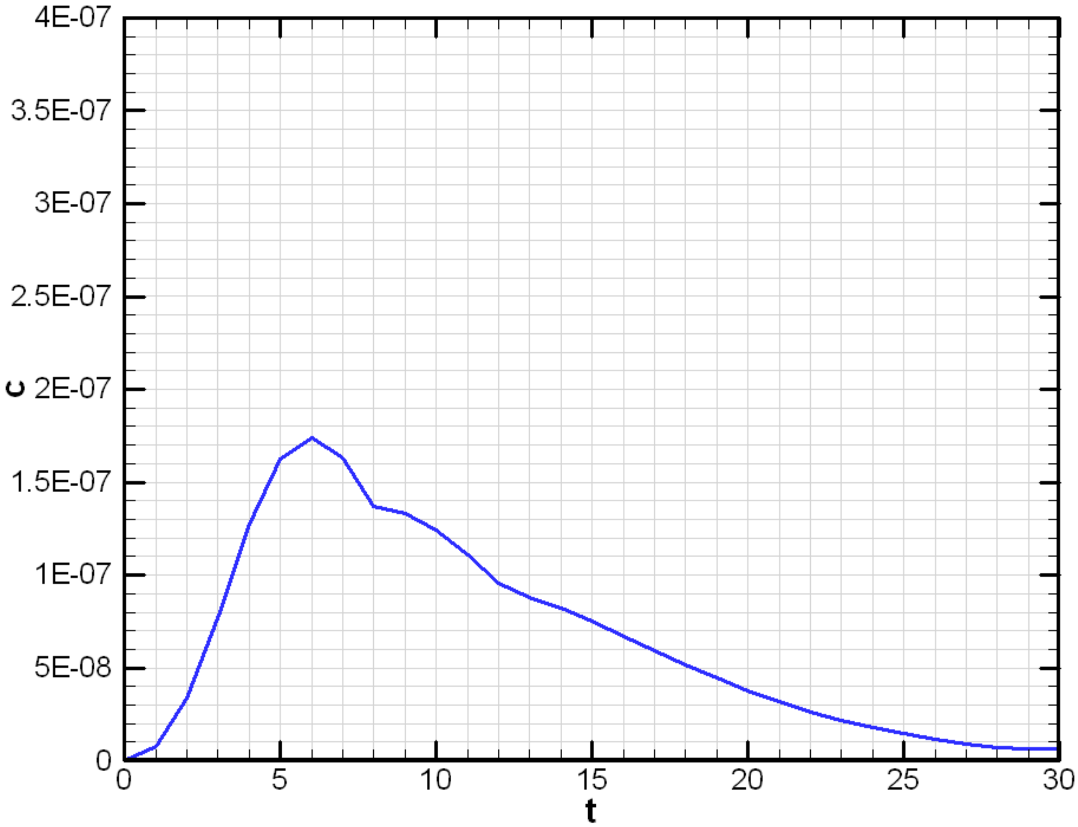

Figure A.0-4: Concentration Breakthrough Curve for a Conservative Constituent Release at the Center of FDC Group 3

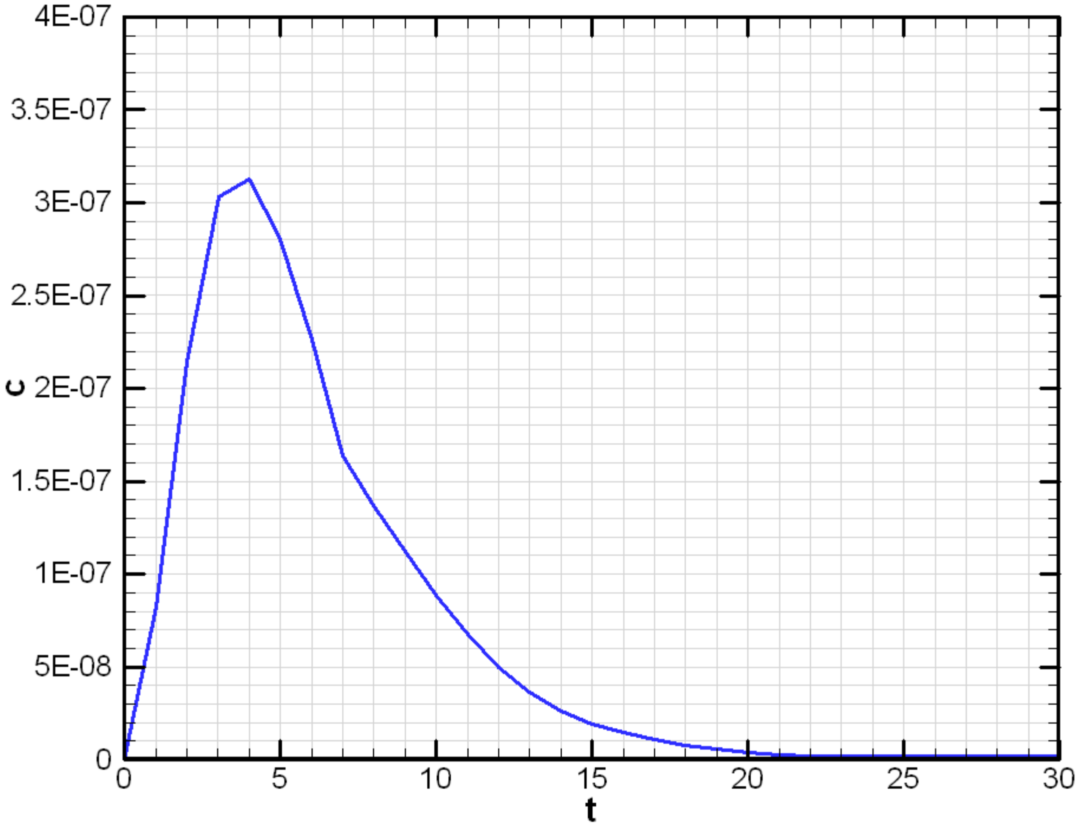

Figure A.0-5: Concentration Breakthrough Curve for a Conservative Constituent Release at the Center of FDC Group 5

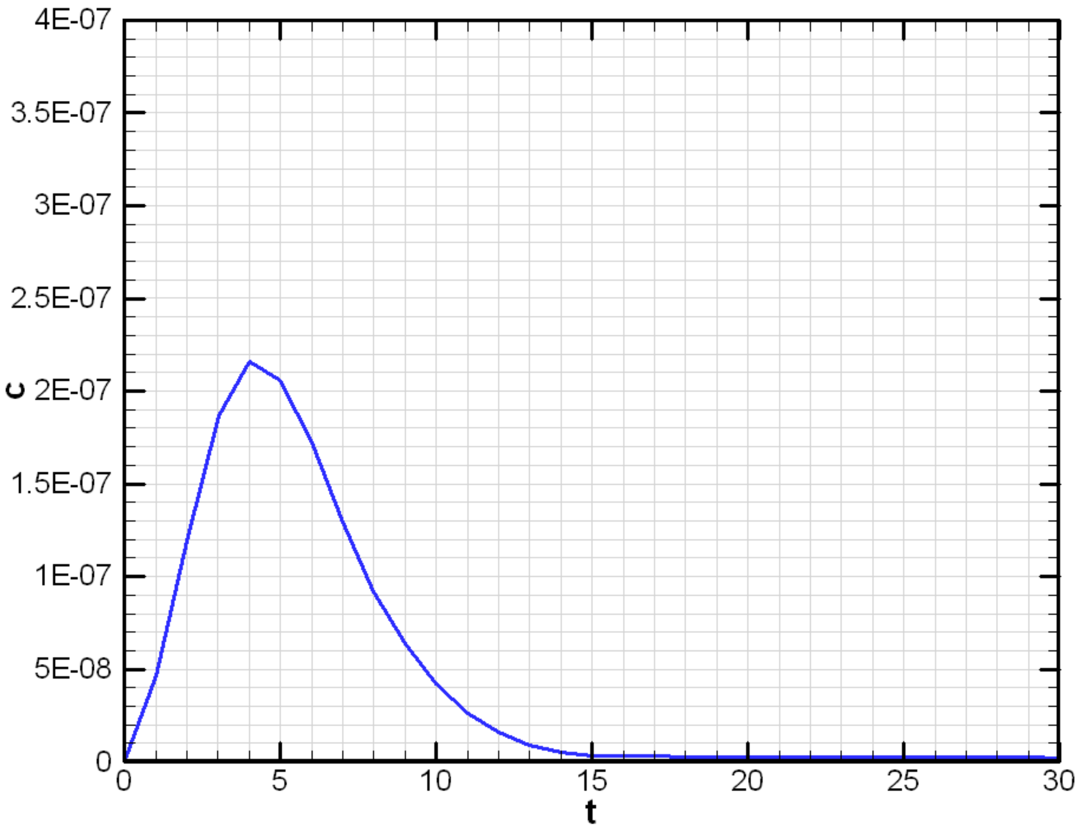

Figure A.0-6: Concentration Breakthrough Curve for a Conservative Constituent Release at the Center of FDC Group 6

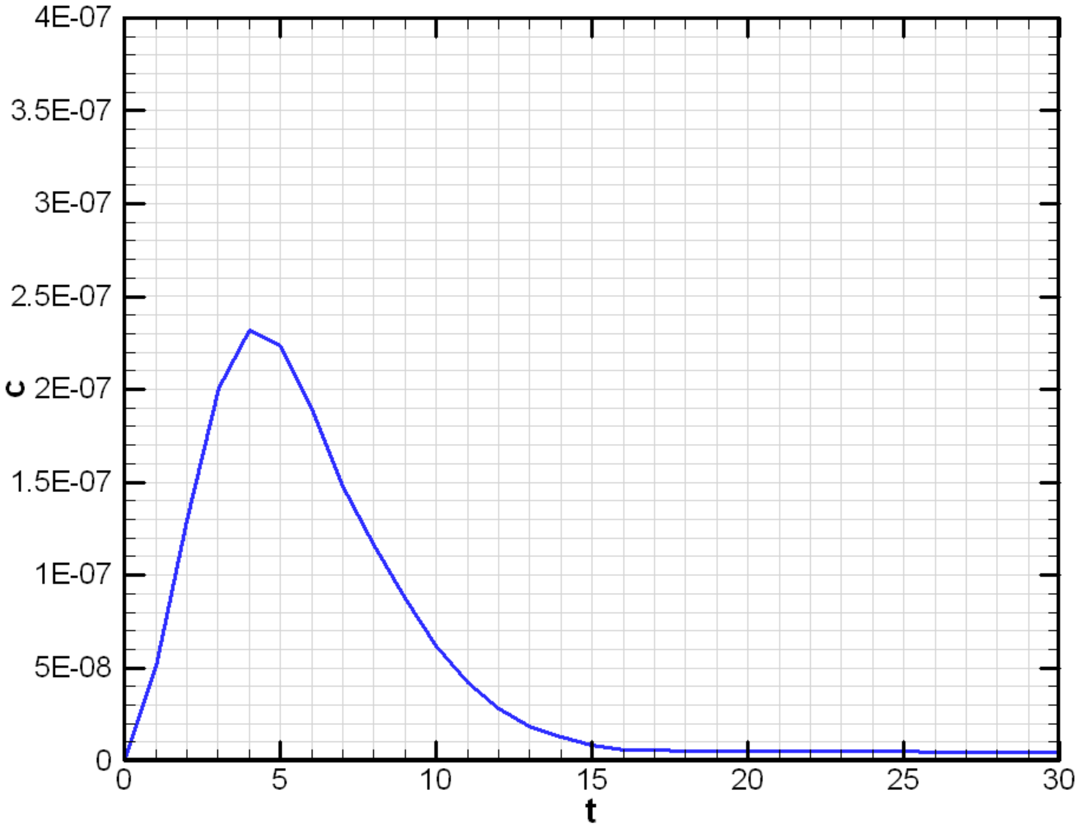

Figure A.0-7: Concentration Breakthrough Curve for a Conservative Constituent Release at the Center of FDC Group 7

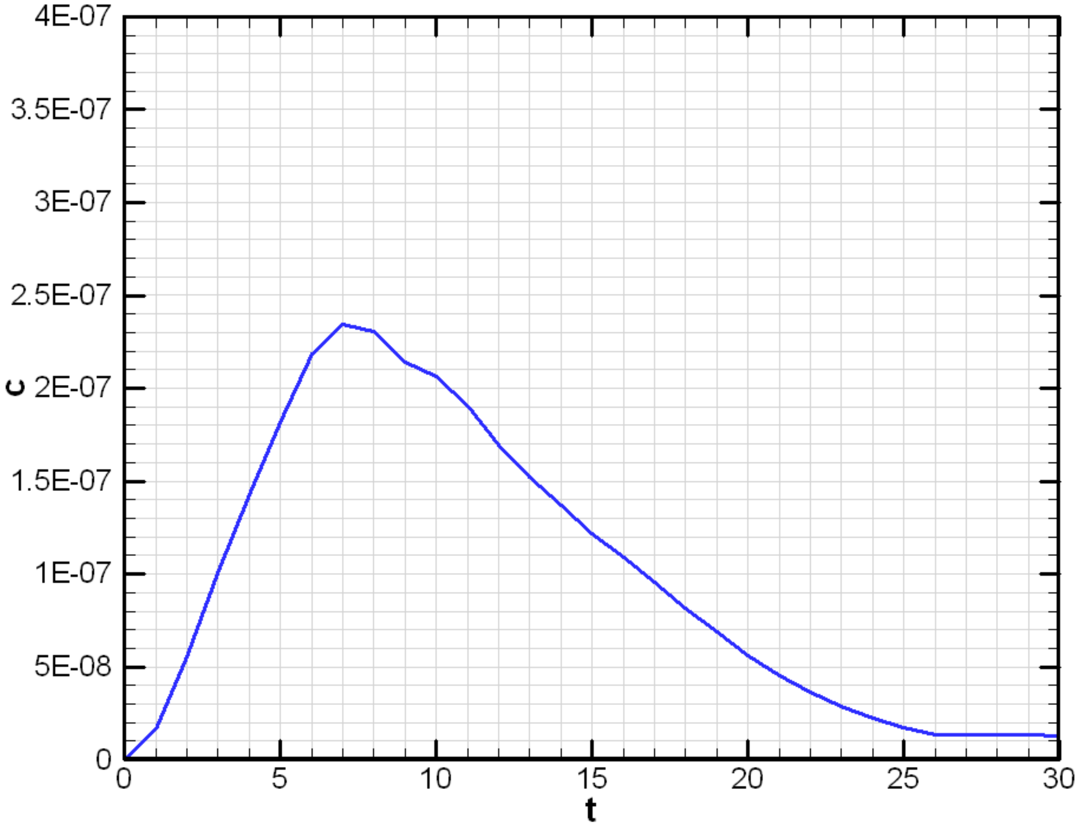

Figure A.0-8: Concentration Breakthrough Curve for a Conservative Constituent Release at the Center of FDC Group 8

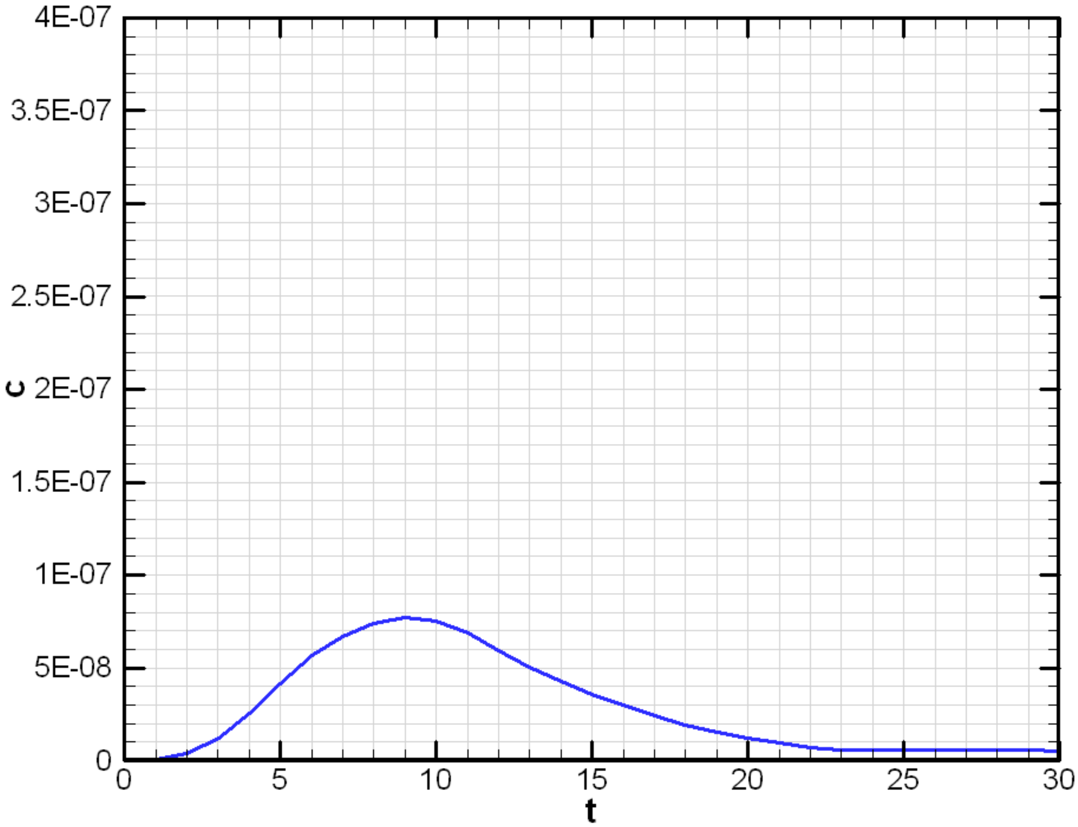

Figure A.0-9: Concentration Breakthrough Curve for a Conservative Constituent Release at the Center of FDC Group 9

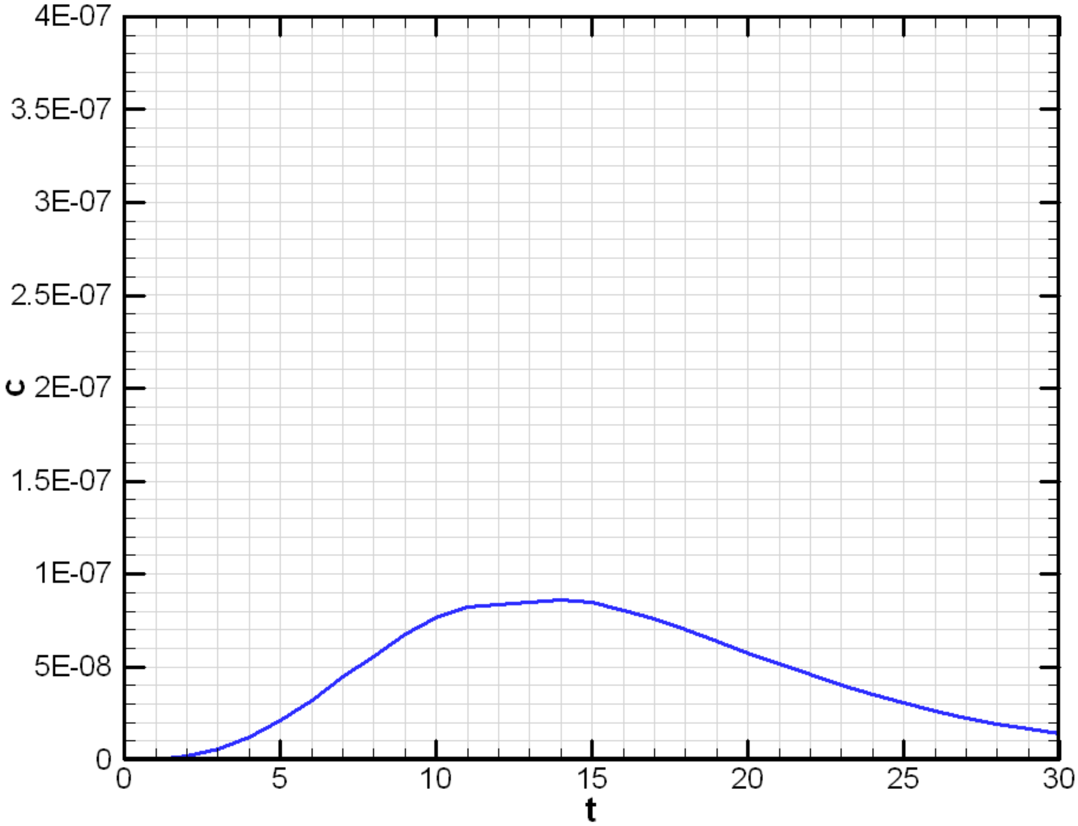

Figure A.0-10: Concentration Breakthrough Curve for a Conservative Constituent Release at the Center of FDC Group 10

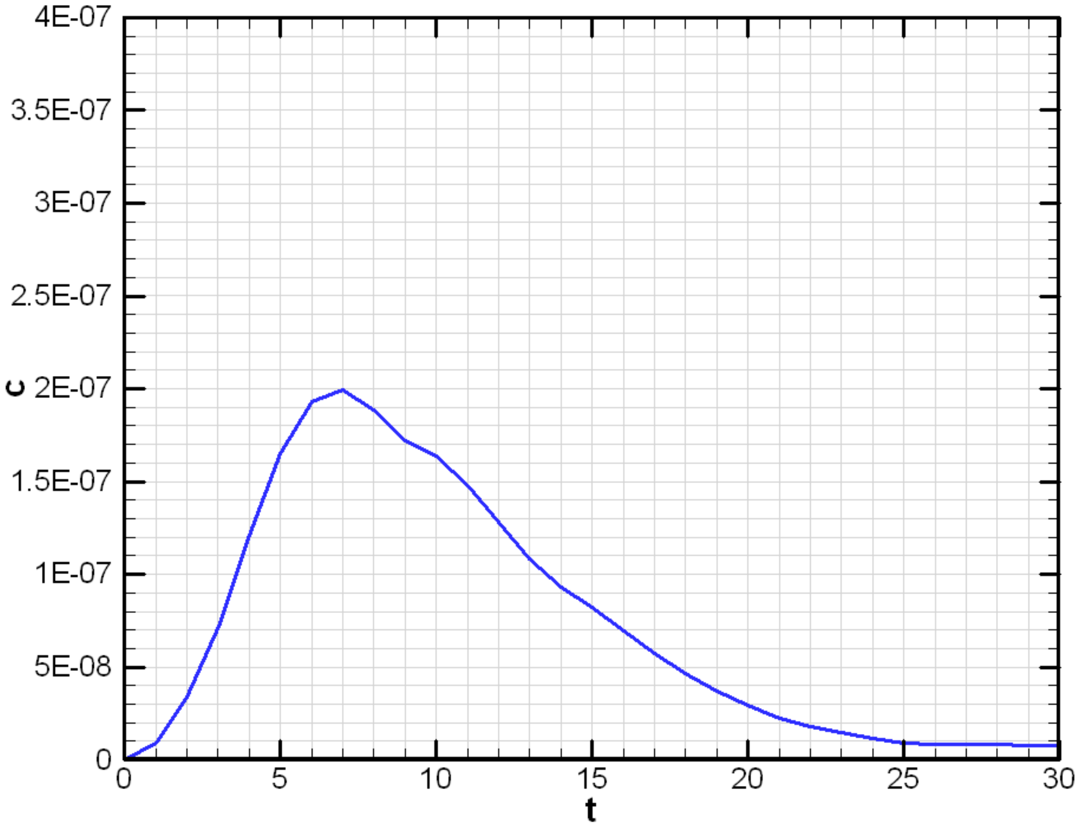

Figure A.0-11: Concentration Breakthrough Curve for a Conservative Constituent Release at the Center of FDC Group 11

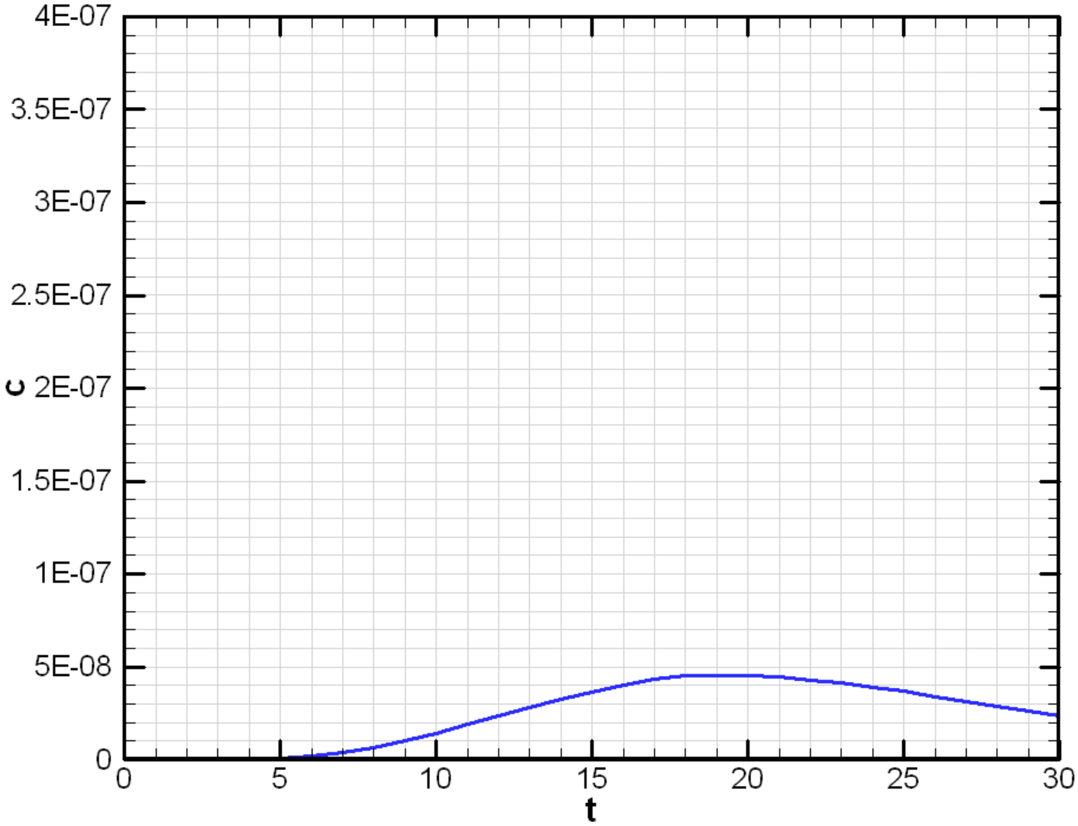

Figure A.0-12: Concentration Breakthrough Curve for a Conservative Constituent Release at the Center of FDC Group 12

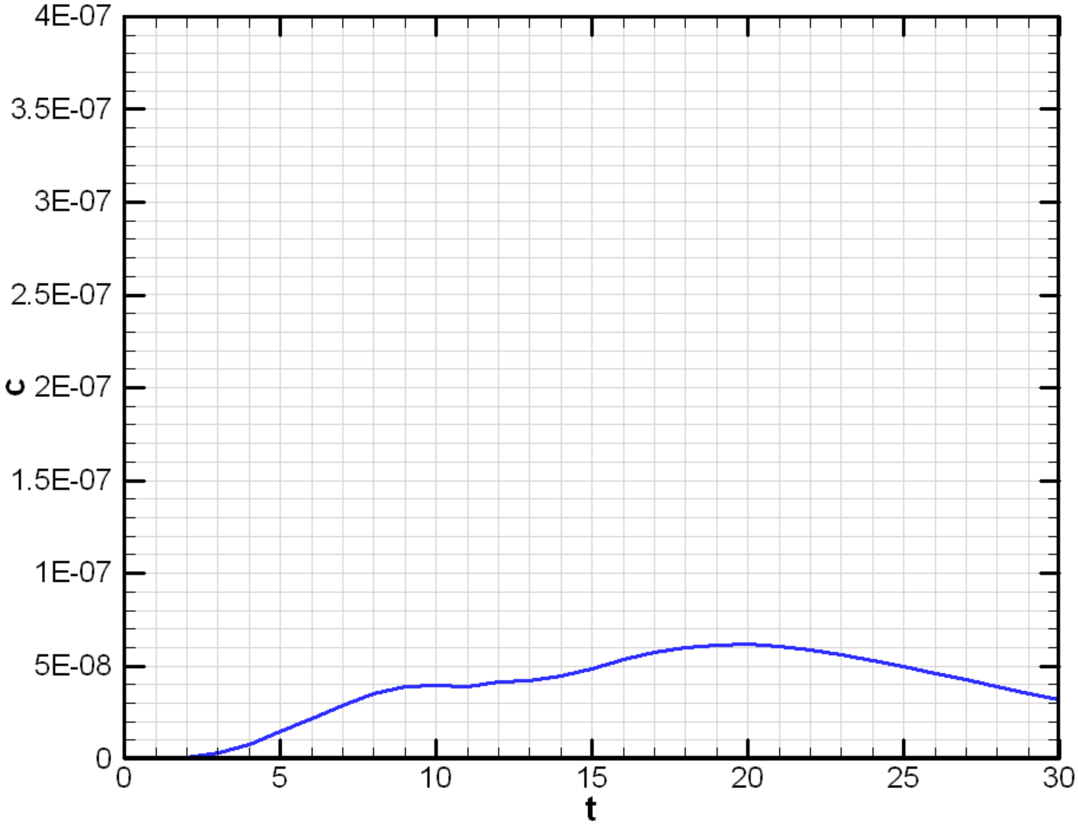

Figure A.0-13: Concentration Breakthrough Curve for a Conservative Constituent Release at the Center of FDC Group 13

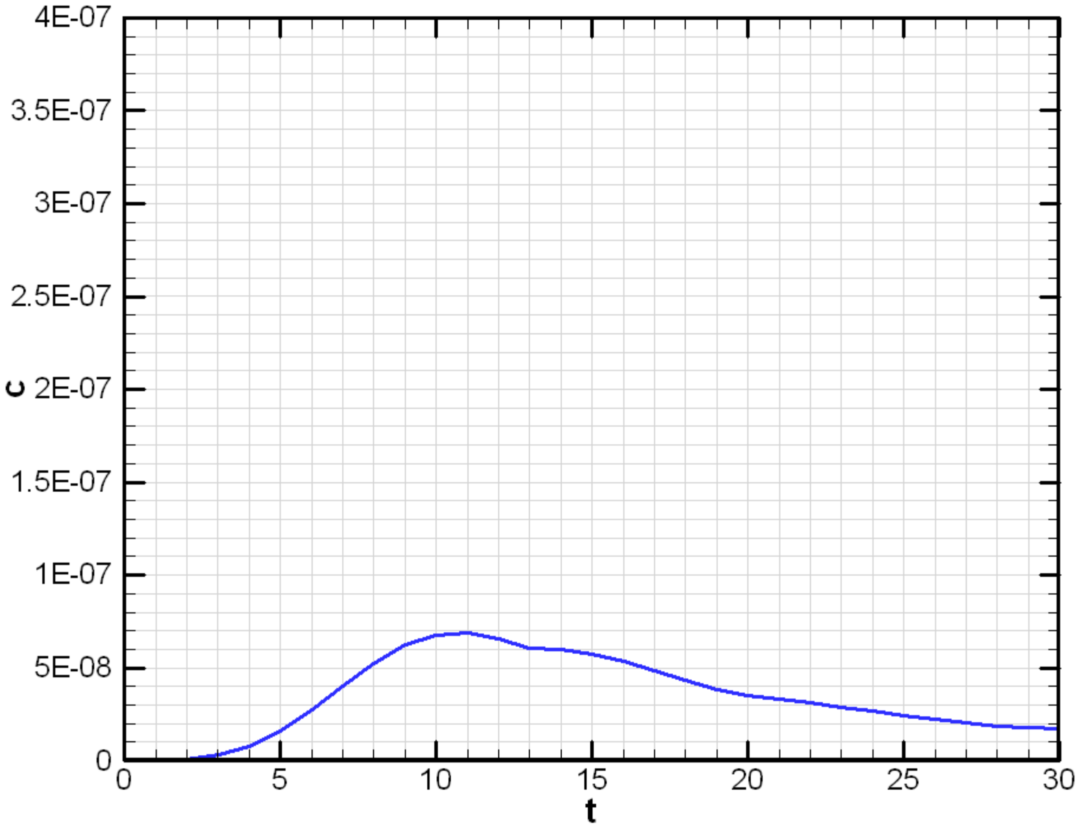

Figure A.0-14: Concentration Breakthrough Curve for a Conservative Constituent Release at the Center of FDC Group 14

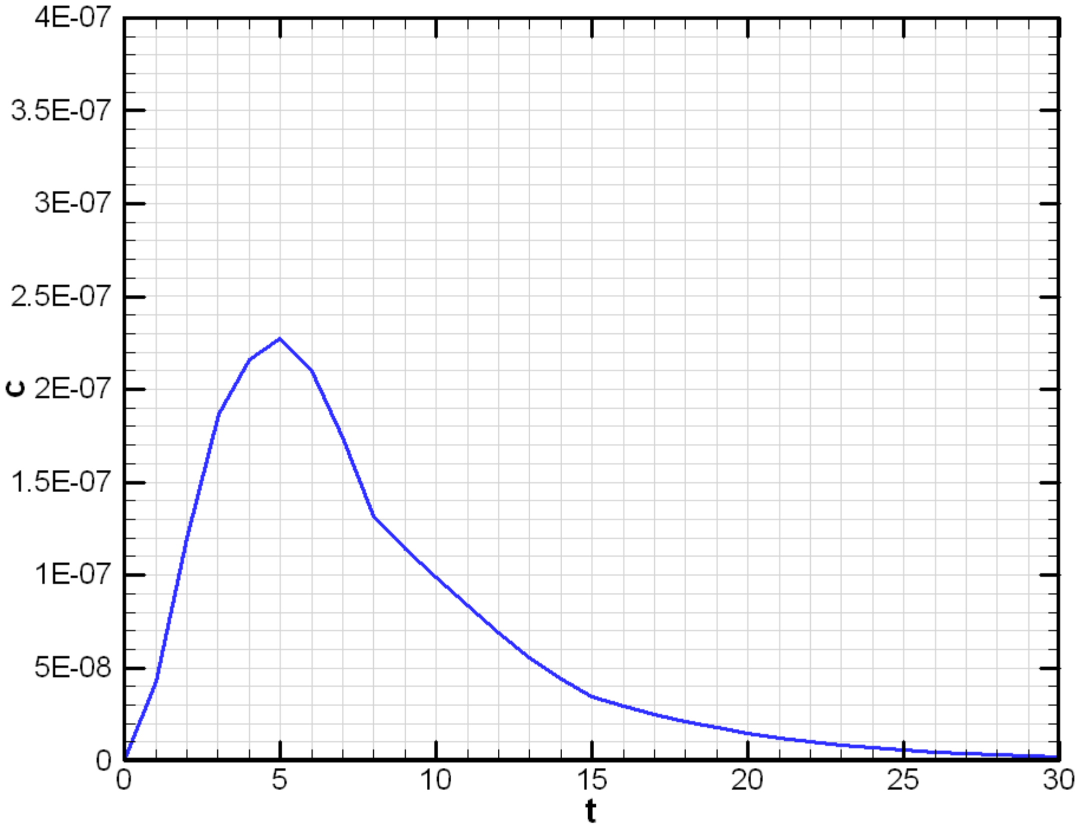

Figure A.0-15: Concentration Breakthrough Curve for a Conservative Constituent Release at the Center of FDC Group 15

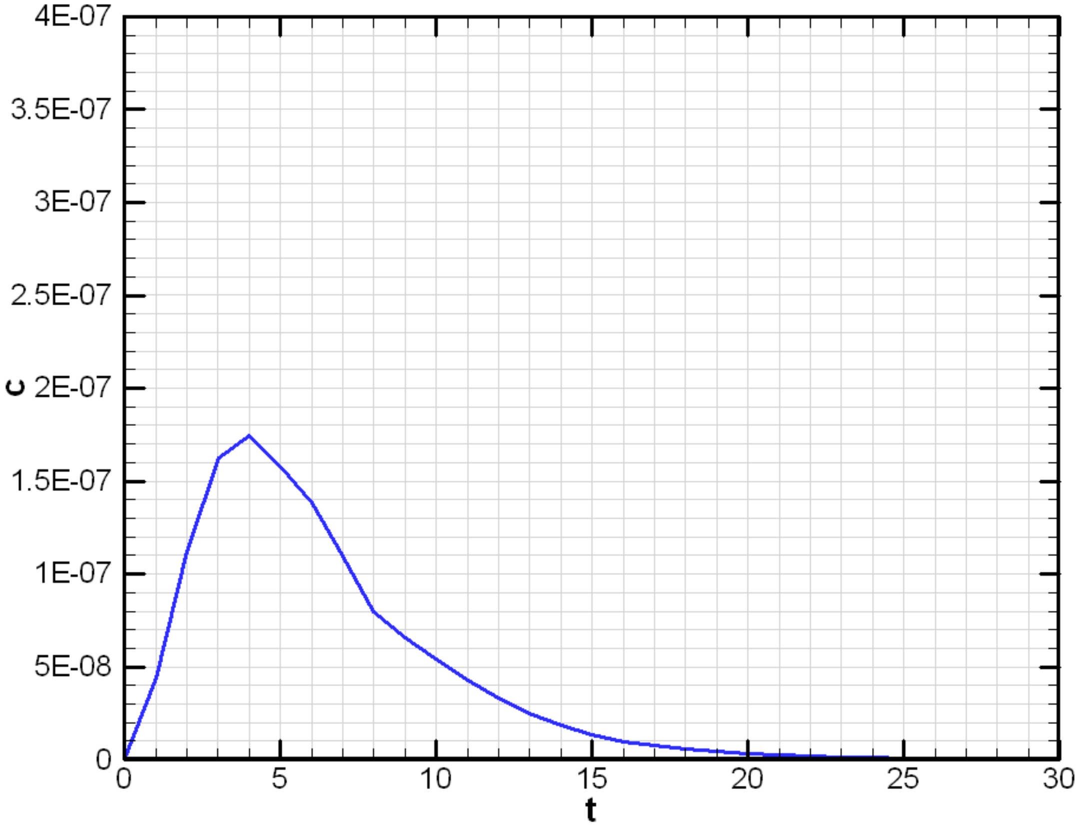

Figure A.0-16: Concentration Breakthrough Curve for a Conservative Constituent Release at the Center of FDC Group 16

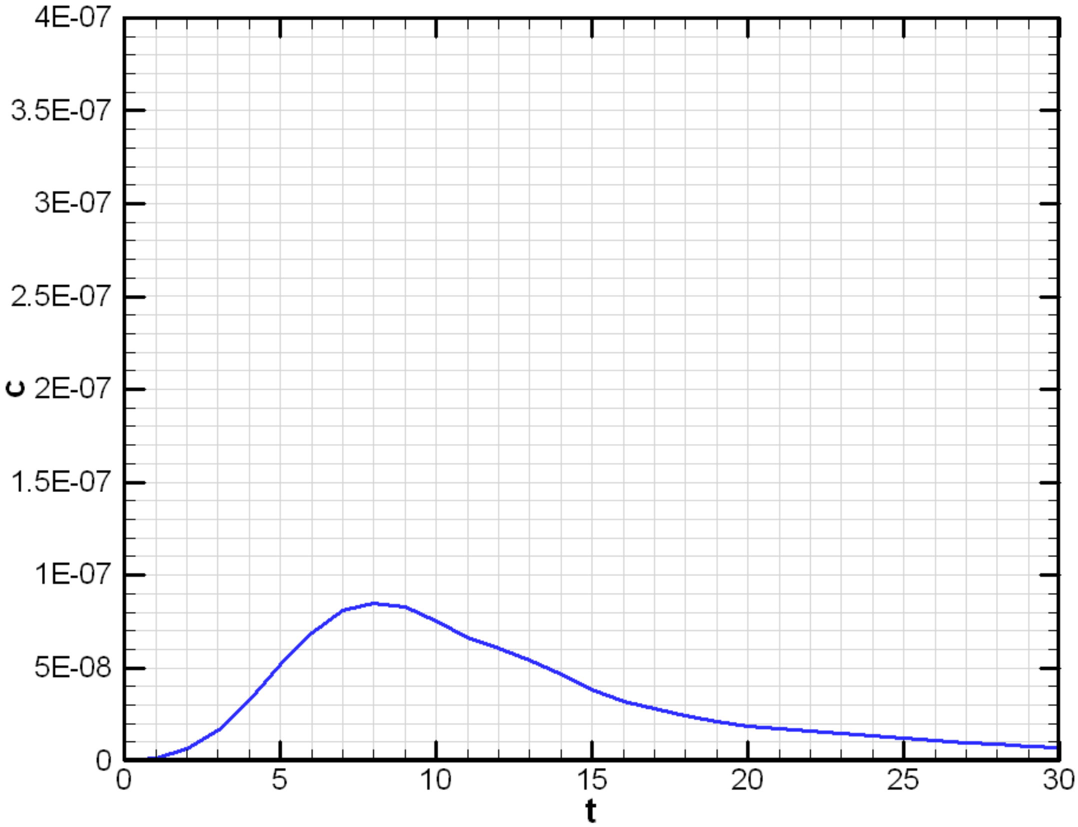

Figure A.0-17: Concentration Breakthrough Curve for a Conservative Constituent Release at the Center of FDC Group 17

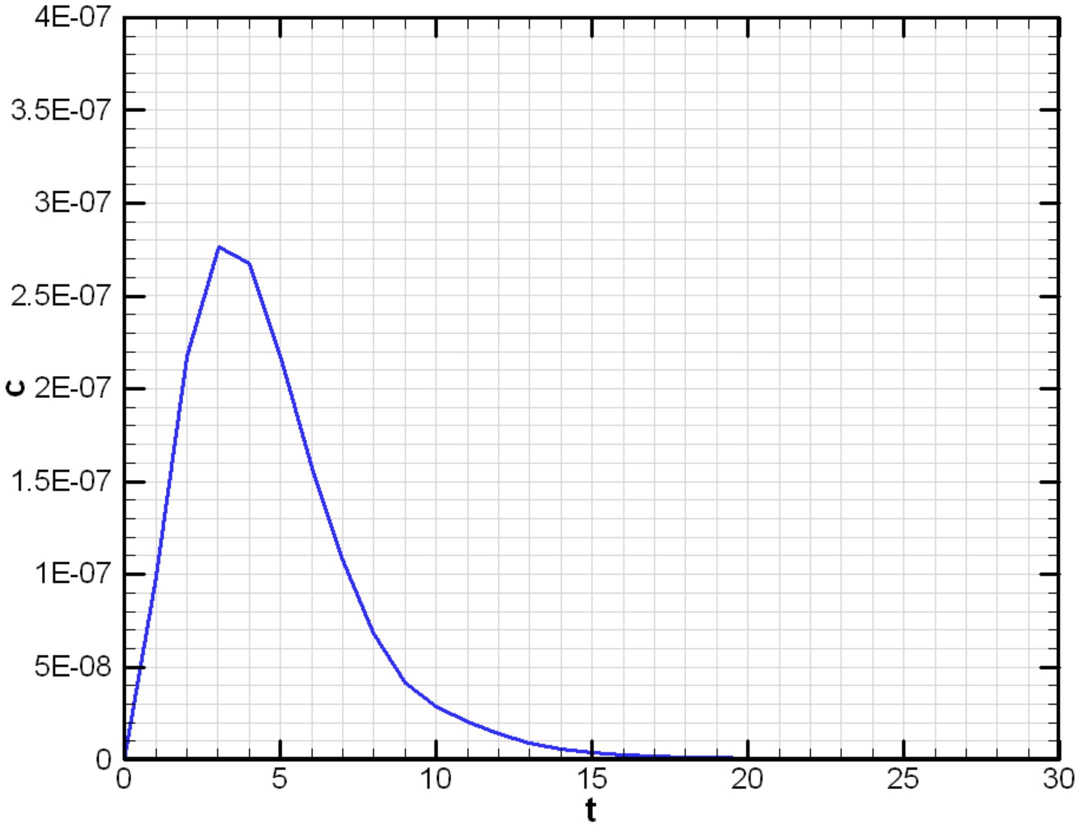

Figure A.0-18: Concentration Breakthrough Curve for a Conservative Constituent Release at the Center of FDC Group 18

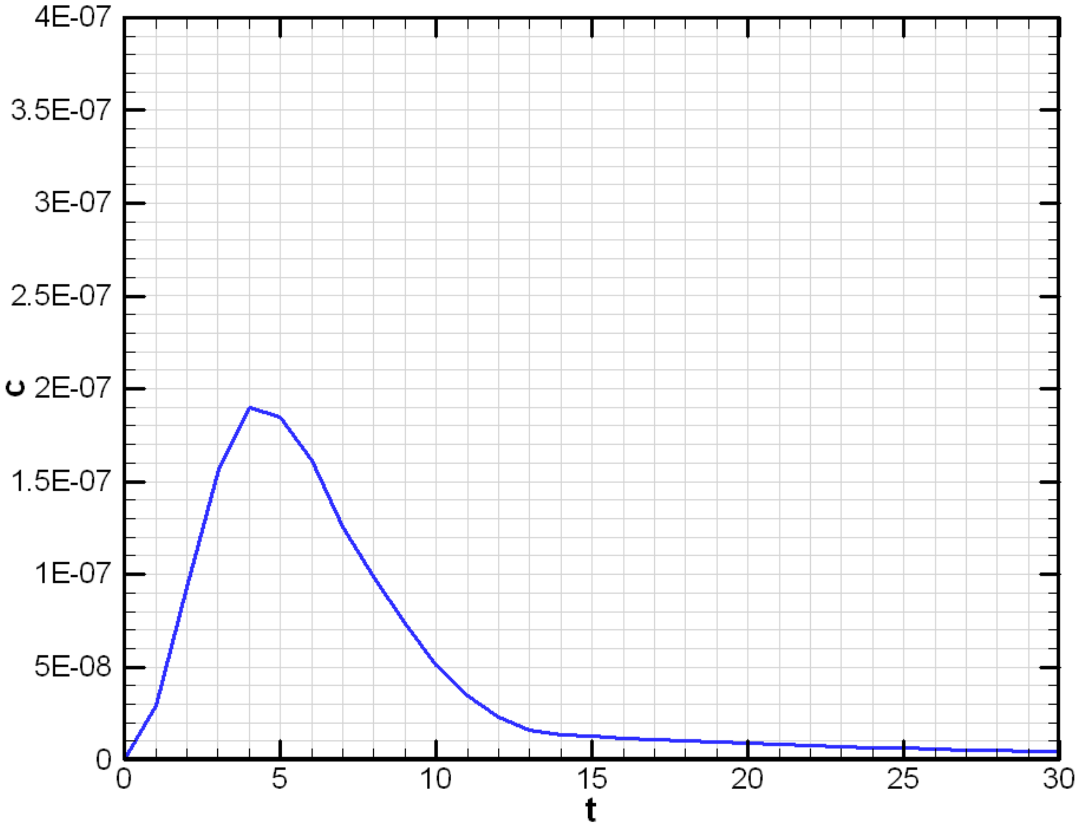

Figure A.0-19: Concentration Breakthrough Curve for a Conservative Constituent Release at the Center of FDC Group 19

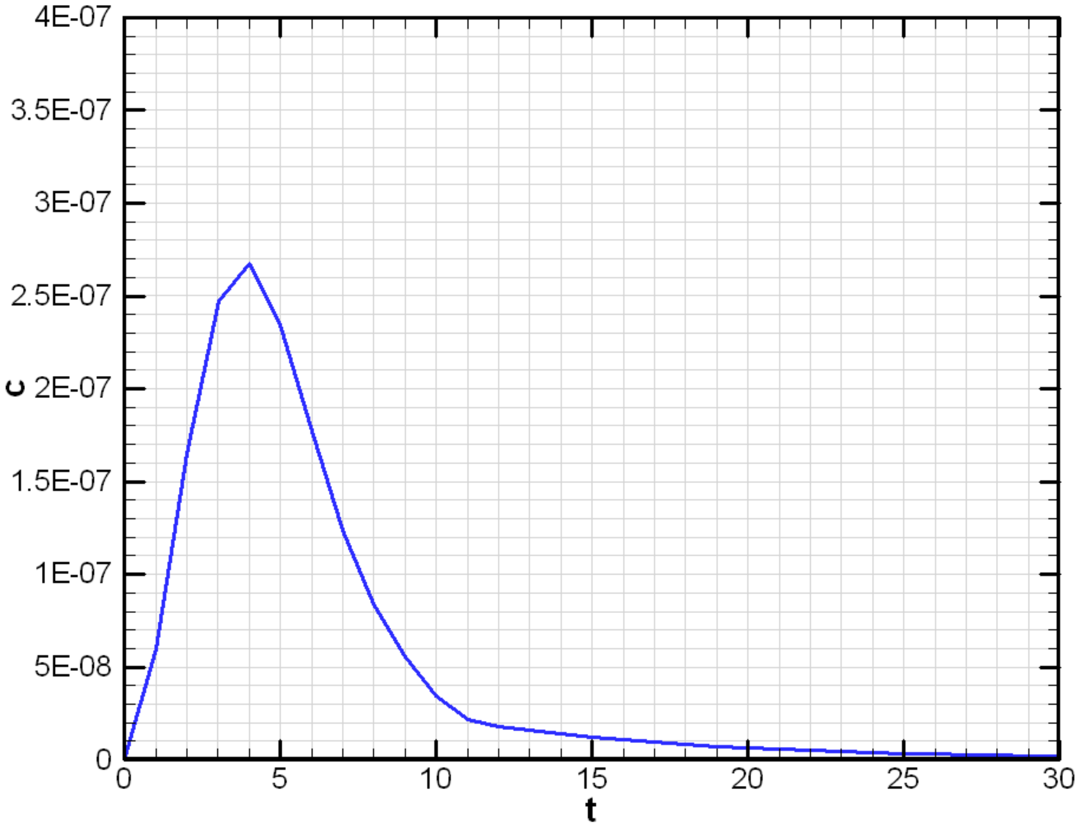

Figure A.0-20: Concentration Breakthrough Curve for a Conservative Constituent Release at the Center of FDC Group 20

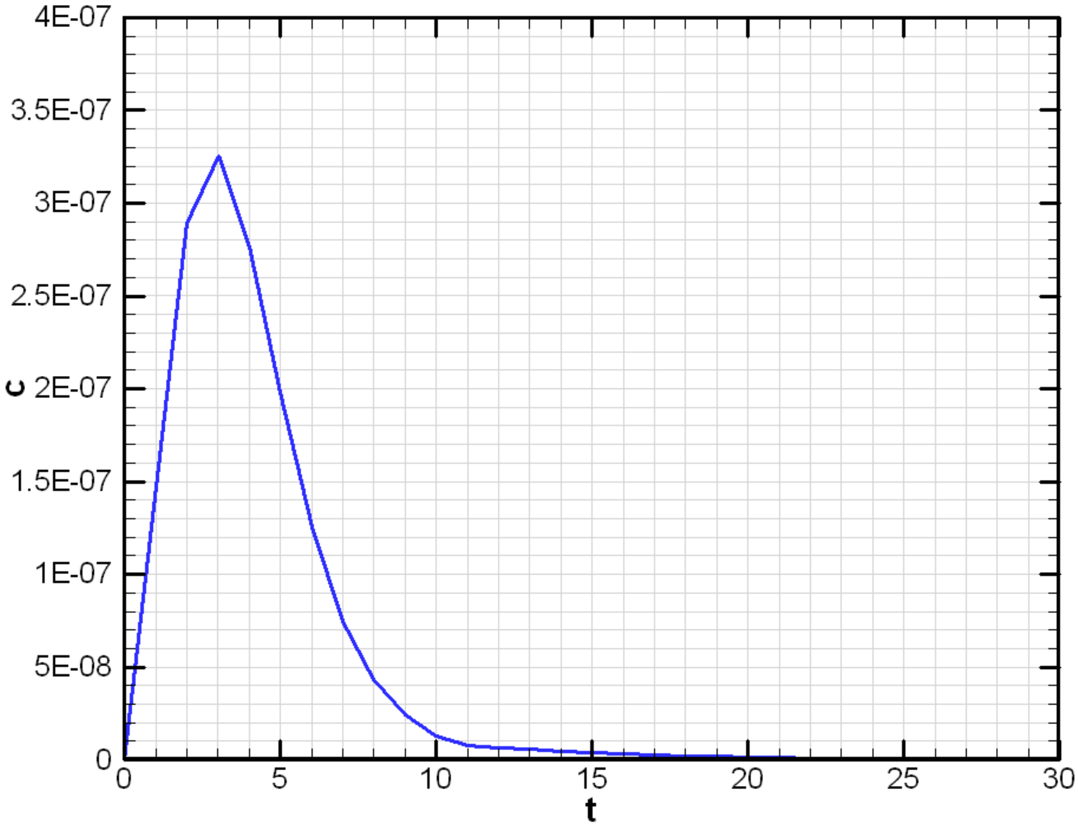

APPENDIX B

Differences between the SDF Stochastic Fate and Transport Model Versions 3.001 and 3.002

Version 3.002 of the SDF GoldSim model represents an update of the initial version (Version 3.001). The updates reflect changes that simplify the organization of the model and the fixing of errata that were found during the checking process. The errata are listed below in Table B.0-1 along with a brief discussion of the implications of the changes. The differences between results generated using Versions 3.001 and 3.002 are quantified in a study presented in Appendix C.

Table B.0-1: Errata Found in Version 3.001 of the SDF GoldSim Model

Update	GoldSim Element	Discussion
1	*GroutBD*	The bulk density of the sandstone was assigned the value for the concrete floor. This doubled the storage capacity due to sorption, slowing down the transport rate and lowering peaks. This parameter is the main driver to the differences between versions documented in Appendix C.
2	*CaseK_FDC_Th230*	Case K value and Case A through Case E value transposed in v3.001. The effect is evaluated in Appendix C.
3	*CaseK_FDC_Ra226*	Case K value and Case A through Case E value transposed in v3.001. The effect is evaluated in Appendix C.
2	*Diffusivity_HDPE*	Case A diffusivity was used in Case K. This would have a limited effect.
3	*UZCELL_** *(Vault 1 and Vault 4)*	When the extra 10 cells were added, the depth-based velocities should have been reordered. This would have little effect.
4	*Min_1stc_K*	Was set to 2,479 pore volumes as opposed to correct value of 2,476 pore volumes. This would have a limited effect.
5	*PF_FlowUZ (Vault 1)*	The benchmark factor for Case 5 was used in Case 6. This has no effect since all benchmark factors are set to 1 in the model.
6	*PF_FlowDirt (Vault 1)*	The benchmark factor for Case 5 was used in Case 6. This has no effect since all benchmark factors are set to 1 in the model.
7	*ConcreteThickness (Vaults 1 and 2)*	Values changed from centimeter to inch. This would have no effect.
8	*SatZoneDarcyVel (Vault 1)*	Value set to Vault 4 velocity in v3.001. This made little difference since the two velocities are 32 (Vault1) and 34 (Vault 4) cm/yr.
9	*PF_FlowSheetDrain1*	Vertical velocities set to zero in v3.001. This would have little effect on results.
10	*Vault_1_Width*	Extra precision added to the value to match SDF PA. This would have little effect on results.
11	*Vault_4_Width*	Extra precision added to the value to match SDF PA. This would have little effect on results.
12	*CaseK_V4_Pu238*	Case A through Case E inventory factor set at 9,300 in v3.001 corrected and reset to 9,100 in v3.002. This would have about a 2 % change in the Pu-238 inventory and thus little change in the results.
13	*SZwell_fraction_clay_east*	This is a benchmark value that is the same as in the SDF PA model, but set to zero in v3.002.
14	*V1_CaseK_Grout1*	Set to values for *Grout Zone 2* in v3.001. This would have a small influence because the velocities are similar in the two zones.
15	*V4_CaseK_UZ*	The top line was incorrect in v3.001. This would have little effect because it only affects the first time step.
16	*NaturalInfiltration.*	Changed from 40 cm/yr to 27 cm/yr to reflect value in the SDF PA. This has no effect since this term is only used in preclosure analysis, which is not presently considered in this model.
17	*SatZoneDarcyVelDist*	The distribution for saturated zone Darcy velocities was updated in v3.002. The standard deviation in v3.001 is the same as in the SDF PA, but reflects negligible variance in the distribution (0.01 times the deterministic velocity value)

Case A = Base Case
Case K = Alternative Sensitivity Case K

APPENDIX C

Assessment of Inventory Discrepancies and Refinements between GoldSim v3.001 and v3.002

INTRODUCTION

Uncertainty and Sensitivity Analyses (UA/SA) were conducted using the refined GoldSim transport model for the Base Case and the Alternative Sensitivity Case K. Alternative Sensitivity Case K was developed to respond to the second round of NRC RAIs. The GoldSim transport model v3.001 was utilized by the Neptune Company to conduct the UA/SA. During subsequent checking when the benchmarking of the refined model was being finalized, discrepancies were discovered in the inventory input and corrected in GoldSim v3.002. In addition, other refinements were made in the model so that GoldSim v3.001 is not identical to GoldSim v3.002. This assessment is conducted to determine the potential impact on the UA/SA results from the inventory input discrepancies and model refinements (see Appendix B) made between GoldSim v3.001 and v3.002.

INPUT DISCREPANCIES

The development of Alternative Sensitivity Case K is described in detail in the response to RAI PA-8, which is found in SRR-CWDA-2011-00044. Included in the development of Alternative Sensitivity Case K were inventory changes as shown in Table C.0-1. The inventory discrepancies are also shown in Table C.0-1 as values presented within brackets "[ ]." Note that the discrepancy in the inventory of Pu-238 in Vault 4 is because of an error in the RAI PA-8 response. The other discrepancies are in the FDC logic, which switched the inventories between the Base Case and Alternative Sensitivity Case K.

Table C.0-1: Inventory Changes for Alternative Sensitivity Case K

Radio-nuclide	Vault 4 Inventory (curies)		FDC (Vault 2, in model) Inventory (curies)	
	Base Case (a)	Case K (RAI PA-8)	Base Case (b)	Case K (RAI PA-8)
Pu-238	9,100 [9,300] (c)	1,000	No change	No change
U-234	26	10	No change	No change
Th-230	7.5	0.01	0.19 [1.3E-04]	1.3E-04 [0.19]
Ra-226	4.1	0.001	7.8E-07 [1.3E-5]	1.3E-5 [7.8E-07]

(a) Provided in SDF PA Table 3.3-3
(b) Provided in SDF PA Table 3.3-5
(c) Value in [ ] is used in GoldSim v3.001

ASSESSMENT METHODOLOGY

To assess the impact of the inventory discrepancies, the GoldSim v3.001 model and the GoldSim v3.002 model were run in deterministic mode to compare the MOP dose results from the different runs. Included in v3.001 and v3.002 of the GoldSim model is the flow data from PORFLOW from Alternative Sensitivity Case K, which is assigned Case Number 6. The Base Case has been assigned Case Number 1. In addition to inventory changes between the Base Case and Alternative Sensitivity Case K, Alternative Sensitivity Case K, as an alternative sensitivity case, differs from the Base Case in the assumed degradation rates and final degradation state of the cementitious barriers within the SDF closure system, the sorption coefficients, as well as the use of a different dose calculation methodology. The Base Case simulation in GoldSim v3.001 (and v3.002) estimates the radiological exposure using both the SDF PA methodology and the RAI methodology.

Assessment for Base Case (GoldSim Case Number 1)

The UA/SA for the Base Case is reported in SDF PA Sections 5.6.4 and 5.6.5, which is based on the GoldSim model v2.009. Because of the refinements made in the GoldSim model (GoldSim v3.001 and v3.002), the UA/SA was repeated for the Base Case to identify any discrepancies between the GoldSim models v2.009 and v3.001. To maintain consistency between the two GoldSim models, the dose methodology used in the UA/SA for the Base Case is founded on the SDF PA methodology. Therefore, this assessment will also only consider the SDF PA dose methodology when comparing the results between GoldSim v3.001 and GoldSim v3.002 for the Base Case.

Tables C.0-2 and C.0-3 present the dose results to a MOP using GoldSim models v3.001 and v3.002. Tables C.0-2 and C.0-3 present the peak dose to the MOP within 10,000 years and 20,000 years after closure, respectively.

Table C.0-2: Peak Dose to the MOP by Sector within 10,000 Years after Closer for Base Case

Results from GoldSim v3.001			Results from GoldSim v3.002		
Sector	Peak Dose (mrem/yr)	Year of Peak Dose	Sector	Peak Dose (mrem/yr)	Year of Peak Dose
[B]	2.46	10,000	[B]	2.72	10,000
[C]	2.45	10,000	[C]	2.69	10,000
[A]	2.45	10,000	[A]	2.68	10,000
[G]	0.61	10,000	[G]	0.77	10,000
[H]	0.61	10,000	[H]	0.76	10,000
[K]	0.61	10,000	[K]	0.76	10,000
[E]	0.60	10,000	[E]	0.73	10,000
[I]	0.60	10,000	[I]	0.73	10,000
[L]	0.60	10,000	[L]	0.73	10,000
[D]	0.60	10,000	[D]	0.72	10,000
[J]	0.59	10,000	[J]	0.70	10,000
[F]	0.59	10,000	[F]	0.68	10,000

Table C.0-3: Peak Dose to MOP by Sector within 20,000 Years after Closure for Base Case

Results from GoldSim v3.001			Results from GoldSim v3.002		
Sector	Peak Dose (mrem/yr)	Year of Peak Dose	Sector	Peak Dose (mrem/yr)	Year of Peak Dose
[B]	4.92	15,800	[B]	5.31	15,800
[C]	4.86	15,800	[C]	5.08	15,800
[A]	4.85	15,800	[A]	4.96	15,800
[G]	2.04	15,200	[G]	3.14	15,200
[H]	1.99	15,200	[H]	3.05	15,200
[K]	1.92	15,200	[K]	2.92	15,200
[E]	1.58	15,200	[E]	2.32	15,200
[I]	1.57	15,200	[I]	2.29	15,200
[L]	1.50	15,200	[L]	2.15	15,200
[D]	1.30	15,200	[D]	1.80	15,200
[J]	1.14	15,800	[J]	1.45	15,200
[F]	1.11	15,800	[F]	1.19	15,800

Tables C.0-2 and C.0-3 indicate that the inventory discrepancies between GoldSim versions v3.001 and v3.002 are not significant. This is to be expected because the Base Case is dominated by the release of contaminants from Vault 4 because of the degraded condition of the vault walls and the assumed initial inventory within the walls to account for the influence of the current weeping of the walls. The dominance of Vault 4 is reflected in the fact that the peak doses occur in Sector B.

To assess the two GoldSim models further, Tables C.0-4 and C.0-5 present the main radionuclide contributors to the peak dose in Sector B within 10,000 years and 20,000 years, respectively. The Ra-226 contribution to the peak dose is not appreciably impacted, thus the inventory discrepancies do not significantly impact the resultant dose. The relative contribution changes for Cs-135 and I-129 between the two models are indicative of other minor refinements made to GoldSim v3.001, which would not significantly impact the UA/SA results.

Table C.0-4: Contribution to Peak Dose in Sector B within 10,000 Years (Base Case)

Results from GoldSim v3.001			**Results from GoldSim v3.002**		
Radio-nuclide	**Dose (mrem/yr)**	**Contribution to Total**	**Radio-nuclide**	**Dose (mrem/yr)**	**Contribution to Total**
[Ra226]	2.36E+00	96.00 %	[Ra226]	2.55E+00	93.76 %
[I129]	3.39E-02	1.38 %	[Cs135]	7.17E-02	2.64 %
[Pb210]	3.16E-02	1.28 %	[I129]	5.27E-02	1.94 %
[Cs135]	2.25E-02	0.92 %	[Pb210]	3.44E-02	1.27 %
[Tc99]	7.49E-03	0.30 %	[Tc99]	7.54E-03	0.28 %
[C14]	9.68E-04	0.04 %	[C14]	1.09E-03	0.04 %
[Pa231]	6.94E-04	0.03 %	[Pa231]	7.35E-04	0.03 %
[Np237]	6.07E-04	0.02 %	[Np237]	6.36E-04	0.02 %
[Nb93m]	5.67E-04	0.02 %	[Nb93m]	6.06E-04	0.02 %
TOTAL	2.46E+00	N/A	**TOTAL**	2.72E+00	N/A

Table C.0-5: Contribution to Peak Dose in Sector B within 20,000 Years (Base Case)

Results from GoldSim v3.001			Results from GoldSim v3.002		
Radio-nuclide	**Dose (mrem/yr)**	**Contribution to Total**	**Radio-nuclide**	**Dose (mrem/yr)**	**Contribution to Total**
[Ra226]	4.01E+00	81.50 %	[Ra226]	4.33E+00	81.48 %
[Tc99]	6.53E-01	13.26 %	[Tc99]	6.80E-01	12.82 %
[I129]	1.06E-01	2.15 %	[I129]	1.47E-01	2.76 %
[Cs135]	7.83E-02	1.59 %	[Cs135]	6.40E-02	1.21 %
[Pb210]	5.41E-02	1.10 %	[Pb210]	5.84E-02	1.10 %
[Pa231]	8.81E-03	0.18 %	[Pa231]	1.70E-02	0.32 %
[Np237]	6.98E-03	0.14 %	[Np237]	1.23E-02	0.23 %
[Nb93m]	2.95E-03	0.06 %	[Nb93m]	3.08E-03	0.06 %
[C14]	7.32E-04	0.01 %	[C14]	8.79E-04	0.02 %
TOTAL	4.92E+00	N/A	**TOTAL**	5.31E+00	N/A

Figure 1 illustrates the dose to the MOP as a function of time for the Base Case for the total dose (from all radionuclides) and from only Ra-226 (which is influenced by the decay of Th-230, U-234, and Pu-238, which produce Ra-226). Figure C.0-1 further illustrates that the inventory discrepancies do not have significant impacts to the deterministic transport runs and thus would not have any appreciable impact on the UA/SA results.

Figure C.0-1: Dose to MOP in Sector B Using GoldSim Models v3.001 and v3.002 (Base Case)

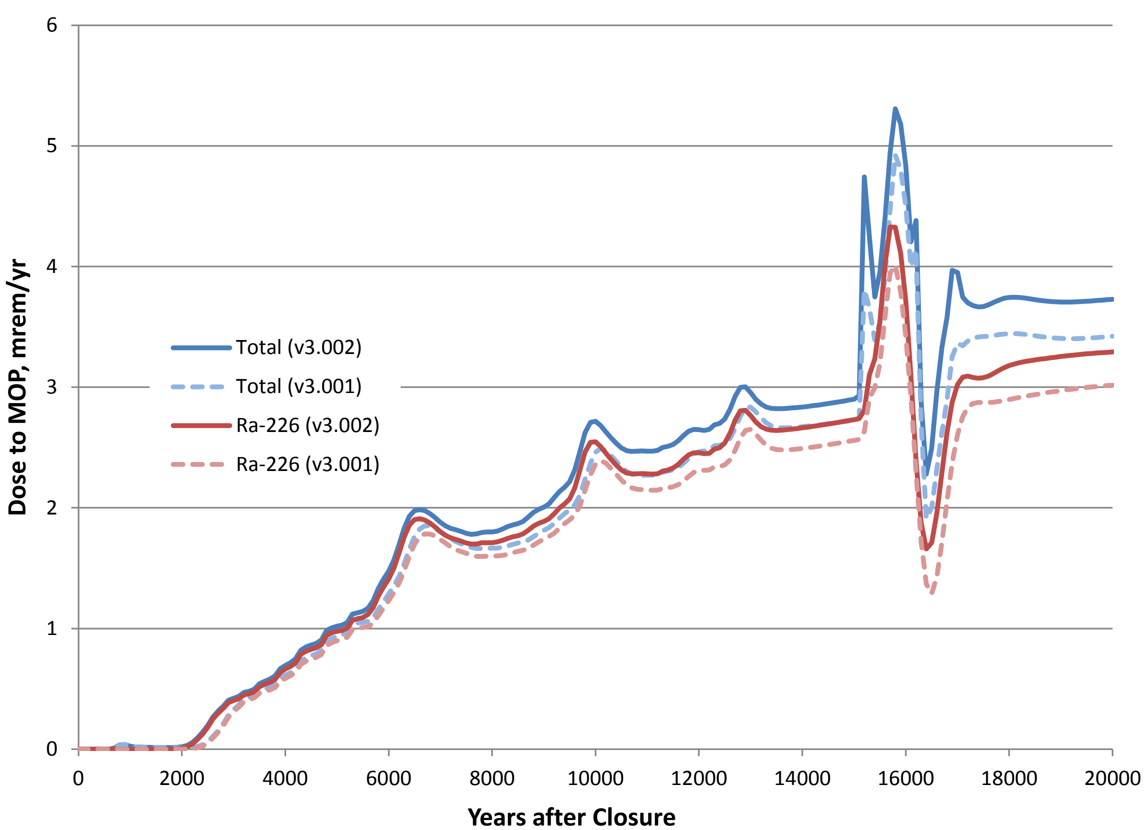

Assessment for RAI Alternative Sensitivity Case K (GoldSim Case Number 6)

The UA/SA for Alternative Sensitivity Case K utilizes the dose methodology developed in the response to RAIs B-2, B-3, and B-4 (SRR-CWDA-2011-00044). This RAI dose methodology was used to evaluate Alternative Sensitivity Case K that is included in the response to RAI PA-8. Therefore, this assessment will also utilize the RAI dose methodology when comparing the results between GoldSim v3.001 and GoldSim v3.002 for Alternative Sensitivity Case K.

Tables C.0-6 and C.0-7 present the dose results to a MOP using GoldSim models v3.001 and v3.002. Because Alternative Sensitivity Case K assumes significant degradation of the cementitious barriers in the disposal units, the dose results are now dominated by the FDCs as indicated by the peak doses occurring in Sector G rather than Sector B as shown for the Base Case. To assess the two GoldSim models further, Tables 8 and 9 present the main radionuclide contributors to the peak dose in Sector G within 10,000 years and 20,000 years, respectively. Tables C.0-8 and C.0-9 illustrate that Ra-226 is not a significant contributor to dose for Alternative Sensitivity Case K; thus, the inventory discrepancies between the two GoldSim models would have no impact on the UA/SA for Alternative Sensitivity Case K.

Table C.0-6: Peak Dose to the MOP by Sector within 10,000 Years after Closure for Alternative Sensitivity Case K

Results from GoldSim v3.001			Results from GoldSim v3.002		
Sector	Peak Dose (mrem/yr)	Year of Peak Dose	Sector	Peak Dose (mrem/yr)	Year of Peak Dose
[G]	19.3	8,600	[G]	15.7	7,300
[H]	18.8	8,600	[H]	15.3	7,300
[K]	17.9	8,600	[K]	14.6	7,300
[B]	15.7	8,600	[B]	13.1	7,300
[E]	13.9	8,600	[E]	11.7	7,300
[I]	13.8	8,600	[I]	11.6	7,300
[L]	12.9	8,600	[L]	10.9	7,300
[D]	10.5	8,600	[D]	9.2	7,300
[C]	10.4	8,600	[C]	9.2	7,300
[A]	9.4	8,600	[A]	8.4	7,300
[J]	8.3	8,600	[J]	7.6	7,800
[F]	5.6	8,600	[F]	5.9	7,800

Table C.0-7: Peak Dose to the MOP by Sector within 20,000 Years after Closure for Alternative Sensitivity Case K

Results from GoldSim v3.001			Results from GoldSim v3.002		
Sector	Peak Dose (mrem/yr)	Year of Peak Dose	Sector	Peak Dose (mrem/yr)	Year of Peak Dose
[G]	79.6	16,200	[G]	84.5	15,800
[H]	76.5	16,200	[H]	81.3	15,800
[K]	72.1	16,200	[K]	76.7	15,800
[B]	62.1	16,200	[B]	65.9	15,800
[E]	51.9	16,200	[E]	55.1	15,800
[I]	51.0	16,200	[I]	54.2	15,800
[L]	46.6	16,200	[L]	49.6	15,800
[C]	34.9	16,200	[C]	36.9	15,800
[D]	34.5	16,200	[D]	36.7	15,800
[A]	29.7	16,200	[A]	31.4	15,800
[J]	23.2	16,200	[J]	24.7	15,800
[F]	9.2	16,200	[F]	9.8	15,800

Table C.0-8: Contribution to Peak Dose in Sector G within 10,000 Years (Alternative Sensitivity Case K)

Results from GoldSim v3.001			Results from GoldSim v3.002		
Radio-nuclide	Dose (mrem/yr)	Contribution to Total	Radio-nuclide	Dose (mrem/yr)	Contribution to Total
[I129]	1.69E+01	87.42 %	[I129]	1.25E+01	79.55 %
[Cs135]	2.34E+00	12.11 %	[Cs135]	3.15E+00	20.05 %
[Tc99]	7.63E-02	0.39 %	[Tc99]	4.50E-02	0.29 %
[K40]	5.58E-03	0.03 %	[K40]	1.44E-02	0.09 %
[Ra226]	4.72E-03	0.02 %	[Nb93m]	2.09E-03	0.01 %
[Nb93m]	2.15E-03	0.01 %	[Ra226]	3.97E-04	0.00 %
TOTAL	1.93E+01	N/A	**TOTAL**	1.57E+01	N/A

Table C.0-9: Contribution to Peak Dose in Sector G within 20,000 Years (Alternative Sensitivity Case K)

Results from GoldSim v3.001			Results from GoldSim v3.002		
Radio-nuclide	Dose (mrem/yr)	Contribution to Total	Radio-nuclide	Dose (mrem/yr)	Contribution to Total
[Tc99]	7.90E+01	99.22 %	[Tc99]	8.44E+01	99.78 %
[Ra226]	5.35E-01	0.67 %	[Ra226]	1.38E-01	0.16 %
[Pb210]	7.15E-02	0.09 %	[Pb210]	3.35E-02	0.04 %
[Nb93m]	9.75E-03	0.01 %	[Nb93m]	8.75E-03	0.01 %
[Pa231]	4.71E-03	0.01 %	[Pa231]	5.43E-03	0.01 %
TOTAL	7.96E+01	N/A	**TOTAL**	8.45E+01	N/A

Tables C.0-8 and C.0-9 indicate that further refinements made in GoldSim v3.002 have an impact on the timing and magnitude of the resulting dose but the inventory discrepancies associated with Ra-226 and its progeny are not the cause. As indicated in Table C.0-8, the dominant contributors to the dose within the first 10,000 years after closure are Cs-135 and I-129. As indicated in Table C.0-9, the dominant contributor to the dose between 10,000 years and 20,000 years after closure is Tc-99. Figure C.0-2 illustrates the dose profiles to the MOP in Sector G, for Alternative Sensitivity Case K, generated using GoldSim v3.001 and v3.002. Figure C.0-2 indicates that the significant differences between GoldSim v3.001 and GoldSim v3.002 are manifested within the 12,000 years after closure.

Figure C.0-2: Dose to MOP in Sector G Using GoldSim Models v3.001 and v3.002 (Alternative Sensitivity Case K)

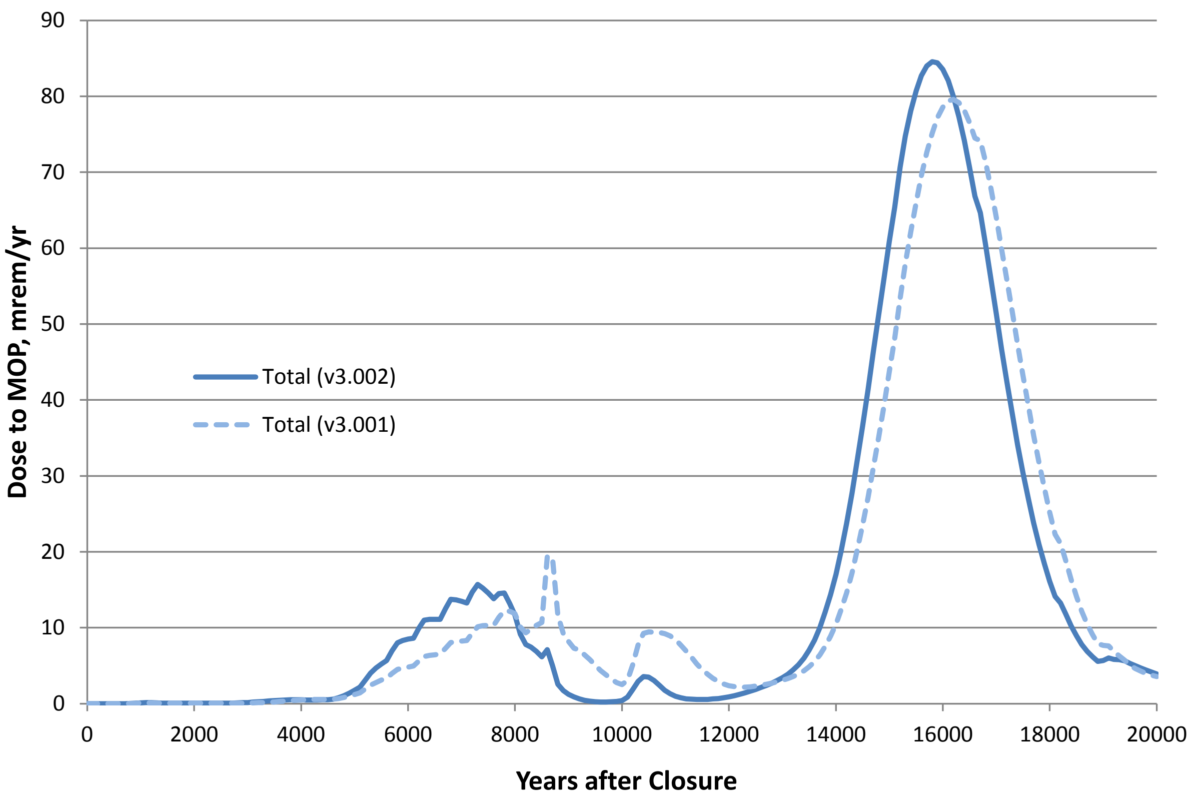

Figure C.0-3 focuses on the time duration up to 12,000 years after closure and illustrates the dose profile to the MOP from the major dose contributors. A closer examination of the two models indicated that the cause of the different dose curves for I-129 and Tc-99 is a correction made to the bulk density of the grout cells in the FDCs (the appropriate values were used for Vault 1 and Vault 4 in GoldSim v3.001). The FDCs dry-bulk density for saltstone is 2.26 g/cm^3 in GoldSim v3.001 however; it was changed to the correct value of 1.01 g/cm^3 in GoldSim v3.002. The dose profile of Cs-135 in Figure C.0-3 shows no appreciable difference between the two models. The Cs-135 contribution to the total dose is almost entirely from the fish ingestion, dose pathway, which is based on stream concentrations that are independent of sector (rather than well locations at 100 meters from the SDF) and is dominated by the Cs-135 release from Vault 4.

Figure C.0-3: Dose to MOP in Sector G Using GoldSim Models v3.001 and v3.002 (Alternative Sensitivity Case K)

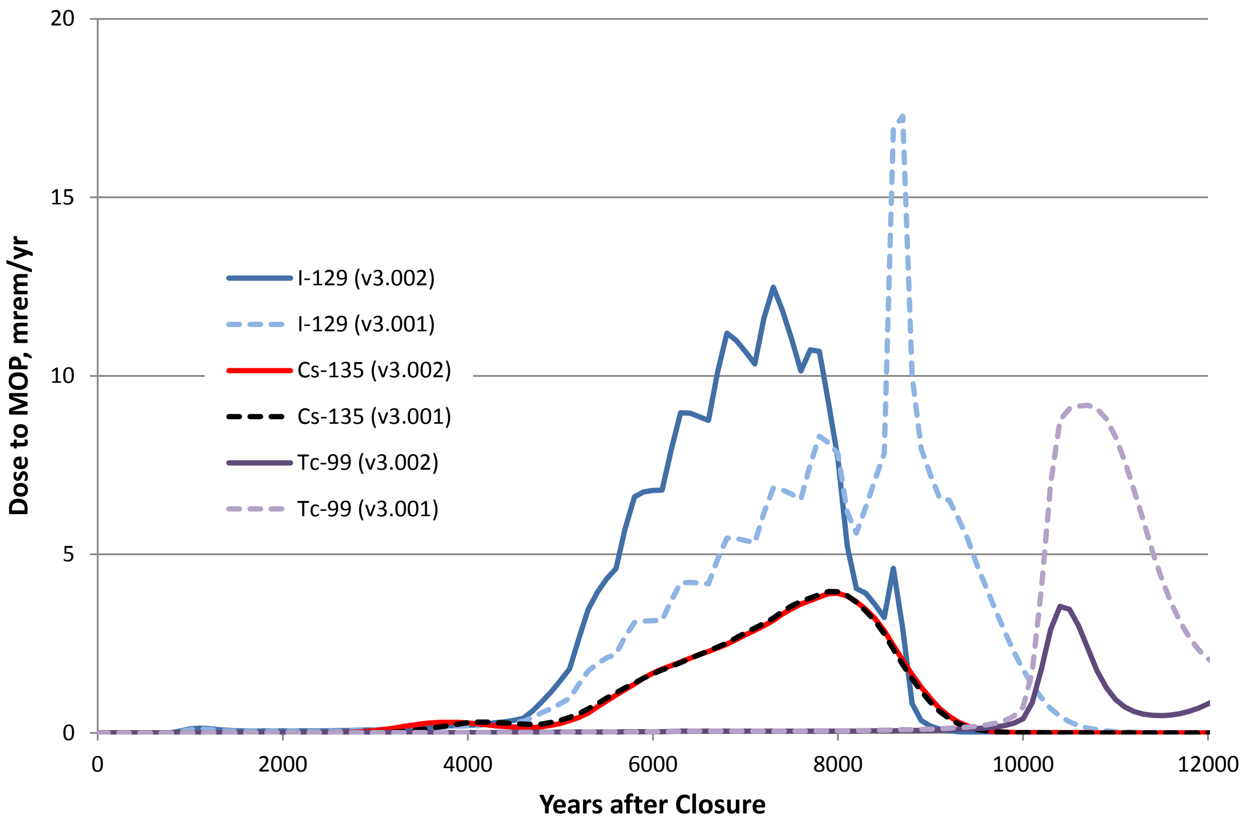

For Alternative Sensitivity Case K, the inventory discrepancies would have no impact of the UA/SA conducted using GoldSim v3.001 because Ra-226 is not a significant contributor to the dose to the MOP. The model refinements made between GoldSim v3.001 and GoldSim v3.002 are shown to either have no impact (for Cs-135) or would over-predict the dose during the time period within 12,000 years after closure (for I-129 and Tc-99). Therefore, the results of the UA/SA conducted using GoldSim v3.001 would bound the results of the UA/SA conducted using GoldSim v3.002 for the duration of time within 10,000 years after closure. For the time period between 10,000 years and 20,000 years, the difference of the dose to the MOP between GoldSim v3.001 and GoldSim v3.002 is not significant; thus, results of the UA/SA conducted using GoldSim v3.001would not be appreciably impacted.

CONCLUSIONS

Based on this assessment it is concluded that the UA/SA conducted using GoldSim model v3.001 is expected to be representative of SDF conceptual model for the Base Case and Alternative Sensitivity Case K.